



THE KINETICS OF PYRITE AND ELEMENTAL SULFUR REACTIONS DURING NITRIC ACID PRE-OXIDATION OF REFRACTORY GOLD ORES

Thesis submitted for the degree of Doctor of Philosophy

by

James R. Flatt
B.A.Sc., M.Eng., Aus.I.M.M., B.C.A.P.E., A.A.E.E

Department of Chemical Engineering
The University of Adelaide

June 1996

DECLARATION

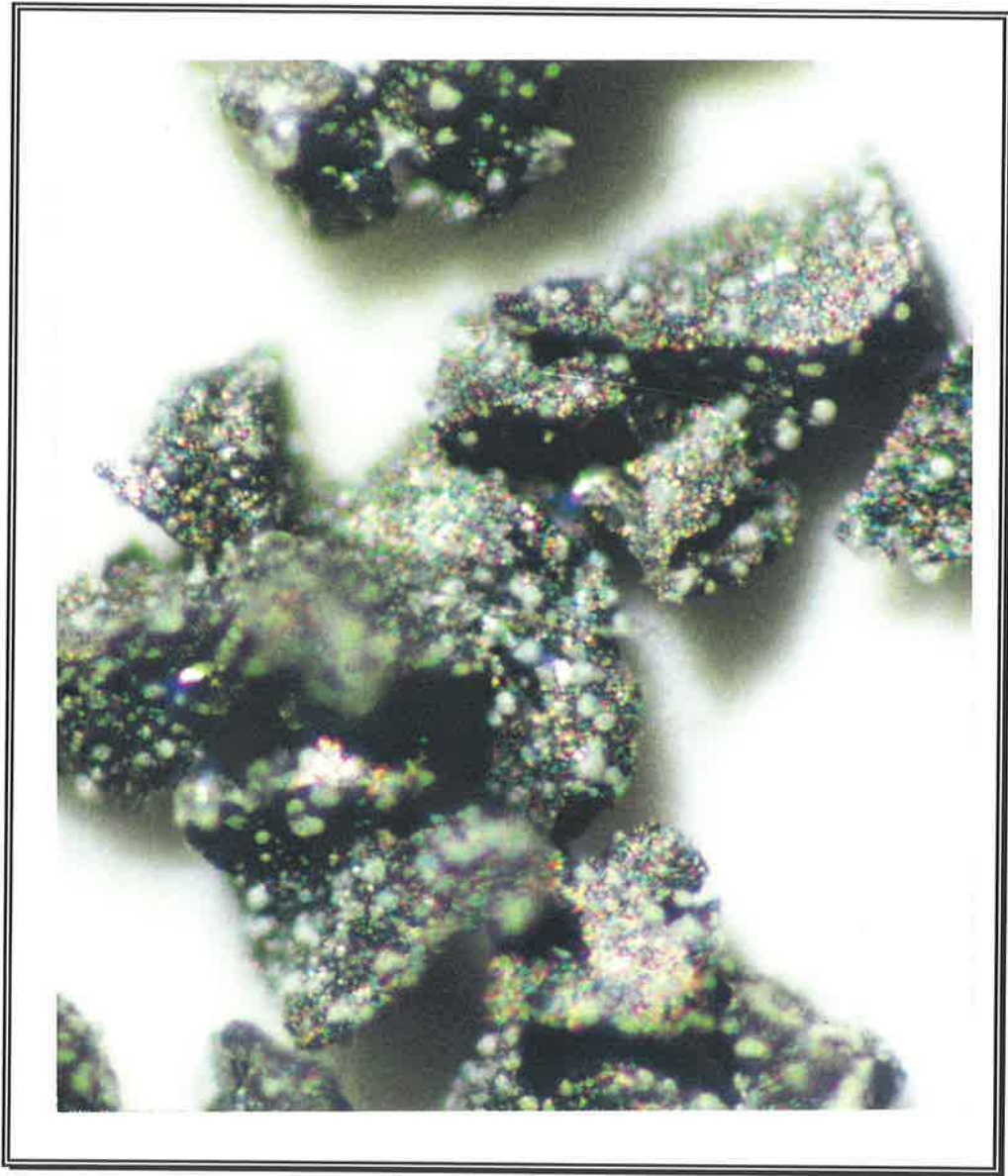
1. This thesis contains no material which has been accepted for the award of any degree or diploma by any University. To the author's knowledge and belief this thesis contains no material previously published or written by any other person, except where due reference is made in the text.
2. I give consent to this copy of my thesis, when deposited in the University Library, being made available for loan and photocopying.

Signed:

James R. Flatt

June 1996

FRONTISPIECE



PYRITE DURING NITRIC ACID LEACH

See page iii of the Appendix for details

THE KINETICS OF PYRITE AND ELEMENTAL SULFUR REACTIONS DURING NITRIC ACID PRE-OXIDATION OF REFRACTORY GOLD ORES

ABSTRACT

Refractory gold deposits are of increasing interest to the mining industry in Australia and overseas. Nitric acid technology for the pre-oxidation of sulfides in such refractory deposits has shown kinetic advantages. Developers of the "Redox" nitric acid process have cited cost advantages to the low temperature process variant, but have also encountered difficulties from elemental sulfur formed during the process. The focus of the present work is to investigate the fundamental kinetics of the pyrite-nitric acid system. Particular attention is paid to the formation and oxidation of elemental sulfur.

Predictive work was undertaken using linear potential-sweep voltammetry. It was shown that the proportion of elemental sulfur formed in 0.22 M nitric acid is independent of temperature but decreases with increasing Eh. Leach tests confirmed the temperature independence. Leach tests were unable to confirm that elemental sulfur would be eliminated at Eh - 1.4 volts SHE. This inability was due to limits of Eh imposed by the nitric acid system itself and also due to difficulties in measuring Eh of hot strongly acidic solutions. Predicted pyrite oxidation rates of $91 \times 10^{-8} \text{ g cm}^{-2}\text{sec}^{-1}$ at 1.20 volts were confirmed by leach tests rates at similar conditions.

Leach tests of pyrite in nitric acid enabled quantification and analysis of seventeen variables and observed phenomena. The data fit a first-order model well, particularly once observed lag period effects were deleted. Lag periods effects were the main differences between pyrites from different sources. These effects are thought to be predominantly caused by rapidly-forming surface layers on pyrite. First-order rate constants from 0.003 min^{-1} to 1.10 min^{-1} were found. However, most tests were in the range considered to be industrially realistic, giving rate constants around 0.1 min^{-1} . The proportion of elemental sulfur which forms from pyrite is higher than expected from the literature, being about twenty percent under conditions typical of the majority of the tests (2.6 M HNO_3). Once formed, this elemental sulfur oxidises slowly compared to the pyrite, with a typical first-order rate constant being 0.007 min^{-1} . Further, the elemental sulfur oxidation rate is an order of magnitude less sensitive to the test variables than the pyrite oxidation rate.

The variation in the oxidation rates of both pyrite and elemental sulfur with experimental conditions accounts for apparently conflicting reports, for both pyrite oxidation rates and elemental sulfur found, in the literature. The present study evaluates more variables than any study found in the literature for pyrite oxidation. The use of nitric acid and elemental sulfur focus goes beyond anything reported.

The independent variables tested proved unable to eliminate elemental sulfur formation, although there is scope for further investigation of silver ion addition, or higher Eh systems. Once formed, elemental sulfur, if it is to be oxidised completely, dictates reaction retention time for the low-temperature "Redox" variant. If less than three percent of elemental sulfur were to be required from a high-sulfide feed, elemental sulfur would dictate unrealistic retention times. This confirms developers' expedient preference for the more expensive high temperature process variant.

Pre-oxidation and cyanidation tests on four refractory gold-bearing materials confirmed the technical capabilities of nitric acid leaching. Gold recoveries were improved from 48-68% to an average of 93%. Reductions of around 2 kg of cyanide and base per tonne of ore were also shown for most materials.

Remaining unrecovered gold could be partially due to elemental sulfur remaining after the pre-oxidation step. This, and other avenues for further investigations, are enumerated in the thesis.

ACKNOWLEDGMENTS

The author gratefully acknowledges the financial assistance provided by Minproc Technology and CRA's Advanced Technical Development. These two companies provided three refractory gold-bearing materials for testing, while Stawell Gold Mines provided the fourth. The joint CSIRO/University of South Australia and CSIRO/University of Adelaide Collaborative Research Funds are also to be thanked for their continuing support and encouragement. In addition the University of South Australia funded two periods of Study Leave during the research program.

The author wishes to thank heartily his supervisor, Dr Brian O'Neill, for his approach, his knowledge and his moral support. Dr O'Neill's approach was one of a colleague who understood the realities of part-time research. He always made time for communication when needed. His knowledge in specialist areas such as mathematical modelling was most helpful. Dr O'Neill even provided occasional funds near the completion of testwork, but it was his continuing moral support which was most appreciated. His sense of humour was a particular asset.

Probably the most rewarding single aspect of the research has been the gaining and support of new colleagues. Dr Ron Woods of C.S.I.R.O. and Dr John Canterford of Minproc have been invaluable throughout. Drs Frank Lawson and David Koch of Monash University are thanked for their insight, guidance and use of equipment for the electrochemical work. The author is grateful to Dr Graham Sparrow and many others at CSIRO Division of Mineral Products. Dr Ernie Peters of the University of British Columbia is thanked for his time and inspiration. The author also wishes to acknowledge the sympathetic timetabling and assistance of colleagues at the University of South Australia, in particular, Dr Ken Strafford, Keith Quast, Ray Newell and David Twigger.

Several pairs of hands contributed to the laboratory work usually on a paid basis or as work experience through C.A.L.U.S.A. These included: Dean Brooks, Dhamendra Bhindi and Siew-Mung Ho for autoclave tests; José Dioses, Hung Ha, Ursula Reimers, Catalin Popescu and Sean Sara for leach tests. Their willing efforts allowed a large number of variables to be evaluated.

Finally, the author is grateful to Mary Barrow for thesis typing, Chris Elford and Alex Kavoukis for help with graphs, and the technical staff of the Department of Chemical Engineering at The University of Adelaide for numerous small favours which were essential to the research.

TABLE OF CONTENTS

Declaration

Acknowledgments

Abstract

| | Page |
|---|-------------|
| Chapter 1: Introduction | |
| 1.1 Reasons for the study | 1 |
| 1.2 Refractory gold ores | 1 |
| 1.3 Specific aims | 2 |
| 1.4 Scope | 2 |
| 1.5 Limitations | 3 |
| 1.6 Summary of Introduction | 4 |
| Chapter 2: Background to Study | |
| 2.1 Chapter content | 5 |
| 2.2 Refractory gold ore | |
| 2.2.1 Practical definition | 5 |
| 2.2.2 Importance | 6 |
| 2.2.3 Causes of refractory behaviour | 6 |
| 2.2.4 Treatment alternatives | 7 |
| 2.2.5 Generalized Flowsheet for Pre-oxidation | 8 |
| 2.2.6 Broader Engineering considerations | 9 |
| 2.3 Nitric acid processes for pre-oxidation | |
| 2.3.1 Preamble | 9 |
| 2.3.2 Brief overview of process chemistry | 10 |
| 2.3.3 Early research | 11 |
| 2.3.4 The "Nitrox" process | 14 |
| 2.3.5 The "Redox" process | 15 |
| 2.3.6 Experimental conditions investigated | 18 |
| 2.3.7 Value of present testwork | 18 |
| 2.4 Elemental Sulfur | |
| 2.4.1 Problems caused during refractory gold processing | 19 |
| 2.4.2 Observations during development testwork | 20 |
| 2.4.3 Pertinent properties | 21 |
| 2.5 Summary | 22 |
| 2.6 References | 24 |
| Chapter 3: Autoclave and Cyanidation Tests | |
| 3.1 Philosophy | 28 |
| 3.2 Scope of Testwork | |
| 3.2.1 Refractory gold-bearing materials tested | 28 |
| 3.2.2 Pre-oxidation and cyanide tests | 29 |

| | Page |
|--|-------------|
| 3.3 Experimental Method | |
| 3.3.1 Rolling bottle cyanidation | 30 |
| 3.3.2 Autoclave pre-oxidation tests | 31 |
| 3.4 Summarised Experimental Results | |
| 3.4.1 Example of individual tests | 32 |
| 3.4.2 Parameters of feed materials | 35 |
| 3.4.3 Effect of nitric acid pre-oxidation on gold cyanidation parameters | 37 |
| 3.4.4 Metal deportment | 38 |
| 3.4.5 Elemental sulfur in pre-oxidation and cyanidation tests | 39 |
| 3.5 Discussion of Results | |
| 3.5.1 Typical individual tests | 40 |
| 3.5.2 Parameters of feed materials | 41 |
| 3.5.3 Effects of pre-oxidation with nitric acid | 41 |
| 3.5.4 Effects on metal deportments | 42 |
| 3.5.5 Findings concerning elemental sulfur | 43 |
| 3.6 Chapter Summary | 45 |
| 3.7 References | 47 |
| Chapter 4: Electrochemistry | |
| 4.1 Philosophy | 48 |
| 4.2 Literature Review | |
| 4.2.1 Linear potential sweep voltammetry | 50 |
| 4.2.2 Related general electrochemical observations | 51 |
| 4.2.3 Elemental sulfur to sulfate ratio | 53 |
| 4.2.4 Nature of the oxidising pyrite surface | 56 |
| 4.3 Experimental Method (General) | |
| 4.3.1 Equipment | 57 |
| 4.3.2 Electrode fabrication | 58 |
| 4.3.3 Electrode polishing | 59 |
| 4.4 Duplication Experiments | |
| 4.4.1 Equipment calibration | 60 |
| 4.4.2 Hamilton and Woods Experiments | 62 |
| 4.5 Ranging Experiments - HNO₃ - H₂SO₄ | |
| 4.5.1 Purpose | 65 |
| 4.5.2 Wide potential-limit experiments | 65 |
| 4.5.3 Higher sensitivity tests | 67 |
| 4.6 Main Test Series | |
| 4.6.1 Experimental Method | 69 |
| 4.6.2 Typical Voltammetric Scan | 70 |
| 4.6.3 Typical Calculations | 71 |
| 4.6.4 Main Test series - Results and Discussion | 74 |
| 4.6.5 Relation to pre-oxidation | 80 |
| 4.7 Summary of Electrochemical Findings | 81 |
| 4.8 References | 83 |

Chapter 5: Pyrite Leach Tests

| | | |
|------------|--|-----------|
| 5.1 | Philosophy | 85 |
| 5.2 | Literature Review | |
| 5.2.1 | Introduction | 88 |
| 5.2.2 | Thermodynamics and metastable sulfur | 88 |
| 5.2.3 | Kinetics of pyrite oxidation | 92 |
| 5.2.4 | Experimental conditions suggested by the literature | 96 |
| 5.2.5 | Section summary | 101 |
| 5.3 | Experimental Method | |
| 5.3.1 | Preparation and analysis of solids | 102 |
| 5.3.2 | Test apparatus and method for main test series | 104 |
| 5.3.3 | Test apparatus and method for attritioning series | 107 |
| 5.3.4 | Liquid assays | 108 |
| 5.3.5 | Sample calculations | 108 |
| 5.4 | Typical Leach Test Results and Discussion | |
| 5.4.1 | Note on grouping of tests | 112 |
| 5.4.2 | Elemental Sulfur formation from pyrite | |
| 5.4.3 | Typical leach test - results | 113 |
| 5.4.4 | Typical leach test - discussion | 114 |
| 5.4.5 | Section summary | 116 |
| 5.5 | Classical Variables - Results and Discussion | |
| 5.5.1 | Stirring rate | 116 |
| 5.5.2 | Temperature | 118 |
| 5.5.3 | Particle size | 120 |
| 5.5.4 | Nitric Acid Concentration | 121 |
| 5.5.5 | Section Summary | 122 |
| 5.6 | Experimental Consistency - Results and Discussion | |
| 5.6.1 | Leach Test method | 123 |
| 5.6.2 | Aging of pyrite samples | 124 |
| 5.6.3 | Sulfur gap | 127 |
| 5.6.4 | Section summary | 128 |
| 5.7 | Industrial Variables - Results and Discussion | |
| 5.7.1 | Sulfuric Acid concentration | 129 |
| 5.7.2 | Ferric Ion concentration | 130 |
| 5.7.3 | Chloride Ion concentration | 132 |
| 5.7.4 | Pulp density | 134 |
| 5.7.5 | Blend of feed sizes | 136 |
| 5.7.6 | Section Summary | 137 |
| 5.8 | Additional Factors - Results and Discussion | |
| 5.8.1 | Attritioning | 138 |
| 5.8.2 | The effect of Eh | 141 |
| 5.8.3 | Addition of Silver ion | 144 |
| 5.8.4 | Additive effect of variables | 146 |
| 5.8.5 | Lag time in pyrite dissolution | 147 |
| 5.8.6 | Pyrite source effects | 149 |
| 5.8.7 | Section summary | 149 |

| | | |
|---|---|------------|
| 5.9 | Mathematical Analysis of Leach Tests | |
| 5.9.1 | Preamble | 150 |
| 5.9.2 | Summary of kinetic data | 151 |
| 5.9.3 | First-order kinetics versus shrinking core model | 159 |
| 5.9.4 | Lag period consideration | 162 |
| 5.9.5 | Variation of pyrite with source | 164 |
| 5.9.6 | Calculation of activation energies | 165 |
| 5.9.7 | Oxidation rate of elemental sulfur | 166 |
| 5.9.8 | Section Summary (Mathematical Analysis) | 177 |
| 5.10 | Relation of Leach Test Findings to the Literature, Electrochemical Results and Refractory Gold Ore Treatment | |
| 5.10.1 | Relation to the literature | 180 |
| 5.10.2 | Relation to the electrochemical findings | 182 |
| 5.10.3 | Relation to refractory gold ore treatment | 185 |
| 5.11 | Chapter Summary | 189 |
| 5.12 | References | 192 |
| Chapter 6: Conclusions and Recommendations | | |
| 6.1 | Preamble - Review of Chapters, Main Findings | 194 |
| 6.2 | Specific Findings New to this Study | 199 |
| 6.3 | General Patterns Found | 201 |
| 6.4 | Recommendations | 202 |
| 6.5 | Summary | 205 |
| | Nomenclature | 206 |
| | Figures | 208 |
| | Tables | 212 |
| Appendix: | Supporting Information | |
| | SEM and XRay Testwork | |

Detailed raw data for Chapters 3, 4 and 5 may be found in the "Supplementary Volume – Raw Experimental Data" (141 pages). Copies of this volume are kept in the libraries of the University of South Australia and the University of Adelaide



1 INTRODUCTION

1.1 REASON FOR THE STUDY

The field of this study is the hydrometallurgical processing of refractory gold ores. The major reason ores are refractory (difficult to treat) is the presence of sulfides. There is a number of technologies for oxidising these sulfides. One developing technology employs nitric acid. When sulfides are reacted with nitric acid, the sulfur content may not oxidise completely to sulfate. Some of the sulfide sulfur may form metastable elemental sulfur. The broad aim of this thesis is to elucidate the chemistry of this sulfide oxidation and of elemental sulfur formation and oxidation.

Development of nitric acid processes has been active for ten years. However, only one, limited, fundamental study of sulfide oxidation by nitric acid has been performed. In particular, little is known about the formation of elemental sulfur other than it is a process nuisance. The present study should be useful to the developer of nitric acid pre-oxidation for refractory gold ores.

1.2 REFRACTORY GOLD ORES

The normal process route for gold ores is crushing and grinding, followed by hydrometallurgical extraction of the gold using alkaline cyanide. Refractory (difficult) deposits respond poorly to this route. Either they exhibit poor gold recoveries or poor economics due to excessive reagent consumption, or both. Such refractory deposits are becoming increasingly important in the world as the easily treatable deposits become exhausted. This is particularly true in Australia, where roughly half the deposits being considered by the mining companies are at least potentially refractory (Canterford (1988)).

The most common reason for refractoriness in gold deposits is the presence of sulfides. In the past, these sulfides were usually pre-oxidised (prior to cyanidation) by roasting. This process route has become environmentally unacceptable. A number of pre-oxidation routes, at various states of industrial use and development, have been proposed to supplant roasting. Of these, nitric acid routes show particularly attractive kinetics (von Michaelis (1992)). Nitric acid

kinetics are not limited by oxygen transfer and solubility restrictions which limit the speed of other hydrometallurgical processes for sulfide oxidation.

Researchers into hydrometallurgical sulfide oxidation have been aware that the sulfides often oxidise incompletely. Elemental sulfur is an intermediate oxidation product which is thermodynamically metastable. Sometimes it is a desired product, as in the treatment of base metal concentrates; more often, however, sulfur is a nuisance about which not much has been studied. For refractory gold ore pre-oxidation, elemental sulfur can have a number of deleterious effects. The degree to which elemental sulfur is a problem varies with combinations of ore and pre-oxidation route. Developers have responded by using harsher oxidation conditions or longer residence times, or both. It is reasonable to expect that a better understanding of the chemistry of elemental sulfur formation and oxidation might lead to less harsh conditions, or else lead to better kinetics and hence to process economies.

Process economies are seldom far from the author's level of conscienceness, owing to his background in industrial ore treatment. He has kept process economics in mind when deciding experimental conditions. It is not much use perfecting a theoretical understanding if that understanding applies only for conditions which are impractical.

1.3 SPECIFIC AIMS OF THIS STUDY

The pyrite-nitric acid system is studied because pyrite is the most common of all minerals associated with refractory gold ores. The applicability of known thermodynamics is examined. The focus of the study is the elucidation of the kinetics of the system.

In particular, the relative rates of formation and oxidation of elemental sulfur are studied. Again, the purpose is to elucidate the fundamentals, with a view to reducing the amount of elemental sulfur formed and to improving its oxidation rate.

1.4 SCOPE OF THIS STUDY

This study begins by providing background on the relevant areas, namely refractory gold, nitric acid processes and the problems and characteristics of elemental sulfur.

The first set of experiments provides background as well. Four gold-bearing materials from known refractory deposits have been tested. Techniques employed

This study begins by providing background on the relevant areas, namely refractory gold, nitric acid processes and the problems and characteristics of elemental sulfur.

The first set of experiments provides background as well. Four gold-bearing materials from known refractory deposits have been tested. Techniques employed were autoclave nitric acid pre-oxidation and rolling bottle cyanide tests. Gold recoveries and reagent consumptions are compared with and without nitric acid pre-oxidation. Included in test results is data on nitric acid oxidation of sulfur in the autoclave.

The next set of experiments investigated fundamentals of pyrite-nitric acid oxidation using cyclic voltammetry techniques. Relative rates of formation of sulfate and sulfur have been calculated at different temperatures.

The largest proportion of experimental work is batch leach tests on pyrite in nitric acid at atmospheric conditions. Variables tested include those that would normally be expected in kinetic studies; included are stirring rate, particle size, temperature and acid concentration. Attempts are made to assess features of likely importance to industrial applications; these include sulfuric acid concentrations, ferric ion concentrations, pulp density, chloride ion concentration (from saline process water) and mixed particle sizes. The reproducibility of tests is evaluated briefly. Attempts to increase solution Eh, consistent with electrochemical findings are outlined. The effects of silver ion addition, and attritioning are evaluated. Reading has pointed to these factors as possibly decreasing the "sulfur gap" between pyrite oxidation and sulfate formation.

Finally, the kinetics of pyrites from different sources, leaching lag periods, and the additive effect of test variables are discussed.

Throughout the study, continued contact has been maintained with the developers of nitric acid pre-oxidation processes. The developers have provided direction, funds and process conditions, at least to the extent compatible with commercial sensitivity. Contact with colleagues working in hydrometallurgical research has also been established. These colleagues have been invaluable, providing advice, equipment and facilities and moral support.

1.5 LIMITATIONS OF THIS STUDY

The four refractory materials of Chapter Three were simply pre-oxidised in the autoclave, to assumed completion. No attempt was made to detail the kinetics of

these four materials. They contained a range of minerals, for which the kinetics differ markedly; it was considered more worthwhile to study pyrite in isolation.

Electrochemical work was limited to cyclic voltammetry. Only one nitric acid concentration was tested. The electrochemical findings, however, justified the travel to Monash University to use their equipment.

Leach tests could be considered limited, depending on the point of view. Divergence between commercial conditions and experimental conditions which allow isolation of individual factors is always a problem. The experimental apparatus was simple, atmospheric and of batch construction. Commercial conditions are constantly changing, as development proceeds, and commercial sensitivity has sometimes limited access to the latest information. This can also limit the extent to which experimental and commercial conditions coincide. Nevertheless, a genuine effort was made to isolate the important variables, both classical and commercial, of the pre-oxidation step.

1.6 SUMMARY OF INTRODUCTION

The intent of this study is practical. The pyrite-nitric acid system is relevant to developers of nitric acid pre-oxidation routes for refractory gold ores. Better understanding of the system and of sulfur formation and oxidation should be useful to such developers.

Conditions employed in this study were such as to elucidate the kinetic effects of classic individual variables; factors of likely industrial significance were also investigated. The realities of commercial progress and laboratory limitations do not always coincide, despite goodwill on both sides.

Communication and support, from both industrial and research colleagues, have been major strengths throughout the study. The work breaks new ground and is relevant to the mining industry in the treatment of refractory gold ores.

1.7 REFERENCES

Caterford, J.H., 1988, Minproc Technology Pty Ltd., Personal communication.

von Michaelis, H., 1992, *Innovations in gold and silver recovery*, Randol International, Denver, pp 4095-4101.

2 BACKGROUND TO THIS STUDY

2.1 CHAPTER CONTENT

This chapter provides a practical definition of refractory gold ores. Causes for refractoriness and technologies available for counteracting it are listed. The technologies for preoxidation are put in their larger flowsheet context.

The history and findings of nitric acid treatment processes for refractory gold ores are outlined. Experimental conditions which have been tested are summarised. The anticipated usefulness of the present study is described.

Elemental sulfur can cause operating problems with gold ore treatment and these problems are outlined. Findings regarding elemental sulfur during "Redox" process development are highlighted. Relevant sulfur characteristics are listed.

2.2 REFRACTORY GOLD ORES

2.2.1 PRACTICAL DEFINITION

Refractory gold-bearing materials are those which are difficult to treat by conventional cyanidation practice. The difficulty manifests itself in either low gold recoveries, high treatment costs, or both. Many refractory materials are simply not economic (and hence are not technically ores) unless additional treatment is applied. A practical quantification of the difficulties has been proposed as any of the following (Flatt, et al. 1991).

Gold recovery below 80%.

Cyanide consumption greater than 1 kg/tonne of ore.

Lime consumption greater than 2 kg/tonne of ore.

Grind finer than 87% passing 72 μm .

Cyanide retention time longer than 70 hours.

The authors also point out that the concepts of "refractory" and "conventional cyanidation practice" are themselves changing.

2.2.2 IMPORTANCE OF REFRACTORY DEPOSITS

Operators are turning their attention to refractory zones as easy "free-milling" deposits become depleted. In many existing mines, the refractory material has been left untreated until the free-milling portion approaches exhaustion. In Australia, roughly half the deposits presently under consideration by mining companies are at least potentially refractory, in that they contain appreciable sulfides (Canterford, 1988). The proportion is perhaps one-third in the United States and one-fifth in Canada (Wells, 1989).

2.2.3 CAUSES OF REFRACTORY BEHAVIOUR

The reasons for a gold ore needing some additional treatment beyond straightforward grinding and cyanidation, fall into seven categories (Dry and Coetzee, 1986).

- a) The gold is encapsulated in sulfides at normal grind sizes. Individual grains of arsenopyrite have been reported at 4000 ppm Au. Historically, many such cases were reported as having gold in "solid solution".

Whether it is disputed by some (ie Lazer, et al., 1986) on the grounds that the gold may be below the detection limit of the SEM (10 μm) but well above a true solid solution size, is of little consequence to those operators considering finer grinding.

- b) The gold is encapsulated at very fine sizes in gangue.
- c) The gold is present as tellurides or electrum, which are only slowly soluble in cyanide without some form of pre-treatment.
- d) Coatings, which are insoluble in cyanide, passivate the gold. These are usually iron compounds (Feather and Koen, 1973), sulfur or else haematite from processes such as roasting (Nagy et al., 1976).
- e) There is a high proportion of oxygen-consuming minerals present. Oxygen is rate-controlling in leaching and most pulps are limited to about 8 ppm dissolved oxygen (lower with saline waters) (Trofe et al., 1988). Therefore, minerals which compete effectively for dissolved oxygen (pyrrhotite is notorious) may slow down the kinetics of cyanidation.

- f) Many minerals of copper, zinc, lead, arsenic and antimony are known consumers of cyanide (Nagy et al. 1976). Flatt, et al. (1991) reported consumptions of over 100 kg/tonne. Oxidized ores containing these elements are often high consumers of cyanide.

- g) Carbonaceous materials in the ore may remove the gold cyanide complexes from the solution as they are formed. The carbonaceous material can be inherent in the ore or may be introduced, such as old mine timbers which have been charred in an underground fire (Scheiner et al., 1972). The degree of activity of carbonaceous materials varies widely. If the material is fine or friable, it will bypass the plant carbon screens and its adsorbed gold will be lost.

Examples have been reported in all cases listed above. The most frequent causes of refractory behaviour appear to be sulfide locking (case a) and cyanicides (case f). In some cases, the sulfides both encapsulate the gold and also are cyanicides or oxygen-consumers.

2.2.4 TREATMENT ALTERNATIVES

Since the dominant reason for refractory behaviour is the presence of interfering sulfides, the dominant pre-treatment processes aim to destroy the sulfides, by oxidation into soluble forms. Until about 1985, roasting was the usual process applied, with all but the oldest plants using fluid-bed roasters.

Roasting, however, has environmental disadvantages and requires careful roaster control. Sometimes subsequent gold and silver recoveries are lower than competing processes (Nagy et al. 1976, Kontopoulos and Stefanakis 1988).

The emerging proven technology is pressure leaching with oxygen and sulfuric acid (The Sheritt-Gordon process). Research has been ongoing since the 1950s, over 100 ores have been successfully tested. Perhaps a dozen plants are currently operating. Autoclaves are large and must resist severe conditions; an oxygen plant is necessary.

Perhaps the technique which gets the most interest has been bacteriological pre-oxidation, using, in most cases, ferrobacillus ferrooxidans. There are currently two successful commercial plants operating in Australia and a number planned for overseas.

A host of processes are in various stages of development and use a range of oxidants from alkaline pressure oxygen (Wells, 1988) through chlorine (Birak and Deter, 1987), Caro's acid (Lakshmanan and Childs, 1984) to bromine (Sehic, 1988) and nitric acid (Leonard, et al., 1990). The "Redox" nitric acid process has been successful at pilot plant level and has the fastest reported kinetics of any method.

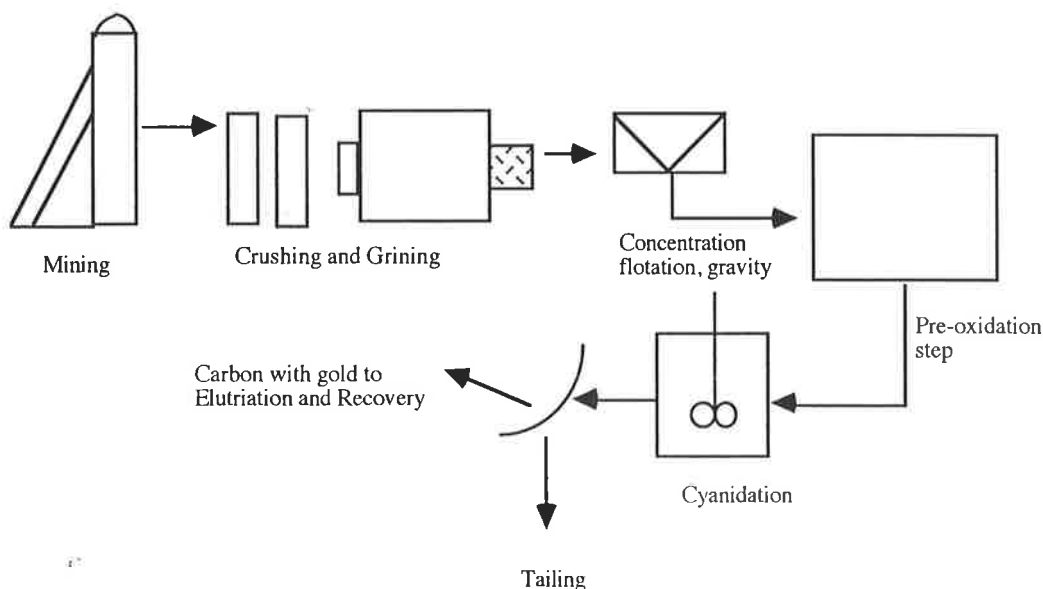
A number of processes have also been suggested with other approaches than pre-oxidation. Ultra-fine grinding (Wells, 1988) will liberate some materials (in Classes a, b, and d of 2.2.3) but its practical limit appears to be about 10 μm . Thiourea has been used successfully at one plant for an ore with high content of cyanicides (Hisshion and Waller, 1980).

Ores with mild "preg-robbing" characteristics often can be treated by carbon-in-leach. Ores with oxygen-consuming minerals are often pre-aerated for from 5 to 12 hours and then cyanided normally. Ores treatable by methods described in this paragraph would usually fall into the category of "pseudo-refractory".

2.2.5 GENERALISED FLOWSHEET FOR PRE-OXIDATION

A generalised flowsheet for treating a material which is refractory due to the presence of sulfides is shown in Figure 2.2.5.1. The pre-oxidation step could be any of the alternatives listed above, including nitric acid. The cyanidation steps are similar to free-milling ores, with carbon-in-leach typical hybrid technology being most often employed in Australian mines.

Figure 2.2.5.1: Generalised Flowsheet for Pre-Oxidation and Cyanidation



2.2.6 BROADER ENGINEERING CONSIDERATIONS

The focus of the present study is on the pre-oxidation step, but this step cannot be considered in isolation. The pre-oxidation step has downstream implications which must be evaluated for any operation to reach industrial viability. The downstream implications can have a dramatic influence on costs, both operating and capital. Costs are generally site-specific (Canterford, 1994a). Metal recovery must be tested for the particular ore and pre-oxidation combinations. Environmental issues must be addressed. Gas-stream emission concerns, especially sulfur dioxide, arsenic and antimony, have militated against conventional roasting in many locations.

A major stumbling-block for would-be developers of many refractory deposit lies in the choice of alternative technologies. Generally, several alternatives will work for a given ore. An ore and treatment alternative must be tested, and the cyanidation results evaluated. The plant must be engineered and subsequent questions (such as residue environmental stability) answered. The plant must be costed and feasibility evaluated. This procedure is expensive, requiring months and hundreds of thousands of dollars. An answer is obtained, but it may not be the most economic answer. Evaluation of another treatment alternative combination with the given ore requires repeating the whole procedure, quite possibly with a different set of subsequent questions.

The engineering considerations which arise for nitric acid pre-oxidation will be discussed under 2.3.5.4.

The focus of the present study is on nitric acid pre-oxidation, with one mineral, pyrite. All the subsequent engineering considerations could not be addressed in the study, but where possible, the implications of testwork findings on subsequent engineering will be discussed.

2.3. NITRIC ACID PROCESSES FOR PRE-OXIDATION

2.3.1 PREAMBLE

Literature on the pre-oxidation treatment of sulfides using nitric acid was sparse prior to 1980. Since then there has been a flurry of development activity. Most of the published papers have concerned two processes which were being developed competitively in the 1980s; these were the "Nitrox" and the "Redox" processes. Elemental sulfur formation has been a problem to both processes, but little study

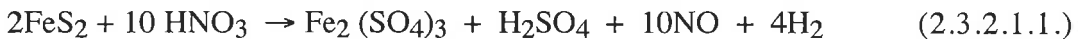
has been done on it. The nature of the literature available on the nitric acid processes and on their problems with elemental sulfur has governed this author's approach to the current section. This section has been organised under the following topics: overall process chemistry, work prior to 1980, the "Nitrox" process, the "Redox" process, elemental sulfur, conditions tested, and a summary.

2.3.2 BRIEF OVERVIEW OF PROCESS CHEMISTRY

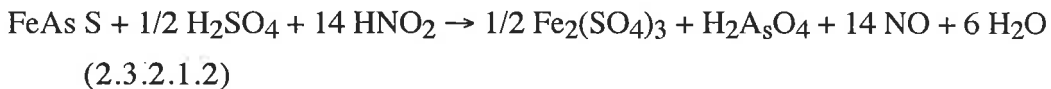
As discussed in subsection 2.2.6, the objective of the nitric acid processes for refractory gold treatment is to pre-oxidize sulfides which would otherwise interfere with gold cyanidation. By far the most common sulfides associated with gold are pyrite and arsenopyrite. Pyrrhotite and marcasite have also been tested at pilot plant level and a host of other sulphides have been found to occur with gold, but pyrite and arsenopyrite are usually the most common sulfides present.

The decision was taken to study pyrite in detail, for a number of reasons. Its common association with refractory gold was foremost, but it also shows reasonable kinetics for a study. There were some arguments against other minerals. For example, galena was ruled out because of tricky photo-chemical side effects. It was thought that high-purity artificial minerals might be required and no-one at Monash (who have experience of the technique) could see a way to make artificial FeAsS. Finally, arsenopyrite poses a danger of producing arsine gas, with its attendant safety risks.

The oxidation of pyrite by nitric acid is complex but can be represented by the overall reaction (Beattie et al., 1989):

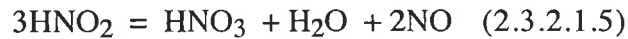
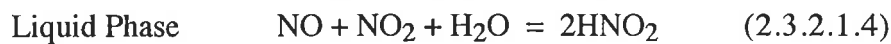
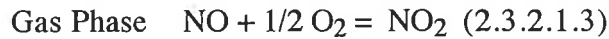


The reactions for arsenopyrite may be summarised as:



Nitrous acid, HNO₂, is thought to be the active species for both sulfides. This is generated through the dissolution of NO which has been oxidised to NO₂. The sulfuric acid required for arsenopyrite may be added but it more commonly generated *in situ* from pyrite normally present in the ore with arsenopyrite.

The loss of nitric acid into the gas phase would be intolerable on both commercial and environmental grounds. The "Redox" process generates and recirculates the nitric acid. Nitrogen oxides reactions are also complex, involving at least five gas phase reactions and three gas-liquid reactions (Newmann and Carta, 1988). The dominant overall reactions are summarised below. These were described in the patent for the "Redox" process (Raudsepp, et al., 1987).



Reaction (2.3.2.1.5) is slow compared to reactions (2.3.2.1.1 through 4). This implies that HNO_2 is probably the active species in sulfides oxidation.

2.3.3 EARLY RESEARCH USING NITRIC ACID

The only researchers who published sulfides leaching studies using nitric acid prior to the 1980s were Bjorling and Kolta (1965) and Prater, Queneau and Hudson (1973). The former researchers treated a range of sulfides and found that nitric acid was an effective "promoter". Lower sulfides (ie pyrrhotite FeS) possessed superior kinetics and hence pyrite was reduced to an artificial pyrrhotite before leaching. Prater et al. tested a range of conditions for nitric acid leaching of copper concentrates. Whilst of considerable scientific interest, the work of both sets of researchers is of limited applicability to the present work. Their focus was on maximising the yield of elemental sulfur. This approach is diametrically opposed to that required for refractory gold ore preoxidation, where elemental sulfur must be avoided.

Prater et al.'s results on reactivity and yield of elemental sulfur for various minerals (Table 2.3.3.1) their limited investigations on the effects of temperature and acids concentration (Table 2.3.3.2) and their relationship between nitric acid strength and sulfur oxidation (Table 2.3.3.3) are of interest.

Table 2.3.3.1: Relative Reactivity and Elemental Sulfur Yield of Pure Minerals Leached with Nitric Acid

| Mineral | Relative Reactivity | Elemental Sulfur Yield, % of Reacted Sulfur |
|----------------------------------|---------------------|---|
| Cu ₃ SbS ₃ | 10 | 40 |
| Cu ₂ S | 8 | 75 |
| FeS (pyrrhotite) | 7 | 60 |
| FeS ₂ (pyrite) | 7 | 3 |
| Cu ₉ S ₅ | 6 | 55 |
| CuS | 6 | 50 |
| Cu ₃ FeS ₄ | 5 | 60 |
| CuFeS ₂ | 2 | 45 |

From Prater et al. (1973)

The low yield of sulfur from pyrite and the low reactivity of chalcopyrite are interesting and have implications for the present work as will be shown in later chapters.

Table 2.3.3.2: Effect of Temperature and Concentration on Elemental Sulfur Formation

| Initial HNO ₃ Concentration % | Temperature °C | Initial H ₂ SO ₄ , Concentration Molarity | Yield of S ⁰ g per g copper extracted |
|--|----------------|---|--|
| 20 | 75 | 0.25 | 0.33 |
| 20 | 95 | 0.25 | 0.44 |
| 20 | 75 | 1.0 | 0.26 |
| 20 | 95 | 1.0 | 0.41 |
| 60 | 75 | 0.25 | 0.40 |
| 60 | 75 | 1.0 | 0.38 |

Leach time, 2 hours, initial HNO₃/Cu. 4:1

From: Prater et al. (1973).

Table 2.3.3.3: Results of HNO₃-H₂SO₄-H₂O Interaction with Elemental Sulfur

| Nitric Acid, % | Temperature, °C | Elemental Sulfur Oxidation, % |
|----------------|-----------------|-------------------------------|
| 60 | 95 | 16.4 |
| 60 | 75 | 8.7 |
| 20 | 95 | 2.5 |
| 20 | 75 | 2.4 |

H₂SO₄ molarity, 1.0 M; leach time, 2 hr; HNO₃/S⁰ = 6

From Prater et al (1973)

Note that only two levels of each variable were tested and that elemental sulfur was oxidized only to a limited extent.

Miller (1980) suggests that kinetic factors dominate over thermodynamic considerations when dealing with sulfide leaching and that concepts developed from corrosion studies are directly applicable. The recent study of Kadioglu et al (1995) is the closest to the present work. It employed conditions which covered a wide range; most tests were less aggressive than those of the present study or those used in industry.

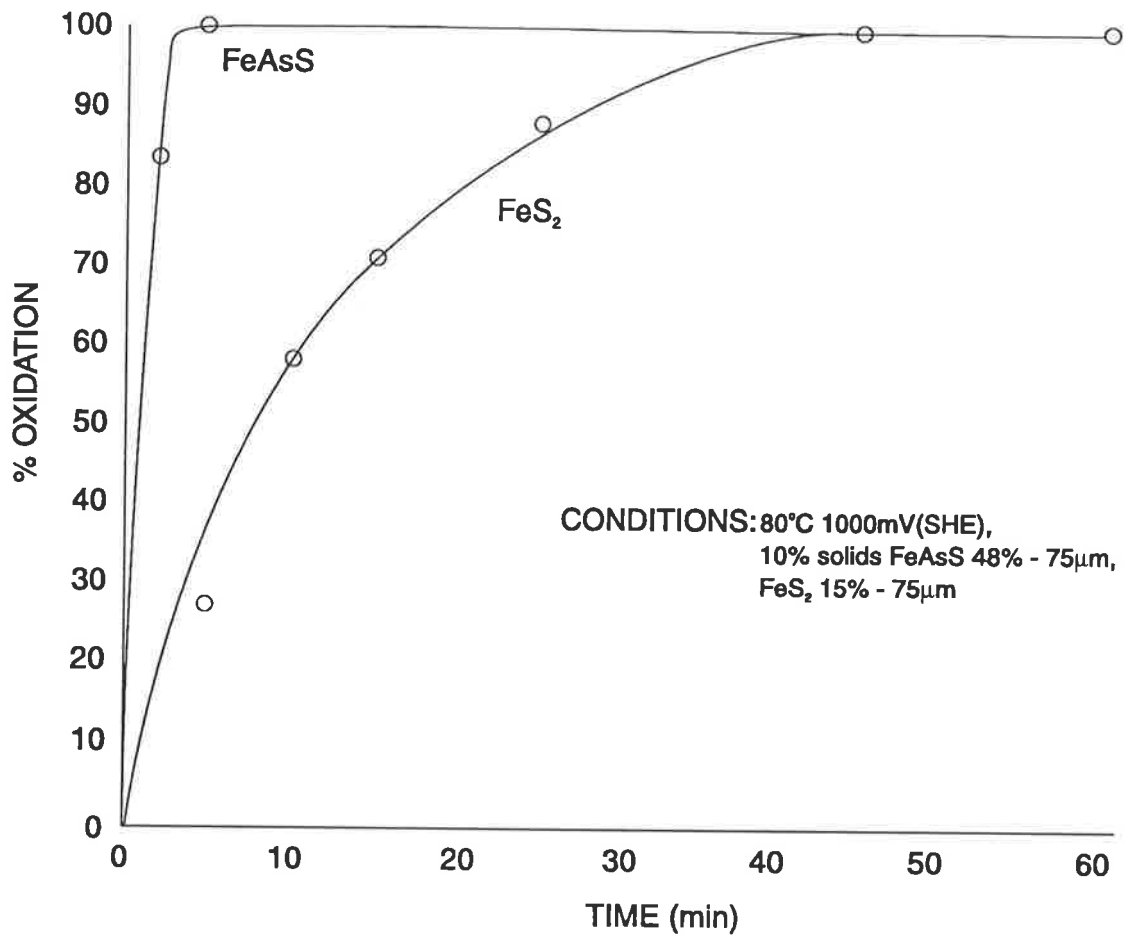


FIGURE 2.3.4.1 Rates of Pyrite and Arsenopyrite Oxidation in Nitric Acid (from Fair et al. 1987)

2.3.4 THE NITROX PROCESS

2.3.4.1 History linked to elemental sulfur

This process is conducted under atmospheric pressure and at temperatures below 100°C. The oxides of nitrogen were reacted to nitric acid in a separate step for recycle. Hydrochem Developments of Toronto published a number of papers between 1986 and 1989. The authors, Fair, et al., (1987), confirmed high elemental sulfur yields (ie 70%) and fast kinetics for arsenopyrite and showed lower yields and slower kinetics for pyrite. Typically arsenopyrite oxidation was complete (but sulfur's was not) after 5 minutes. Pyrite was oxidized after 50 minutes. See Figure 2.3.4.1 opposite.

In van Weert, et al., (1988) and van Weert and Fair (1989) testwork and pilot plant design for testing Dickenson arsenopyrite concentrate is described. The authors stated that the formation of elemental sulfur extended the test programme by at least a year. The developers opted to accept the formation of elemental sulfur on the basis that a "narrowly defined nitric acid oxidation regime" might not be compatible with a wide range of feedstocks. This decision complicated the flowsheet, indicating the inclusion of sulfur separation and oxidation steps (flotation and hot lime treatment). This complication had a great deal to do with the cessation of development work on the Nitrox process (Anonymous (1991)).

It is noteworthy that the authors never confirmed the existence of such a "narrowly defined nitric acid oxidation regime" which will oxidise all sulfur to sulphate in commercially-acceptable times.

2.3.4.2 Other findings

It was stated that trace elements effect the rate of pyrite oxidation (silver was singled out) and perhaps the yield of elemental sulfur. Van Weert et al. (1988) includes Ernie Peter's interesting suggestion that S₈ rings (the most stable form) are not formed during oxidation but rather subsequently at slower rate in the oxidation residue.

During an interview (van Weert, 1989) Gus van Weert stated that the sole work on kinetics (to his knowledge) was by Russian authors, was not available in translation, on arsenopyrite. He also claimed that no rational explanation for the formation of elemental sulfur on which to postulate a mechanism.

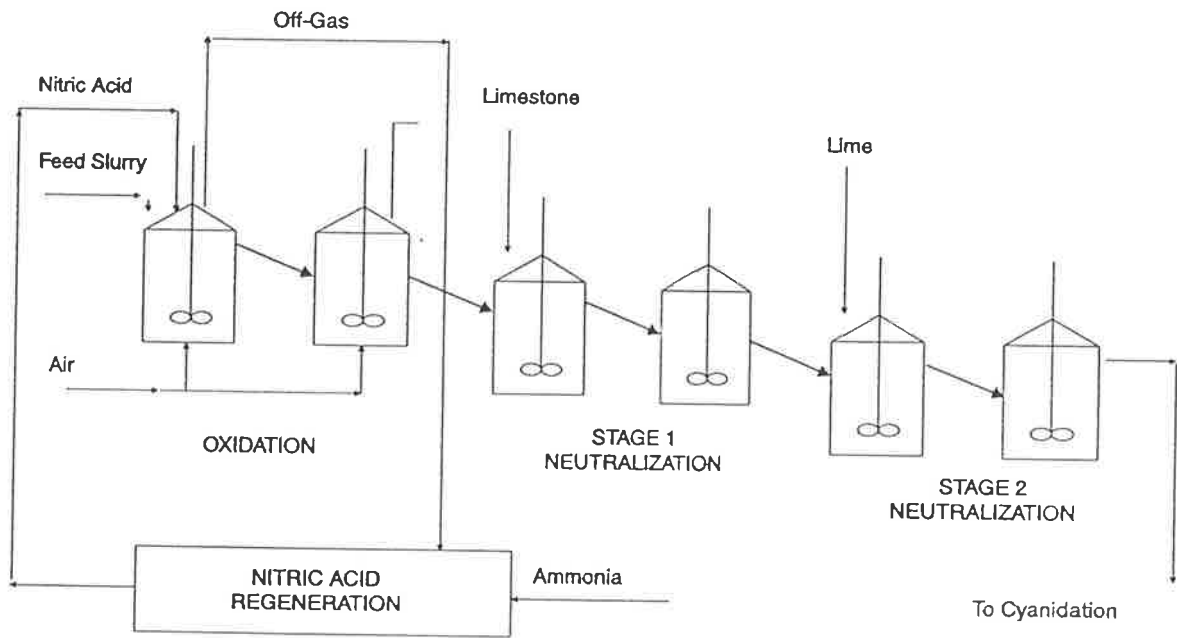


FIGURE 2.3.5.1 Low Temperature Redox Process Flow Sheet (from Canterford 1994b)

2.3.5 THE "REDOX" PROCESS

2.3.5.1 History

This process was proposed in 1981 and has been under development since then. Formerly called the "Arseno" process, it was re-named the "Redox" process in 1988. In 1991, the Australian firm Minproc bought the process from its Canadian Developers (Bacon, Donaldson and Associates). The process underwent several changes during this period.

The process has proven very successful at improving gold recoveries in the subsequent cyanidation step (Beattie, et al., 1985). Recoveries from gold-bearing materials have shown improvements of from 74% (to 94% from 20% with conventional cyanidation only) to 15% (to 96% from 81%). "Preg-robbing" carbonaceous ores have been successfully treated as well as ores which were refractory due to sulfides. Materials of construction requirements are reasonable. 310 or 304 L stainless steel suffices as opposed to lead-lined brick for pressure leaching with sulfuric acid (Berezowsky and Weir, 1984). Finally, reaction times are generally shorter than with sulfuric acid, which is usually 120 minutes and pressures are lower than the 1500 - 3000 kPa required for sulphuric acid leaching. In addition continuous pilot plant runs have been successful on Snow Lake and Bakyrchik concentrates, the latter at 15 kg/hr. A 500 kg/hour small scale commercial plant was commissioned at Bakyrchik in 1994 (Whellock, 1994).

2.3.5.2 Alternative Flowsheets

The "Redox" process evolved into two variants, based mainly on heat balance considerations (Leonard, 1990). The low-temperature variant is used for whole ores, with sulfur contents below 7%. Typical conditions are 85°C, atmospheric pressure, with nitric acid concentration in the 2.2-2.5 M (140-155 g L⁻¹) range (Sobel et al. 1994). The nitric acid is regenerated in a separate step developed by Minproc. Figure 2.3.5.1 gives a typical flowsheet.

Elemental sulfur was not found to be a problem with the low-temperature variant, although reasons were not given. Reaction times varied from 90 to 120 minutes for Cinola ore in pilot tests (Beattie, et al., 1989).

The high-temperature option is typically performed in autoclaves at 195°C, 700 kPa of oxygen overpressure and Eh's 900 millivolts relative to the Standard Hydrogen Electrodes (Leonard, et al., 1990). The oxygen over-pressure is dictated by the

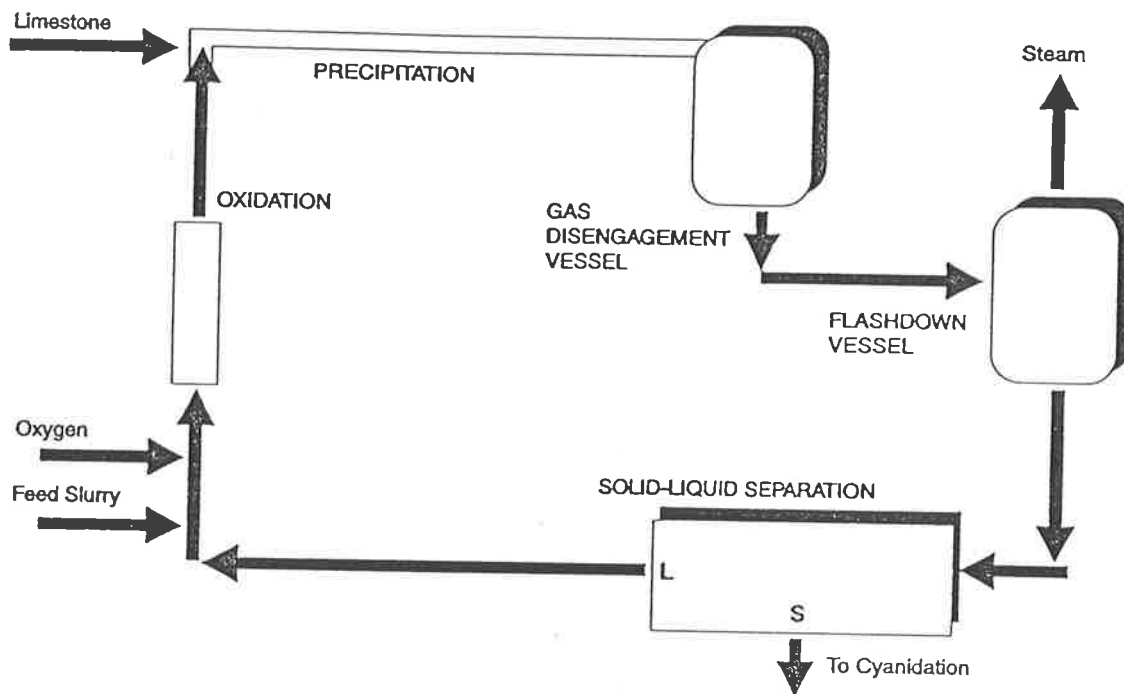


FIGURE 2.3.5.2 High Temperature Redox Typical Process Flow Sheet (from Canterford 1994b)

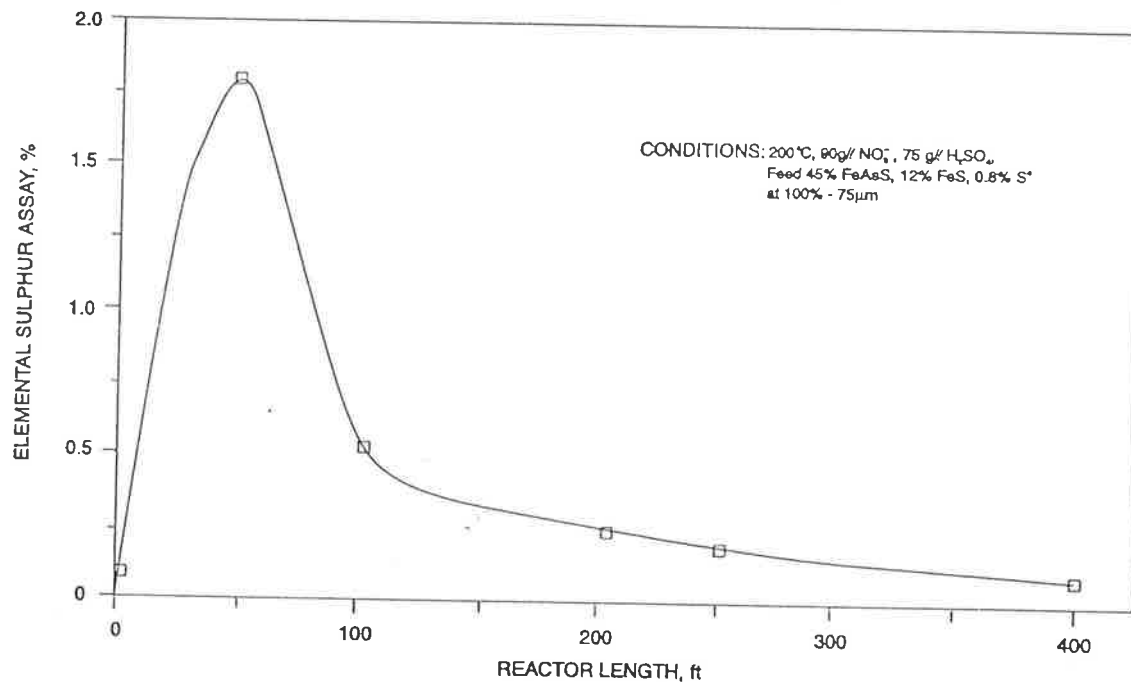


FIGURE 2.3.5.3 Elemental Sulphur Formation and Oxidation in Pipe Reactor (from Leonard, 1990)

need to convert NO_x to HNO₃. The reaction time was only eight minutes for Snow Lake arsenopyrite concentrates. A typical flow sheet is shown in Figure 2.3.5.2.

2.3.5.3 Findings of Development Testwork

Development testwork on the "Redox" process has focussed on economic factors rather than fundamental research. However, some very relevant findings concern elemental sulfur.

Apparently the oxidation of sulfide to sulfate dictates residence time, rather than the oxidation of metal sulfide to metal ions. For the Snow Lake pipe reactor, the metal was liberated and elemental sulfur produced within 2 minutes; oxidation of all the S⁰ required an additional 6 mins (see Figure 2.3.5.3 opposite).

During one pilot run on Bakyrchik concentrate, the temperature was allowed to fall to 125°C from its normal (180-210°C) range. Subsequent gold recovery fell to 50% from its normal (85-95%) range. This fall was attributed to elemental sulfur although the cause was not proven.

The "Redox" process also appeared to passivate the carbon content of the Bakyrchik material (Sobel et al. 1994). The Shungite carbonaceous material had a history of being preg-robbing. Bakyrchik recovery was normally about 60%.

2.3.5.4 Flowsheet Engineering Considerations

Canterford (1994b) listed flowsheet considerations, beyond the pre-oxidation leaching stage, which are important in nitric acid processes for refractory gold. They include nitric acid regeneration, which must be external to the leaching vessel for the low-temperature "Redox" variant. Any NO_x in off-gases must be catalytically oxidised. Effluents must be treated to meet environmental nitrate levels. (1.5 g l⁻¹ NO₃⁻ in Canada, for instance).

There are implications here for nitric acid makeup as well; pilot runs show 1-2% nitrate loss. Finally, materials of construction (stainless steel will suffice for most parts) and mass and energy balance implications must be reviewed. As intimated earlier, these considerations are beyond the range of the present study.

2.3.5.5 Economics of the "Redox" Process

Minproc, the developer of the "Redox" process, claim favourable economics for the nitric-acid based pre-oxidation alternative. Minproc have the engineering know-how to cost such facilities, but they warn that costs are project-specific. Table 2.3.5.1 gives comparative data for nitric acid, pressure oxidation ($\text{H}_2\text{SO}_4 + \text{O}_2$) and biological oxidation (Canterford, 1994b).

Table 2.3.5.1: Relative Costs for Pre-Oxidation Processes (Canterford, 1994b)

a) Low Temperature Redox cost comparison (normalised)

| Process | Capital Cost | Operating Cost |
|----------------------|--------------|----------------|
| Redox | 1.00 | 1.00 |
| Whole ore roasting | 1.11 | 1.01 |
| Pressure oxidation | 3.64 | 0.64 |
| Biological oxidation | 1.62 | 0.69 |

b) High Temperature Redox cost comparison (normalised)

| Process | Capital Cost | Operating Cost |
|----------------------|--------------|----------------|
| Redox | 1.00 | 1.00 |
| Concentrate roasting | 1.82 | 1.51 |
| Pressure oxidation | 2.24 | 1.29 |
| Biological oxidation | 0.62 | 3.23 |

c) Basis for cost comparison

| | Low temperature | High temperature |
|------------------|-----------------|------------------|
| Throughput (t/h) | 161.0 | 8.0 |
| Au (g/t) | 6.0 | 64.5 |
| S (%) | 1.5 | 21.0 |

Battery limits: Slurry feed to oxidation
 Oxidation discharge to cyanidation
 All ancillaries required for oxidation are included

Generally, the low-temperature process is likely to require about 60% of the capital of the high-temperature process, due to the need for autoclaves when operating at 190°C.

Table 2.3.6.1: Previous Experimental Conditions Tested.

| Workers | Minerals | HNO ₃ Conc | Other Reagents | Eh | Ph | Temperature | Atmosphere | Other | Comments |
|--|--|--|---|-------------------|-----------------------------|--|---|---|--|
| Bjorling and Kolta (1964) | 5 pyrrhotites both natural and reduced from pyrite Sphalerite, Galeua, Molybdenite concentrates 7 copper slags and scrap | Stoichiometric 1:10 1:14 | | | 20% HNO ₃ to 3.8 | 50-90°C 120°C 150°C 90° and 120°C 120°C | | Pulp density 1.5-20% 10 atm 5% pulp density | 1. Limited testing of any given combination of parameters; typically only two tests. 2. Leaching times 120- 180 minutes |
| Prater, Quenacu and Hudson, 1973 | Copper concentrates (Chalco pyrite and Bornite) | 13-60% | H ₂ SO ₄ 0.25-2.0 M | | | 75°C and 95°C | Atmospheric pressure oxygen absent | 14 and 33% solids | 3 Limited qualitative tests on other copper minerals, pyrite and pyrrhotite 4. As per comment 1 conditions optimised by factorial design 5. Times 30-240 mins |
| Van Weert, Fair, Schneider, and Aprahamian 1983-90 | Ores and concentrates arsenopyrite and pyrite pyrite | 100 g l ⁻¹ | 77 g l ⁻¹ SO ₄ ²⁻ 39 g l ⁻¹ Fe ³⁺ | +75 mV (SCE) | 0 | 85°C 88° | | 40-50% solids in pilot 10% 75% - 75µm | 6. pilot plant development work; few details given 7. laboratory - used pilot liquid |
| Beattie, Peters, Randsepp Sarkar, and Childs, Foo, Balderson, Ismay, Bath, Canterford, Leonard, Christensen, and Dawson, 1983-90 | Ores and concentrate containing pyrite and pyrite pyrite arsenopyrite whole ore pyrite and arsenopyrite Arsenopyrite concentrate 47% aspy 12% pyrrhotite | 0.25 M 3.0 M (16 - 190 g l ⁻¹) 0, 23 g l ⁻¹ HNO ₃ 23 & 140 g l ⁻¹ 6, 11, 23 140 g l ⁻¹ 63g 126 g l ⁻¹ | 0 - 3.0 M H ₂ SO ₄ 60-90 g l ⁻¹ acidity as H ₂ SO ₄ | 0.75 - 1.20 volts | | 80-195°C Mostly at either 85-95°C or 185-195°C 100, 125, 160°C 100°C 80°C 85°C 190-210°C | 50-200 psig O ₂ air ambient 1600-2275 kPa O ₂ 125% of stoichiometric | 85-200 g/l pulp density 50%-60µm 77% - 37 µm 10-20% solids | 8. development work; more conditions reported than 6. but still not exhaustive. Reported conditions tended to be limits (Patent) or else specific tests on a specific ore. 9. Low temperature. Time requirements to 120 minutes. High temperatures low as 8 minutes 10. pilot plant 11. 85-110°C gave elemental sulfur problems |
| Kadioglu et al. (1995) | Pyrite | 50-300 g/l | none | not stated | | 13-80°C | air | sizes 75-850 µm Speed 800 rpm | |

Any pressure oxidation step in a flowsheet is expensive, particularly because of the oxygen plant required. Capital cost for one high temperature plant treating 250 tpd of sulfide concentrates (20%S) was estimated at \$25 Million (Canadian) in 1988; operating costs were estimated at \$42/tonne (Canadian). In 1995 Australian dollars, these figures translate to roughly \$35 million for capital and \$60 per tonne.

Finally the cost of the process will include waste disposal. Neutralisation costs of the resulting sulfuric acid can dwarf all others.

2.3.6 EXPERIMENTAL CONDITIONS INVESTIGATED

Table 2.3.6.1 gives the conditions tested (at least those which have been published) by workers with nitric acid.

2.3.7 VALUE OF PRESENT TESTWORK

2.3.7.1 Relation to Previous Work

The conditions tested by Bjorling et al. and Prater et al. were clearly laid out. They tested wide ranges of industrial materials with limited variation of parameters. The development work of van Weert et al. ("Nitrox" process) and Beattie et al. ("Redox" process) has been less clearly reported. This is understandable for development work in a commercially-sensitive environment. These latter authors have tended to report proposed ranges of parameters (ie, from 0.75 to 1.20 volts Eh) with fewer specific tests conditions. In all cases, the materials tested were natural ores or concentrates.

The writer thought that more specific test conditions and results might be obtained by visiting some of the workers quoted. While other authors were helpful and encouraging, they were unable to release further specifics due to commercial sensitivity. This writer is, therefore, confident that any such specifics, if they exist, are unlikely to be published in the near future.

The work of Kadioglu et al. covered the classical kinetic variables, but the majority of their experiments were under conditions too slow to be of industrial interest for refractory gold ore processing. The Turkish workers were mainly interested in leaching pyrite from coal deposits.

Details of the experimental leach conditions for the present work are found in Chapter 5. Conditions were selected as much as possible to be within the range of

industrial interest - that is to give complete pyrite oxidation within two hours. No fundamental study of the nitric-acid pyrite system exists which is predominantly within this range of conditions. In addition to the classical kinetic variables, the present study incorporates five industrial variables such as ferric ion concentration and pulp density. A number of tests are used to check experimental consistency. Finally, six other factors suggested by the literature or by the testwork itself, are investigated. This is probably the largest fundamental study reported. Hopefully, its focus on near-industrial conditions will also keep it relevant to process developers, not merely of academic interest.

2.3.7.2 Low Temperature Variant of "Redox" Process

As stated earlier, the low temperature variant of the "Redox" process is seen by Minproc to have cost advantages over other pre-oxidation processes and capital cost advantages over the high-temperature "Redox" variant. The good kinetics and efficient oxygen mass-transfer of nitric acid allow a process to work at 80-90°C, but at fairly long residence times 90-120 minutes for pyrite. Any fundamental work which significantly speeds this up could be a real benefit to the developers. They have not quantified all the variables to date. Also, there is indication that elemental sulfur and its effect on subsequent gold cyanidation may be the limiting consideration. The formation of elemental sulfur is known to occur, but its formation and oxidation have been noted, rather than studied. Accordingly, the present work is both original and prospectively of economic benefit to the oxidation of refractory gold deposits.

2.4 ELEMENTAL SULFUR

2.4.1 PROBLEMS CAUSED DURING REFRACTORY GOLD PROCESSING

For refractory gold pre-oxidation, the production of elemental sulfur can be a major problem. Hiskey and Schlilt (1982), in their review of aqueous oxidation of pyrite, cite the following problems which may arise when treating gold ores:

- a) oxidation of sulfides may be inhibited by the formation of surface layers of sulfur.
- b) the sulfur can act as a "glue", forming large pellets of unreacted sulfides.
- c) elemental sulfur can occlude gold, rendering it unavailable for cyanide complexation.

- d) the sulfur may itself be a cyanicide, consuming expensive reagent by reaction to thiocyanate. In addition, the workers (already cited) with the "Redox" process have suggested the potential problem of the formation of soluble polysulfides during lime neutralisation. Sulfur may also dictate other process steps, such as when lime is injected to precipitate arsenic. Of the potential problems, occlusion of gold by the elemental sulfur appears to be the most serious. "Nitrox" tests on Dickenson concentrates (van Weert et al. 1988) showed that 90% of the gold in the "Nitrox" residue reported to the sulfur fraction, which was 36% of the residue weight. Beattie and Ismay (1990) reported that 50% of the gold reported to the elemental sulfur, which was 10% of the process feed weight. The sulfur was fairly coarse, being 6% + 150 μm . For the Snow Lake pilot test program, elemental sulfur occlusion of the gold caused rejection of the low-temperature option (Foo et al. 1989).

2.4.2 OBSERVATIONS DURING DEVELOPMENT WORK

Developers of nitric acid routes have not systematically studied sulfur formation, but have recorded a number of observations as follows:

- a) It is often the deviations from process stability that seem to increase sulfur yield (Leonard et al. 1990).
- b) Pyrite begins to react with nitric acid at 60°C and gives minor sulfur yield (Beattie et al. 1989).
- c) Arsenopyrite begins to react with nitric acid at ambient temperatures and yields about 20% sulfur.
- d) Despite melting at 113°C, elemental sulfur still presents a problem if the process is conducted at 150-185°C (Beattie and Ismay 1990). A minimum temperature of 195°C is required to eliminate it. Workers in related fields have attributed this is the fact that molten elemental sulfur S_8 rings begin to polymerise above 159°C. The polymerised sulfur shows a strong viscosity increase (Papangelakis and Demopoulos 1991, working on $\text{H}_2\text{SO}_4\text{-O}_2$ pressure leaching).
- e) Redox potential (Eh) is important when attempting to oxidise elemental sulfur (Raudsepp et al. 1987). Below an Eh of 0.90 volts (vs SHE) S^0 oxidation is minimal, at Eh 0.94 volts it is rapid enough to destroy protective coatings, and about Eh 1.05 volts it was reported that all sulfur is oxidised to sulfate.

- f) Some researchers (Buckley et al. 1988) present evidence which they suggest indicates the process of a sulfur-rich layer on the surface of oxidising sulfides. They suggest this "metal deficient sulfide" is not elemental sulfur.

Elemental sulfur has been found to be a nuisance during nitric acid developmental work. It has dictated the high-temperature option for one ore and has caused unattractive flowsheet complications for another. Despite this, no systematic study of elemental sulfur formation or its elimination has been published. Further, unpublished sources have stated that no such study has been undertaken. It is in the hope that such a study may prove worthwhile to the Industry that the current doctorate program was undertaken.

2.4.3 PERTINENT PROPERTIES OF ELEMENTAL SULFUR

The physical chemistry of elemental sulfur is complex. The stable form to 95.6°C is rhombic S_{α} . However, amorphous sulfur may take years to transfer to α at room temperature (Tuller, 1954) S_{α} has appreciable solubility in CS_2 , but 5 μm amorphous sulfur is stated to be insoluble. The sulfur precipitated from CS_2 takes the λ form, which slowly transforms to rhombic. Extensive allotropy occurs with rings and chains from 6 to 18 atoms identified. Rhombic sulfur melts at 113°C, monoclinic at 118°C and nacreous monoclinic at 107°C. All these are thought to be made up of S_8 rings. Liquid sulfur can exhibit exceptional supercooling. Droplets of 3 mm diameter can remain liquid at room temperature for weeks. Liquid sulfur is viscous at all temperatures.

Liquid sulfur S_8 rings begin to polymerise at 160°C (Powell and Timms, 1974), giving a marked viscosity increase. At higher temperatures, depolymerisation occurs; the interaction is very complex. Chains do not branch. Sulfur bond length varies widely in different compounds.

It is generally agreed that the S_8 ring (Figure 2.4.3.1) is the most stable. However, extensive allotropy, and persistent metastability and supercooling make it very difficult to predict the form of elemental sulfur present at a given time from a given set of conditions.

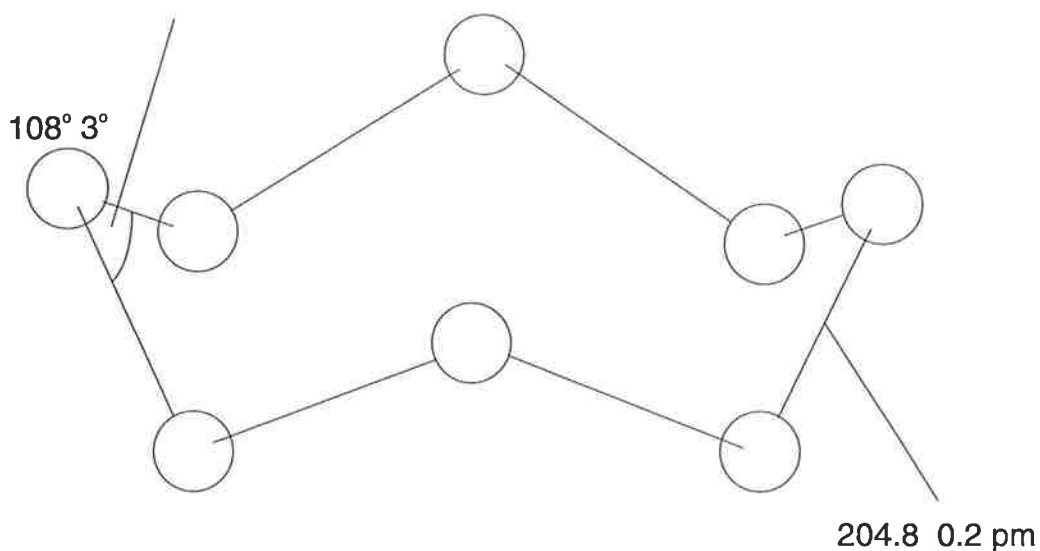


FIGURE 2.4.3.1 S₈ Ring Structure (from Powell and Timms, 1974)

2.5 SUMMARY

Although nearly twenty papers have been written on nitric acid treatment of sulfide-bearing materials, limited fundamental kinetics have been published. The early workers concentrated on showing that nitric acid would successfully treat a range of feeds and their economic goal was to solubilise base metals while yielding sulfur in the elemental form.

Developers of nitric-acid pre-oxidation processes have brought the technology to the brink of commercialisation. Cost advantages are anticipated by developers of the "Redox" process, with an added capital cost incentive for the low-temperature variant. Developers of nitric acid processes have not been as complete in their reporting as the early researchers. Such experiments as have been reported have tended to be at only two levels of a given variable. While elemental sulfur was recognised as a problem, it was eliminated either in a separate stage, or by operating at 195°C. Its formation and oxidation was not addressed in any detail. In fact, these authors have pointed out the need for more study of the sulfur question.

The nitric acid testwork carried out in Chapter 4 and 5 of this thesis uses a single mineral, pyrite. The leaching and electrochemical work is aimed at understanding the kinetics, and the relevant parameters are studied individually. A second focus of the work is the formation and oxidation of elemental sulfur.

The writer submits that the aspects of kinetics and of elemental sulfur have not been adequately studied previously. The previous work has not been investigated at

enough levels of parameters, nor focussed on anything other than the raw results. Discussions with a number of the other workers cited support this writer's views.

2.6 REFERENCES:

- Beattie, M.J.V., Raudsepp, R., and Ismay, A., 1989, Arseno/Redox process for refractory gold ores, in *Processing of Complex Ores*, Dobby, G.S. and Rao, S.R., editors, 28th Annual Conference of Metallurgists of CIM, Pergamon Press, Toronto, pp 431-439.
- Beattie, M.J.V., Raudsepp, R., Sarkar, K.M. and Childs, A.M., 1985, The arseno process for refractory gold ores, unpublished report.
- Beattie, M.J.V., and Ismay, A., 1990, Applying the redox process to arsenical concentrates, *J.Mining*, 42, pp 31-35.
- Berezowsky, R.C.M.S. and Weir, D.R., 1984 Pressure oxidation pretreatment of refractory gold, *Minerals and Metallurgical Processing*, 1, pp 1-14.
- Birak, D.J. and Deter, K.W., 1987 *International Symposium on Gold Metallurgy*, Winnipeg (Editors Salter, Wyslowzil and McDonald) pp 135-140.
- Bjorling, G. and Kolta, G.A., 1965, Oxidizing leach of sulfide concentrates and other materials catalysed by nitric acid, Proceedings, *International Mineral Processing Congress*, New York, pp 127-138.
- Buckley A.N., Hamilton, I.C. and Woods, R., 1988, Studies of the surface oxidation of pyrite and pyrrhotite using X-ray photoelectron spectroscopy and linear potential sweep voltammetry in Richardson, P.E. and Woods R. (Eds) *Electrochemistry in Mineral and Metal Processing II*, The Electrochemical Society Inc. Pennington, N.J., pp 234-246.
- Canterford J.H., 1988, see Chapter 1.
- Canterford, J.H., 1994b, Nitric acid and hydrometallurgy Reinventing the wheel or exploiting new opportunities, Gold Annual Conference, Brisbane, 3-6 July, pp 111-115.
- Canterford, J.H., 1994a, The need for and pitfalls in new process technologies AusIMM 6th Extractive Metallurgy Conference, Brisbane 3-6 July, pp 7-10.

- Dry M.J. and Coetzee, C.F.D., 1986, The recovery of gold from refractory ores, Gold 100 Conference Proceedings SAIMM Johannesburg (Fivas, C.E. and King R.P., eds) pp 259-274.
- Fair, K.J., Schneider, J.C. and Van Weert, G., 1987 Options in the nitrox process, *International Symposium on Gold Metallurgy*, CIM Aug 23-26, 1987.
- Feather, C.E. and Koen, G.M., 1973, The significance of the mineralogical and surface characteristics of gold grains in the recovery process, *J. of SAIMM*, 73, pp 223-235.
- Flatt, J.R., Dunlop, G., Fander, W.H., Wong, K., and O'Neill, B.K., 1991, An overview of refractory gold testwork and research in Adelaide, World Gold '91 AusIMM Conference Cairns, April 21-25, pp 78-86.
- Foo, K.A., Bath, M.D., Ismay, A. and Canterford, J.H., 1989 New gold processing technologies: an Engineer's perspective, in *Gold Forum on Technology and Practices (World Gold '89)*, SME-AusIMM, Reno, Nevada, Nov 5-8, pp 233-250.
- Fraser, D.M. Zacharaides, J.C., A Comparison of alternative models for non-linear leaching kinetics, *J.S.Aft.Inst. Min. Metal*, pp 365-372.
- Hiskey, J.B. and Schlitt, W.J., Aqueous oxidation of pyrite, in Schlitt N.S. (Ed) *Interfacing Technologies in Solution Mining*, AIME, USA, pp 55-74.
- Hisshion, R.J. and Waller, C.G., 1980, Recovering gold with thioarea, *Mining Magazine*, September 1984, 151, (3), pp 237-243.
- Kadioglu, Y., Karaca, S. and Bayakceken, S., 1995, Kinetics of pyrite oxidation in aqueous suspension by nitric acid *Fuel Processing Technology*, 41 Elsevier, pp 273-287.
- Kantopoulos, A. and Stefanakis, M., 1988, Treatment of the Olympias refractory gold concentrate, *Perth International Gold Conference* 28 Oct-1Nov 1988. Randol International, Denver.
- Lakshmanan, V.L. and Childs, A.M., 1984, Treatment of refractory gold ores, *14th Annual CIM Hydrometallurgical Meeting*, Oct 14-17, 1984.

- Lazer, M.J, Southwood, M.J. and Southwood, A.J., 1986, The release of refractory gold from sulphide minerals during bacterial leaching *Gold 100 Proceedings of International Conference on Gold*, SAIMM, Vol 2, pp 287-197.
- Leonard, R. (1990b) Private communication
- Leonard, R.C., Christensen, K.S. and Dawson, P.A, 1990, Treatment of arsenopyrite ores with the "Redox" process, *Randol Gold Forum '90*, 13-15 Sept 1990, Squaw Valley, Ca (Publisher, Randol International, Denver, Co)
- Miller, J.D., 1980, Unit processes in extractive metallurgy - hydrometallurgy, Module 1, Course Notes.
- Nagy, I., Mrkusic, P. and McCulloch, H., 1976, Chemical treatment of refractory gold ores - literature survey, Report No. 38, *National Institute of Metallurgy (Mintec)* Johannesburg, South Africa.
- Newman, B.L. and Carta, C., 1988, Mass transfer in the absorption of nitrogen oxides in alkaline solutions, *AIChE Journal*, 34, (7), July 1988, pp 1190-1199.
- Papangelakis, V.G. and Demopoulos, G.P., 1991, Acid pressure oxidation of pyrite; reaction kinetics, *Hydrometallurgy*: 26 Elsevier Amsterdam, pp 309-325.
- Powell, P. and Timms, P., 1974, The chemistry of the non-metals, Chapman and Hall, London, pp 176-182, 203-206.
- Prater, J.D., Queneau, P.B. and Hudson, J.T., 1973, Nitric acid route to processing copper concentrates, *Transactions, AIME*, 254, pp 117-122.
- Raudsepp, R., Peters, E., Beattie, M.J.V., 1987, Process for recovering gold and silver from refractory ores, U.S. Patent No 4, 647, 307, March 3, 1987.
- Scheiner, B.J., Lindstrom, R.E., Guay, W.V. and Peterson, D.G., 1972, Extraction of gold from carbonaceous ores: Pilot plant studies, *U.S. Dept of the Interior Report 7597*.
- Sehic, A., 1988, An update of the K-process, *Perth International Gold Conference*, 28 Oct- 1 Nov, Randol International Denver, pp 184-187.

Sobel, K.E., Bolinski, L. and Foo, K.A., 1994, Pilot plant evaluation of the Redox process for Bakyrchik gold PLC, Volume 8 Minerals Engineering '94 Conference.

Trofe, T.W., Galagher, D.J., Reuter, C.O. and Findlay, S., 1988, Evaluation of high TDS water on mining operations in Western Australia, *Perth International Gold Conference*, Oct 28 - Nov 1 Randol International, pp 206-311.

Tuller W.N., 1954, Sulfur data book, McGraw Hill, New York.

Van Weert, G. (1989) Personal communication

Van Weert, G., Fair, K.J., 1989, Optimizing the Nitrox process through elemental sulphur formation, Processings, *Thirteenth International Precious Metals Institute Conference*, Montreal, Quebec, Canada pp 305-317.

Van Weert, G., Fair, K.J. and Aprahamian, V.H., 1988, Design and operating results of the Nitrox process, *2nd International Gold Conference No 7-9 1988*, Vancouver, B.C., Canada.

Van Weert, G., Fair, K.J. and Schneider, J.C., 1986, Prochem's Nitrox process, CIM Bulletin, 79, (895), pp 84-85.

Wells, J.A., 1989, A Generic study of the capital and operating costs for the recovery of precious metals from refractory ores, Canadian Mineral Processors - Annual Conference, Ottawa, Canada, Jan 18-20.

Wells, J.A., 1988, Vibro energy milling and its application to gold recovery, *Canadian Mineral Processor's Conference*, Ottawa, 19-21 January.

Whellock, J.G., 1994, Application of the Redox process of the Bakyrchik gold deposit, Randol International Gold Conference, Vancouver.

3 AUTOCLAVE AND CYANIDATION TESTS

3.1 PHILOSOPHY

When the work which comprises this thesis commenced, the field chosen was the treatment of refractory gold ores. Sponsorship was obtained from Minproc Technology Pty Ltd and from CRA's Advanced Technical Development Division. CRA provided one gold-bearing refractory material for testwork. Two other materials were obtained from Stawell Gold Mines of Victoria, Australia. Some months later, Minproc obtained small samples from two overseas deposits. Naturally, all companies were interested in testing of their gold-bearing materials. Talks with sponsors and research personnel working on various treatment techniques (Kandemir 1988) narrowed the choice of technology to pressure oxidation, with an emphasis on nitric acid. CSIRO's Division of Mineral Products, Port Melbourne, had been visited by the writer. Permission was obtained to work with their titanium autoclaves for pressure pre-oxidation.

A niche of research, original and deep enough for a Doctoral study, had not been identified at this point. The parties agreed that the field, and especially nitric acid treatment, had many unanswered questions which might constitute original research and be useful for the industry. The University of Adelaide approved proceeding, and the University of South Australia granted a period of Study Leave to begin the work.

The autoclave and cyanidation tests were therefore preliminary work to the main investigation. They were undertaken to gain a feel for the field, to provide data on the sponsors' materials, and to identify a specific area of research which would be both suitable for a Doctorate and useful to the industry.

3.2 SCOPE OF TESTWORK

3.2.1 REFRACTORY GOLD-BEARING MATERIALS

Five gold-bearing materials were obtained, four of which were tested. The CRA feedstock was a pyrite concentrate from their Bougainville operation. Several thousand tonnes per week of this material was being produced in 1988. Stawell

Gold's materials were from their "Wonga" and "Magdala" lodes; time restricted testwork to the former material. Minproc's sources were the Cinola deposit from Vancouver Island in Canada and the Tonkin Springs operation in Nevada, USA. These last four materials were whole ore samples. Bulk assays (by Amdel) of the four materials tested gave the following chemical analyses shown in Table 3.2.1.1.

Table 3.2.1.1: Chemical Analysis of Feedstocks

| Element | | | | | | | | | | |
|------------------------------|---------|--------|---------|-----------|-----------|-----------|-----------|-----------|-----------|-----------|
| Material | Fe % | S % | Cu % | Zn ppm | Ni ppm | As ppm | Sb ppm | Pb ppm | Te ppm | Ag ppm |
| Bougainville (code "Auber") | 38.0 | 45.0 | 0.85 | 105 | 95 | 340 | 18 | 75 | 25 | 12 |
| Stawell (code "Brahms") | 5.05 | 1.00 | 0.007 | 110 | 40 | 4950 | 18 | - | < 10 | 2 |
| Cinola (code "Elgar") | 2.25 | 2.10 | 0.008 | 15 | 305 | 370 | 118 | 75 | 210 | 4.2 |
| Tonkin Spring (code "Fauré") | 1.60 | 1.30 | 0.005 | 105 | 320 | 3700 | 114 | 22 | 210 | 13 |

Gold assays are addressed under section 3.4

3.2.2 PRE-OXIDATION AND CYANIDATION TESTS

Five tests were carried out at CSIRO in beakers to establish conditions. These were followed by twenty-six autoclave tests on the various feedstocks, at conditions given in section 3.4. The Bougainville material required several parallel tests to provide enough residue for cyanidation. These parallel tests, two in beakers and thirty-three in a four litre stainless steel autoclave, were carried out in Adelaide after the CSIRO period. One test was carried out with only elemental sulfur, nitric acid, and oxygen in the autoclave.

Twenty-four rolling-bottle cyanidation tests were carried out. Two were on Orabanda gold ore, a non-refractory material available in the laboratory, to familiarise the writer with the methodology. Thirteen were on the four feedstock refractory materials to establish their base cyanidation behaviour, without preoxidation. Nine were on pre-oxidation residues.

Very little optimisation was attempted for either the base cyanide tests, or the pre-oxidation runs. For the base tests, the grinds as suggested by the companies supplying the feedstock were used. (Stawell "Wonga" cyanidation samples proved very slow to filter and a coarser grind was resorted to for later tests.)

Standard reagent concentrations were maintained throughout all tests, although each feedstock was pre-tested to determine initial cyanide and base additions. For the autoclave tests, pressure conditions were adopted that were close to those for the "Redox" high-temperature variant. A residence time of one hour was used in order to ensure complete sulfide oxidation for all feedstocks.

3.3 EXPERIMENTAL METHODS

3.3.1 ROLLING BOTTLE CYANIDATION

The method followed was that of Dorr and Bosqui (1950). Preliminary cyanide and base consumptions were determined for each new material. For cyanide, the preliminary test was to leach 100 g of ore in 100 ml of 1% NaCN solution for 20 minutes with 4 g of NaOH. The residual cyanide in 10 ml of filtered solution was then titrated with $0.8663 \text{ g l}^{-1} \text{ AgNO}_3$ to determine preliminary cyanide consumption. Potassium iodide was added to sharpen the end point. For base, the preliminary test was to leach 12.5 g of ore in 50 ml of $4 \text{ g l}^{-1} \text{ NaOH}$ solution for 5 minutes at $25 \text{ }^\circ\text{C}$. Residual base in 20 ml of filtered solution was then titrated using 0.7889 g l^{-1} oxalic acid, with phenolphthalein indicator.

The target minimum solution strength for rolling-bottle leaching was 0.050 w/o NaCN and 0.025 w/o NaOH. The initial additions of both reagents were therefore enough to satisfy the preliminary consumptions plus enough to give 0.05% NaCN and 0.025% NaOH solution.

For most tests, 200 g of ore were put into the rolling bottle with 500 g of de-ionised water to give 28.6% slurry. Initial base and cyanide additions were made and the bottle set to rolling. After 1 hour, the bottle was stopped, the bottle allowed to stand a few minutes, and a sample withdrawn and filtered through a $5 \text{ }\mu\text{m}$ 'millipore' membrane. This sample was then titrated, sequentially with silver nitrate and oxalic acid, to determine residual cyanide and base solution strengths. The amount of slurry withdrawn and titrated varied with the difficulty of filtering and end-point detection. Slurry withdrawn was in the range of 10-40 ml and titrations were in the range of 5-20 ml. All samples were measured by pipette. A wide-mouth pipette was used for slurry sampling because in most cases settling was slow. Time that the bottle was off the roller generally was about 20 minutes; such time was accounted for as non-leaching time. The bottle was restarted as soon as the solution had been made up to its target reagent strengths. Reagent additions were made in the solid form, weighed to nearest milligram. Sample volume was replaced by de-ionised water. Samples were also taken at 3 hours, 6 hours, 24

hours and 48 hours. A few tests were extended to 72 hours. The tests was boosted at the end - extra cyanide was added to redissolve any gold precipitated from solution during the test.

In the case of Tonkin Springs material, the cyanide titration was obscured by a dark colour in solution. This was eliminated by adding about 0.02 g of litharge for each ml of sample to be titrated. Tonkin Springs autoclave residue was also extremely fine, requiring pressure filtration.

At the end of each run the bottle was weighed to account for evaporative losses. The contents were filtered, the filtrate weighed, and the residue dried after washing with weak cyanide solution and de-ionized water. Residues were sampled and sent to Amdel Laboratories for fire-assaying. Solutions were analysed for gold by atomic absorption spectrometry. Calculations included the weights of solids in samples, with solid samples' gold contents back-calculated from the solutions.

3.3.2 AUTOCLAVE PRE-OXIDATION TESTS

The method detailed describes that used in the 1 litre capacity titanium autoclave at CSIRO. The method was essentially the same when the four-litre autoclave was used, but quantities were quadrupled.

A 100 g sample of ore was cut out by riffing. The material had been previously dry-ground to size for cyanidation, and this size was used for pre-oxidation. 500 ml of 3 M nitric acid solution was added to the ore in the autoclave. The autoclave was bolted closed. For "Nitrox" tests the pressure generated was measured in the closed autoclave. For "Redox" tests, an overpressure of 680 kPa was added to that obtained from the "Nitrox" test for that particular material. Commercial oxygen was used to provide the atmosphere for "Redox" tests.

The autoclave was heated to 85°C and maintained at this temperature for one hour. Cooling water was used to maintain temperature for the high-sulfide Bougainville material, but temperature control was not good for this material. After 1 hour, the reactor was allowed to cool to about 50-60°C at which point it was opened. Both warm-up and cool-down periods were in the order of 30-40 minutes.

The contents of the autoclave were filtered in a large vacuum filter through #1 Whatman paper. The filtrate was then polished through a 5 µm 'millipore' membrane. The residue was washed with 1 M HNO₃ then distilled water. It was then dried at 90°C, weighed and sampled for fire analysis for gold. All filtrate and

washings were weighed. Filtrate was retained and filtrate and washings were sampled for analysis.

Liquid samples were assayed by the author at CSIRO for gold and iron by AAS, and by Amdel (then Classic Comlabs) by AAS (method 4). Amdel also determined copper and silver by AAS (method 4 and 2) arsenic by WAT4A and antimony by WAT 4C vapour generation - atomic absorption methods. Several months later, mercury analysis was attempted using WAT4.

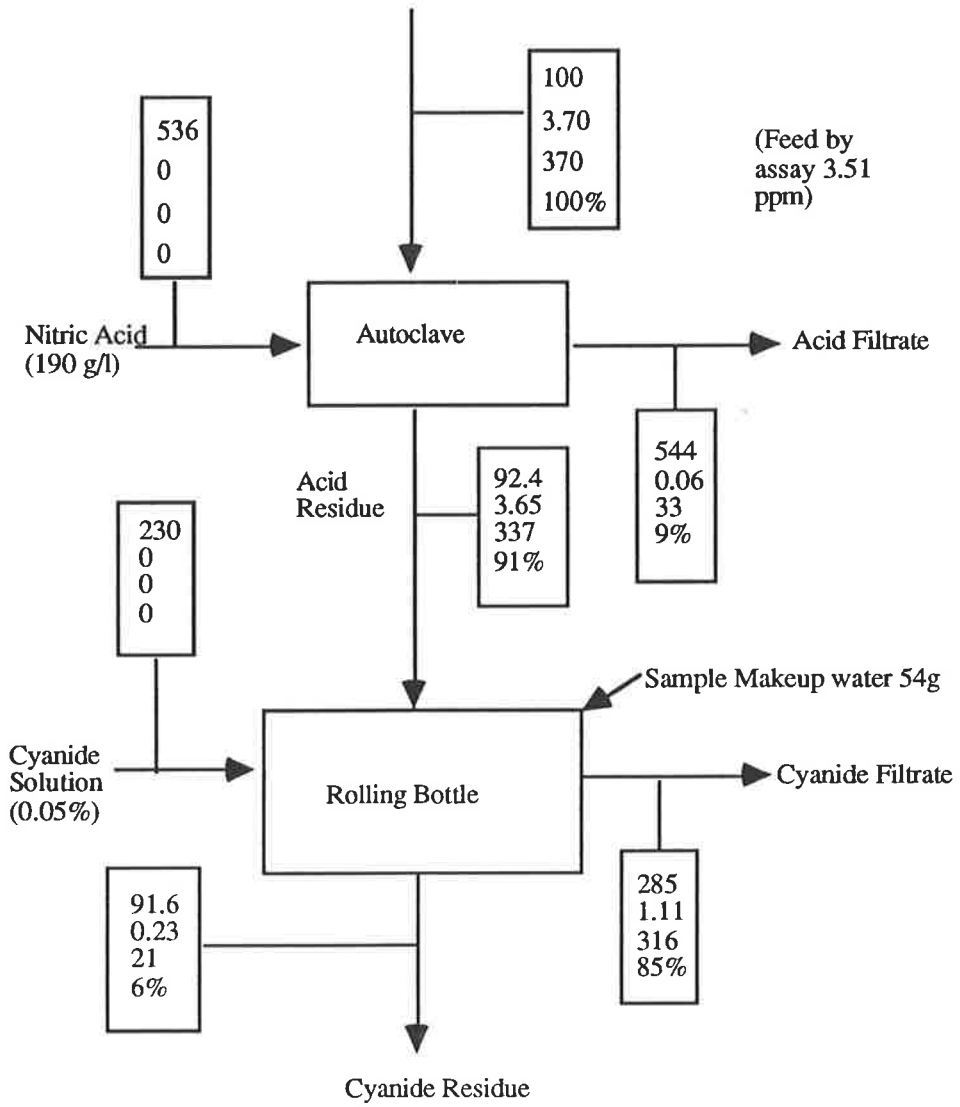
Solids were analysed by Amdel using AAS4 for iron and copper and XRF for antimony and arsenic. Mercury analysis was attempted using method AAS5.

3.4 SUMMARISED EXPERIMENTAL RESULTS

3.4.1 EXAMPLES OF INDIVIDUAL TESTS

Given that autoclave and cyanidation work were preliminary to the pyrite-nitric acid work of Chapters four and five, the majority of the results of the former are only summarised here. However, the typical mass and metal balances of Figure 3.4.1.1 and 3.4.1.2 and Table 3.4.1.1 are included for clarity. They represent tests for which no accounting problems occurred. Section C of the "Supplementary Volume - Raw Results" gives examples of the technical problems encountered when undertaking metal balances. The "Supplemental Volume" also gives detailed test results and mass balances.

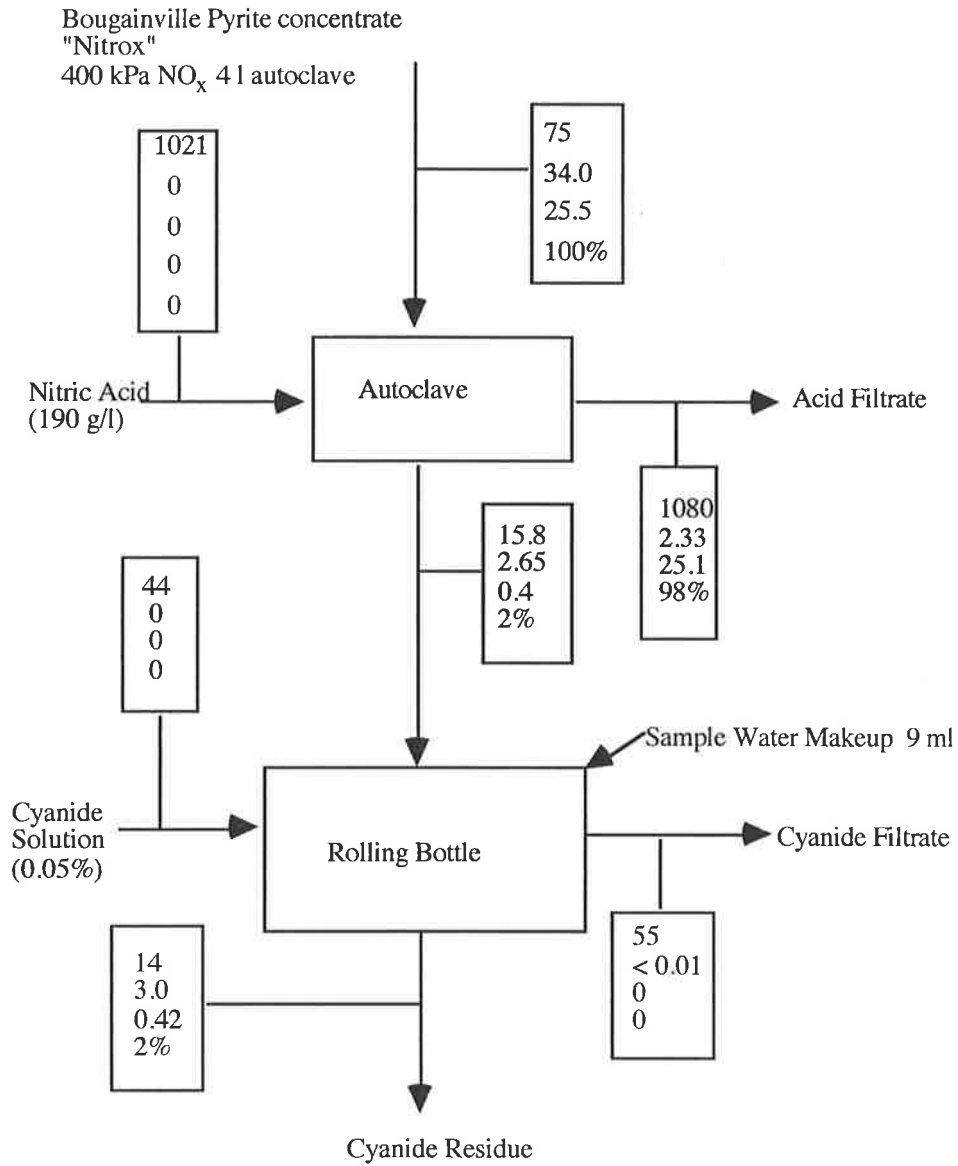
Figure 3.4.1.1: Whole Ore Gold Balance
 Tonkin Spring Whole Ore "Redox: 770 kPa O₂ 1litre autoclave



Legend

| |
|---|
| grams |
| ppm Au |
| µg Au |
| distribution |
| Filtrate figures include Evaporation estimates |

Figure 3.4.1.2: Sulfide Concentrate Iron Balance
 Bougainville Pyrite Concentrate "Nitrox" 400 kPa NO_x 4 litre autoclave



Legend

| |
|--|
| grams |
| % Fe |
| g Fe |
| distribution |
| Filtrate figures include Evaporation estimates |

Table 3.4.1.1: Typical Rolling Bottle Log

Combined "Redox" Residue Tonkin Springs

Initial Conditions

Solids 199.9 g H₂O 493.3 g

NaCN 309 mg NaOH 508 mg

| Time | Liquid withdrawn ml | Titration | | | Solution % | | Additions | | | Gold | |
|----------|------------------------|-----------|-------------------|------|------------|----------|------------------|--------------|--------------|------|------------|
| | | Sample | AgNO ₃ | Acid | NaCN | NaC N | H ₂ O | NaCN (mg) | NaOH (mg) | ppm | Extraction |
| 1 hour | 20 | 5 | 7.5 | 8.2 | 0.075 | 0.082 | 20 | – | – | 0.91 | 60% |
| 3 hours | 40 | 5 | 5.8 | 8.0 | 0.058 | 0.080 | 40 | – | – | 1.17 | 79% |
| 6 hours | sample | missed | | | | | | | | | |
| 24 hours | 30 | 5 | 2.3 | 7.8 | 0.023 | 0.078 | 30 | 139 | – | 1.25 | 87% |
| 48 hours | 30 | 4 | 1.7 | | 0.022 | | 29 | 158 | – | | |
| Boost | | 5 | 6.9 | 3.7 | 0.068 | | – | – | – | 1.28 | 96% |

Consumptions: NaCN 309 + 139 + 158 – 382 → 224 mg/199.9 g = 1.12 kg/tonne ore

NaOH 808 – 275 → 533 mg/199.9 g = 2.67 kg/tonne ore

3.4.2 PARAMETERS OF FEED MATERIALS

Mineralogical examination using a geological reflected-light microscope was used with the chemical analyses from Amdel to generate approximations of mineral contents of the four feedstock materials. Table 3.4.2.1 gives the approximate results.

Table 3.4.2.1: Approximate Mineralogy of Gold Bearing Materials

| Source | Major Minerals | Minor Minerals | Potential Cyanicides |
|----------------------------------|---|--|----------------------|
| Bougainville Sulfide concentrate | pyrite 82% clear species 16% (quartz ?) | chalcopyrite 2.3 % bornite 0.1% | 2.4% |
| Stawell "Wonga" ore | clear species 93% pyrite 5% | arsenopyrite 1% magnetite, 1% pyrrhotite | 1% |
| Cinola | clear species 95% pyrite 4% | pyrrhotite? | 0.1% |
| Tonkin Springs | clear species 97% | pyrite 2% arsenopyrite 0.8% | 0.9% |

Table 3.4.2.2 provides screen analysis of the four gold-bearing materials used for the tests. Table 3.4.2.3 gives approximate free-gold values for the feed materials. Amalgamation tests are generally considered to recover gold particles which are completely freed from gangue, not merely partially locked and hence exposed to cyanide. The amalgamable portion would presumably be recoverable by gravity methods unless extremely fine.

Table 3.4.2.2: Grinding Data for Cyanide and Autoclave Test Feeds

| Source | Size (% retained) | | | | | |
|------------------------------------|---------------------|---------------------|--------------------|--------------------|--------------------|----------------------------|
| | + 300 μm | + 150 μm | +106 μm | + 75 μm | + 45 μm | - 75 μm nominal |
| Bougainville Sulfide concentrate | - | 3.9 | 9.9 | 20 | 38 | 80% |
| Stawell "Wonga" (milled and pulv.) | - | 0.4 | 7.6 | 13.3 | 29.6 | 87% |
| crushed only | 35 | 50 | - | 63 | 48 | 63% |
| Cinola | 0.6 | 9.7 | 15.3 | 21.7 | 39.6 | 78% |
| Tonkin Springs | - | 7 | 15.5 | 24 | 42 | 76% |

The crushed only Stawell material was used for later cyanide tests and autoclave tests because of the difficulty in filtering cyanided slurry samples.

Table 3.4.2.3: Amalgamation Test Data

| Source | % Gold recoverable by Hg Amalgamation |
|----------------------|---------------------------------------|
| Bougainville Sulfide | 73 |
| Stawell "Wonga" | 19 |
| Cinola | 18 |
| Tonkin Springs | 2 |

Table 3.4.2.4 gives a summary of the statistics on gold analyses in the feed materials. Sampling for gold is notoriously difficult, so the feed values which were calculated from residues and cyanide solutions are more reliable. Gold recoveries are based on these calculated feed values.

Table 3.4.2.4: Variability of Feed Samples for Gold

| Material | Samples (n) | Assay g/t | σ | Precision (2S) |
|----------------------|-------------|-----------|----------|----------------|
| Bougainville Sulfide | 13 | 3.96 | 0.72 | $\pm 38\%$ |
| Stawell "Wonga" | 17 | 3.99 | 0.55 | $\pm 28\%$ |
| Cinola | 3 | 3.13 | 0.37 | $\pm 29\%$ |
| Tonkin Springs | 3 | 3.70 | 0.51 | $\pm 34\%$ |

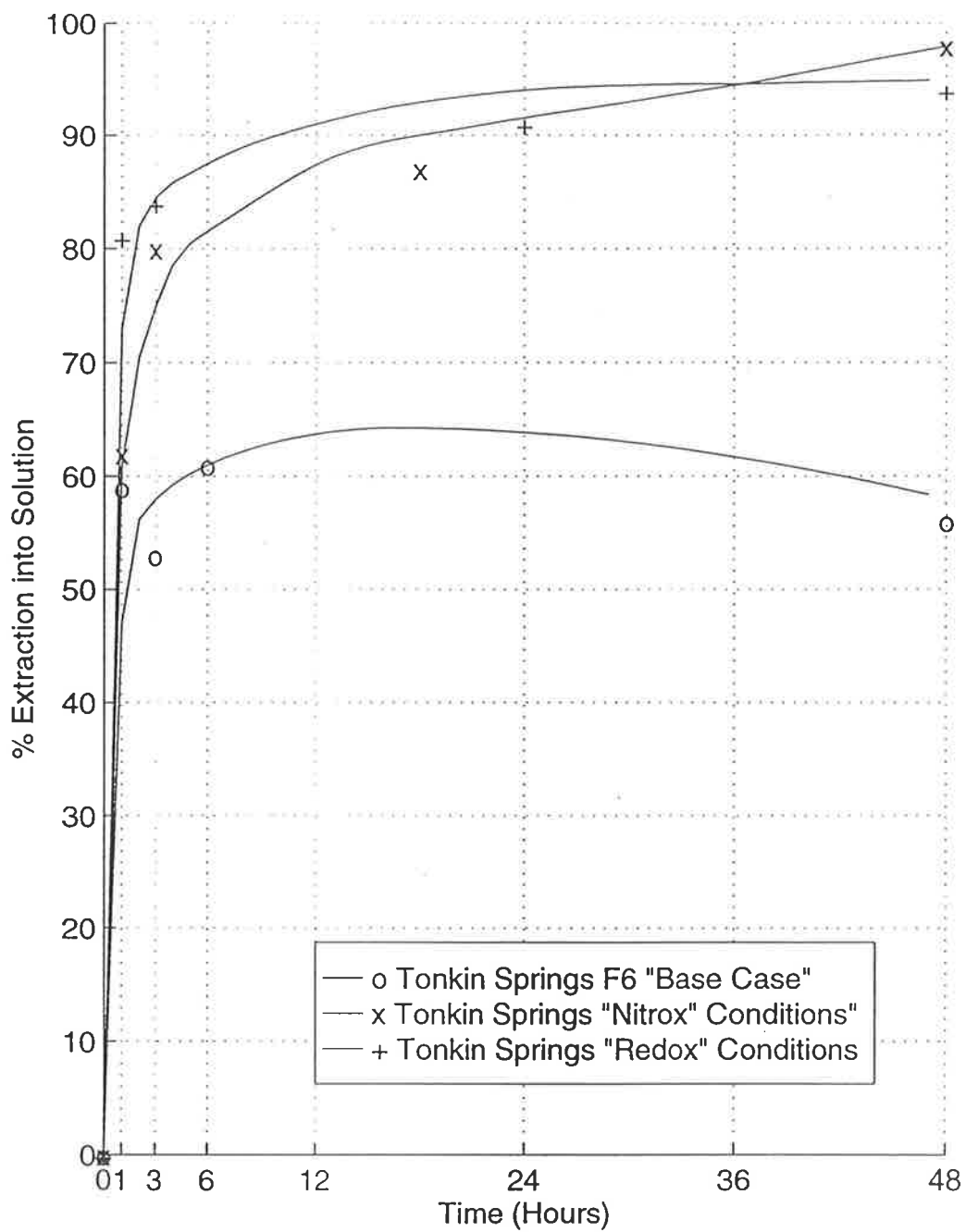


Figure 3.4.3.1: Typical Effect of Pre-Oxidation on Gold Recovery

3.4.3 EFFECT OF NITRIC ACID PRE-OXIDATION ON GOLD CYANIDATION PARAMETERS

Table 3.4.3.1 gives oxidation degree, gold recovery, and reagent consumption for the four materials tested.

Table 3.4.3.1: The Effect of Pre-oxidation with Nitric Acid on Cyanidation for Four Gold-bearing Materials

| Material | | "Base Tests" (no pre-oxidation) | "Nitrox" Tests | "Redox" Tests |
|---------------------------------|--------------------------|------------------------------------|-------------------|------------------|
| Bougainville pyrite concentrate | % oxidation [#] | – | 98 | 98 |
| | Recovery (Au) | 63% | 95% | 97% |
| | consumption. NaCN (kg/t) | 9.3 | *1.4 | *0.6 |
| | consumption. NaOH (kg/t) | 2.3 | *0.6 | *1.7 |
| Stawell ore | % oxidation [#] | – | 87 | 80 |
| | Recovery (Au) | 68% | 93% | 96% |
| | consumption. NaCN (kg/t) | 0.7 | 3.9 | 4.7 |
| | consumption. NaOH (kg/t) | 2.0 | 4.7 | 3.5 |
| Cinola ore | % oxidation [#] | – | 78 | 84 |
| | Recovery (Au) | 48% | 86% | 95% |
| | consumption. NaCN (kg/t) | 0.8 | 1.7 | 0.8 |
| | consumption. NaOH (kg/t) | 4.7 | 1.0 | 1.1 |
| Tonkin Springs ore | % oxidation [#] | – | 70 | 75 |
| | Recovery (Au) | 60% | 91% | 94% |
| | consumption. NaCN (kg/t) | 7.0 | 1.2 | 0.8 |
| | consumption. NaOH (kg/t) | 9.0 | 1.9 | 2.7 |

Note: # % oxidation was taken from the iron balances as the % of the iron in the feed which reported to the acid filtrates.

* reagents consumptions were calculated on the basis of original feed material. In the case of the pyrite concentrate, 79% of the original feed was dissolved in the autoclave.

Recovery of gold in the acid filtrate was assumed to be 98% and is included above. The values shown in Table 3.4.3.1 are final values. The figures are averages of the tests performed on any given feed materials with some judgemental culling; seven Stawell base tests were performed, but most pre-oxidized cyanidations were performed only once. Accordingly, statistics are not given. More data may be seen under metal departments - subsection 3.4.4.

A typical cyanidation curve is shown in Figure 3.4.3.1. Gold recovery is plotted with time, for Tonkin Springs ore with and without nitric acid pre-oxidation. The effect of pre-oxidation on reagent consumption for the same material is shown in Figure 3.4.3.2. As for Figure 3.4.3.1, these are specific single test results for the cyanidation step, and as such, do not correspond directly to Table 3.4.3.1, which is based on metal balances around the two steps. However, the data of Table 3.4.2.2 does correspond to the Tonkin Springs "Redox" lines on the two figures.

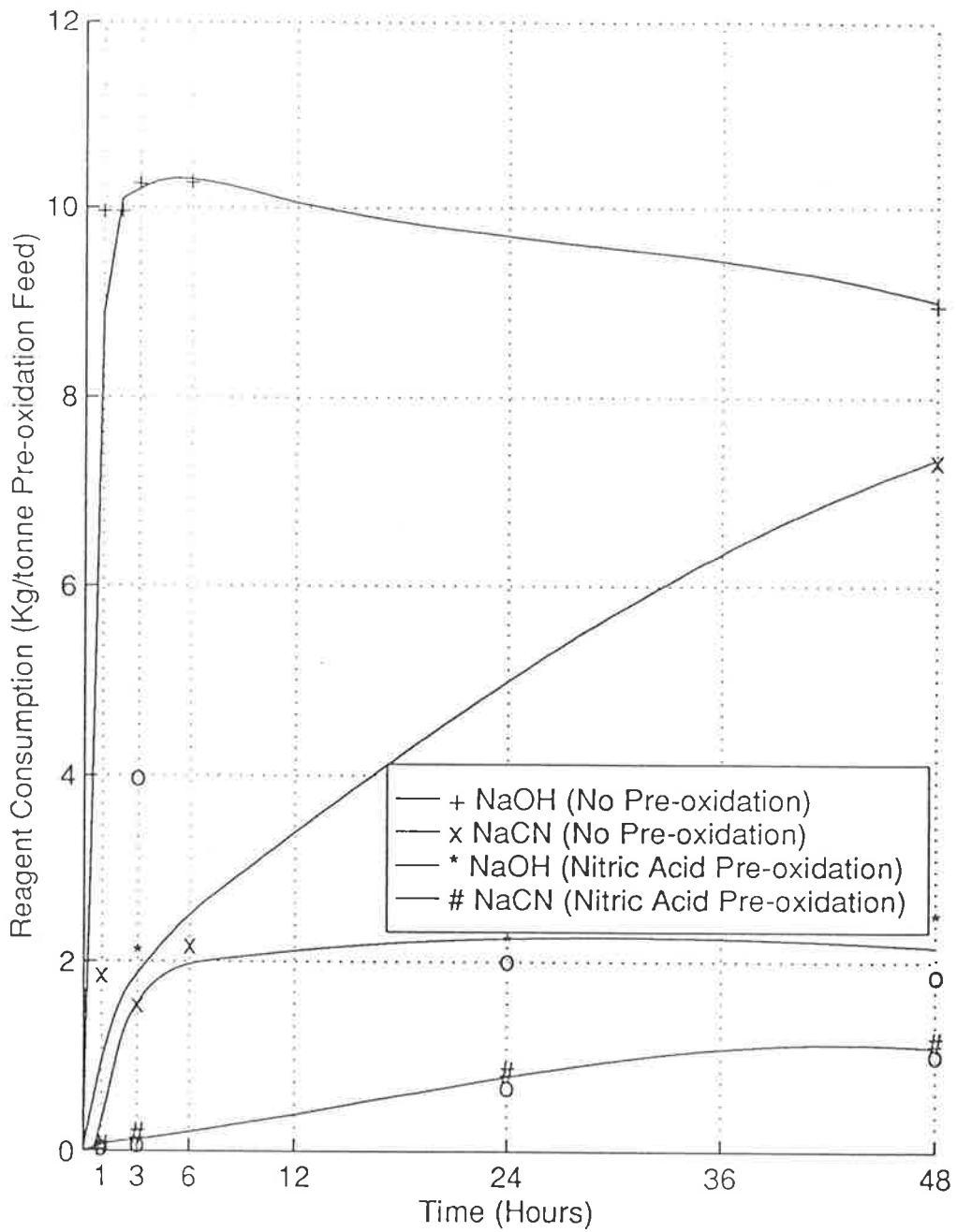


Figure 3.4.3.2: Typical Effect of Pre-Oxidation on Reagent Consumptions
 Rolling bottle Cyanidation Tests on Tonkin Springs Ore. "Redox" # and "Nitrox" o results are very close. Solution strengths 0.25% NaCN 0.025% NaOH

3.4.4 METAL DEPARTMENTS

Metal departments for gold and silver are summarised for the four feed materials in Table 3.4.4.1. Again, these are based on balances which may be found in the Supplemental Volume. Many of the balances required adjusting of assays, and some did not close within limits justified by assay or sampling variabilities.

Table 3.4.4.1: Gold and Silver Departments

| Feed Material | Test Conditions | Acid Filtrate % | Cyanide Filtrate % | Cyanide Residue % | Balance Quality |
|---------------------|-----------------|---------------------------|--------------------|-------------------|---------------------|
| Bougainville pyrite | "Nitrox" | 13 70 | 82 20 | 5 10 | poor poor |
| Bougainville pyrite | "Redox" | 1.5 Ag not assayed for | 95 | 3.5 | good |
| Stawell "Wonga" ore | "Nitrox" | 8 39 | 85 61 | 7 0 | good good |
| Stawell "Wonga" ore | "Redox" | 6 Ag not assayed for | 90 | 4 | fair |
| Cinola ore | "Nitrox" | 20 41 | 67 41 | 13 18 | good good |
| | "Redox" | 17 36 | 78 57 | 5 5 | poor poor |
| Tonkin Springs Ore | "Nitrox" | 24 30 | 68 56 | 8 14 | good good |
| | "Redox" | 9 13 | 85 72 | 6 15 | good good |

Legend: Gold
 Silver

Departments of iron, copper, antimony and arsenic are reported in Table 3.4.4.2. Iron oxidation was used to indicate oxidation degree of the minerals in each feed material. Arsenic and antimony have environmental implications and copper, arsenic and antimony minerals are potential cyanicides. Mercury balances were attempted, but were abandoned as none closed. Bougainville and Stawell mercury contents were very low, but Cinola ore contained 500 ppm and Tonkin Springs 900 ppm of mercury.

Table 3.4.4.2: Iron, Copper, Arsenic and Antimony Departments

| Feed Material | Test Conditions | Acid Filtrate % | Cyanide Filtrate % | Cyanide Residue % | Balance Quality |
|---------------------|-----------------|-----------------|--------------------|-------------------|-----------------|
| Bougainville pyrite | "Nitrox" | 98 | 0 | 2 | poor |
| | | 77 | 2 | 21 | poor |
| | | 96 | 0 | 4 | good |
| | "Redox" | 44 | 6 | 50 | fair |
| | | 98 | 0 | 2 | good |
| | | 99 | 0 | 1 | dubious |
| Stawell "Wonga" ore | "Nitrox" | 50 | 6 | 44 | good |
| | | 87 | 0 | 13 | poor |
| | | 97 | 0 | 80 | fair |
| | "Redox" | 13 | 7 | 80 | fair |
| | | 80 | 0 | 20 | poor |
| | | 97 | 0 | 3 | poor |
| Cinola ore | "Nitrox" | 6 | 7 | 87 | good |
| | | 78 | 0 | 22 | poor |
| | | 39 | 29 | 32 | poor |
| | "Redox" | 90 | 2 | 8 | poor |
| | | 10 | 13 | 77 | good |
| | | 84 | 1 | 15 | poor |
| Tonkin Springs Ore | "Nitrox" | 97 | 1 | 2 | fair |
| | | 8 | 26 | 66 | good |
| | | 69 | 0 | 31 | poor |
| | "Redox" | 81 | 2 | 17 | poor |
| | | 18 | 2 | 80 | poor |
| | | 74 | 0 | 26 | good |
| | "Redox" | 48 | 37 | 15 | poor |
| | | 90 | 0 | 10 | poor |
| | | 19 | 9 | 72 | good |

Legend: Iron, **Copper**, Arsenic, *Antimony*

Note: Cu not assayed for in five cases

3.4.5 ELEMENTAL SULFUR IN PRE-OXIDATION AND CYANIDE TESTS

Elemental sulfur was noted in some tests using Bougainville pyrite concentrate in beakers. It made its appearance as a hydrophobic scum. It was not noticed in most autoclave tests, or with any of the other gold-bearing materials. Since gold recoveries from pre-oxidised samples were good, elemental sulfur was not originally considered to be causing problems with these tests.

However, one test was run which tested the susceptibility of elemental sulfur to oxidation at the conditions which had been used. Table 3.4.5.1 provides the conditions and test results.

Table 3.4.5.1: Autoclave Test on Elemental Sulfur

| | |
|------------------|--|
| Feed conditions: | S ^o 20.0 g, – 75 µm (fine powder) |
| | 1500 ml of 190 g l ⁻¹ HNO ₃ |
| | 1 hour @ 100°C and 1000 kPa O ₂ pressure. |
| Residue | 19.3 g glazed, brittle agglomerates |
| | S ^o oxidation less than 4% |

After the findings of Chapter 5, it was decided to have another look at the autoclave residues for elemental sulfur. The results of the assays by Amdel are given in Table 3.4.5.2.

Table 3.4.5.2: Elemental Sulfur in Autoclave Residues

| Feed Material | Cyanide Residue | | | | | g S ^o in residue for 200 g feed | Sulfur in feed reporting as S ^o in residue (%) | Gold in residue as % of feed |
|---------------------|-----------------------|------|------------------|-----------------------|--------------------|--|---|------------------------------|
| | Au ^φ g/t φ | % S= | % weight of feed | Au ^φ (g/l) | S ^o (%) | | | |
| Bougainville pyrite | 4.6 | 45 | 19 | 1.28 | 2.0 [#] | 0.8 | 1 | 5 |
| Stawell ore | 4.6 | 1 | 82 | 0.24 ^φ | 0.05 [*] | 0.1 | 4 | 4 |
| Cinola ore | 3.6 | 2.1 | 94 | 0.18 ^φ | 0.1 [*] | 0.2 | 4.5 | 5 |
| Tonkin Springs ore | 3.5 | 1.3 | 90 | 0.32 | 0.1 [#] | 0.2 | 7 | 8 |

"Nitrox" conditions, * "Redox" conditions

φ from metal balances; adjusted within assay/sampling limits

3.5 DISCUSSION OF RESULTS

3.5.1 TYPICAL INDIVIDUAL TESTS

The gold balance on Tonkin Springs ore Figure 3.4.1.1, is typical in that it shows good recovery of gold (85%) to cyanide solution. It also shows an appreciable dissolution of (9%) of gold into nitric acid. This latter value is ore-dependent, but cannot be neglected for any of the four feed materials. Pilot plant testwork on Cinola found that the gold reached a saturation level in "Redox" liquors. Otherwise gold in acid has been assumed recoverable (98%) on carbon. A bleed and neutralisation would be required.

The iron balance on Bougainville pyrite (Figure 3.4.1.2) is typical for this material, in that almost all the iron is dissolved in the autoclave. Cyanidation of the "Redox"

Tonkin Springs acid residue typifies the cyanide tests. (This line is shown in Figure 3.4.3.1 as well as in Table 3.4.1.1.) The gold extraction pattern is a normal cyanidation curve, with the bulk of the gold solubilised within three hours.

3.5.2 PARAMETERS OF FEED MATERIALS

It can be seen from Table 3.4.2.1 that all four materials contain enough sulfides to explain their refractory behaviour. However, there is no correlation between the potential cyanicides column and the actual base case cyanide consumptions of Table 3.4.3.1. Obviously the arsenopyrite and other sulfides present are not equally cyanide-consuming in the four materials. Also, there is some indication from the declining portion of the base case curve in Figure 2.4.3.1, that there may be preg-robbing constituents in Tonkin Springs ore.

The grinding parameters of Table 3.4.2.2 show that the materials were close to plant grinds for the subsequent tests. The exception is the Stawell crushed only sample, which was resorted to overcome a bottleneck in filtering samples. Surprisingly, the considerably coarser grind (63% vs 87% passing 75 μm) showed a gold recovery drop of only 2%, which was not even statistically significant for the eight tests conducted on Stawell.

Only ore amalgamation test was performed on each material. The Bougainville result is considered to be anomalous, as it is higher than the base cyanide gold recoveries. The other materials would merit separate gravity treatment if there were some gold particles present which was too coarse to dissolve during the plant cyanidation retention time. The variation in feed gold assays which is shown in Table 3.4.3.4 is annoying, but unfortunately, entirely typical for gold-bearing materials. Such variation is inherent for gold and is one of the reasons making mass balances awkward. It was not until a fairly large number of assays were on hand that the degree of imprecision was appreciated.

3.5.3 EFFECTS OF PRE-OXIDATION WITH NITRIC ACID

The results of Table 3.4.3.1, as illustrated by Figures 3.4.3.1 and 3.4.3.2, strongly point out the advantages of pre-oxidation for the four materials tested. Gold recovery improvements ranged from 25% to 47% (absolute). Cyanide consumption was reduced in three cases, but by a factor of seven for Tonkin Springs. Base consumption also went down in three of four cases, by a factor of four for Tonkin Springs. It is thought that the higher reagent consumptions for Stawell may have been due to the difficulty of washing the very fine residue in a vacuum filter.

In a plant design, attention would be required for washing Stawell and Tonkin Springs residues, both of which are very fine. Inadequate washing would raise reagent costs, so a compromise would be called for.

While design of the entire plant is out of the scope of this thesis, nitric acid pre-oxidation and subsequent processes steps must be costed. Nevertheless, the magnitude of the recovery improvements and reagent costs are very encouraging.

3.5.4. EFFECTS ON METAL DEPARTMENTS

Table 3.4.4.1 not only confirms the improved gold recovery figures, but shows good silver recoveries as well. Of the materials tested, none have enough silver to be interesting (Bougainville contains perhaps \$A2.00 per tonne). However, the implications for high-silver ores are worthwhile.

Kontopoulos and Stefanakis (1988) gave typical silver recoveries of the various processes on Olympias refractory sulfide concentrate. He stated during his conference presentation that nitric acid pre-oxidation showed advantages in silver recovery of about 20% over roasting and 85% over pressure oxidation. The present work confirms the high dissolution rates of silver with nitric acid and points out its advantage for high silver bearing materials.

The metal balances of Table 3.4.4.2 show trends strongly. Iron minerals which can be oxidised to soluble form report to acid filtrate, with virtually all of the rest remaining in cyanide residues. Almost all of the arsenic reports to the acid filtrate, except for Tonkin Springs ore, where 10-17% remains in the cyanide residue. This could be an already partially oxidised arsenic mineral, which might explain the high cyanide consumption of Tonkin Springs material. From the acid filtrate, arsenic can be precipitated as a coarse ferric arsenate (Canterford 1994b) which is environmentally stable.

The deportment of antimony is more problematical. Cinola and Tonkin Springs contain 100 ppm Sb, and although the majority remains in the cyanide residue, appreciable amounts report to both filtrates. Study of antimony's behaviour in these solutions has environmental implications, but is beyond the scope of this study.

Copper was assayed for as an alternative gauge of % oxidation to iron. Sulfate would have been a more logical choice but discussions with CSIRO at the time indicated the extremely tedious nature of gravimetric determination. In any event

the copper oxidation was much slower than iron, and the balances were erratic. Iron values were therefore used for Chapter three to indicate completeness of oxidation. Repeat individual autoclave tests showed quite good correlation. For example, five of six Stawell tests showed iron oxidation within 1%.

The mass and metal balances of Tables 3.4.4.1 and 3.4.4.2 are forty-one in number. Of these, twenty-two are considered good to satisfactory. Those balances could be adjusted within the limits of sampling or assay precision. Sample precision of feeds is given in Table 3.4.2.4 and was in the order of $\pm 30\%$. Several weeks of frustration led the author to question the published chemical analysis accuracies. This proved fruitful in that accuracies were revealed (Francis, 1990) to be a function of level in relation to detection limit instead of a fixed value. Gold in solutions, for example, should be $\pm 10\%$ accurate at 1 ppm (100 x the detection limit) but only $\pm 50\%$ at 0.1 ppm and $\pm 100\%$ at 0.01 ppm. Approximations using this information allowed the metal balances which are reported. Details on the balances and an example calculation of how they were adjusted may be found in the Supplemental Volume. The nineteen questionable or unsatisfactory balances may be attributable to a host of causes, such as poor sampling, but the reasons have not been isolated. The exception is sodium interference with gold analyses by AAS (Brooks and Flatt, 1992) which gives artificially high values of about 8%. Certainly some chemical interference with determinations occurs, as for example, copper in acid filtrates reporting at double the content reported in the feeds.

The lesson to be learned is that refractory gold-bearing materials are likely not only to be refractory, but individual, and difficult to assay.

3.5.5 FINDINGS CONCERNING ELEMENTAL SULFUR

The test of Table 3.4.5.1 shows the extremely slow rate of oxidation of elemental sulfur. Given imperfection in mass recovery when washing out the autoclave, it cannot be said with assurance that any of the elemental sulfur was oxidised. The conditions were identical to that of "Redox" oxidation of the other samples, but not to that used in industry. (Where elemental sulfur is known to be a problem, as with arsenopyrite concentrates, the "Redox" process is run at 190°C). This finding agrees with those of Prater, et al., (1973).

The conclusion here is that the elemental sulfur formed for the four materials tested must either be in fairly low proportion to the total sulfur in the ore, or else it must be oxidised appreciably while it is still at micro or submicro size. If elemental sulfur reached, say, fifty microns in size, it would not oxidise under the test conditions.

That the proportion of elemental sulfur formed is low, or that the elemental sulfur formed is oxidised early is evident from Table 3.4.5.2. Under the conditions of "Redox" and "Nitrox" pre-oxidation, only 4-8% of the sulfur in the four materials is still present in the autoclave residues. The proportion present in the residues would seem to be ore-dependent. A quick estimation based on the mineralogy of Table 3.4.2.1 gave the correlation below on elemental sulfur in autoclave residues. For this prediction, pyrite was assumed to yield 3% of its sulfur content as elemental sulfur, and arsenopyrite 20%. These approximations after severe nitric acid pre-oxidation are to be found in Prater, et al., (1973) and Beattie et al. (1989), respectively..

Table 3.5.5.1: Predicted Elemental Sulfur in Autoclave Residues

| Material | Pyrite % | Arsenopyrite | S= % | Residue S ^o Predicted | Actual Residue S ^o |
|---------------------|----------|--------------|-------------|-------------------------------------|----------------------------------|
| Bougainville pyrite | 82 | — | 43.9 | 1.3% | 2.0% |
| Stawell ore | 5 | 1% | 2.7 0.33 | 0.08 0.07 } 0.15% | 0.05% |
| Cinola Ore | 4 | — | 2.1 | 0.06% | 0.1% |
| Tonkin Springs | 2 | 0.8% | 1.1 0.26 | 0.03 0.05 } 0.08% | 0.1% |

In an absolute sense, the correlation is very good between predicted and assayed elemental sulfur. This is particularly valid when errors in sampling and assaying are considered. It can be safely stated that the elemental sulfur is ore-dependent and dependent on the type and proportion of the sulfides present.

Whether elemental sulfur is responsible for the loss of gold in autoclave residues is less clear from Table 3.4.5.2. A case could be made that the gold loss is proportional to the fraction of sulfide sulfur left as S^o for the last three feed materials. The Bougainville material has a much higher ratio of gold lost to fraction of sulfur left as S^o, but this could be accounted for by the higher absolute proportion of S^o in the Bougainville autoclave residue. The question would require more work and better designed specific tests, to be settled. One path with promise might be to float the elemental sulfur and assay it for gold. There are, of course, a great many alternate explanations, including gold encapsulated in gangue or sulfides agglomerated by elemental sulfur.

3.6. CHAPTER SUMMARY

The autoclave and rolling bottle tests of this chapter have given the author a feel for the field of research, and revealed an original area of study suitable for a Doctoral investigation. The study has now been narrowed down to the pyrite-nitric acid system and the behaviour of elemental sulfur in that system.

The material in this chapter is preliminary to that study, but has provided considerable confirming data on four gold-bearing materials from three different Australian mining companies. The tests approximated industrial conditions, particularly of the "Nitrox" process, and the low-temperature variant of the "Redox" process. "Redox" tests under oxygen pressure are also conducted, although at lower temperatures than the industrial high-temperature variant.

The four materials tested all fit the definition of refractory, at the grinds tested. Using conventional cyanidation, recoveries were in the range of 48-68%. Cyanide consumption of two of the materials were high at 7-9 kg/tonne. Caustic consumptions were high for all four materials at 2-9 kg/tonne. Reagent consumptions did not appear predictable from mineralogy. The four materials were quite different, coming as they did from locations in Australia, Solomon Islands, Canada and the United States. Three were ore with sulfur 1-2% and the fourth a pyrite concentrate. Arsenic and antimony levels varied widely.

The difference in the four materials tested revealed itself in cyanidation behaviour and also in difficulties which arose in obtaining satisfactory metal balances, at least part of which was related to difficulties in assaying.

All four materials responded very well to pre-oxidation with nitric acid. Gold recoveries improved from 25 to 47% absolute. Cyanide consumptions were reduced for two of four cases, by about 7 kg/tonne ore. Caustic soda was reduced for three of four materials, in the range of 0.6-7 kg/tonne.

Good silver recoveries were obtained from the four materials tested. Arsenic reported mostly to autoclave acid filtrates. Two of the ores were very difficult to filter.

Elemental sulfur was formed in all cases, in a proportion predictable from the mineralogy. The question of elemental sulfur's relation to gold losses bears further investigation. Certainly the elemental sulfur, once it has formed particles of any size, is refractory to the nitric acid and oxygen conditions tested in this Chapter.

The tests of this chapter were not optimised and even then it could be argued that too many were done. This was largely a function of wanting to provide information for sponsors on four materials. However, working on four diverse materials has helped the author appreciate the diversity, and especially the difficulties of refractory gold ores. In addition, many valuable contacts have been made in industry and in the research community. Most importantly, the work has underlined the importance of elemental sulfur in refractory gold pre-oxidation, and provided the original research niche which makes up the bulk of this thesis.

3.7 REFERENCES

Beattie, M.J.V., Randsepp, R. and Ismay, A., 1989, See chapter 2.

Brooks, D.S. and Flatt, J.R., 1992, Copper, iron and sodium interferences in the determination of gold by atomic absorption spectrometry with particular reference to cyanide solutions, *Analytica Chimica Acta* 264, pp 107-114.

Canterford, J.H., 1994b, See chapter 2.

Dorr J.V.N. and Bosqui F.L., 1950, Cyanidation and concentration of gold and silver ores, 2nd Ed. McGraw-Hill, New York.

Francis, T., 1990, Amdel Laboratories - personal communication.

Kandemir, H., 1988, Personal communication.

Kontopoulos, A. and Stefanakis, M., 1988, See chapter 2.

Prater, J.D., Quenean, P.B. and Hudson, T.J., 1993, See chapter 2.

4 ELECTROCHEMISTRY

4.1 PHILOSOPHY

4.1.1 ADVANTAGES OF ELECTROCHEMISTRY

Electrochemical experimentation can be a very useful part of hydrometallurgical studies. Electrochemical tests, once set up, are relatively quick and can cover numerous variables in a relatively short time. Tests can be quite accurate, and reproducible if meticulous care is taken to duplicate all conditions. The technique is useful for interfacial phenomena, and mostly applied to the early stages of leaching. In the present work, it should predict what will happen at the pyrite-acid interface, although not necessarily at those percentages of oxidation, where, for example, flocculation of individual particles may occur. The equipment can be fairly simple at a cost of say \$10,000. More advanced computerised packages are available from such companies as Princeton Applied Research, for say \$80,000 if justified.

4.1.2 DISADVANTAGES TO ELECTROCHEMISTRY

On the downside, electrochemical experimentation is hypersensitive to technique, and is extremely interpretative in nature. A particular current peak at a given voltage (Eh) may not represent a single phenomenon (such as $\text{Fe}^{2+} \rightarrow \text{Fe}^{3+}$). Many peaks of interest are masked by other, larger occurrences (such as water decomposing). Location of peaks depends on the system, equipment setup, the test variables, the sequence of testing, sample history and just about any other factor imaginable. The literature is extensive, but has never been systematised to provide, for example, a catalogue of peak phenomenon Eh values (Woods 1992).

Without the availability, advice and experience of other workers, electrochemistry is probably not a good idea. The author was fortunate in being able to use equipment at Monash University and to draw on the experience of staff there and from CSIRO Port Melbourne.

4.1.3 EXPERIMENTAL APPROACH

Given the sensitivity and interpretative nature of electrochemical testwork, the decision was made to begin by duplicating previous work. Initially tests were chosen from the equipment calibration manual. Next, the work of Hamilton and Woods (1981) using pyrite in acetic acid buffer (pH 4.6) was duplicated. Ranging tests using 0.5 M H₂SO₄ and then 0.22 M HNO₃ were conducted to determine useful voltage (Eh) ranges and overall pattern.

The bulk of the work considered under "Experimental Results" was conducted using pyrite in 0.22 M HNO₃ (pH 0.7). Tests were done on freshly ground surfaces, taken to different anodic scan limits. The anodic voltage oxidised the pyrite. Sweeping down to a constant cathodic Eh followed in each case, to provide data to analyse the oxidation products. This sequence was repeated at four different temperatures. This work has not been done before, using pyrite in nitric acid.

The thrust of the electrochemical work was to provide insight into the relative formation of elemental sulfur and sulfate. A paper (Flatt and Woods, 1995) summarising this work has been published.

4.1.4 CHAPTER SEQUENCE

Section 4.2 surveys the literature on related work. It begins with a brief description of the technique employed plus interpretation, to help readers unfamiliar with electrochemical experimentation. Some related general points are made. Subsection 4.2.3 deals with previous findings on the ratio of production of elemental sulfur as opposed to sulfate. The majority of this subsection concerns work with at least a component of electrochemistry. Almost no work has been carried out in nitric acid medium. Work by developers of nitric acid processes on sulfur/sulfate ratio is contrasted to electrochemical researchers' results. A broader literature review of nitric acid process testwork and development was given in Chapter 2, Section 2.3.

Section 4.3 outlines the general experimental methods followed, with emphasis on the work which is original to the field. Section 4.4 summarises experimental results of the duplication work which was done to provide confidence in the original work. A brief discussion is included.

Section 4.5 provides results and discussion for Ranging experiments. These were used to target more detailed experiments. The main test series follows in Section 4.6. The method and a typical calculation are followed by summarised results and a

discussion of this series. The main series findings are compared to the literature and related to pre-oxidation of refractory gold ores.

The chapter is summarised in section 4.7

4.2 LITERATURE REVIEW

The method of linear potential sweep voltammetry will be considered first. Interpretation of a relevant sweep trace will be discussed. Some related general observations will be cited. Applicable electrochemical investigations by other researchers will be reviewed. These fall mainly into two key areas. The first is the ratio of elemental sulfur to sulfate produced when oxidising pyrite. The second is the nature of the oxidising sulfide surface.

4.2.1 LINEAR POTENTIAL SWEEP VOLTAMMETRY

4.2.1.1 Technique

The experimental technique follows that of Hamilton and Woods (1981) with minor modifications. A three-electrode cell is used with the working electrode made from the mineral being studied. The counter electrode is platinum and the voltage between the two is measured by a reference electrode (generally calomel). The reference electrode makes use of a Luggin probe to minimise I-R drop. The electrolyte, scan speed, and sweep limits can be varied at the researcher's will. Output from the cell is measured as the current flowing between the working and counter electrodes.

In linear potential sweep voltammetry, measurements commence at a potential at which no current flows. The voltage is increased to a predetermined limit (anodic in the present case) then reduced to a predetermined cathodic limit, then increased to roughly the open-circuit potential, when the scan is terminated. The common term "cyclic voltammetry" is more correctly used when the scan is continued for a number of cycles. The bulk of the present work used only a single cycle, hence the term preferred is linear potential sweep voltammetry (Woods, 1992).

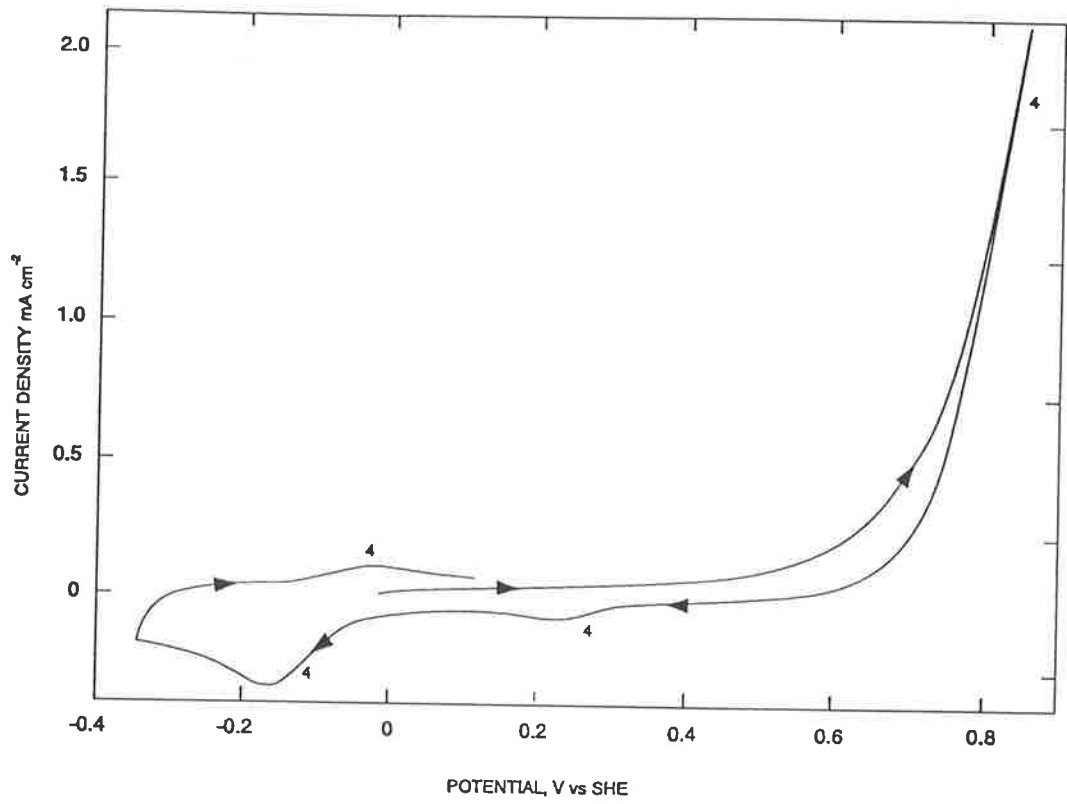


Figure 4.2.1.1: Voltammograms for Stationery Pyrite Electrode at pH 4.6
(from Hamilton and Woods, 1982)

4.2.1.2 Interpretation

Sweep data for fresh-ground pyrite in pH 4.6 acetic buffer electrolyte is given in Figure 4.2.1.1. Sweep 4 was begun at about 0 volts, increased to about + 0.82 volts (vs SHE), then reduced to about - 0.34 volts, then increased back to about + 0.1 volts. The anodic current increases sharply in the region from about + 0.62 volts to + 0.82 volts and then drops rapidly as the potential is reduced. The amount of pyrite oxidised in this region can be calculated from the charge transferred in the region. This in turn can be calculated from the total anodic area under the curve including both the forward and reverse curves. As will be explained later, this region includes oxidation of sulfide sulfur to both sulfate and elemental sulfur.

While the sulfate formed cannot be reduced (Hamilton and Woods, 1981) the elemental sulfur, which remains at the surface, can be reduced. It forms H_2S , giving a cathodic hump which peaks at about - 0.15 volts. Since the sulfur reduced will equal that formed on the anodic portion of the sweep, the sulfate formed at the same time can be calculated. Therefore, as long as the peaks can be resolved (separated from other phenomena) the ratio of elemental sulfur to sulfate formed can be estimated. A typical calculation is given in section 4.3.5.

4.2.1.3 Modifications to Method

The literature is generally in agreement on the importance of fresh polishing of sulfide electrode surfaces to obtain consistent results. Researchers vary in the lengths to which they have gone to ensure that the electrode does not oxidise while it is being polished. Sato (in Hiskey and Schlitt 1982) deoxygenated his polishing water using nitrogen. The nitrogen itself had been dried with $CaCl_2$ and passed over a heated copper plate to ensure it was oxygen free. Hamilton and Woods performed all experiments in a nitrogen-filled glove bag. Ramprakesh et al. (1991) found that polishing in deoxygenated water and then transferring the wet electrode to the cell worked satisfactorily. A second cycle gave the same peak heights as the first scan, showing negligible oxidation had occurred during polishing.

4.2.2 RELATED GENERAL ELECTROCHEMICAL OBSERVATIONS

4.2.2.1 Nature of Pyrite Oxidation

The electrochemical nature of pyrite oxidation was clearly established in the work by Bailey and Peters (1976), Hiskey (1982) cites their "unequivocal evidence" obtained using O^{18} tracer tests. Bailey and Peters proved, in some very clever

work, that the oxygen for pyrite oxidation originates from the water and not the gas phase.

4.2.2.2 Mineral History

Wadsley (1992), approaching the question from a thermodynamics viewpoint, dislikes testing single mineral electrodes. He maintains that history (thermal, physical chemistry) of mineral electrodes from different pyrite sources could lead to different behaviours. He maintains that pyrite in contact with a second mineral phase would have more closely defined properties. For example, it is known that different specimens of pyrite can act as either "n" or "p" type semi-conductors. However, Beigler (1976) (Hiskey and Schlitt 1982) found there was no correlation between electrochemical behaviour of pyrite and its semi-conductor properties. This finding was reinforced by Springer (Hiskey and Schlitt 1982). While these are only two examples, it would seem that mineral history is unlikely to be a cause for electrochemical experimental variation. However, trace impurities, crystal morphology and prior surface oxidation are known to be important.

4.2.2.3 Mechanism Proposals

Hiskey and Schlitt's review (1982) of work on pyrite electrochemistry is an excellent source of information. Amongst other points, the reviewers comment that the mechanisms for pyrite oxidation are very difficult to evaluate. For example, Beigler and Swift (1979) propose one mechanism which shows lower Tafel slopes than those determined experimentally. Other mechanisms have been advanced, but have not been accurate in predicting kinetics. It seems to this writer that there has been little success in postulating detailed mechanisms and rate controlling steps for pyrite oxidation. This view is supported by wide variations in experimental observations as covered in 4.2.3.

4.2.2.4 Active/Passive Pyrite

Hiskey and Schlitt (1982) state at one point that "experimenters cannot agree on rest potentials" for pyrite. This would seem to be mostly a function of the voltammetry experiments themselves. The rest potential should be + 0.34 volts (SHE) based on equilibrium considerations. Peters and Majima (1968) fix it at + 0.62 volts, which actually makes pyrite refractory compared to other base-metal sulfides. This is true for natural pyrite which has undergone some (anodic) oxidation over time. Such pyrite is "passive". However, once the pyrite has been subjected to cathodic currents it becomes "active" with a rest potential close to the equilibrium value.

Thus the source of disagreement cited appears to be the electrochemical experimental history of particular pyrite specimens.

4.2.3 ELEMENTAL SULFUR TO SULFATE RATIO

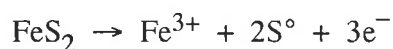
4.2.3.1 Thermodynamic/Equilibrium Considerations

The usual starting point for consideration of oxidising processes, such as pre-oxidation of sulfides for refractory gold ores, is thermodynamics. A generally useful aid in the Eh-pH diagram or Pourbaix diagram. The relevant one for pyrite oxidation is given in Chapter 5, section 2, page (91). Thermodynamics will be discussed in detail in this section.

At the conditions used for the bulk of the electrochemistry testing in this chapter, the equilibrium phase should be pyrite between about Eh 0 volts and + 0.35 volts (vs Standard Hydrogen Electrode (SHE)). Above about + 0.35 volts, the equilibrium phases should be ferrous ion (Fe^{2+}) and sulfate ion ($\text{SO}_4^{=}$). Above about + 0.7 volts ferric ion (Fe^{3+}) and sulfate should be present. Suffice it to say for the present chapter, that equilibrium does not apply. Pyrite requires an over-voltage before it will oxidise, and elemental sulfur persists well beyond its equilibrium conditions. These facts lead to competing reactions for pyrite oxidation.

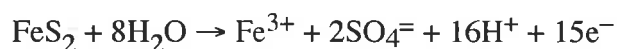
4.2.3.2 Competing Reactions

There are two predominant reactions for pyrite in acid oxidation (Hiskey and Schlitt, 1982)



$$\text{Eh} = 0.340 + .0295 \log a_{\text{Fe}^{2+}} \quad (4.2.3.1.1)$$

and



$$\text{Eh} = 0.354 - 0.067 \text{pH} + 0.0084 \log a_{\text{SO}_4^{=}} \quad (4.2.3.1.2)$$

These two reactions proceed independently at different speeds, which vary widely with test conditions. Elemental sulfur is not an intermediate to sulfate formation, and elemental sulfur once formed, oxidises only slowly. Elemental sulfur once

formed may be stable up to Eh 1.7 volts, a value at which sulfate formation is favoured (Beigler and Swift, 1979).

4.2.3.3 Early Evidence

Workers cited in the review by Hiskey and Schlitt have reported substantial elemental sulfur formation from pyrite although many did not quantify it. These included McKay and Halpern (1958), Garrels and Thompson (1960), Dutrizac and MacDonald (1974). Their conditions and oxidising solutions varied widely.

4.2.3.4 Quantified S⁰/SO₄⁼

There is qualitative agreement that high Eh favours sulfate over elemental sulfur. Hiskey and Schlitt attempted to correlate such quantitative evidence which seemed to correspond to similar conditions. Figure 4.2.3.1 shows sulfate yield as % (the sulfur yield can be taken as 100 - sulfate yield) for work by Bailey and Peters (1976), Meyer (1979) and Beigler and Swift (1979). The range is wide; for example at Eh + 1.0 volts (vs SHE) the workers found from 65 to 90% sulfate yield. (35 to 10% elemental sulfur). Sulfur that was considered negligible above Eh = 1.5 volts).

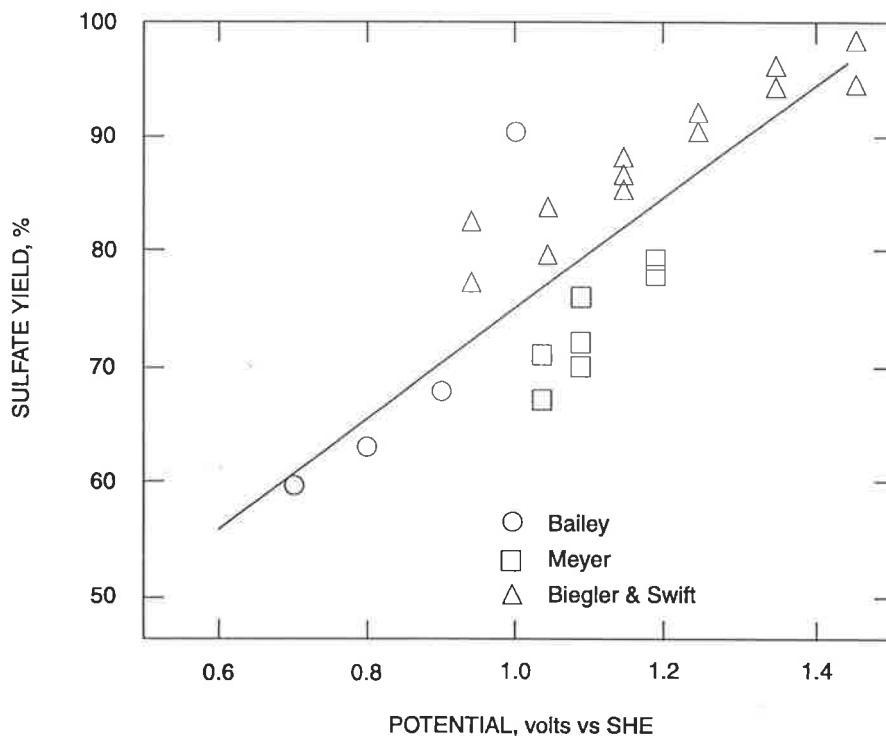


FIGURE 4.2.3.1 Sulfide conversions to Sulphate as Found by various researchers (from Hiskey and Schlitt 1982)

4.2.3.5 Oxidant

It is still evident that the ratio of elemental sulfur to sulfate varies with the oxidising reactant and its concentration. Most work was done in sulfuric acid. Bailey and Peters (1976) working with 1 M H₂SO₄, found 50-90% SO₄⁼ formed. Peters' earlier work with Majima (1968) using 1 M HClO₄ found no elemental sulfur, at 1.05 volts Eh.

4.2.3.6 Temperature Effects

Bailey and Peters (1976) found there was no consistent trend in the S⁰/SO₄⁼ ratio with temperature using 1 M H₂SO₄. Beigler and Swift (1979) stated that there was evidence that the ratio is independent of temperature.

4.2.3.7 Nitric Acid Experimentation

The only electrochemical test using nitric acid was one run by Beigler and Swift (1979). They stated only that 1 M HNO₃ gave a similar Tafel slope to 1 M H₂SO₄.

The bulk of evidence on elemental sulfur yields from pyrite, using nitric acid, comes from the developers of nitric acid processes. None of this work was electrochemical but it is included here, because the thrust of the electrochemical experimentation is elemental sulfur yield in nitric acid.

Almost without exception, the developers using chemical analysis found that pyrite produced very little elemental sulfur. Prater, et al., (1973) found 3% sulfur yields from pyrite oxidation. Van Weert et al. (1988) quoted 3.3% elemental sulfur from pyrite. Beattie et al. (1989) stated elemental sulfur yield was "minor" for pyrite, 20% for arsenopyrite and up to 100% for pyrrhotite. Beattie and Ismay (1990) stated 6% of elemental sulfur was formed, mostly as pellets, from pyrite at 100°C.

The point is that these figures are totally at odds with the electrochemical experiments. Reasons for this will be advanced in Chapter 5 on the pyrite leach tests.

4.2.3.8 Summary S⁰/SO₄⁼ Ratio

The literature is in general agreement that there are two reactions describing pyrite oxidation (Formulas 4.2.3.1 and 4.2.3.2). The reactions are competing and elemental sulfur is a separate product, not an intermediate to sulfate. Once the

elemental sulfur is a separate product, not an intermediate to sulfate. Once the elemental sulfur is formed, it oxidises slowly. High Eh favours sulfate formation, but experimental factors have varied and the sulfur/sulfate yields vary widely. Temperature effects are unclear.

No electrochemical studies using nitric acid have been conducted. The leach work done by developers of nitric acid processes has quoted low (3%) elemental sulfur yield. This disagrees with electrochemical studies performed in other mediums than nitric acid. The discrepancy provided some hope that nitric acid would produce less elemental sulfur than other lixiviants for pyrite.

4.2.4 NATURE OF THE OXIDISING PYRITE SURFACE

4.2.4.1 Technique Advances

More attention has begun to be paid to the actual surface of the pyrite as it oxidises, in an attempt to understand the complex mechanisms. Buckley et al. (1988) state that electrochemistry lacks the molecular specificity to unequivocally identify species. The favoured technique is a combination of electrochemical experiments with techniques which not only quantify elements on the surface of specimens but also the chemical state of these elements. XPS (Xray Photoelectron Spectroscopy) and Raman Spectroscopy have been used.

4.2.4.2 Metal-deficient Sulfides

Work by Buckley et al. (1988) on the surface layers of oxidised pyrite (pH 4.6) cast doubt on the formation of elemental sulfur. XPS showed that the supposed sulfur layer lacked 2 p electron binding energies and also the volatility which would be expected of sulfur (of S₈ at least). The suggestion of the authors was that the resulting layer was a metal-deficient sulfide - the sulfur lattice was unchanged but there were a great many cation vacancies. The stoichiometry of such a layer would be well outside the stable range, but then we know we are dealing with metastability.

Raman Spectroscopic studies by Turcotte et al. (1993) suggest that anodic pyrite oxidation produces polysulfides plus elemental sulfur. The tested range of Eh was + 0.65 - 1.25 volts.

4.2.4.3 Comment

For our present work, Woods (1992) has suggested that no polysulfides will be present below pH2 "to confuse things".

The author cannot help but wonder whether some of the electrochemical experiments were taken far enough (ie % oxidation) to produce elemental sulfur. There may be metal-deficient sulfide present, particularly at low degrees of oxidation, but the evidence for formation of sulfur in leach tests is very strong.

This author has only an exposure to XPS technology. It seems highly interpretative in nature and requires a great deal of experience. The author would not presume to question the interpretation of experts.

4.3. EXPERIMENTAL METHOD (GENERAL)

4.3.1 EQUIPMENT

The experimental equipment consists of three electrodes in an electrochemical cell development by CSIRO

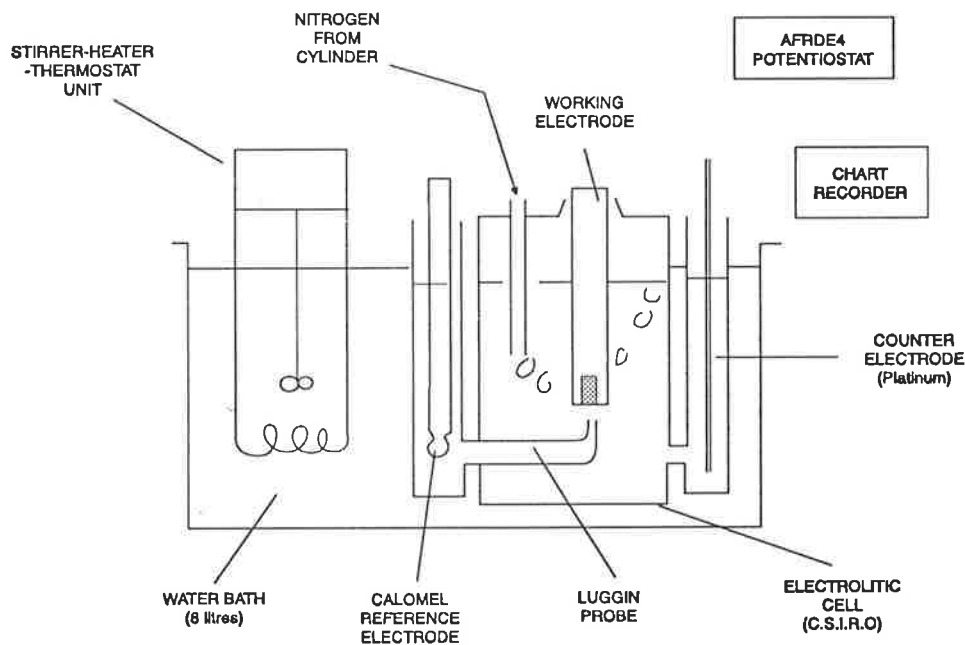


FIGURE 4.3.1.1 Schematic view of Electrochemical equipment arrangement

Figure 4.3.1.1 provides a schematic view of the equipment. The temperature of the cell and electrodes could be maintained within $\pm 1^\circ\text{C}$ by a thermostat-controlled heater in a water bath. The voltage was varied, and current measured, using a Pine Instruments Model AFRDE4 Potentiostat with built-in sweep generator. Current-potential relationships were plotted on a Rikadenki X-Y recorder. Potentials were measured against a saturated calomel reference electrode contained in the cell's side compartment and connected to the main cell via a Luggin probe. All potentials were converted from SCE to SHE (standard hydrogen electrode) scales, taking readings on SCE to be + 0.242 volts against the SHE (Weast et al. 1984). A Pine Instruments electrode rotator was used for early work; later scans mostly left the working electrode stationary.

4.3.2 ELECTRODE FABRICATION

Electrodes were cut from massive crystals of pyrite from Gumeracha, South Australia. Two Gumeracha pyrite electrodes were used, however, with one being an old CSIRO electrode, the other prepared for this work from a massive pyrite sample purchased from Australian Minerals of Hahndorf, S.A. Both electrodes were used on duplication runs at different times and yielded effectively identical results.

Pyrite specimens were connected to threaded brass fittings using silver epoxy. The fittings and pyrite were then "potted" in non-conducting epoxy resin. The epoxy was machined so that the pyrite crystal and the epoxy itself were centred to avoid uneven flowlines in the electrolyte for three experiments requiring electrode rotation.

4.3.3 ELECTRODE POLISHING

Electrodes were rough polished on a finisher. Before voltammetric experiments, a fresh pyrite surface was created by polishing on 200 grade silicon carbide paper. A schematic of the apparatus is shown in Figure 4.3.1.2.

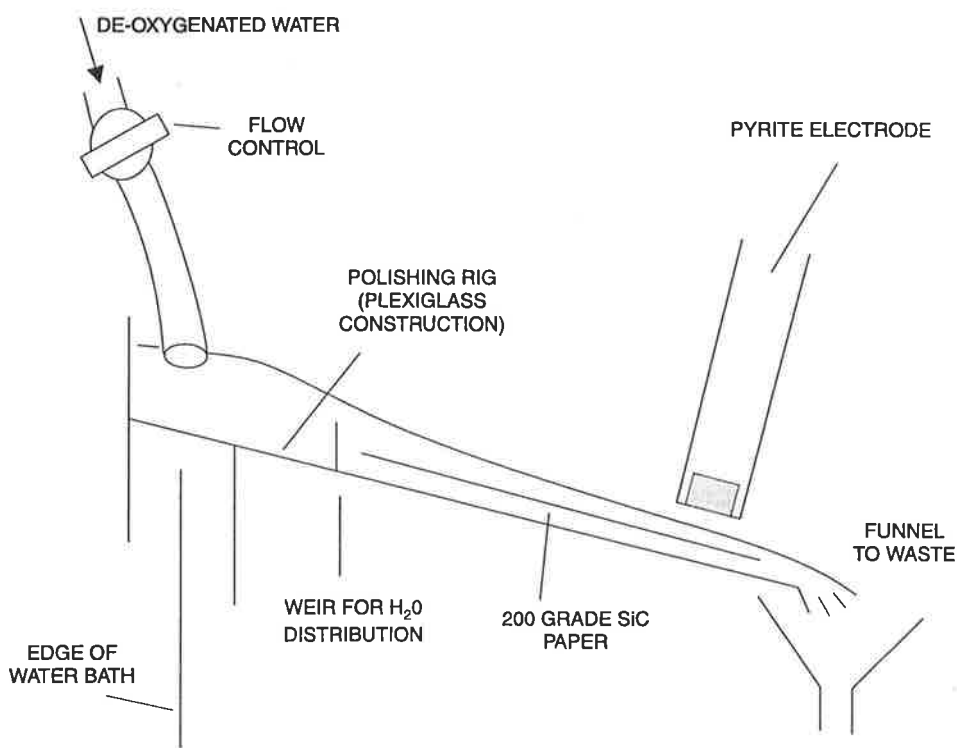


FIGURE 4.3.1.2 Schematic view of Electrode Polishing Apparatus

A stream of distilled water which had been deoxygenated with nitrogen was used for polishing. The method originally included wiping the electrode free of abrasive debris with a tissue. However, more consistent results were found, when the method was modified to let the water stream wash away the debris. The electrode was then transferred, with a layer of water still adhering to its surface, to the experimental cell. The improved consistency of results was attributed to oxidation of the partially cleaned pyrite when a tissue was used. Care was required with the modified method to begin polishing at the "bottom" end of the silicon carbide paper and to move the electrode up the paper for subsequent polishings. This meant the water could not carry debris from the paper to the electrode face. Transfer from washing apparatus to the cell took less than a second.

A number of such refinements were found to be necessary for consistency in the linear potential sweep experiments. The washing refinement is included as an example showing the hypersensitivity of the technique.

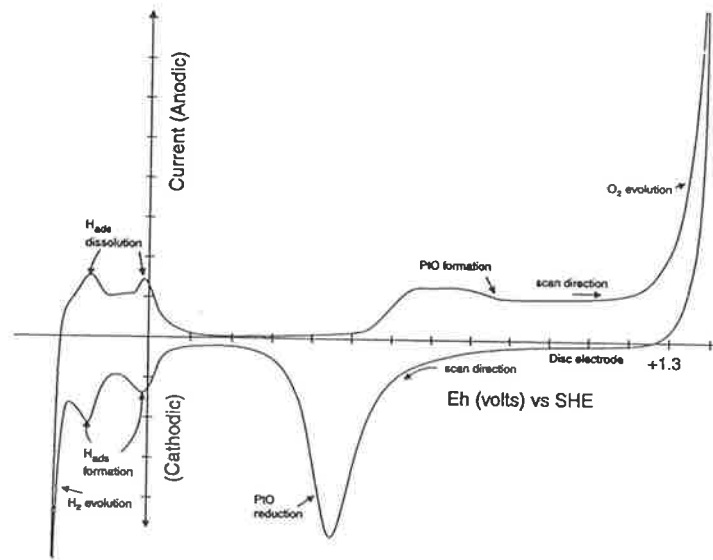


FIGURE 4.4.1.1 Test "A" from Manual

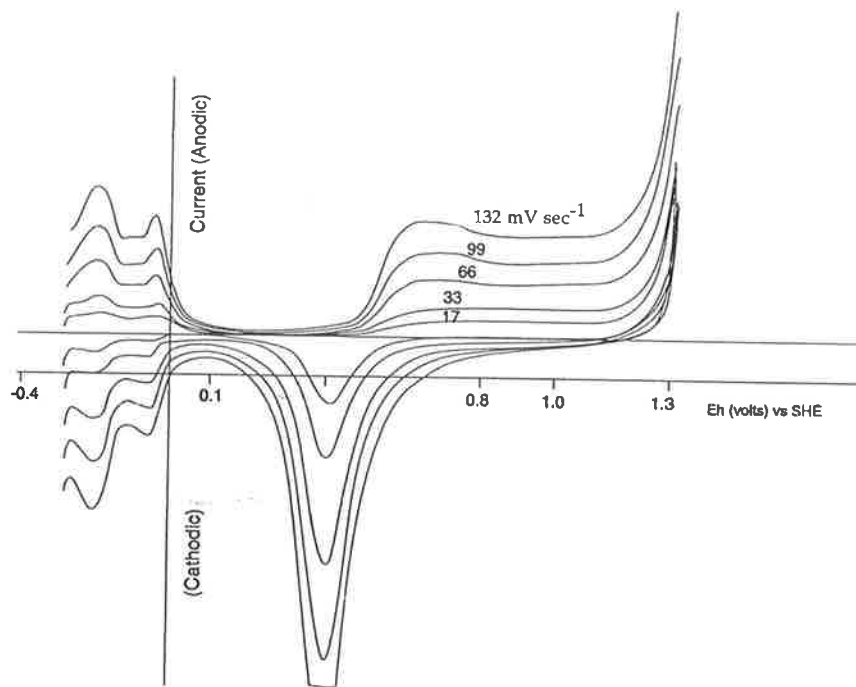


FIGURE 4.4.1.2 Duplication of Manual Tests "A"

4.4 DUPLICATION EXPERIMENTS

4.4.1 EQUIPMENT CALIBRATION

4.4.1.1 Method of Tests From AFRDE 4 Manual

Two experiments from the Pine Instruments manual, using a platinum working electrode were performed. These are recommended by the manufacturer for instrument and equipment calibration. They are also useful learning exercises. The first experiment simply involves the electrochemical decomposition of water. The second involves the effect of rotation speeds on current flow.

4.4.1.2 Results for Equipment Calibration

Figure 4.4.1.1 is a copy of the platinum electrode disc electrode voltammetric sweep trace from the AFRDE4 manual, Test "A". The manual's figure is shown upside down; this is because the American electrochemical convention is opposite to the Australian convention. The Australian convention is used throughout this thesis. The scan rate was not stated.

Figure 4.4.1.2 shows a series of voltammetric sweeps performed. This was using the provided platinum disc electrode as the working electrode, with the identical electrolyte to that of the manual's sweep, namely 0.5 Molar H_2SO_4 . The series consists of 5 different scan rates, as noted on the figure. In both figures the scans are for a "stabilised" electrode, that is, after four-six scans, when the pattern had ceased to change.

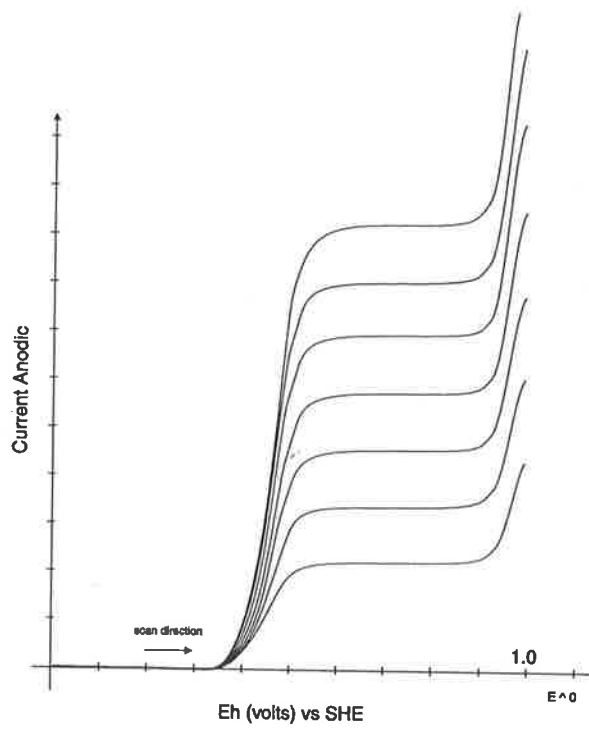


FIGURE 4.4.1.3 Test "B" from Manual

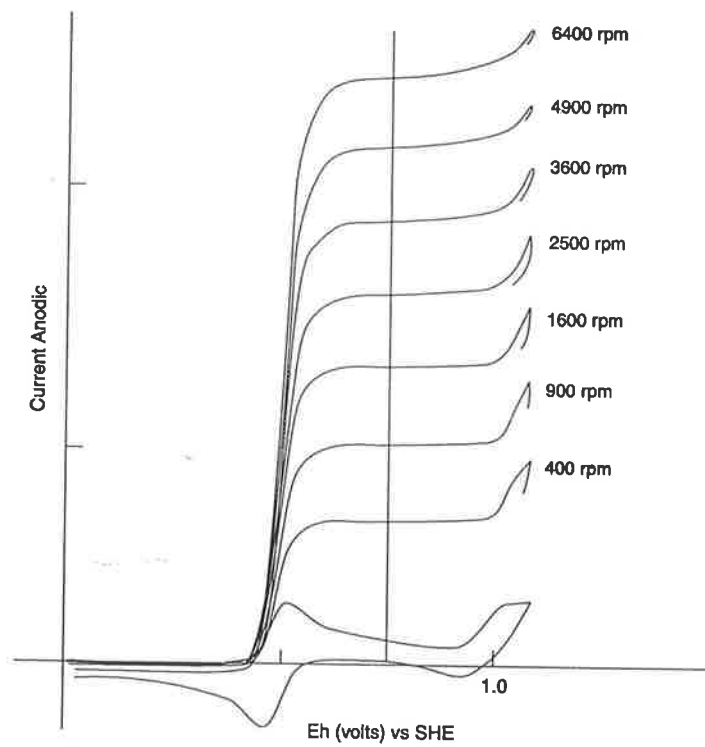


FIGURE 4.4.1.4 Duplication of Test "B"

Figure 4.4.1.3 shows the effect of rotating the platinum electrode at different speeds. This is experiment "B" from the AFRDE4 manual and figure 4.4.1.3 is a copy of the manual's figure. The calculated diffusion coefficient for Iodine from this figure was $0.9 \times 10^{-5} \text{ cm}^2 \text{ sec}^{-1}$.

Figure 4.4.1.4 is the experimental result of a duplicate run to that in the manual. The experimental scans were recorded at slightly lower Eh than those of the manual, due to sensitivity of the chart recorder. The diffusion coefficient for Iodine for this figure was $1.5 \times 10^{-5} \text{ cm}^2 \text{ sec}^{-1}$.

The two experimental figures shown are from some 63 voltammograms which were generated while learning the technique and becoming familiar with the equipment for linear potential sweep voltammetry.

4.4.1.3 Discussion for Equipment Calibration Tests

Platinum Electrode Test "A"

The graphs for platinum electrodes (Figures 4.4.1.1 and 4.4.1.2 page 60) are identical in all important aspects. While both horizontal and vertical scales are different, both figures show similar peaks at similar Eh values.

In the positive-going direction (Australian convention) there is a pronounced, though wide, peak which begins at Eh +0.55 volts, with the current remaining nearly constant to Eh 1.2 volts. This is PtO formation. On the negative-going scan, the PtO reduces, beginning at about +0.6 volts, with a pronounced peak having a maximum value at +0.4 volts. The shape of experimental figure 4.4.1.2 at 66 or 99 mV sec^{-1} most closely approximates the AFRDE4 manual figure.

The figures both show a major peak beginning at Eh = + 1.23 volts and rising rapidly off-graph by Eh = + 1.33 volts. This is the classic water decomposition reaction.



for which Eh = + 1.225 volts (Weast et al. 1984)

Further, both experimental and manual figures show similar mirror-image peaks below 0.0 volts, becoming large cathodic peaks at - 0.30 volts. The first two peaks

are associated with adsorbed hydrogen formation; the large cathodic peak is for hydrogen evolution.

Manual Experiment "B"

Figures 4.4.1.3 and 4.4.1.4 (page 61) are quite similar as well. Both show the same pattern of a current beginning at + 0.4 volts which is pretty much constant in the range 0.5 - 0.9 volts before rising rapidly at about 0.95 volts. Both curves show similar increases in current with increased speed of rotation.

The results of these two experiments showed that the equipment was working properly and calibrated to reasonable accuracy.

4.4.2 HAMILTON AND WOODS EXPERIMENTS

4.4.2.1 Method

The tests of Hamilton and Woods (1981) were duplicated for pyrite and pyrrhotite at pH4.6. The electrolyte was 0.5 M acid plus 0.5 m sodium acetate buffer solution. All experimental conditions were duplicated, namely scan-rate 20 m V sec⁻¹, anodic scan limit + 0.82 volts (SHE), cathodic scan limit - 0.35 volts, X-axis (potential) scale was 0.05 volts cm⁻¹, Y axis scale was 0.02 m A cm⁻¹. The electrode was fresh ground and stationary, although the present work included a second run with the electrode freshground then rotated at 1000 rpm. This was for interpretive purposes. The reference paper (Hamilton and Woods 1981) mentioned effects on rotating the electrode.

These experiments give confidence with the sulfide electrodes, their preparation, the interpretation of the resultant graphs and with subsequent calculations.

4.4.2.2 Results for Hamilton and Woods Duplication

Figure 4.4.2.1. is from Hamilton and Woods (1981). The figure shows only the single scan which was reversed at an anodic limit of + 0.82 volts (SHE). The result is for a freshly ground Gumeracha pyrite electrode.

The current density at Eh = + 0.70 volts (SHE) was 0.45 mA cm⁻² pH was 4.6 with an electrolyte of 0.5 M acetic acid and 0.5 M sodium acetate.

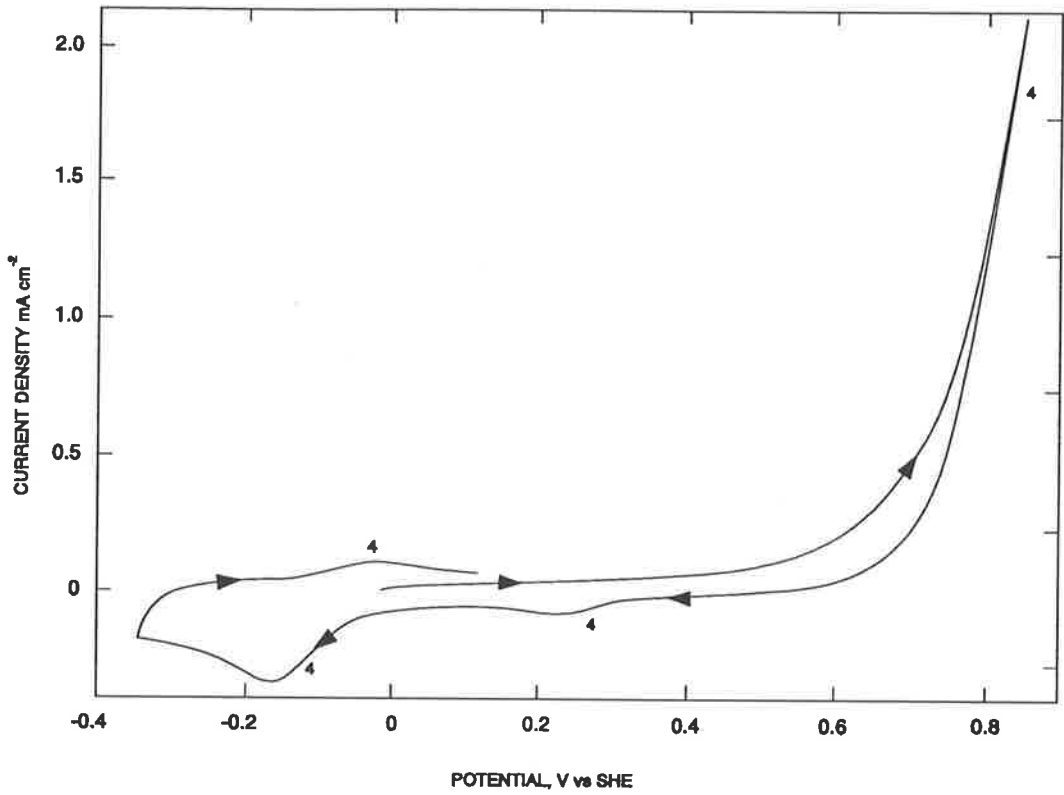


FIGURE 4.4.2.1 Hamilton and Woods Experiment Results

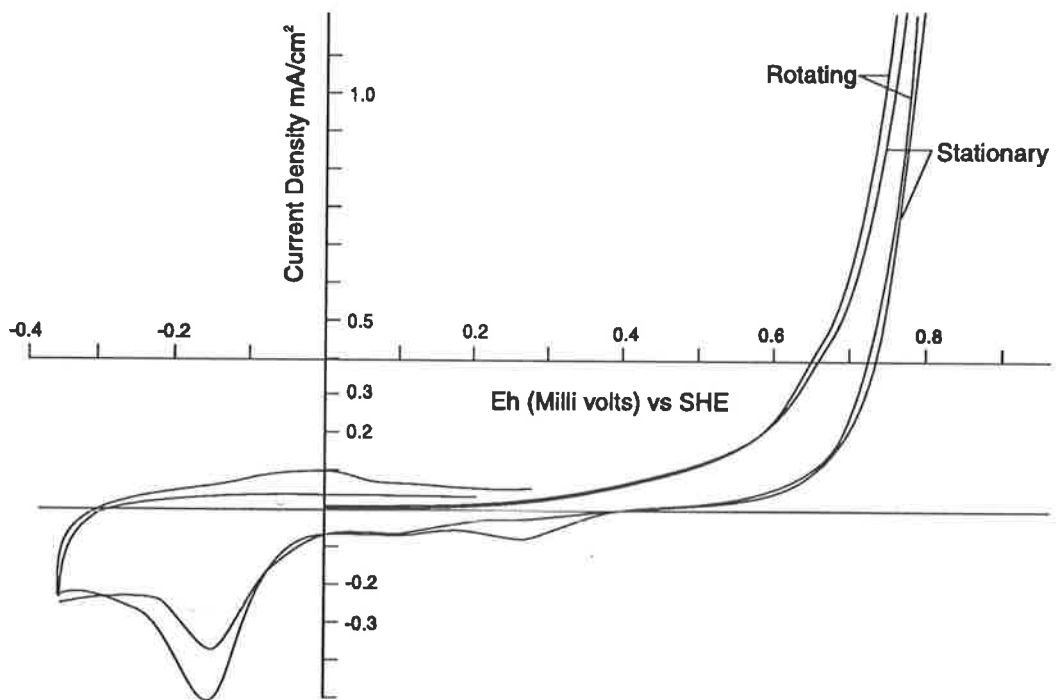


FIGURE 4.4.2.2 Duplication of Hamilton and Woods Experiment

Figure 4.4.2.2 shows the author's experimental duplication of Hamilton and Woods' work. The voltammogram shows two scans, one with a fresh-ground Gumeracha pyrite electrode in the stationary position, the second, with the electrode rotated at 1000 rpm.

All other conditions were a duplicate of those used for Hamilton and Woods' work.

The current density at Eh + 0.700 volts (SHE) was 0.58 mA cm^{-2} .

An identical scan in July 1993 showed a figure essentially the same as figure 4.4.2.2. The current density at Eh + 0.70 volts (SHE) was 0.60 mA cm^{-2} .

In work not presented here, the author also tested a pyrrhotite electrode at pH 4.6. Identical conditions were used to those of Hamilton and Woods (1981).

The two experimental figures shown are from some 15 voltammograms generated while duplicating the Hamilton and Woods work.

4.4.2.3 Discussion for Hamilton and Woods' Duplication

Voltammogram Comparison

Figure 4.4.2.1 (from Hamilton and Woods 1981) and Figure 4.4.2.2 (experimental results from March 1992) are essentially identical. The drawing scales of the two curves are different; figure 4.4.2.2 has a height to width ratio just under double that of figure 4.4.2.1. The peaks are, therefore, slightly more pronounced on figure 4.4.2.2. In electrochemical terms, however, the two match.

Consider the stationary electrode curve of 4.4.2.2. (The rotating electrode curve was run only to help the author's understanding of the electrochemistry.) Both figures show a rise in current beginning at about + 0.40 volts (SHE) and becoming very steep at + 0.60 volts. At + 0.40 volts Fe^{2+} begins to oxidise to Fe^{3+} . The reverse reaction shows on the negative-going sweep as a small, distinct peak which begins at about + 0.35 volts and has a maximum at about +0.28 volts. This peak appears at the identical location on both the experimental and the Hamilton and Woods figures. (The peak disappears when the electrode is rotated (figure 4.4.2.2 only) because soluble ferric ion at the surface has been dispersed by the rotation.)

As the potential falls below 0.0 volts (SHE) a larger cathodic peak appears, attaining a current density of -0.3 mA cm^{-2} at about -0.15 volts. (This value is

for the stationary curve of figure 4.4.2.2 and also for figure 4.4.2.1.) This peak is elemental sulfur reducing to H₂S gas at the electrode surface ($S^0 + 2e^- \rightarrow S^{2-}$).

As the potential returns from the lower limit in a positive-going direction a peak begins to form and reaches a maximum at about 0.0 volts. This is caused by some H₂S which remains at the electrode surface being re-oxidised to S⁰. (For the rotating electrode case in figure 4.4.2.2, the rotation disperses all the H₂S, so the peak is not evident.) Again both the Hamilton-Woods and stationary experimental traces are identical.

Current Density Comparison

The only noticeable difference between the two curves is the higher current density from the author's experimental voltammogram. For a typical potential of + 0.70 volts the current density of the experimental sweep was 0.58 mA cm⁻² vs 0.45 mA cm⁻² or about 30% higher than the Hamilton-Woods sweep. (This is a calculated result, not merely one of drawing scale.) The difference, however, is not significant and could be easily accounted for by a difference in roughness factor for the two electrodes (Woods 1992). Two different experimenters can be expected to achieve different degrees of polishing.

Polishing Technique Modification

As presaged in section 4.2.1.3, oxidation of the electrode during and immediately after polishing the electrode is always a concern. The technique described in section 4.3.1.3 was used with sulfide electrodes. After some time taken to refine the technique it was found to be satisfactory. A second and third scan of a polished electrode (not shown here) would appear at the same heights as the first scan. This shows that no negligible oxide layer was on the electrode before the first scan.

Duplication Standard

The accuracy of duplication was quite acceptable in working with pyrite electrodes and in the polishing and other techniques. This part of the work was particularly helpful in learning about interpretation of the curves. Duplicating the Hamilton-Woods experiment gave considerable confidence to subsequent findings.

4.5 RANGING EXPERIMENTS $\text{HNO}_3\text{-H}_2\text{SO}_4$

4.5.1 PURPOSE

A significant limitation of the equipment was the inflexibility of the chart recorder. While the potentiostat was capable of limits of ± 4.0 volts, the chart recorded was limited to a normal A4 page. Currents can increase dramatically, meaning readings go off-scale and are lost. Extreme currents can also cause the equipment to destabilise. On the other hand, many important features are lost if the scale is too small. All of this means quite a number of tests may be required to deduce appropriate potentiostat amplification and chart settings before a useful recording is achieved.

4.5.2 WIDE POTENTIAL-LIMIT EXPERIMENTS

4.5.2.1 Method for Wide Potential-Limit Experiments

The electrolyte (0.5 Molar H_2SO_4) was chosen as about mid-range of much of the electrochemical literature for pyrite testwork. 0.22 molar HNO_3 was about right for the same pH (0.67 and 0.69 respectively). The electrode was stationary. Scan rates were 20 mV sec^{-1} , reversed at + 1.7 volts SHE (anodic) and - 0.7 volts SHE. X axis (potential) scale was $0.2 \text{ volts cm}^{-1}$ and Y axis (current) scales were 0.2 V cm^{-1} and 10 mA volt^{-1} giving 2.0 mA cm^{-1} . (The potential axis was one quarter as sensitive as for the duplication experiments, the current axes one-tenth as sensitive).

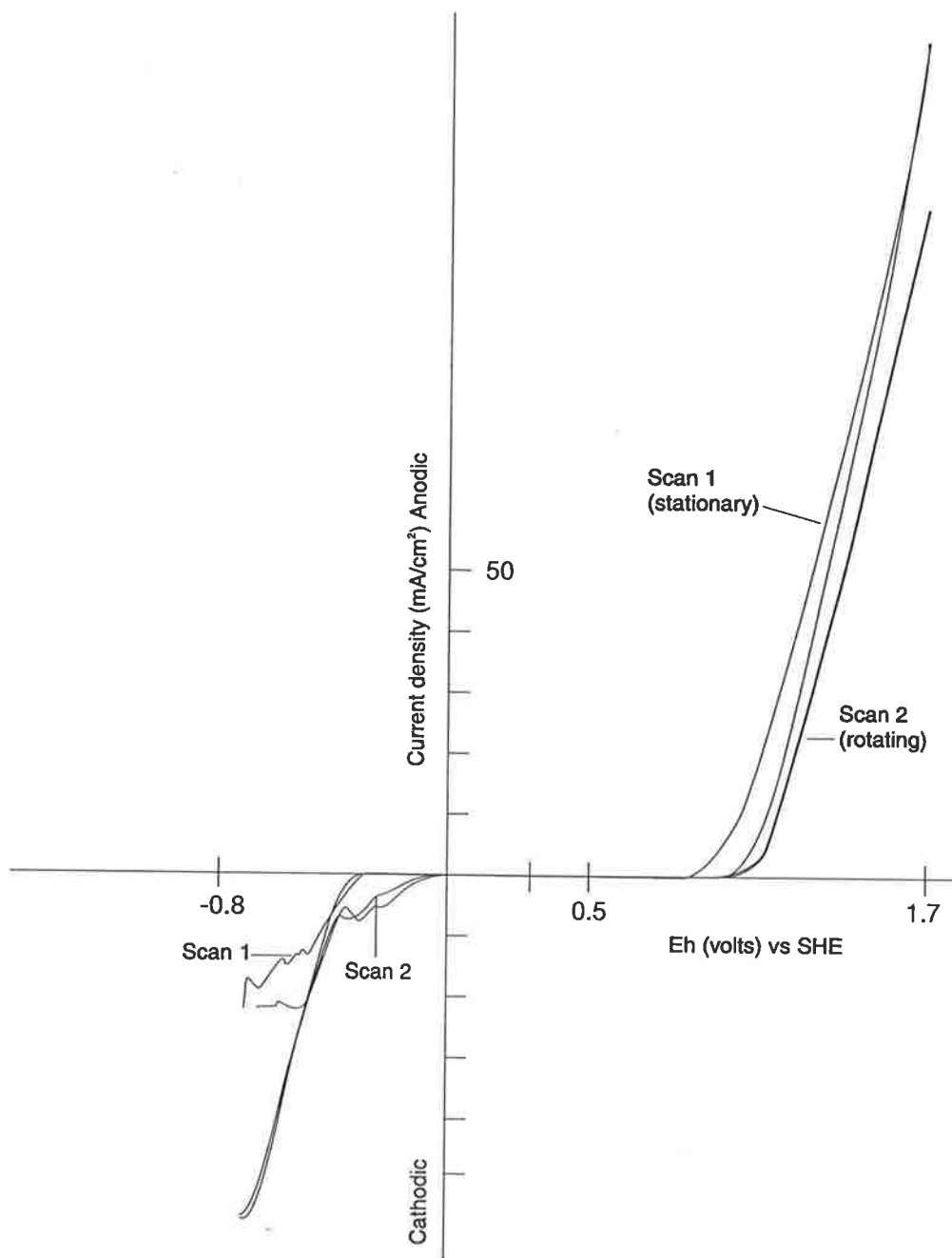


FIGURE 4.5.2.1 Voltammetric sweep for pyrite electrode + 1.7, -0.75 volts in 0.5 M H₂SO₄

4.5.2.2 Results for Wide Potential-Limit Experiments

Figure 4.5.2.1 (opposite page) shows the voltammetric sweep for a pyrite electrode in 0.5 M H_2SO_4 , taken over a wide scan range from + 1.7 volt (SHE) to - 0.75 volts (SHE). The electrode was stationary, with a fresh-ground surface. At these high Eh limits, quite high current densities were achieved - 150 mA cm^{-2} anodic, and over 60 mA cm^{-2} cathodic (the chart went to its limit)

Figure 4.5.2.2 shows the identical sweep for the pyrite electrode in 0.22 M HNO_3 (same pH as the previous figure). This time the anodic current density reached the limit of the chart recorder, but was in excess of 190 mA cm^{-2} . The cathodic current density reached a maximum of 64 mA cm^{-2} at Eh = - 0.7 volts (SHE).

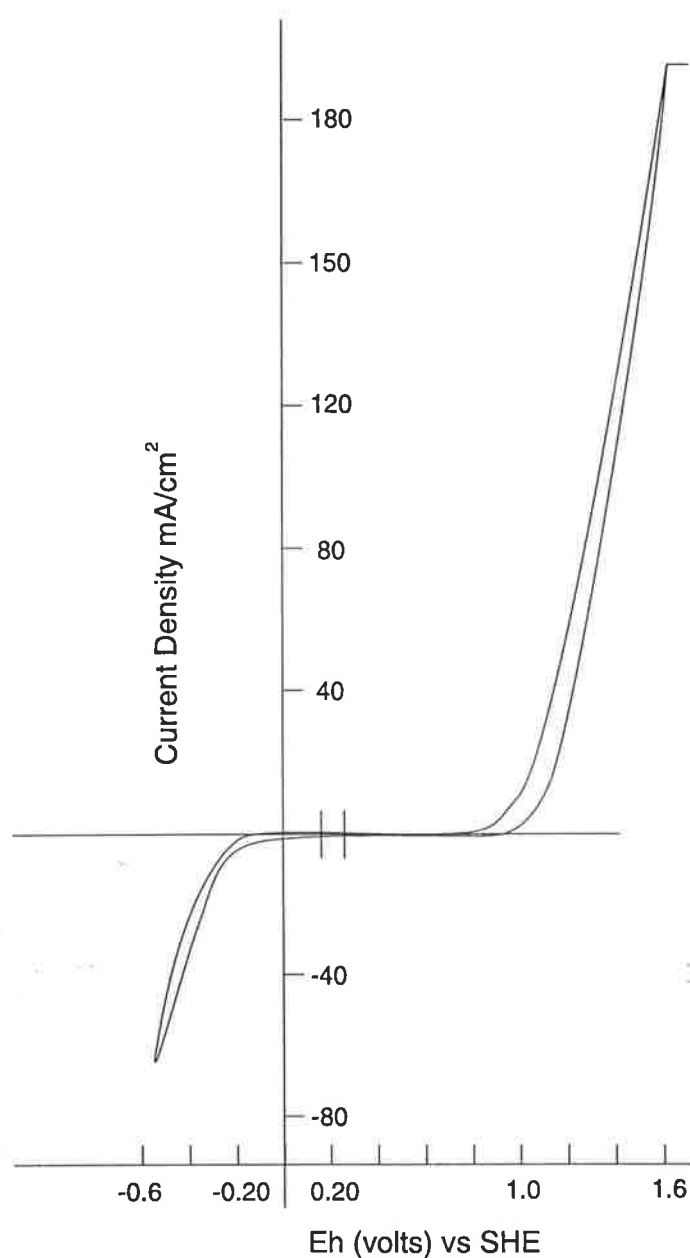


FIGURE 4.5.2.2 Voltammetric sweep for pyrite electrode + 1.7, -0.6 volts in 0.22 M HNO_3

4.5.2.3 Discussion for Wide Potential-Limit Experiments

Figures 4.5.2.1 and 4.5.2.2 (previous pages) are comparable but show a number of interesting differences. The most noteworthy is the significant cathodic double peak which begins at $E_h = -0.05$ volts (SHE) and reaches maximum at -0.30 volts. The peak is present in sulfuric acid and but not for nitric acid. The peak was interpreted as elemental sulfur reducing to H_2S . This led to the hope that for high anodic sweep limits ($+1.7$ volts in this case) nitric acid oxidation of pyrite might not produce elemental sulfur at low temperatures. A relevant fact known from autoclave experience (Chapter 2) is that sulfuric acid does produce sulfur in quantities sufficient to agglomerate unreacted sulfides and to prevent their complete oxidation.

The current densities attained at the larger E_h values of these experiments were both quite high. The nitric acid anodic currents were about 25% higher than for sulfuric acid, showing that HNO_3 is a stronger oxidant. This is for similar pH volumes (0.68) through for lower concentration of nitric acid (0.22 M vs 0.5 M for H_2SO_4). Again this points to the powerful oxidising nature of nitric acid. Cathodic reduction current densities were similar.

4.5.3 HIGHER SENSITIVITY TESTS

4.5.3.1 Method for Higher Sensitivity Tests -- HNO_3 vs H_2SO_4

Linear-potential sweeps were run comparing a pyrite electrode in 0.5 M H_2SO_4 and 0.22 M HNO_3 . The difference from the "ranging" tests were lower scan limits ($+0.970$ volts SHE anodic and -0.280 volts cathodic) and higher sensitivities .05 Volts cm^{-1} for potential and .04 Volts cm^{-1} for current. These tests were for the purpose of observing more subtle differences between the acids with pyrite. Scan speeds were 20 mV/sec $^{-1}$ and the electrode was fresh-ground and stationary for both tests.

4.5.3.2 Results - Higher Sensivity Tests HNO₃ vs H₂SO₄

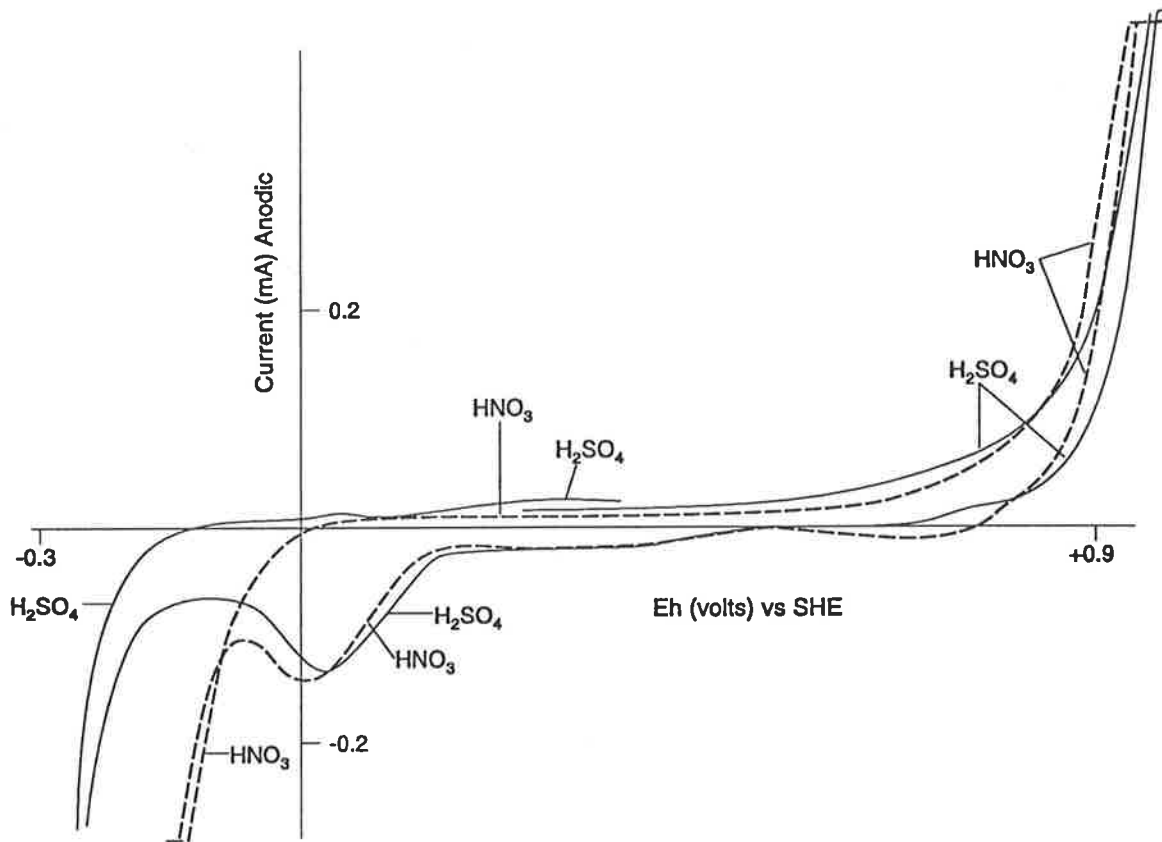


FIGURE 4.5.3.1 Voltammetric sweeps for pyrite electrode + 0.97, -0.28 volts in 0.5 M H₂SO₄ and 0.22 M HNO₃

Cyclic voltammograms for a pyrite electrode at 25°C in —·—·—· 0.22 mol dm⁻³ nitric acid and — 0.5 mol dm⁻³ sulfuric acid. Scans at 20mVs⁻¹ commenced at 0.2V and taken initially in the positive-going direction.

Figure 4.5.3.1 shows a pyrite electrode in both 0.5 H₂SO₄ and 0.22 M HNO₃ on the same figure. The conditions are identical to those of figures 4.5.2.1 and 4.5.2.2 except with much reduced scan limits. Both electrolytes were tested to +0.970 volts (anodic) and -0.280 volts (cathodic). The anodic currents at Eh + 0.70 volts (SHE) were + 0.20 and + 0.26 mA cm⁻² for nitric acid and sulfuric acid, respectively.

4.5.3.3 Discussion for Higher Sensivity Tests

Figure 4.5.3.1 shows the pyrite electrode in the two electrolytes.

Of significance are the cathodic peaks which are located in the range of + 0.15 to - 0.1 volts (SHE). Both electrolytes show this peak, which is sulfur reducing to H₂S, whereas it was not evident for nitric acid in figure 4.5.2.2. The reason for this is that, for the nitric acid - pyrite system, significant elemental sulfur is formed

Table 4.6.1.1: Anodic Settings for Main Test Series

| 26°C Series | | | | | |
|-----------------------------|------|----------------------------|-------------------|-------------------------|---|
| Potential Limit (volts SHE) | Scan | Potential Scale (volts/cm) | Time Scale sec/cm | Current Scale (mAmp/cm) | Charge Scale (mCoulombs/cm ²) |
| + 0.92 | | 0.2 | 10 | 0.2 | 2 |
| 1.02 | | 0.2 | 10 | 2.0 | 20 |
| 1.13 | | 0.2 | 10 | 2.0 | 20 |
| 1.23 | | 0.2 | 10 | 2.0 | 20 |
| 1.33 | | 0.2 | 10 | 2.0 | 20 |
| 1.43 | | 0.2 | 10 | 2.0 | 20 |
| 40°C Series | | | | | |
| + 0.82 | | 0.2 | 10 | 0.04 | 0.4 |
| + 0.92 | | 0.2 | 10 | 0.1 | 1.0 |
| + 1.02 | | 0.2 | 10 | 0.4 | 4.0 |
| + 1.12 | | 0.2 | 10 | 1.0 | 10 |
| + 1.22 | | 0.2 | 10 | 2.0 | 20 |
| + 1.32 | | 0.2 | 10 | 2.0 | 20 |
| + 1.42 | | 0.2 | 10 | 2.0 | 20 |
| + 1.52 | | 0.2 | 10 | 4.0 | 40 |
| 60°C Series | | | | | |
| + 0.92 | | 0.05 | 2.5 | 0.02 | 0.05 |
| 1.03 | | 0.2 | 10 | 2.0 | 20 |
| 1.13 | | 0.2 | 10 | 2.0 | 20 |
| 1.23 | | 0.2 | 10 | 2.0 | 20 |
| 1.33 | | 0.2 | 10 | 2.0 | 20 |
| 1.45 | | 0.2 | 10 | 2.0 | 20 |
| 80°C Series | | | | | |
| + 0.82 | | 0.2 | 10 | 0.1 | 1.0 |
| + 0.92 | | 0.2 | 10 | 0.4 | 4.0 |
| + 1.02 | | 0.2 | 10 | 2.0 | 20 |
| + 1.12 | | 0.2 | 10 | 2.0 | 20 |
| + 1.22 | | 0.2 | 10 | 2.0 | 20 |
| + 1.32 | | 0.2 | 10 | 4.0 | 40 |
| + 1.42 | | 0.2 | 10 | 4.0 | 40 |

Calculations: Column 3 = Column 2/scan speed
 Sec/cm = volts.H_s cm⁻¹/volts sec⁻¹
 Column 5 = Column 4 x Column 3

Milliamp-sec/cm² = mAmp cm⁻¹ x sec cm⁻¹ (1 amp.sec = 1 coulomb)

at lower potentials, but not higher. This was not explained until the following set of experiments (of Section 4.6) were analysed.

Another evident difference in the electrolytes was that the large cathodic peak (which goes off-scale in Figure 4.5.3.1) commences perhaps 0.1 volts sooner for nitric acid than for sulfuric acid. In the case of sulfuric acid, the expected major cathodic reaction is the reduction of pyrite, while for nitric acid it is the reduction of the electrolyte (Flatt and Woods, 1995).

The major anodic peaks which becomes very steep at + 0.8 volts is slightly steeper for nitric acid than for sulfuric. This confirms the greater oxidising power of nitric acid. Finally, there is a slight anodic peak beginning at about $E_h = + 0.2$ volts for sulfuric acid which is not noticeable for the nitric acid. This is likely the $H_2S \rightarrow S^0$ peak for any H_2S which remains at the stationary electrode surface (it disappeared upon rotating). It could be that less S^0 was formed for the nitric acid; a more likely possibility is that the decomposition of the electrolyte at the surface for an extended period from $- 0.1$ to $- 0.28$ volts (9 seconds) dispersed the H_2S gas better for the nitric acid case.

4.6 MAIN TEST SERIES

4.6.1 EXPERIMENTAL METHOD

4.6.1.1 General Conditions

These tests constitute the main electrochemical findings of the present thesis. They were performed to quantify the relative amounts of elemental sulfur and sulfate formed when oxidising pyrite anodically to different anodic potentials (E_h s). All tests were performed in 0.22 Molar HNO_3 electrolyte. The working electrode was Gumeracha pyrite, freshly ground in each case, and stationary. All scans were at 20 mV sec^{-1} . Cathodic settings were similar for each test. The cathodic limit was reversed in the range of $- 0.20$ to $- 0.23$ volts. The potentiostat scale was generally $0.05 \text{ volts cm}^{-1}$ in the cathodic region and the cathodic current scale was usually $0.2 \text{ milliamps cm}^{-1}$. The resulting cathodic charge scale was usually $0.5 \text{ millicoulombs cm}^{-2}$.

4.6.1.2 Anodic Conditions

The independent variable for the different sweeps in a series was the anodic potential limit. This meant that in order to stay on scale and still achieve reasonable

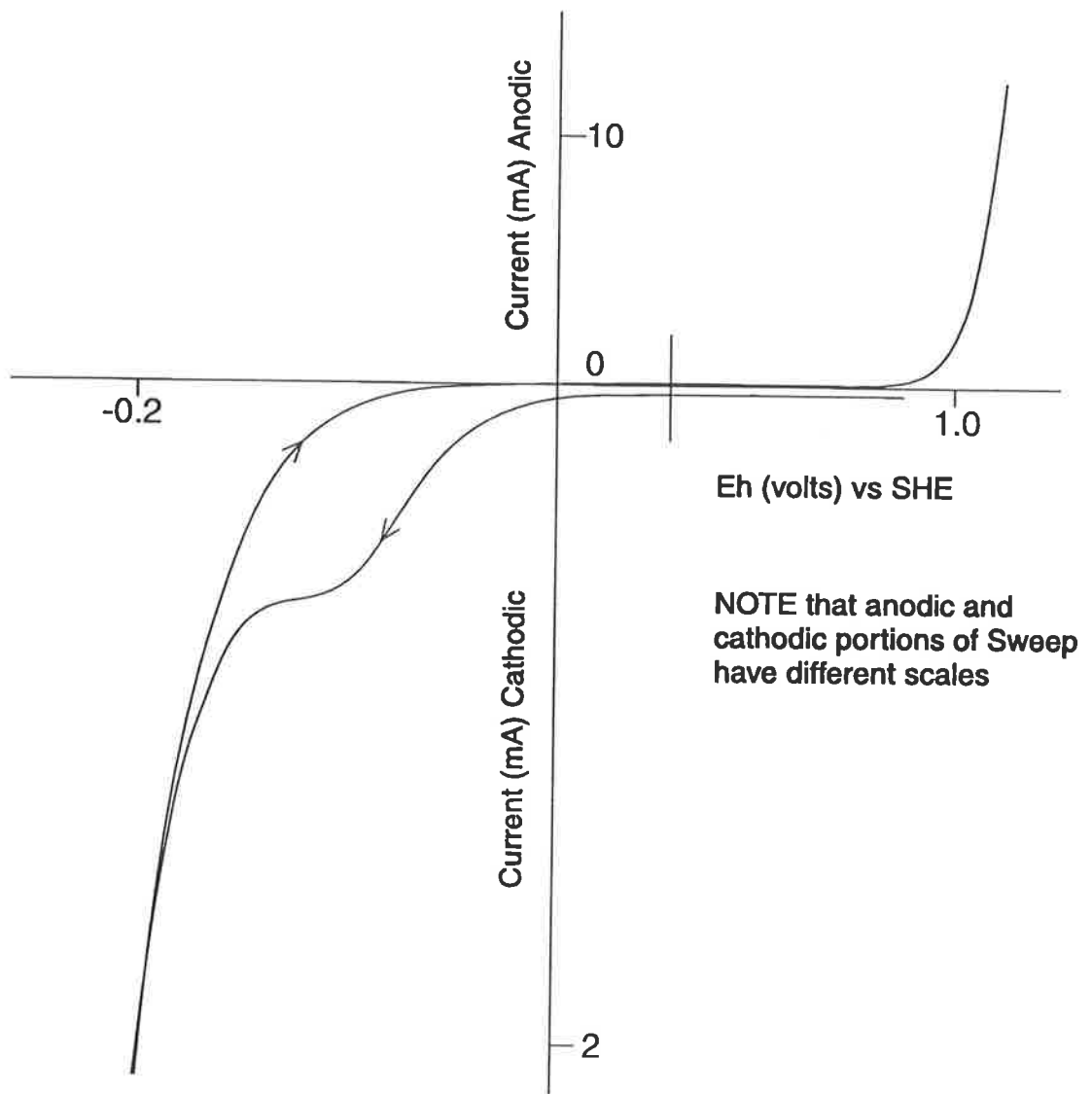


FIGURE 4.6.2.1 Typical voltammetric scan main test series
Pyrite electrode in 0.22 M HNO₃ at 60°C

sensitivity for any measurement, the settings had to be changed during a given sweep. The changeover was affected in the low-current section of the curve as the potential moved below + 0.6 volts towards 0 volts SHE. Any introduced errors appeared minimal and no instrument instability was induced. Anodic sweep settings are given in table 4.6.1.1 (opposite page 69). As can be seen, a series was run at each of room temperature, 40°C, 60°C and 80°C.

4.6.2 TYPICAL VOLTAMMETRIC SCAN

4.6.2.1 Results for Typical Single Scan

Figure 4.6.2.1 (opposite) shows a typical voltammogram in its original form. It shows the entire sweep at 60°C for Gumeracha pyrite in 0.22 M HNO₃. The electrode is fresh-ground and stationary. The upper scan limit was + 1.13 volts for the sweep; that and the temperature were the variables being tested.

4.6.2.2 Discussion for Typical Single Scan

The typical voltammogram shows all the features expected from the ranging experiments. These features are masked for some individual scans but can be deduced from changing trends as the experiments progress. Figure 4.6.2.1 shows an anodic peak beginning at about Eh - 0.80 volts. This is pyrite oxidising to elemental sulfur and sulfate. The scale of this anodic peak is 1/40th of the cathodic section of the sweep, in order to keep the anodic trace within the chart limits.

The cathodic sulfur reduction peak begins at about + 0.12 volts (SHE) and reaches a maximum about - 0.05 volts. Before this reaction is completed, however, the electrolyte reduction peak (which begins at - 0.10 volts at room temperature, probably sooner at 60°C) rises and obscures the second half of the sulfur reduction peak. From Figure 4.5.3.1 this electrolyte reduction appears completely irreversible - the trace comes back on itself, despite the reaction being continued for 9 seconds. Therefore, it is reasonable to assume that for Figure 4.6.2.1, the negative-going cathodic reaction for electrolyte reduction follows the same curve as the subsequent positive-going cathodic reaction for electrolyte reduction. Accordingly, the difference between the negative-going total cathodic curve and the positive-going (or negative-going) electrolyte reaction curve must be attributable to elemental sulfur reduction. This conclusion justifies the method of sulfur charge estimation used in the calculations. Section 4.6.3 gives an example.

4.6.3 TYPICAL CALCULATIONS

4.6.3.1 Data Source

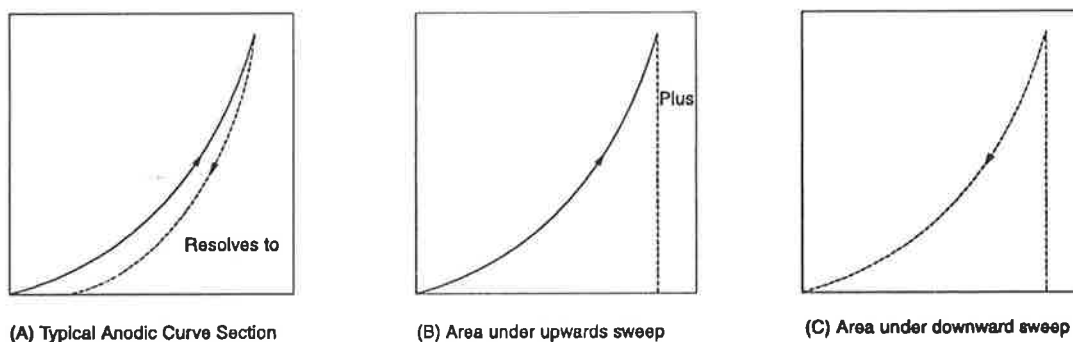
Calculation of the amount of pyrite leached (moles) to elemental sulfur and to sulfate requires two source of information. From the experimental voltammetric sweep graphs, the charge passed may be ascertained. From the reaction chemistry, the stoichiometry and then the charge required for oxidation and reduction reactions can be obtained.

4.6.3.2 Charge Passed

Figure 4.6.2.1 (page 70) gives the linear potential sweep data for 60°C at an anodic limit of 1.13 volts (SHE). The effect of the change in current scale (mentioned previously) is that the cathodic region is amplified 40 times compared to the anodic region (0.5 mC cm⁻² vs 20 mC cm⁻² respectively).

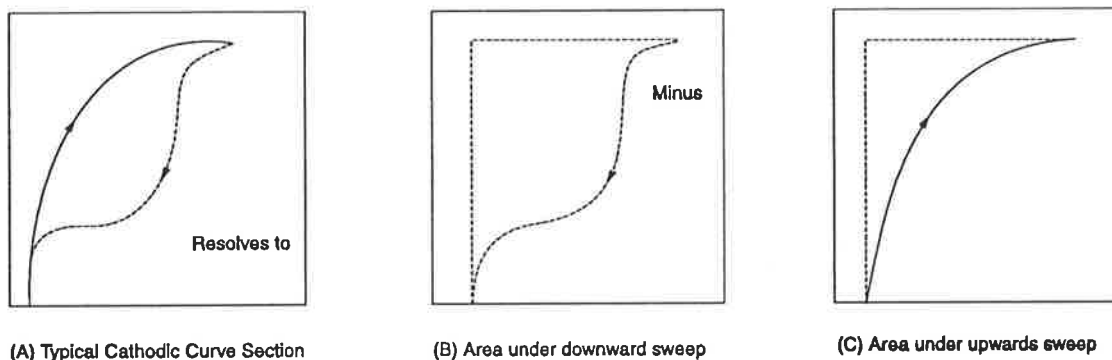
To calculate the charge it is necessary to integrate the appropriate areas under the curve.

From Figure 4.6.2.1, the anodic area is fairly straightforward. The charge passed is proportional to the area under the curve on the upwards sweep plus the area under the curve on the downwards sweep. Both upwards and downwards sweeps in this region are anodic-pyrite is being oxidised to ferric ion plus sulfate plus sulfur. The upwards area marginally exceeds the downwards area - this is probably because the surface which has undergone some oxidation is marginally less active due to coatings of, for example, iron hydroxides. Repeated scans without intermediate polishing display the same trend.



SKETCH 4.6.3.1.

The cathodic curve area of concern becomes a little more tricky to resolve as the anodic limit is increased. At 60°C and an anodic scan limit of + 1.03 volts the $S^0 \rightarrow H_2S$ "bump" is fairly separate and distinct. At + 1.13 volts (Figure 4.6.2.1), the sulfur reduction "bump" begins to merge with the larger peak which results from the reduction of the electrolyte $HNO_3 + 3H^+ + 3e^- \rightarrow NO + 2 H_2O$. Accordingly, the area of the sulfur reduction "bump" was considered to be that under the negative going sweep minus that of the return sweep for electrolyte reduction.



SKETCH 4.6.3.2.

The logic of this subtraction is that electrolyte reduction could be expected to follow curve 4.6.3.2c) if there were no elemental sulfur present.

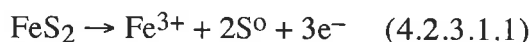
The curves were integrated by the rudimentary method of expanding the experimental graphs on a photocopier, cutting out the curves with scissors and weighing them, then applying appropriate scaling factors. Sophisticated computer packages are available for this task with such equipment as the PAR voltammeter but the equipment was in use by others when the author was at Monash University.

For Figure 4.6.2.1

| | Anodic | Sulfur |
|-------------------------------------|--------|--------|
| Area weight (g) | 0.0341 | 0.0630 |
| Area (cm ²) | 4.53 | 8.37 |
| Charge scale (mC cm ⁻²) | 20 | 0.5 |
| Area (millicoulombs) | 90.7 | 4.18 |

4.6.3.3 Reaction Chemistry

The anodic reactions given earlier were



and



If x moles of pyrite are oxidised to elemental sulfur and y moles of pyrite are oxidised to sulfate, then the total charge passed is $(3x + 15y)F$ coulombs where F is Faraday's constant.

The sulfate formed anodically is irreversible, but the sulfur will be reduced when the voltage is sufficiently cathodic viz:



resulting in the transfer of $4F$ coulombs per mole of pyrite oxidised to sulfur on the preceding anodic sweep.

Thus the amount of charge passed for sulfate formation and the moles of sulfate formed, can be calculated for a given curve.

4.6.3.4 Fraction of Pyrite Oxidised to $\text{S}^0/\text{SO}_4^{2-}$

For the example of Figure 4.6.2.1 (+1.13 volts anodic limit; 60°C , electrode area 0.15 cm^2) the calculation is as follows:

$$\begin{array}{ll} \text{Anodic moles} & 90.7 \times 10^{-3}\text{C} = (3x + 15y) \times 96,500 \\ \text{(sulfate + sulfur)} & (4.6.3.2) \end{array}$$

$$\begin{array}{ll} \text{Cathodic sulfur moles} & 4.18 \times 10^{-3}\text{C} = (4x) 96,500 \text{ C mole}^{-1} \\ (4.6.3.3) & \end{array}$$

$$\text{From (4.6.3.3)} \quad x = 1.08 \times 10^{-8} \text{ moles } \text{S}^0 \text{ produced.}$$

Then from (4.6.3.2)

$$y = 6.05 \times 10^{-8} \text{ moles } \text{SO}_4^{2-} \text{ produced}$$

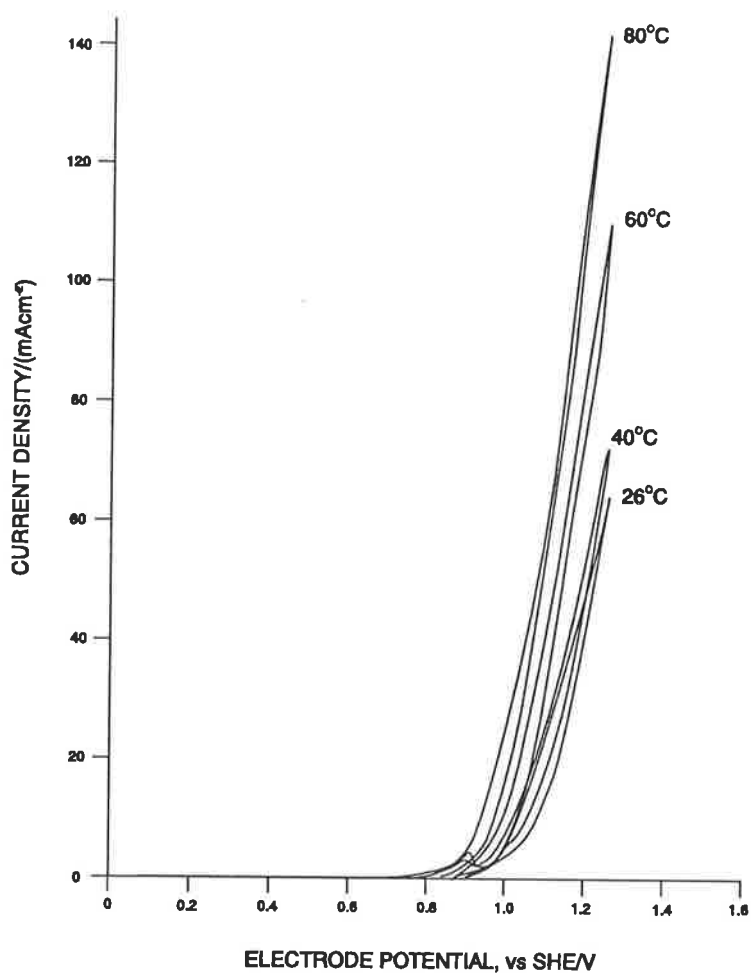


FIGURE 4.6.4.1. Anodic sections of voltammograms for a pyrite electrode in 0.22 mol dm^{-3} nitric at 25°C , 40°C , 60°C , and 80°C . Scans at 20 mVs^{-1} taken in the positive-going direction from near the rest potential and reversed at 1.23 V in each case.

This means the conversion of pyrite was:

$$\frac{x}{x+y} \times 100\% = \frac{1.08}{(1.08 + 6.05)} \frac{x10^{-8}}{x10^{-8}} \times 100\% \approx 15\% \quad \text{to sulfur for this particular voltametric sweep}$$

4.6.3.5 Oxidation Rate

For this Gumeracha pyrite electrode, the exposed area was 0.15 cm². Therefore the oxidation rate was:

$$\text{to sulfur } \frac{1.08 \times 10^{-8}}{0.15} = 7.2 \times 10^{-8} \text{ moles/cm}^2$$

$$\text{to sulfate } \frac{6.05 \times 10^{-8}}{0.15} = 40.3 \times 10^{-8} \text{ moles/cm}^2$$

4.6.4 MAIN TEST SERIES RESULTS AND DISCUSSION

4.6.4.1 Data Presentation

The data in this section is a summary of some 26 voltammograms generated (in June-July 1993) on pyrite in nitric acid. The work in that period comprised some 108 voltammograms in all. Many were for the purposes of setting up, familiarization and re-calibrating.

Only summary figures are presented here, chosen to show overall trends as to how increasing temperature and scan limits affect the pyrite-nitric acid system. The emphasis of calculations was on the relative rates of formation of elemental sulfur and sulfate.

4.6.4.2 Results - Temperature Effect on Current Density

Figure 4.6.4.1 (page opposite) is a summary of the anodic segments of 4 voltammograms at different temperatures. In each case, the anodic scan limit was + 1.23 volts (SHE). All curves are to the same scale.

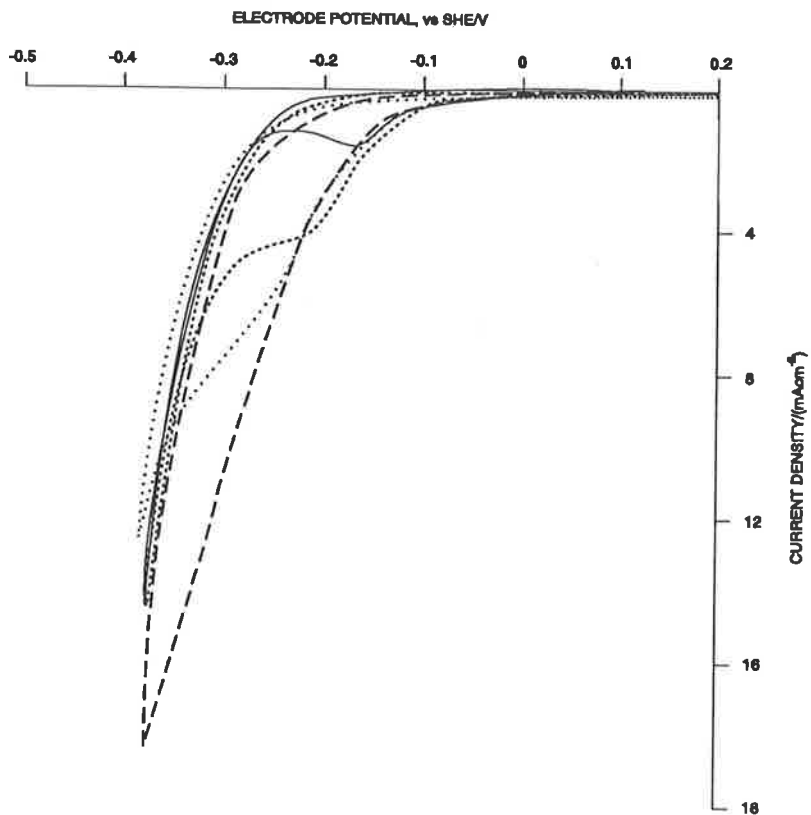


FIGURE 4.6.4.2 Cathodic portions of cyclic voltammograms for a pyrite electrode at 60°C taken initially in the positive-going direction from near the rest potential and reversed at ——— 1.03, ······ 1.13, - - - - - 1.23 and - · - · - 1.33 V. Scan rate 20mVs⁻¹.

4.6.4.3 Discussion - Temperature Effect on Current Density

Figure 4.6.4.1 shows the effect of temperature on current density. While the current density and, therefore, the reaction speed, increases with temperature, the effect is not as marked as could be expected. As a broad rule, 10°C of temperature increase can be expected to double the rate of a reaction; however, the current density shows an increase which averages 23% per decade of temperature, at this anodic potential limit (+ 1.2 volts). Whether this approximation from electrochemical data translates into any meaningful kinetic data remains to be seen, in Chapter 5. It must be remembered that these particular voltammograms apply to a pyrite oxidation time of about 42 seconds only.

4.6.4.4 Results - Anodic Scan Limit Effect on Sulfur Produced

Figure 4.6.4.2 (page opposite) is a summary of the cathodic segments of 4 voltammograms at 60°C, but with different anodic limits.

4.6.4.5 Discussion - Anodic Scan Limit Effect on Sulfur Produced

Figure 4.6.4.2 shows the effect of scan anodic limit on sulfur reduced during the cathodic portions of the sweeps. It is the areas of the cathodic peaks which are important. The amount of elemental sulfur produced during the anodic portion of the sweeps increases as the sweep limits increase. This make perfect sense as long as some elemental sulfur is produced as well as sulfate. The increase in area of the cathodic peaks with higher (anodic!) limits means there was more anodic sulfur available to be reduced. The increasing amount of sulfur is evident from the increasing area of the cathodic peaks as the anodic limit increases. The four curves of figure 4.6.4.2 convert to the figures in Table 4.6.4.1.

4.6.4.6 Results - Fraction of Pyrite Oxidised to S⁰/SO₄⁼

Table 4.6.4.1 is a summary of all the calculated data from the 26 voltammograms testing temperature and anodic limit. The data is tabulated in the form of moles of elemental sulfur or sulfate per cm² of pyrite electrode. (See section 4.6.3 for a typical calculation). Tests were conducted at four temperatures and 5 to 8 anodic limits.

Table 4.6.4.1: Moles of sulphur and sulphate produced by electrochemical oxidation of pyrite in nitric acid on potential scans at 20 m Vs⁻¹.

| Upper potential limited | 26°C | | 40°C | | 60°C | | 80°C | |
|-------------------------|--|------------------------------|------|------------------------------|------|------------------------------|------|------------------------------|
| Volts vs SHE | Moles / 10 ⁸ cm ⁻² of Pyrite | | | | | | | |
| | S° | SO ₄ ⁼ | S° | SO ₄ ⁼ | S° | SO ₄ ⁼ | S° | SO ₄ ⁼ |
| 0.82 | | | 1.1 | 0.2 | | | 2.2 | 1.5 |
| 0.92 | 0.43 | 0.69 | 1.8 | 1.4 | | | 28% | 5.7 |
| 1.02 | 1.7 | 2.6 | 2.5 | 8.9 | 2.5 | 9.4 | 6.4 | 24 |
| 1.12 | 3.9 | 19 | 4.5 | 21 | 7.2 | 40 | 15 | 73 |
| 1.22 | 4.7 | 52 | 7.3 | 56 | 11 | 83 | 16 | 215 |
| 1.32 | 4.1 | 107 | 5.4 | 103 | 14 | 212 | 11 | 310 |
| 1.42 | 2.6 | 196 | 2.8 | 185 | 1 | 335 | 3.3 | 426 |
| 1.52 | | | 2.4 | 245 | | | | |

The data from table 4.6.4.1 was recalculated to give % of sulfide sulfur (from pyrite) oxidised to elemental sulfur (as opposed to sulfate). These figures were plotted against anodic limit in figure 4.6.4.3.

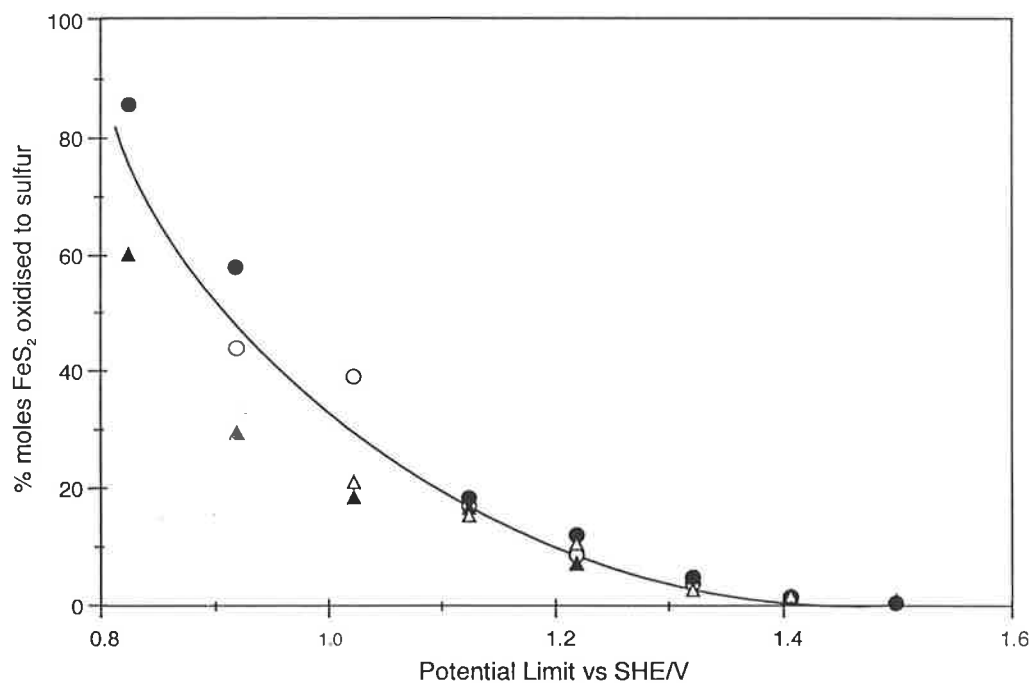


FIGURE 4.6.4.3 Dependence of proportion of pyrite sulfur oxidised to sulphate as a function of the upper potential limit of the scan
 ○, 25°C; ●, 40°C; △, 60°C; ▲, 80°C.

4.6.4.7 Discussion - Fraction of Pyrite Oxidised S^0/SO_4^{2-}

The calculations for the 60°C series of scans are given in Table 4.6.4.2.

Table 4.6.4.2:

| Anodic Limit (volts) | Cathodic Curve Area (cm ²) | S^0 mC S^0 | moles x 10 ⁻⁸ per cm ² S^0 |
|----------------------|--|----------------|--|
| 1.03 | 2.83 | 1.42 | 2.5 |
| 1.13 | 8.37 | 4.18 | 7.2 |
| 1.23 | 12.45 | 6.22 | 11 |
| 1.33 | 15.41 | 7.71 | 14 |

Although it is not shown in this table, the amount of elemental sulfur produced generally levels off as the anodic scan limit reaches about 1.3 volts. All voltammograms showed less sulfur available to be reduced at an anodic scan limit of + 1.3 volts or higher. That effect is apparent from Table 4.6.4.1 (page 76).

Anodic Scan Limit Effect on Sulfate Produced

While the total area under the anodic curves increases with temperature at constant Eh, as in figure 4.6.4.1, it increases much more dramatically with anodic limit at a given temperature. The effect is shown clearly in Table 4.6.4.1. Most of this increase is due to sulfate produced at higher Eh values.

Anodic Scan Limit Effect on S^0/SO_4^{2-} Ratio

Table 4.6.4.1 also shows the fundamental findings of the electrochemical work. The moles of sulfur and sulfate formed by pyrite oxidation are tabled for each scan limit and each temperature. The effect of anodic scan limit is obvious - the amount of sulfate increases by factors of from 280 to over 1200 when increasing the anodic limit from + 0.82 volts + 1.42 volts, depending on the temperature.

Meanwhile, the amount of elemental sulfur peaks for each temperature at between 1.22 and 1.32 volts. Whether this is due to less S^0 being actually formed at Eh > 1.22 volts, or to that S^0 which is formed being itself oxidised to sulfate, is not evident from the electrochemical work. That question brings up the further question of the oxidation rate of elemental sulfur, which is addressed in Chapter 5 of the present thesis.

The data from Table 4.6.4.1 is easily converted to % of pyrite oxidised to sulfur. The converted figures are presented in Figure 4.6.4.3 (page 76). Two trends are clear. First, the % of sulfur formed drops off rapidly with Eh. Second, the % of the elemental sulfur is more or less independent of temperature.

4.6.4.8 Comparison to Literature

The Eh-S⁰ trend in Figure 4.6.4.3 is in keeping with various findings in the literature. The "best" of the literature reviewed suggested a correlation which was plotted as Figure 4.2.3.1 (Page 54). Figure 4.6.4.4 below is that same figure, with the asterisks added to show the findings of the present work.

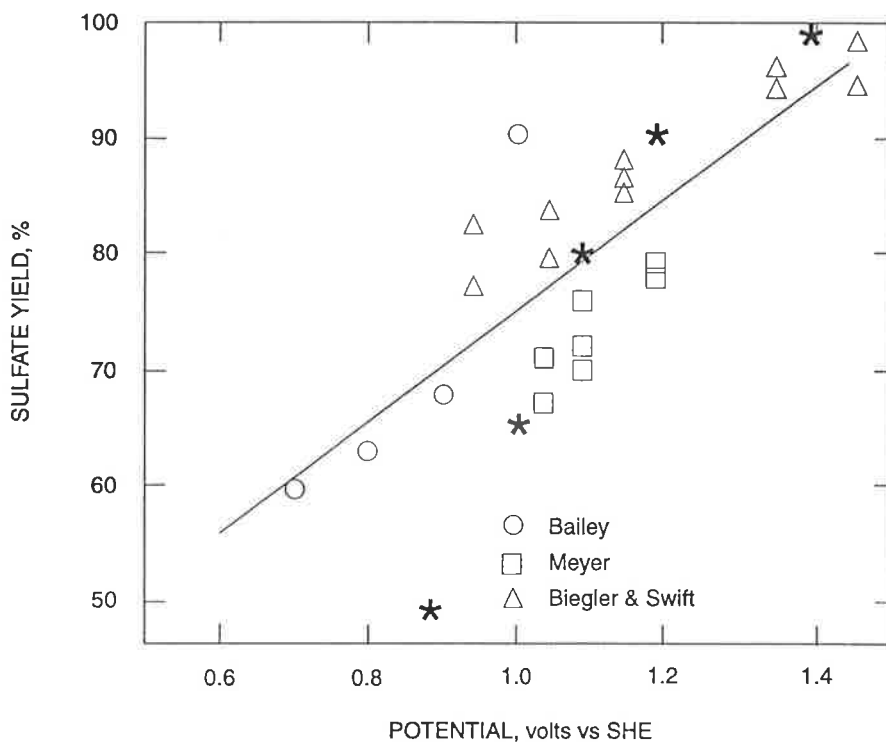


FIGURE 4.6.4.4. Comparison of experimental sulfate yield to literature

The results are not strictly comparable. The Hiskey and Schlitt (1982) plot was a compilation of three researchers' work. Not all of their results were from electrochemical work and none of it was in nitric acid. Nevertheless, the general trend is similar and the results above Eh about + 1.0 volts are within the cited researchers' range. The present work indicates that little S⁰ will be found if the Eh is above + 1.4 volts (SHE).

Below Eh about + 1.0 volt, at least in nitric acid, the present work shows that a considerably higher proportion of elemental sulfur is formed than was previously reported in the literature.

The second trend, that the proportion of elemental sulfur is independent of temperature, also has a precedent. Beigler and Swift (1979) using electrochemistry and 1.0 M H₂SO₄ electrolyte, found that "there are indications that the sulphate yield at fixed potential is independent of temperature". The present work would seem to present strong evidence to that effect.

It should be mentioned that the present work is for a specific system. Only one acid, at a single concentration, was tested. Only pyrite, from a single source, was tested. As with the other work cited from the literature, the findings here cannot necessarily be extended to all sulfide oxidation, or to all refractory gold pre-oxidation processes. The pyrite-nitric acid system is much more thoroughly investigated, using leach tests, in Chapter 5.

4.6.4.9 Nature of the Oxidising Pyrite Surface

Inspection of Figure 4.6.4.2 (page 75) will show that there is a subtle shift in the location of the sulfur peak with anodic limit. As the anodic limit increases by 0.1 volts, the maximum of the sulfur peak shifts to the left by perhaps 50 millivolts for Figure 4.6.4.2. This pattern is evident at all temperatures, at least for as long as the sulfur peak maximum is distinguishable. The shift varies widely but seems to average about - 30 millivolts per 0.1 volt increase in anodic limit. The sulfur peak appears to keep moving leftwards even in those cases where the absolute amount of sulfur decreases. (There are the scans for which it was very difficult to distinguish sulfur peaks from electrolyte peaks.) If this is true, the shift cannot be due merely to an increased thickness of any sulfur layer on the surface (Flatt and Woods, 1995). Thus there would seem to be a change in the nature of the layer itself.

This change would be consistent with those authors who suggest that sulfur may be present in another chemical state at the electrode surface. There is no indication from the electrochemical work as to whether this could be metal-deficient sulfide or polysulfides.

A calculation on the "sulfur" coverage of the electrode surface was performed for the 80°C, 1.22 volts anodic limit case. 9 millicoulombs charge was passed, giving about 16×10^{-8} moles of "sulfur" per cm² of pyrite. Given sulfur's density of 2, a guesstimated amorphous atomic packing factor of 0.5, and a guesstimated surface relative roughness of 2, the sulfur layer would be ≈ 60 atomic layers thick. This would seem awfully thick for a metal-deficient lattice to exist.

4.6.5 RELATION TO PRE-OXIDATION

4.6.5.1 Relation to Literature

As discussed in section 4.2.3.7, developers of nitric acid processes reported very little (< 3%) elemental sulfur produced when pre-oxidising pyrite. The present work has found that there is significant elemental sulfur produced at Eh values which are achievable with nitric acid systems - less than + 0.97 volts (SHE). At this value, 40% sulfur could be expected. This is more in keeping with other researchers' findings. That the present electrochemical findings are not totally inconsistent with the developers' reported figures will be addressed in Chapter 5.

4.6.5.2 Temperature Independence

That the temperature does not affect the proportion of elemental sulfur formed is also significant for developers. They tend to operate at + 180°C and report no elemental sulfur problems at those temperatures. If the electrochemical findings are correct, the S⁰ must have roughly the same activation energy as SO₄⁼, since the relative rates are temperature independent. This would tend to suggest that the developers are using conditions which allow all the S⁰ already formed to itself oxidise to sulfate.

4.6.5.3 Kinetic Oxidation Rate

A calculation was performed using the data from the voltammogram at + 1.02 volts anodic limit, 80°C. The Eh in the region for pyrite oxidation would be in the range of 1.02 to 0.82 volts, since oxidation only begins at the lower figure. The average weighted by the current is 0.95 volts (SHE); at 20 mV sec⁻¹ scan rate, it would apply over 20 seconds (up and back). A solution Eh of 0.97 volts should be about the limit attainable with nitric acid (Weast et al. 1984). According to the electrochemical data, a sweep which averaged 0.95 volts would oxidise 15 x 10⁻⁸ moles of pyrite in 20 seconds per cm² of surface area. (This would produce 6 x 10⁻⁸ moles cm⁻² of S⁰ and 24 x 10⁻⁸ moles cm⁻² of SO₄⁼ in that time, see table 4.6.4.1). This is equivalent to 91 x 10⁻⁸ grams of pyrite oxidised per second per cm² of pyrite surface area. This figure will be compared to appropriate leach test rates in Chapter 5.

4.7 SUMMARY OF ELECTROCHEMICAL FINDINGS

4.7.1 MAIN FINDINGS

The main linear sweep voltammetry series showed that pyrite in nitric acid oxidised to both elemental sulfur and sulfate. Sulfur is not an intermediate, it is a separate product. The proportion that oxidises to elemental sulfur decreases as the Eh of the system is increased. This parallels similar findings, in other electrolytes, reported in the literature. The results in nitric acid compare well quantitatively to those parallel findings above Eh + 1.0 volts (SHE). However, considerably more S⁰ was found, for example 50% S⁰ at + 0.90 volts Eh, than had been reported below + 1.0 volts.

The proportion of pyrite oxidising to elemental sulfur was found to be independent of temperature. This agrees with limited data in the literature. Unexpected peak shifts from the voltammograms suggest the nature of the oxidising surface of the pyrite changes with Eh. This could be consistent with a metal-deficient sulfide.

4.7.2 RELEVANCE TO REFRACTORY GOLD PRE-OXIDATION

Developers of nitric acid pre-oxidation routes have reported little (< 3%) elemental sulfur formed. The contrary findings of the present work, plus the temperature independence of sulfur proportion, could be important to developers. Besides improving fundamental understanding, the present work could be important if lower-temperature routes are explored.

The present results indicate that above Eh = + 1.4 volts no elemental sulfur would result. However, this Eh is unattainable in commercial nitric acid leaching systems.

4.7.3 QUESTIONS RAISED BY ELECTROCHEMICAL WORK

The present work has raised several questions which may be answered in part by the leaching work to be described in Chapter 5. Foremost of these questions is the oxidation rate of the elemental sulfur once it is formed. The kinetics of the elemental sulfur to sulfate reaction will be critical to developers of nitric acid routes, since it appears almost certain that formation of some sulfur cannot be avoided.

The extent to which electrochemical data can predict actual leaching kinetics remains to be demonstrated. The nature of the oxidising surface has only been hinted at.

Whether this is important at the macroscale and whether elemental sulfur morphology becomes important, remain to be addressed by the leach tests in the next chapter.

4.8 REFERENCES

- Bailey, L.K. and Peters, E., 1976, Decomposition of Pyrite in acid by pressure leaching and anodization; the case for an electrochemical mechanism, *Canadian Metallurgical Quarterly*, 15, (4), pp 333-344.
- Beattie, M.J.V. and Ismay, A., 1990, see chapter 2.
- Beattie, M.J.V., Randsepp, R. and Ismay, A., 1989, see chapter 2.
- Beigler, T. and Swift, D.A., 1979, Anodic behaviour of pyrite in acid solutions, *Electrochimica Acta*, 24, Pergamon Press, 415-420.
- Buckley, A.N., Hamilton, I.C. and Woods, R., 1988, See chapter 2.
- Flatt, J.R. and Woods, R., 1995, A voltammetric investigation of the oxidation of pyrite in nitric acid solutions: Relations for treatment of refractory gold ores, *J.Applied Electrochemistry*, 25, pp 852-856.
- Hamilton, I.C. and Woods, R., 1981, An investigation of the surface oxidation of pyrite and pyrrhotite by linear potential sweep voltammetry, *JElectroanalytical Chemistry*, 118, pp 327-343.
- Hiskey, J.B. and Schlitt, W.J., 1982, See chapter 2.
- Peters, E. and Majima, H., 1968, Electrochemical reactions at pyrite in acid perchlorate solutions, *Canadian Metallurgical Quarterly*, 7(3), pp 111-117.
- Prater and Queneau, 1973, See chapter 2.
- Ramprakash, Y., Koch, D.F.A. and Woods, R., 1991, The interaction of ion species with pyrite surfaces, *J.Applied Electrochemistry*, 21, 531-536.
- Turcotte, S.B., Benner, R.E., Riley, A.M., Li, J., Wadsworth, M.E. and Bodily, D.M., 1993, Surface analysis of electrochemically oxidized metal sulfides using raman spectroscopy", *J.Electroanalytical Chemistry*, 347, 158.
- Van Weert, et. al., 1988, See chapter 2.
- Wadsley, M., 1992, verbal communication.

Weast, R.D., Astle, M.J. and Bayers, W.K., 1984, CRC handbook of chemistry and physics, CRC Press Inc., Bass Rate, Fla., D-157.

Woods, R., 1992, verbal communication.

5 PYRITE LEACH TESTS

5.1 PHILOSOPHY

5.1.1 AIMS OF LEACH TESTS

The broad aim of this chapter is to elucidate the chemistry of the pyrite-nitric acid system. The approach adopted is to study variables relevant to, and in ranges relevant to, the pre-oxidation of refractory gold-bearing sulfides.

Elemental sulfur often causes problems in sulfide leaching systems. Limited studies of its formation and role are available in the literature. In particular, its occurrence during nitric acid leaching has not been studied in detail. A specific goal of the leach testwork then, is to elucidate and quantify the formation and oxidation of elemental sulfur. Hopefully, the formation can be avoided, or the oxidation accelerated, to the point where elemental sulfur is eliminated as a problem.

Both the broad and specific goals are seen as being useful to developers of nitric acid pre-oxidation routes.

5.1.2 GROUPING OF VARIABLES

It will be shown that a range of variables which can affect oxidation rates in the pyrite-nitric acid system is large. This leads to a large study and in turn to a long chapter. Long chapters are apt to lose the reader, so it has been thought wise to group the variables and factors studied.

Classical kinetic variables will constitute the first group. The effects of the classical variables are usually anticipated from general kinetic knowledge. This study will quantify the order of chemical dependencies and the rate constants. Classical variables include stirring rate, temperature, particle size and the concentration of the principal reagent. For the present study, an investigation of the low-temperature variants of nitric acid pre-oxidation, the principal reagent is nitric acid. For low-temperature variants, acid is regenerated externally to the leach step and recycled.

The second group of tests will verify internal consistency of experimentation. The basic leach method was duplicated to establish variability of results. Concerns that the pyrite itself may age will be addressed. This could have a serious effect on the test program itself, more so because the study was undertaken part-time over thirty months.

The third group of variables include those of a more practical nature. These variables may not be as satisfying for a theoretical study, but have commercial implications. The industrial group includes sulfuric acid and ferric iron concentrations. Both will be present in plant recycle liquors. Chloride ions effect will also be studied. It is present in significant amounts in most mine waters. Pulp density will be studied in this group, as will blends of feed particle sizes. All other work was performed on narrow size fractions, as this aids the study of other variables' effects. Most products from grinding circuits, however, have a considerably wider size range. Again the effect of these industrial variables on pyrite leach kinetics will be quantified.

The final group of tests has been named "additional factors". It includes variables suggested by reading or discussion, plus phenomena which have been observed from the leach tests and are considered worthy of discussion. The former category will include attritioning, attempts to modify the Eh of the system, and silver ion addition. The observed phenomena which will be studied further include additivity of variables' effects and presence of lag or induction period after which the leach rate accelerates. The variation of pyrite leach behaviour with source was not an intentional variable of the study. However, sample quantity requirements dictated using two pyrite sources and these will be compared as part of this group.

5.1.3 CHAPTER SEQUENCE

The chapter will follow a standard logical sequence but be ordered by the grouping described above. Section 5.2 is the literature review. It will address the applicability of thermodynamics to the pyrite-nitric acid system and to elemental-sulfur formation in particular. It will summarise previous kinetic studies. Finally, the levels of specific variables suggested by the literature will be addressed. Those variables will be grouped as described above: classical; industrial; and other. The literature review will finish with a summary.

Section 5.3 is a general description of the leach-test method and the rationale behind the author's decisions. The specific levels at which the variables have been tested will be left to their appropriate "results and discussion" sections. The list is long and would need repeating later anyway.

Section 5.4 will describe one typical test in some detail. This is to familiarise the reader with the form of results from most tests and how the elemental sulfur is quantified. A single test will show the pattern for sulfur. Later sections summarise the series of tests. These summaries do not show the sulfur present as clearly. The reader intrepid enough to want to see original data for the individual tests is referred to the "Supplementary Volume - Raw Data". While this volume is not officially part of this thesis, copies are kept in the libraries of the University of Adelaide and the University of South Australia. Section 5.4 will also address the question of elemental sulfur as opposed to a metal-deficient lattice, which was raised in Chapter 4.

Section 5.5 will present the summarised results and discussion for the four classical variables of the first grouping. Included will be the effects of the variables on the measured "sulfur gap".

Section 5.6 will summarise and discuss the results for leach test consistency and possible pyrite aging.

Section 5.7 will summarise results and discuss the five series of tests for industrial variables.

Section 5.8 will provide and discuss summarised results for the six factors of the additional factors category. This will bring the total series analysed to seventeen.

Section 5.9 is the mathematical analysis section. It is here that the reader will find most of the quantification of variables' effects on leach rates. Here too, will be tackled the quantification of the rates of elemental sulfur formation and oxidation. Simulation of these two rates will be related to the observed sulfur gaps for a number of cases.

Section 5.10 will relate the findings of the leach tests to the literature, to the electrochemical work described in Chapter 4, and to pre-oxidation of refractory gold deposits.

Section 5.11 will summarise the findings of the chapter. This will simply be an overview, as most sections will include their own summaries. Although this structure has some repetition, it was thought wise for such a long chapter. The philosophy will be to guide the reader so he or she does not lose his or her way in the labyrinth of experimental conditions addressed by the leach tests.

5.2 LITERATURE REVIEW

5.2.1 INTRODUCTION

Extensive literature exists on pyrite oxidation. However, the range of experimental conditions described are varied. Hiskey and Schlitt (1982) alone quote roughly twenty sources. A number of references naturally overlap with Chapter 4 of this thesis. Individual findings are often conflicting. In order to rationalise this amount of material, this review has been organised into three subsections, namely, thermodynamics, kinetics and experimental conditions. The *thermodynamics* subsection will discuss the relevant classical equilibrium diagrams. The emphasis will be on the limitations of such diagrams, leading to the concept of metastable, elemental sulfur.

The *kinetics* subsection will review the bulk of the literature on pyrite oxidation kinetics, originating before 1982, in summary form. A recent investigation concurrent to that of this thesis, and specific to nitric acid and pyrite, will be dealt with in more detail.

It became obvious early in the present investigation, that the results varied widely with experimental conditions. The third subsection will focus on conditions suggested by the literature. (Details of these experimental conditions are the subject of Section 5.3.) The present chapter's experimentation covers some seventeen variables. Therefore, this subsection will be further broken down, into the same classification as the variables themselves. These are, somewhat arbitrarily, '*classical*' kinetic variables, '*industrial*' variables and '*additional*' variables.

The literature review will finish with a summary.

5.2.2 THERMODYNAMICS AND METASTABLE SULFUR

The application of classical thermodynamics to the modelling of metallurgical processes encounters a number of limitations. These seriously constrain the

application of thermodynamics analysis to the present work. If thermodynamic equilibrium was to be attained, elemental sulfur (S^0) and the sulfide from which it is formed, should not exist at the conditions of Eh and pH used in the present study.

Past efforts towards applying thermodynamics to sulfide mineral oxidation are summarised. Measures to try to reconcile classical Eh-pH diagrams with kinetic limitations are outlined.

5.2.2.1 Classical Thermodynamics of Sulfide Oxidation

The most popular method for describing the reactions which occur during sulfide oxidation is the Eh-pH diagram or Pourbaix diagram.

For the process being studied, nitric acid functions as a catalyst (Raudsepp, Peters and Beatie, 1987). Hence, from a thermodynamic perspective, the Me-S-H₂O systems are of interest, rather than those systems containing nitrate (Wadsley 1990, Wong 1991).

House (1987) summarises a number of limitations of classical Eh-pH diagrams:

- experiments which form the basis for such diagrams are conducted at unrealistically low concentrations in order to assume unit activities of reactants.
- the diagrams represent reactions assuming dissolved species whereas leaching occurs at phase interfaces.
- most thermodynamic data was generated at room temperature.
- equilibrium is seldom economic in an industrial process; sometimes it is not even approached.
- solid reactants and products vary considerably and may have important effects not anticipated by the classical diagram.

Table 5.2.2.1 lists conditions assumed by classical analysis, as opposed to "real" conditions for the "Redox" and similar industrial processes. It can be expected that such limitations also apply to computerised data bases, such as CSIRO's "Thermodata" package.

House's bibliography on metal-water system Eh-pH diagrams is comprehensive. He identifies the Cu-Fe-S-H₂O system as the best researched.

Table 5.2.2.1 Limitations of Classical Eh-pH Diagrams

| Limitations | Classical Conditions | Industrial Conditions ("Redox" Process) |
|-----------------------------|---------------------------------|--|
| Concentrations of reactants | 10 ⁻⁶ M | 3m nitric acid; 10 ⁻² to 10 ⁰ M iron species |
| Reaction location | Between dissolved species | gas-solid interfaces or gas-liquid interfaces |
| Temperature | 25°C | 85-180°C |
| Equilibrium | Assumed | Seldom attained due to time (financial) constraints |
| Nature of solid species | Defined only as "unit activity" | Affected by other species, impurities, history of mineral and surface morphology |

Sato (1960) reviewed alternative approaches to studying sulfide oxidation. Analytical approaches are imprecise because sulfur possesses many oxidation states (-II through to + VI) and oxidation proceeds by a series of consecutive reactions. Mineralogical data fails to provide direct information on mechanisms and rates, although it can give clues on the direction and relative rates of reactions. Kinetic studies can be inconclusive due to system complexity and rate-limiting factors. Electrochemical work also has disadvantages such as synergistic effects and mineral potentials which drift.

Sato proposed oxidation steps for the Cu-S, Pb-S, Ag-S, Zn-S and Fe-S systems. He also suggested that S₂ molecules are released from sulfide-matrix surfaces during oxidation.

In the conclusions of his paper, Sato immediately leaps from broad principles to suggested specific oxidation steps for the common sulfide minerals. Although his experiments may well have substantiated this leap, it is not justified in the paper reviewed. Accordingly, Sato's paper was flawed; admittedly, this is a facile statement by this writer, given his easy historical perspective and subsequent investigators' findings.

Sato spelled out the need to fit experimental observations on electrode sign, potential magnitude, pH dependency and variation of production activity with any proposed reaction step. In this, he pointed out some of the difficulties workers have encountered in this field.

*

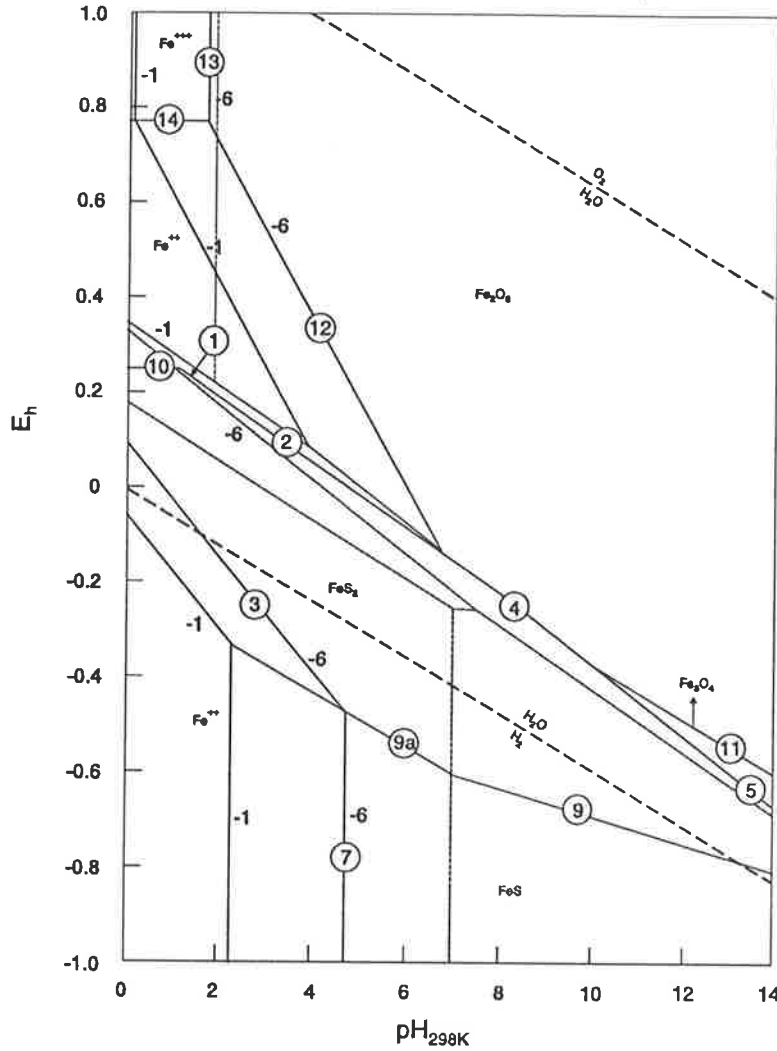


FIGURE 5.2.2.1 Equilibrium Eh-pH diagrams for Fe-S-H₂O systems at 25°C, 1 atm (from Ferreira, 1995)

Iron Oxides and Sulphides-Water System

Reactions

- (1) $Fe^{2+} + 2HSO_4^- + 7H_2 = FeS_2 + 8H_2O$
($Fe^{2+} + 2HSO_4^- + 14H^+ + 14e = FeS_2 + 8H_2O$)
- (2) $Fe^{2+} + 2SO_4^{2-} + 2H^+ + 7H_2 = FeS_2 + 8H_2O$
($Fe^{2+} + 2SO_4^{2-} + 16H^+ + 14e = FeS_2 + 8H_2O$)
- (3) $FeS_2 + 2H^+ + H_2 = Fe^{2+} + 2H_2S_{(aq)}$
($FeS_2 + 4H^+ + 2e = Fe^{2+} + 2H_2S_{(aq)}$)
- (4) $Fe_2O_3 + 4SO_4^{2-} + 8H^+ + 15H_2 = 2FeS_2 + 19H_2O$
($Fe_2O_3 + 4SO_4^{2-} + 38H^+ + 30e = 2FeS_2 + 19H_2O$)
- (5) $Fe_2O_3 + 6SO_4^{2-} + 12H^+ + 22H_2 = 3FeS_2 + 28H_2O$
($Fe_2O_3 + 6SO_4^{2-} + 56H^+ + 44e = 3FeS_2 + 28H_2O$)
- (6) $3FeS_2 + 4H_2O + 2H_2 = Fe_3O_4 + 6HS^- + 6H^+$
($3FeS_2 + 4H_2O + 4e = Fe_3O_4 + 6HS^- + 2H^+$)
- (7) $FeS + 2H^+ = Fe^{2+} + H_2S_{(aq)}$
- (8) $Fe_2O_3 + 3HS^- + 3H^+ + H_2 = 3FeS + 4H_2O$
($Fe_2O_3 + 3HS^- + 5H^+ + 2e = 3FeS + 4H_2O$)
- (9) $FeS_2 + H_2 = FeS + HS^- + H^+$
($FeS_2 + H^+ + 2e = FeS + HS^-$)
- (10) $Fe^{2+} + 2S + H_2 = FeS_2 + 2H^+$
($Fe^{2+} + 2S + 2e = FeS_2$)
- (11) $3Fe_2O_3 + H_2 = 2Fe_3O_4 + H_2O$
($3Fe_2O_3 + 6H^+ + 2e = 2Fe_3O_4 + 3H_2O$)
- (12) $Fe_2O_3 + 4H^+ + H_2 = 2Fe^{2+} + 3H_2O$
($Fe_2O_3 + 6H^+ + 2e = 2Fe^{2+} + 3H_2O$)
- (13) $Fe_2O_3 + 6H^+ = 2Fe^{3+} + 3H_2O$
- (14) $Fe^{3+} + 1/2H_2 = Fe^{2+} + H^+$
($Fe^{3+} + e = Fe^{2+}$)

The following equilibrium relations were also considered

- (4 (a)) $Fe_2O_3 + 4SO_4^{2-} + 4H^+ + 17H_2 = 2FeS_2 + 19H_2O$
($Fe_2O_3 + 4SO_4^{2-} + 34H^+ + 30e = 2FeS_2 + 19H_2O$)
- (6(a)) $3FeS_2 + 4H_2O + 2H_2 = Fe_3O_4 + 6S^{2-} + 12H^+$
($3FeS_2 + 4H_2O + 4e = Fe_3O_4 + 6S^{2-} + 8H^+$)
- (8(a)) $Fe_2O_3 + 3S^{2-} + 6H^+ + H_2 = 3FeS + 4H_2O$
($Fe_2O_3 + 3S^{2-} + 8H^+ + 2e = 3FeS + 4H_2O$)
- (9(a)) $FeS_2 + H_2 = FeS + H_2S_{(aq)}$
($FeS_2 + 2H^+ + 2e = FeS + H_2S_{(aq)}$)

Ferreira (1975) constructed Eh-pH diagrams for the sulfur-water, copper oxides and sulfides-water, and iron oxides and sulfides-water systems at 25°C, 100°C and 150°C using theoretical considerations. He argues that normal calculations based on half-cell reactions were inaccurate because they ignore the entropy of electrons. He provides a complete set of reactions and thermodynamic constants for the systems he studied. The effect of temperature on these diagrams is small. He acknowledges the theoretical co-existence of S^0 and Fe^{++} , also of pyrite and Fe^{++} for 150°C.

Figure 5.2.2.1 (opposite) presents the classical Eh-pH diagram at 25°C for the Fe-S-H₂O system. Solid lines are for the iron species, at activities 10^{-1} and 10^{-6} M, dashed lines are for sulfur species at 10^{-1} M. Identifying numbers on the lines are those of the corresponding equations.

The asterisk * identifies the approximate position of autoclave conditions when the writer tested Bougainville pyrite material (pH – 0.48). The stable phases should be Fe^{3+} and HSO_4^- .

5.2.2.2 Metastable Phases

The major problem with these "classical" diagrams is that they do not agree with the experimental evidence of a wide range of researchers. Time after time, sulfides have failed to oxidise under predicted conditions, elemental sulfur has been produced when it was not predicted and reactions were either slower or less complete than expected. Resolution of the problem was not helped by disagreement between investigators' findings. Depending on the system, and test conditions, different non-equilibrium sulfides were also reported.

The elemental sulfur, which should not be present according to the Eh-pH diagram, has been termed "metastable sulfur". It is this metastable sulfur which causes such problems in leaching operations. In nitric acid processes, it forces operators to use more severe conditions (Beattie and Ismay, 1990) or to incorporate extra treatment steps (Fair and Van Weert, 1989) into the flowsheet.

5.2.3 KINETICS OF PYRITE OXIDATION

5.2.3.1 Investigations prior to 1982

Hiskey and Schlitt (1982) reviewed the aqueous oxidation of pyrite from thermodynamic, kinetic, electrochemical and bacteriological viewpoints.

This review is probably the most useful starting point for the future student. These authors explain the many discrepancies of previous authors in terms of slow kinetics, which meant that different authors were finding different products. Iron (III) hydroxide persists 6-8 days at 25°C (Fe₂O₃ is the stable form) and elemental sulfur's kinetics are slow and vary widely with conditions. Both products can form passivating layers.

There is considerable divergence in investigators' reported rates of sulfide oxidation.

Table 5.2.3.1 summarises various investigators' results for oxygen dependence, activation energy and mechanism.

Table 5.2.3.1: Summary of the Kinetics of Aqueous Oxidation of Pyrite (from Hiskey)

| Material | Conditions | Medium | O ₂ Dependence | Activation Energy kJ/mol | Mechanism | Reference |
|---------------------------------------|--|--------------------------------|---------------------------|--------------------------|--|-------------------------------|
| Natural FeS ₂ | 130-210°C 2.7-13.9 atm P _{O₂} | H ₂ O | 0.5 | 83.7 | Surface controlled chemisorption | Warren (1956) |
| Upgraded FeS ₂ Concentrate | 100-130°C 0-4 atm P _{O₂} | H ₂ SO ₄ | 1.0 | 55.7 | Surface controlled chemisorption | McKay and Kelpern (1958) |
| Upgraded FeS ₂ concentrate | 130-165°C 6.1-23.8 atm P _{O₂} | H ₂ O | 0.5 | 70.3-77.4 | Chemical control | Cornelius and Woodcock (1958) |
| Natural FeS ₂ | 33°C 4 x 10 ⁻⁵ -2 x 10 ⁻³ M Fe ³⁺ deoxygenated | Acid ferric sulfate | — | — | Controlled by Eh | Garrels and Christ (1960) |
| Natural FeS ₂ | See text | H ₂ O | 0.5 | 58.6 | Fe ³⁺ Adsorption | Smith and Shumate (1970) |
| Natural FeS ₂ | 40-90°C 1 atm P _{O₂} | H ₂ O | — | 51.9 | Linear kinetics chemical control | Mishra (1973) |
| Natural FeS ₂ | 80-100°C 0-9.2 at 0-1.0 M Fe ³⁺ | H ₂ SO ₄ | 0.5 | 39.6-46.0 | Linear kinetics chemical control | King and Lewis (1980) |
| Natural FeS ₂ | 85-130°C 0-66.5 atm P _{O₂} | H ₂ O ₄ | 0.5 | 51.1 | Electrochemical /controlled by the mixed potential | Bailey and Peters (1975) |

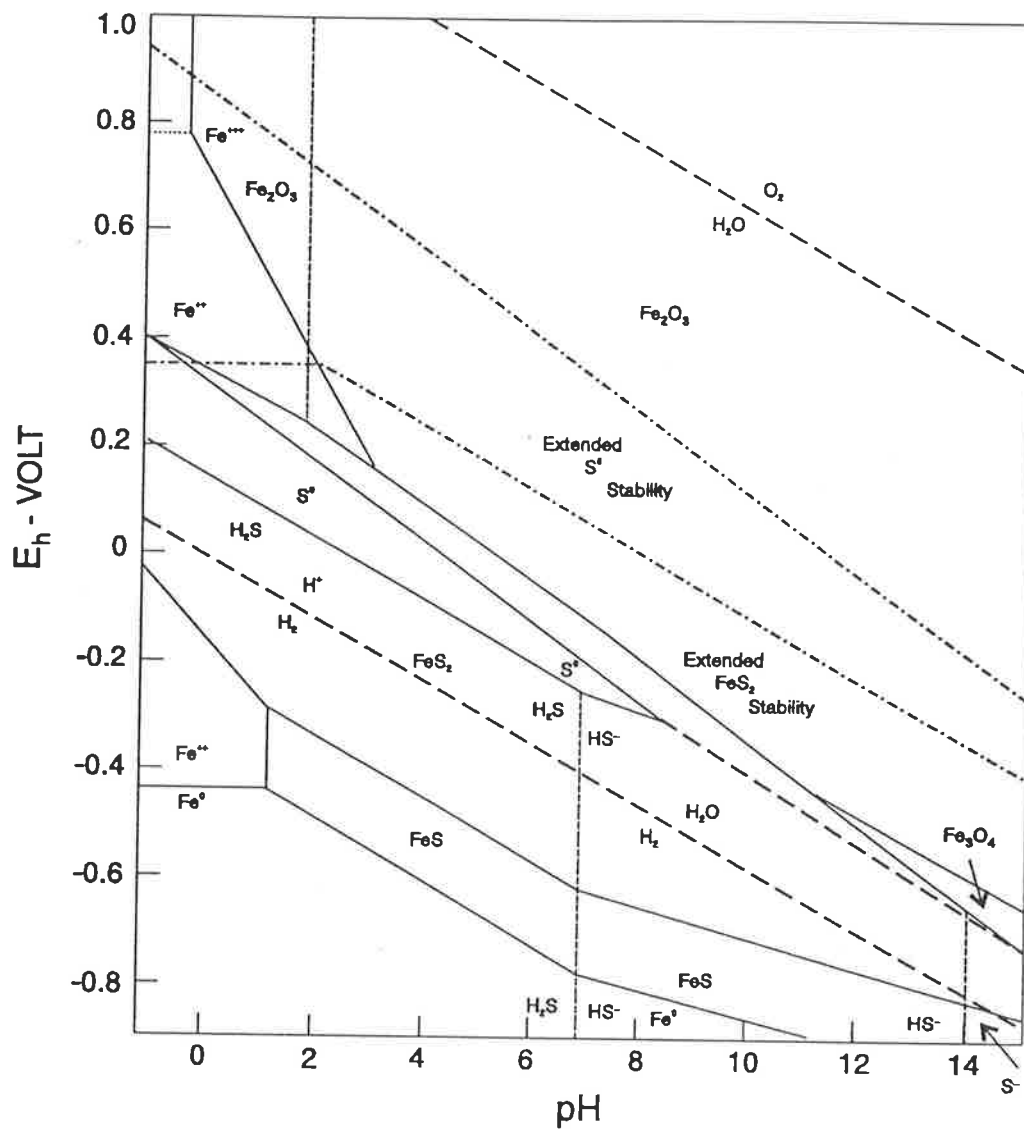
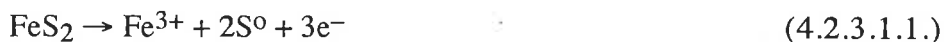
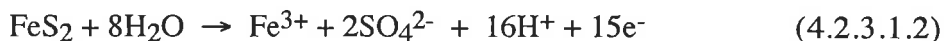


FIGURE 5.2.3.1. Eh -pH diagram of the Fe-S-H₂O system with extended metastable zones (from Peters 1984)

The literature confirms that there are two competing reactions (as seen in Chapter 4).



and



Depending on the conditions, the relative rates of these reactions vary. Accordingly, so will the amount of elemental sulfur formed vary and so will its effects. For example, if reaction (4.2.3.1.2) accounts for more than 27% of the total pyrite oxidised, volume changes are such that any S^0 formed will not be passivating. Iron (III) concentration also effects the kinetics and iron concentration, of course, is changing during leaching. At Ehs above 1050 mV (vs SHE) Peters and Maijima (1968) found only SO_4^{2-} existed.

The work of Ernest Peters of UBC best reconciles the classical thermodynamics and real kinetics of sulfide oxidation. Peters (1981) suggests that if geologists are keen to use thermodynamics it is because their processes have had a little longer to occur. Overvoltages (H_2 , O_2) are common in metallurgical processes. Peters (1984) suggests that since species such as S^0 are formed irreversibly and SO_4^{2-} and HSO_4^- are kinetically inert, classical diagrams fail. Further, metallurgists are generally uninterested in species such as H_2O , HS^- and $\text{S}^{=}$ for leaching applications. Using a wide background of experimental conditions, he proposed adding 75 kcal/mole (314 kJ/mol) to the formal energy of formation of S^0 . He also increased the predominance area of metastable pyrite to account for the oft-observed overpotentials necessary for its oxidation. His resultant diagram is shown in Figure 5.2.3.1 (opposite).

It can be seen that this writer's experimental autoclave conditions are still in the HSO_4^- region but only just so.

Another means of modifying the classical diagram to overcome kinetic limitations was devised by Woods et al. (1987). Following work on the Cu-S- H_2O system by Koch, who proposed several metastable Cu_yS species, Woods et al. used a Swedish computer programme to modify the classical diagram for the observed metastable species.

Modifications were also made for the experimental observation that the only stable aqueous states of sulfur are – II (SO etc) and + VI (SO_4^{2-} etc). Like Peters,

Woods et al. do not consider the $S^{\circ} \rightarrow SO_4^{2-}$ reaction and this enlarges their stability regions for S° .

Woods' and Peters' modified diagrams agree below $pH = 5$.

5.2.3.2 Proposed Mechanisms for Pyrite Oxidation

To attempt to describe a mechanism for pyrite oxidation is to open a can of worms, even more confused and conflicting than that raised by varying experimental conditions. Hiskey and Schlitt (1982) content themselves with referring to a "complex dissolution mechanism with intermediates like thiosulfate, sulfite, dithionate and dithionite". Smith and Shumate (in Hiskey and Schlitt, (1982)) had proposed a four-step mechanism involving an activated complex. The activation energies found by researchers in Table 5.2.3.1 range from 40 to 85 kJ mol^{-1} . It would seem likely that these values at least point to chemical control but beyond that the researchers proposed mechanisms scatter.

Chander and Briceno (1987) proposed a seven-step mechanism to explain the kinetics of pyrite leaching. Their proposal is complex and appears virtually unsubstantiated.

A number of researchers have proposed models of the rate-controlling process for pyrite leaching. The shrinking core model, for example will be discussed under 5.2.3.3. As far as the mechanisms which might be behind such models are concerned, perhaps the best which can be said is that the experts have largely ignored them.

5.2.3.3 Recent Investigation Specific to Pyrite - Nitric Acid

Work aimed at leaching pyrite from coal has also been published at intervals. A recent investigation, which must have been going on at the same time as that in this thesis, was published by the Turkish researchers, Kadioglu et al. (1995). It has several interesting findings, and is the only paper found which deals directly with pyrite-nitric acid and elemental sulfur.

Kadioglu and his co-workers tested what are called in the present work the classical kinetics variables. These included stirring rate, temperature, nitric-acid concentration, and particle size. The range of these variables in the two investigations (Kadioglu and the present thesis) are different, although there is some overlap. For example, parts of the Turkish work investigated very low

temperatures and acid strengths. While these may be of academic interest, they are not of industrial significance, and resulted in very low extractions - 0.8%.

Perhaps the most interesting of these workers' findings was the amount of elemental sulfur found. Their figure 5 is reproduced as Figure 5.2.3.2 below.

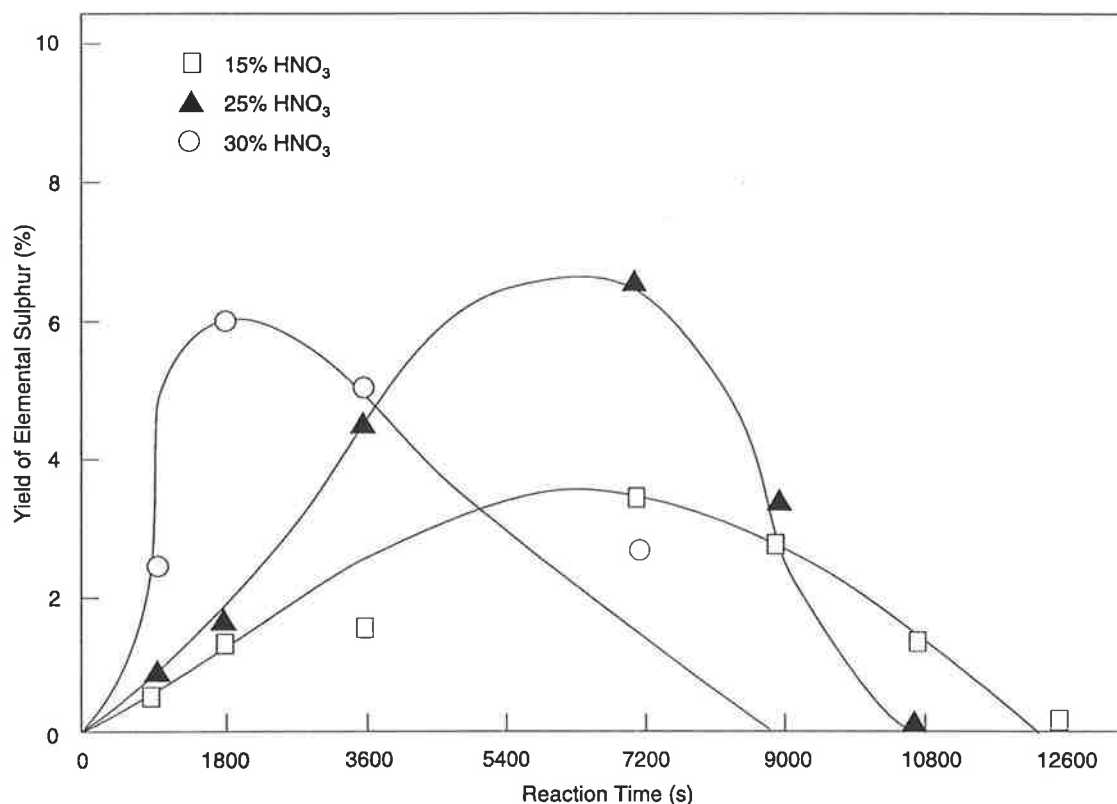


FIGURE 5.2.3.2 Extent of elemental sulphur formed as a function of nitric acid concentration and time at 70°C (from Kadioglu et al. 1995)

The results of Figure 5.2.3.3 show elemental sulfur yield peaking at about 6% for 25-30% HNO₃ (3.9-4.7 molar) and at about 3% for 2.4 molar acid. Their explanation is in terms of competing reactions - the same as equations 4.2.3.1.1. and 4.2.3.1.2 - plus the oxidation of elemental sulfur to sulfate. The latter rate is not quantified.

The experimental methods employed by Kadioglu et al. are quite different from those of the present work. They ground small amounts of pyrite in a porcelain mill "to ensure that the particles obtained were spherical". After washing, acetone drying, and sieving, small (0.2g) samples were leached. Leach tests were stopped at a given time (15, 30, 60 or 120 minutes) and the residue extracted with carbon disulfide. Solution iron was determined by titration and sulfate by gravimetry. This means four sets of determinations for each curve. The writer considered gravimetry and performed a few CS₂ Soxhlet extraction.

The amount of routine laboratory work done by the Turkish investigators is staggering. Their sulfur balances are almost incredibly accurate, although only final balances are shown. Kadioglu et al (1995) report chemical control of pyrite leaching in nitric acid. They found activation energy varied with acid strength, reporting values of 52 and 27 kJ mol⁻¹. They stated they found a good fit for some of their data with the shrinking core model. This agreed with findings by King and Lewis (1980) and Bailey and Peters (1976) (both in Hickey and Schlitt (1982)). The former authors, however, worked at 30 and 120 psig (200-800 kPa) oxygen overpressure and the latter at 6800 kPa.

5.2.3.4. Summary of Literature on Kinetics

The oxidation of pyrite is complex because a great many variables affect its kinetics. These kinetics are reasonably slow. This has meant different investigators found different products, not only because of something different about their experimental conditions, but also because they looked at different times. A wide range of activation energies has been reported. Mechanisms have been largely ignored due to being perceived as too difficult. Recent specifically pyrite-nitric acid work by Kadioglu et al. has presented worthwhile results on classical kinetic variables. It will be interesting to compare these to the results of the present work. As with other work on pyrite oxidation, care will be required to ensure comparable experimental conditions are being used.

5.2.4 EXPERIMENTAL CONDITIONS SUGGESTED BY THE LITERATURE

These will be dealt with in the groups, and in the order, of which there are tested subsequently. Reference was not necessarily found, or sought, for all seventeen variables.

5.2.4.1 Classical Kinetics Variables

As is true throughout the present investigation, an attempt was made to keep the classical kinetic variables within realistic commercial bounds. For the low-temperature variant of the "Redox" process the following conditions apply: (Raudsepp et al. 1987):

- Stirring Speed - sufficient for suspension
- Temperature - 85 - 90°C
- Particle size - P80 governed by sulfide liberation - usually 120-60µm
- HNO₃ concentration - 150 g/l

Kadioglu et al. (1995) found that the dissolution rate of pyrite was practically independent of stirring speed in the range 300 to 1200 rpm. Their leaching rates were extremely slow, one might say negligible, in the range 25-40°C.

Bailey and Peters (1976) found the initial reaction speed was proportional to the surface area of the pyrite. This was also found to be the case by Kadioglu et al. (1995).

A number of workers have found that the leaching rate increases dramatically with HNO₃ concentration. This has been dealt with in some detail in Chapter 2. A considerable increase in leaching rate has been observed above 1.6 Molar (100 g/l).

5.2.4.2 Industrial Kinetic Variables

Limited testing on sulfuric acid added to the leach was covered in Chapter 2. Sulfuric acid increases the leach rate.

Ferric iron is well documented as an oxidising agent. Three sets of authors reviewed in Hiskey and Schlitt (1982) mention this. King and Lewis showed that 1 molar Fe³⁺ doubled the reaction rate of pyrite. Their data is shown as Figure 5.2.4.1.

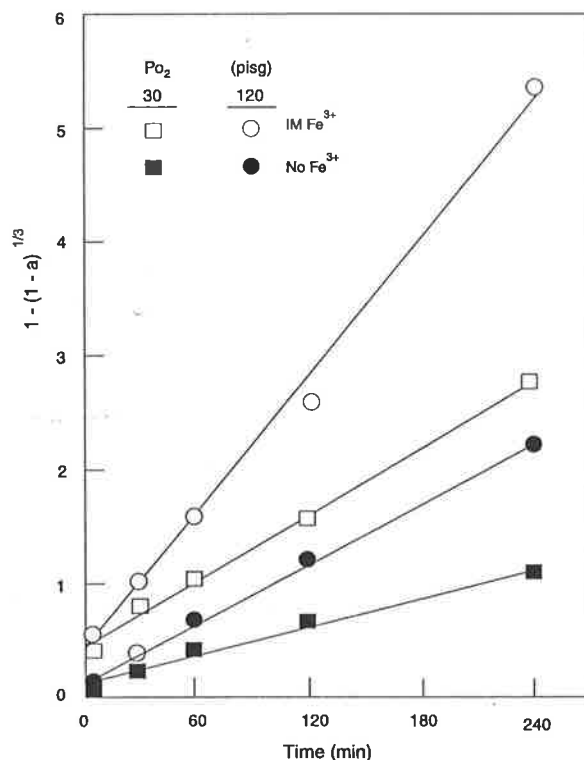


FIGURE 5.2.4.1 Correlation of Pyrite Dissolution data with surface reaction rate equation (from King and Lewis 1980)

Chloride ion is stated to increase the rate of pyrite oxidation (Ichikuni (1982) and Sheenan and Strickland (1957)). All three references are given in Hiskey and Schlitt (1982)).

Pulp density is an important variable for industrial processes. It has implications for the reactor vessel size. Pulp density may well be governed by the heat balance in the reactor. In some cases, reacted solids are recycled to dilute the percent sulfur in the reactor feed (Berozowski et al. (1991)). This can be for heat balance purposes or to reduce the incidence of sulfur tying up unreacted sulfides as pellets.

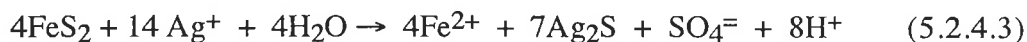
5.2.4.3 Additional Kinetic "Variables"

Under this category, and the reason for the inverted commas around "variables", are both controlled test variables and phenomena observed during the test.

From the literature on the "Redox" process, it was noted that sulfide concentrates produced elemental sulfur in quantities which caused problems, but whole ores did not. In particular see Leonard et al. (1990)). Also whole ores were run at higher (30%) pulp densities. From this it was suspected that the sulfur might be being rubbed off the surface of the pyrite as it formed for whole ores. This is called "attritioning" for the purposes of this thesis and was tested as such. The Berozowski et al. (1991) paper recently underlined that this is an operating strategy for sulfuric acid based pressure leaching.

Chapter 4 focussed on the effect of Eh on the sulfur/sulfate ratio during pyrite leaching. Although the literature varied, the work in Chapter 4 suggested no sulfur would be found above Eh 1.4 volts, that about 9% sulfur could be expected at 1.2 volts and more at lower Eh. Limited attempts were made to increase Eh as a leach test variable.

Several researchers suggest that silver ion may inhibit the formation of elemental sulfur. Shashi et al. (1987) suggest that silver ion slows pyrite corrosion rates. Van Weert et al. (1988) states "there is some indication that silver may affect sulfur yield". The most complete work on the topic is Buckley et al. (1989). In it, the authors suggest that when Ag_2S is present on the surface of pyrite, as long as one atom in eight of pyrite sulfur oxidises direct to SO_4^{2-} , the rest will not form elemental sulfur. This was proposed to occur via:



These researchers found no sulfur occurring at 10^{-2} M Ag^+ , but some S^0 occurred at 10^{-3} molar Ag^+ . Further, when acidified solution containing ferric ion was tested at 10^{-2} molar Ag^+ sulfur was found. It seems that silver ion suppression of elemental sulfur formation will depend upon the mixed system. Any such system must be tested. Further, the work combined electrochemistry and XPS, but not actual leach tests.

No reference was found which referred to whether the effects of individual variables were additive or otherwise. It is probably fair to say that no study has been complete enough to address this issue.

A common feature of the leach tests in the present work was an initial period when the leaching rate was low. This "lag time" was followed by an accelerated leaching rate. Shashi et al. (1987) gave electrochemical evidence that this phenomenon was autocatalysis due to ferric ion. Their finding is shown in Figure 5.2.4.2.

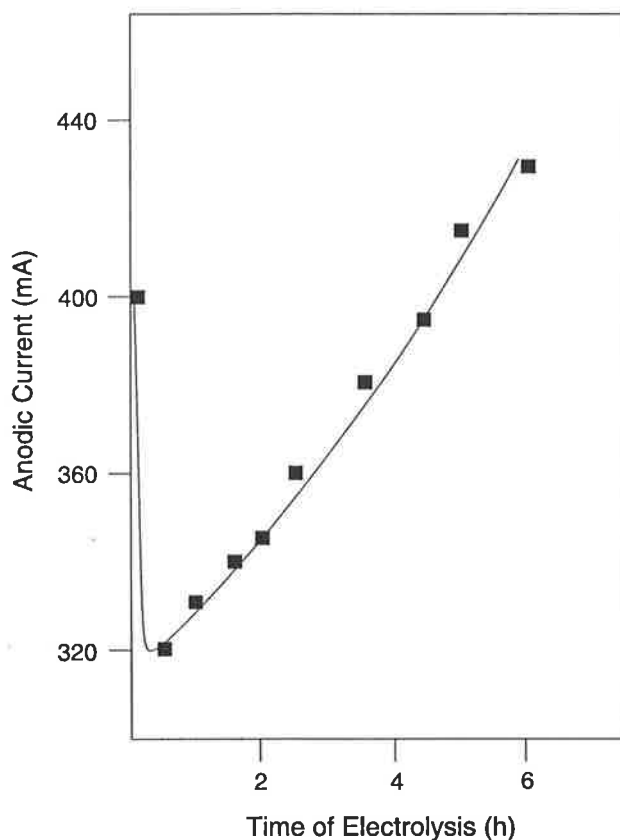


FIGURE 5.2.4.2 Electrolytic current at constant voltage (from Shashi et al. 1987)

Peters (1984) stated that six atomic layers of elemental sulfur, formed due to air oxidation of pyrite, could passivate it. A change from passive to active pyrite could account for the leach rate acceleration. Hiskey and Schlitt (1982) mention the general presence of surface films which retard pyrite oxidation at low Eh.

McKay and Halpern (1958 - in Hiskey and Schlitt (1982)) mention surface etching and pitting of pyrite during leaching. This could possibly affect the leach rate by increasing the effective surface area during the leach.

The source of the pyrite is recognised to be a variable. It is generally recognised that trace elements, or mineral geological history, have effects on surface-related phenomena such as flotation or cyclic voltammetry. Bailey and Peters (1976) found that pyrites from Sullivan Mine were more reactive than those from three other sources due to the more uneven surface morphology of the former.

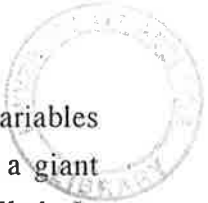
Finally, one variable conspicuous by its absence from this chapter is the oxygen partial pressure. Hiskey and Schlitt (1982) quote various effects of P_{O_2} from none to 0.5th order. It was considered that variations of at least a factor of 5 would be needed to see any effect. The glass leach vessel make such variation impractical. No autoclave tests were done for PO_2 as there is a fair amount of data extant, if not in agreement, in the literature.

5.2.5 SECTION SUMMARY (Literature Review)

Understanding hydrometallurgical oxidation of sulfides has proved a daunting and uncompleted task. Initial attempts were made in 1830. After 1966, the favoured method became the use of Pourbaix diagrams. These have proved inadequate. Experimental results interpreted in the light of Eh-pH diagrams were often conflicting and confusing. Diagrams with extended metastable regions may prove to be more useful but it is early days for these and the Fe-S-H₂O extended diagram has not been verified experimentally (Peters (1991)).

The problem of elemental sulfur in nitric acid pre-oxidation processes would appear to be a kinetic one rather than a thermodynamic problem. Finding a range of useful kinetics for commercially realistic conditions will be attempted as part of this present work. The generation of kinetically-modified Eh-pH diagrams is a challenge which will have to remain outside the present scope.

This review has given a number of starting points for the various variables proposed for the testwork in Chapter 5. The literature has shown that for the pyrite - nitric acid system the classical kinetic variables have been only partially



investigated and that very recently. For a host of industrial and other variables there is very little reported. The puzzle of sulfide oxidation is like a giant multidimensional crossword, with most of the white squares as yet unfilled. In one corner of the giant crossword is pyrite, with nitric acid and elemental sulfur being dimensions of the pyrite sub-puzzle. Again, going by the literature, most of the white squares are blank, or only pencilled in qualitatively. It is believed that the findings of this thesis will fill in a significant portion of the crossword puzzle.

5.3 EXPERIMENTAL METHOD

This section will describe the methods used for the kinetic leach tests. Leach tests fell into two categories - those in a glass reactor and those in an attritioning vessel. Both apparatuses and methods will be described. Beyond this difference in methods, the individual tests differed only in the values of certain variables, such as temperature. Accordingly, those variables are categorised and quantified in the 'results' part of five section (5.4 through 5.8) rather than in the present section.

5.3.1 PREPARATION AND ANALYSIS OF SOLIDS

5.3.1.1 Crushing and Storage of Pyrite

Approximately two kilograms of pyrite, originally from Gumeracha, South Australia, was available from the Geology stores at the University of South Australia. Large single-crystal samples of Gumeracha pyrite were obtained from Australian Minerals of Hahndorf, South Australia, for electrochemical and XPS work. Australian Minerals also supplied several kilograms of moderately-coarse pyrite originating from Huanzala, Peru.

Solids were crushed using a rocking cast-iron pestle on a flat cast-iron plate. Gumeracha pyrite was crushed 13 May 1992 and Huanzala 4 June 1992 and again 28 July 1994. Samples were dry-screened and the fractions stored in plastic phials with snap-on tops. After it began to be suspected that the pyrite was aging (July 1992) phials were filled with nitrogen after use and stored in a freezer at -5°C . The entire contents of a given phial were riffled to provide the pyrite sample for a given test - usually 3.00 grams, weighed to four decimal places on a Mettler AE 166 balance. Dry screening proved adequate for Gumeracha pyrite but Huanzala pyrite was deslimed by wet screening at $45\ \mu\text{m}$ after the initial test series.

5.3.1.2 Composition of Solid Pyrites

Analysis of pyrites was performed by Amdel Laboratories of Thebarton, South Australia. Iron was determined volumetrically (Method 1A) and sulfur gravimetrically (Method 1B). The sulfur method took some refining including slow bromine dissolution in an ice bath. Trace elements were determined by ICP (Method 4A). Table 5.3.1.1 below gives the reconciled main component analysis from both pyrites.

Table 5.3.1.1: Pyrite Assays (%)

| | Gumeracha | Huanzala |
|-----------------------|--------------------------|--------------------------|
| Fe | 44.7 | 45.5 |
| S | 51.8 | 50.9 |
| | } 96.5% FeS ₂ | } 96.5% FeS ₂ |
| All trace metals | 0.8 | 0.2 |
| Silica | 2.12 | 4.0 |
| Other gangue minerals | 0.76 | 1.0 |
| total | 100.2 | 101.6 |
| Trace As | 0.045 | <0.010 |
| Metals: Sn | <0.005 | 0.008 |
| Mo | <0.005 | <0.005 |
| Cr | 0.009 | 0.008 |
| Zn | 0.015 | 0.006 |
| Pb | 0.065 | 0.010 |
| Cd | 0.20 | <0.002 |
| Co | 0.20 | <0.005 |
| Ni | 0.045 | <0.005 |
| Ba | 0.015 | 0.030 |
| Ta | <0.005 | 0.007 |
| Nb | <0.005 | <0.005 |
| V | 0.004 | 0.007 |
| Be | <0.002 | <0.002 |
| Cu | 0.43 | 0.060 |
| La | <0.005 | <0.005 |
| Zr | 0.003 | 0.004 |
| Sc | <0.002 | <0.002 |
| Y | <0.002 | <0.002 |
| Sr | 0.010 | 0.010 |
| Ce | <0.010 | <0.010 |

In contrast to the results of Table 5.3.1.1, the nitric acid leach tests indicated values of purity of 98.5% FeS₂ for Gumeracha and 99.5% FeS₂ for Huanzala. (It was assumed no gangue dissolved in HNO₃.) The differences may well have been one of sampling and are not considered significant. The values of 98.5% and 99.5% pyrite purity, respectively, were used throughout the leach test calculations when checking extraction values.

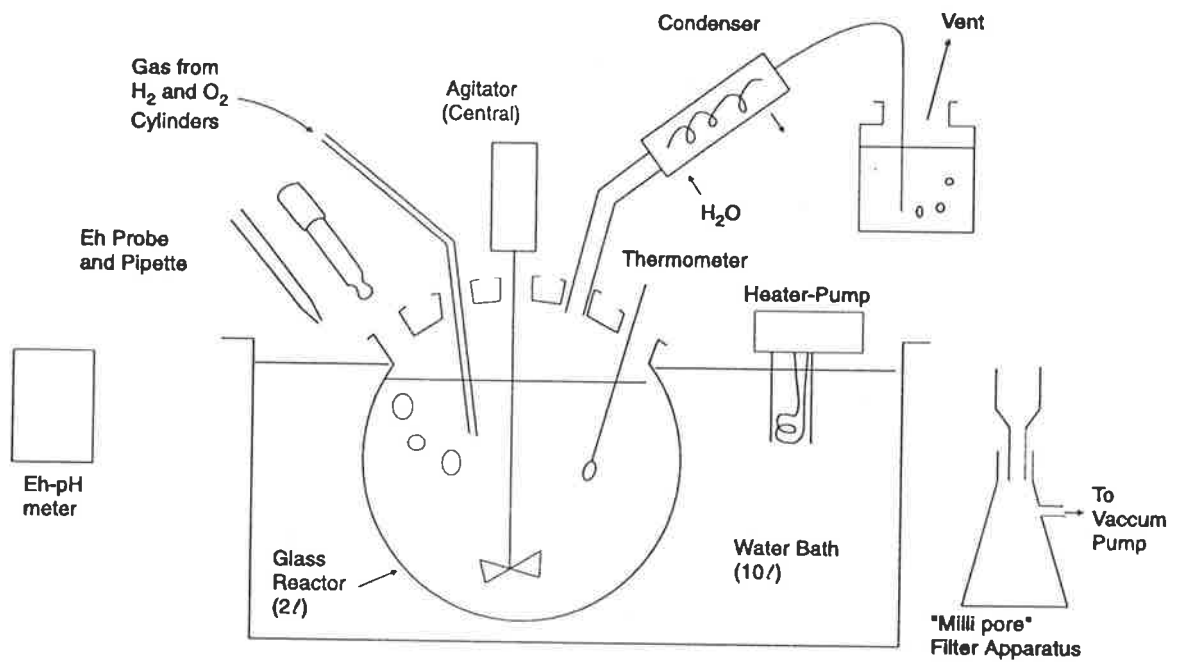


Figure 5.3.2.1: Schematic of leach test apparatus

5.3.1.3 Composition of Leach Residues

Leach test residues were filtered, washed with 1.0 M HNO₃ and distilled water and allowed to dry in air overnight. They were then accurately weighed and examined under a microscope - usually an Olympic SZH binocular optical microscope. Volume percentages were estimated using a visual comparison chart. These were converted to a percent by weight using pyrite density of 4.5, sulfur of 2.0 and gangue at 2.7 g cm⁻³ respectively. Given that the residues were generally about 5% of the feed weight, the method provided acceptable accuracy.

As a check on this, a number of residues were extracted with carbon disulfide in a Soxhlet apparatus, then separated using tetrachloro-ethanol for more accurate determinations. These agreed closely with the visual estimate, the worst error being less than 5% of the original feed for a case with 25% residue. Given the comparative time demands - a half an hour for microscopic estimation and two days for Soxhlet-heavy liquid determination - the visual estimation method was used for all other tests.

5.3.2 TEST APPARATUS AND METHOD FOR MAIN TEST SERIES

5.3.2.1 Apparatus - Glass Reactor

A schematic of the test apparatus for the majority of the leach tests is shown in Figure 5.3.2.1. The reactor was a spherical glass vessel of 2.0 l capacity, with five ports in its top surface. The vessel was scrounged originally, modified at a cost of three hundreds dollars, and amazingly never dropped through some ninety leach tests.

The central port was used for the stirrer, consisting of hinged teflon paddles on a stainless steel shaft. One port was used for a condenser, one for a thermometer and one for a gas inlet. The fifth port was used for an Eh probe, and also for sample introduction and liquid samples removal. The whole apparatus was maintained within $\pm 1^\circ\text{C}$ in a 10 litre water bath. Bath heating was via a variable Circon 2000 Watt pump-heater. Control was manual.

Exit gases from the condenser were scrubbed through 1.0 litre of 1.0 M sodium carbonate solution before venting to atmosphere.

5.3.2.2 Typical Test Method

The apparatus was set up. Cold acid was then added to the reactor and the liquid was saturated with commercial oxygen by bubbling O₂ through the acid for at least thirty minutes. Hot water was added to the bath and then it was brought up to temperature. Just prior to the addition of solid, the Eh probe (Pt - Ag/Ag Cl saturated Cl) was checked against a standard solution at room temperature and then transferred to the leach vessel. Stirrer speed was checked with a stopwatch (4:1 gear ratio). The gas flow was changed to commercial nitrogen directly over the liquid surface during each test. This was done to be consistent with the electrochemical tests of Chapter 4.

Pyrite was added via a funnel and the experimental log begun. Liquid samples were extracted using a pipette - a wide mouth pipette was used when solid samples were desired. Liquid samples (20 ml) were generally extracted at 5, 10, 20, 30, 45, 60, 90 and 120 minutes. This was varied depending on the expected speed of the test. Liquid quantities were generally not made up. The liquid samples were filtered through a 5 µm 'millipore' filter. The receiving vessels were 1 litre Erlenmeyer flasks with side-arm connected to a vacuum pump. Samples were bottled and the receiving flasks were drained, not washed, between samples.

5.3.2.3 Rationale

The test method and levels of variables chosen were a compromise based on the desire to emulate industrial conditions, the need to isolate the effects of individual variables for a fundamental study, and the available equipment. Most work was done at 0.2% solids (3.0 g pyrite in 1.5 l of acid). This gave virtually constant composition of the liquid throughout the test. Thus the reaction could be tracked in terms of pyrite concentration alone. (The reverse was actually used, namely pyrite extraction - this is a common way of expressing hydrometallurgical reaction completion.) While 0.2% pulp density is much lower than those used in industry (10 - 20% for 15% sulfide feeds) higher pulp densities would have required sophisticated acid makeup equipment, which was not available. Crude acid makeup was used in the pulp density series, which it was hoped would show any effect inherent in higher pulp densities

A single screen fraction of pyrite was used for most tests (ie, - 90 + 125 µm). A wide range of particle sizes tends to blur kinetic effects and it can be difficult to assure that a wide range is consistent. Sampling of solids tends to be affected by size effects.

The apparatus used limited stirring speeds attainable and the pressure which could be used. The autoclave which had been used in Chapter 3 proved difficult for sampling purposes and reaction progress could not be followed visually. In addition, several other authors have covered the oxygen pressure dependence of pyrite leaching (Hiskey and Schlitt 1982) although not using nitric acid.

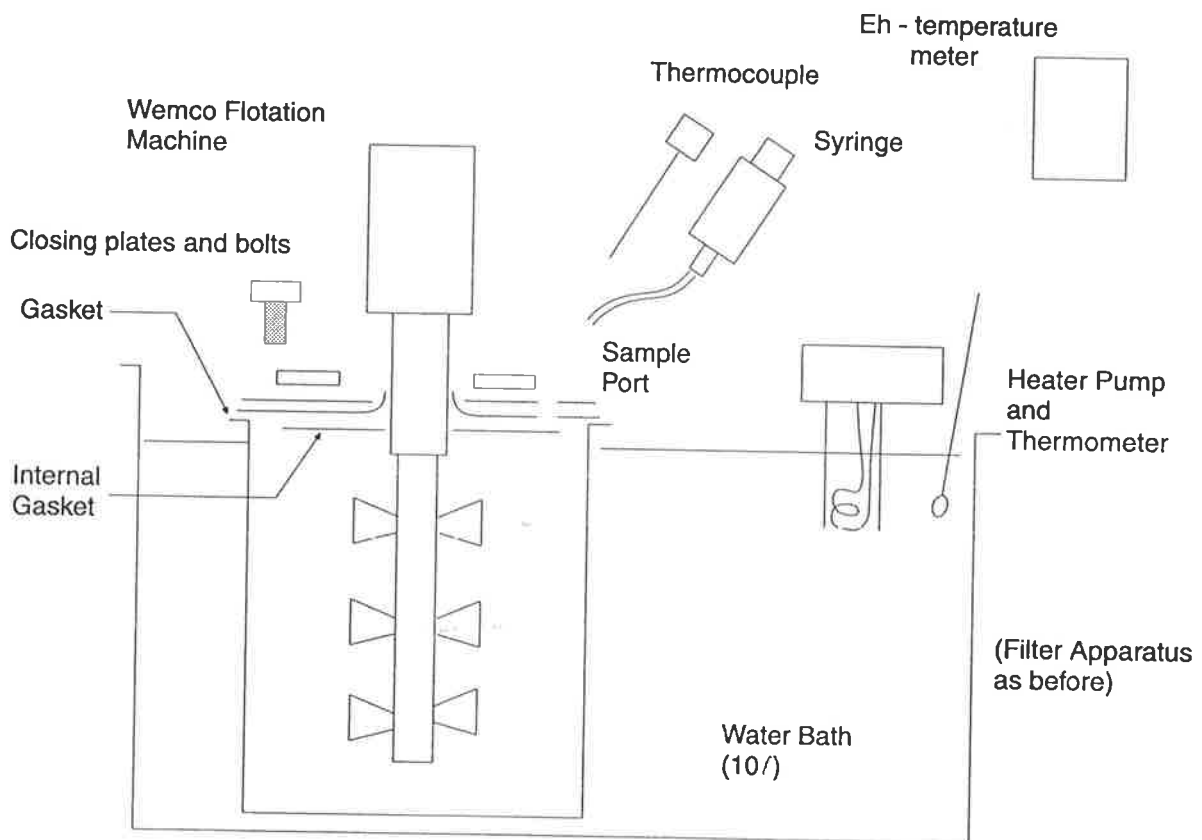


Figure 5.3.3.1: Schematic of attritioning apparatus

5.3.3 TEST APPARATUS AND METHOD - ATTRITIONING SERIES

5.3.3.1 Apparatus - Attritioning Cell

Figure 5.3.3.1 (opposite) is a schematic of the attritioning test apparatus. The octagonal stainless steel attritioning vessel had a stainless steel lid. Modifications were required because tests involved hot nitric acid. The modifications included rubber gaskets (later modified to teflon) and heavy bolted plates to press the gasket between lid and vessel and lid and stirrer shaft. Sample addition and sampling were via a 5 mm port fitted with a tube to avoid liquid splashing out. Samples were taken with a 50 ml syringe fitted with a teflon tube. For heating and temperature control, the same water bath was used as for the glass reactor.

The attritioner itself was a Wemco laboratory flotation machine. A condenser could not be fitted to the attritioner vessel, so evaporation losses had to be accounted for by weight loss.

5.3.3.2 Test Method - Attritioner Tests

The experimental procedure was a crude version of that for the glass reactor. No oxygen saturation was attempted.

The vessel was positioned under the attritioner and the shaft lowered into the vessel. 728 ml of acid were added, along with 300 g of glass balls. (This was about the pulp density reported for whole-ore "Redox" test. The 3.0 mm ϕ soda - lime glass balls had a density of about 1.45 g cm⁻³ and so the inert solids in the vessel were 23% by volume. Most attritioner tests are run at 50% by weight solids which would be 27% by volume for silica.) The gasket and lid were put on and the vessel bolted shut. The water bath was filled and brought up to temperature. Temperature in the vessel was checked by inserting a thermocouple through the sample port. The thermocouple was checked regularly against the thermometer in the water bath. Once temperature was attained, the attritioner was shut off and solid pyrite added by blowing it in through a plastic drinking straw. (The pyrite was weighed in this straw and the straw weight deducted afterwards, as a few particles tended to adhere to the straw.) About 1.50 grams of pyrite was used per test, giving the same percent solids initially as the main test series. The original purpose of the series was only to prove that attritioning would eliminate elemental sulfur. Later, two tests were employed in the "additive effects" tests and they are discussed in Section 5.8.

At 10, 20, 30, 60, 90 and 120 minutes, the attritioner was shut off to allow sampling. The temperature inside the vessel was checked and 15 ml of liquid withdrawn. The reduced number and quantity of solids were used because they were a larger proportion of the whole. That, plus the problem of evaporation losses, meant liquid samples had to be accounted for in detail for the attritioning series. Liquid samples were filtered as before.

At the end of the run the solids were retained on a 45 μm screen. The slurry that passed through was filtered on a 5 μm millipore filter. The balls on the screen were washed and the adhered solids added to that on the millipore for analysis. The balls were dried and weighed.

5.3.4 LIQUID ASSAYS

Analysis of liquids was attempted by AAS. Iron, always difficult, proved more so in 3 M HNO_3 . Several days' work gave optimised settings which still intimated nine (9) % error. Sulfate assays by barium gravimetry are time-consuming. It was decided to use professional analysis. Amdel Laboratories offered very fair rates and were most reasonable about small, erratic sample batches over a long period. Some problems resulted and these are discussed in the Supplemental Volume.

Iron analysis were performed using ICPMES (Inductively Coupled Plasma). The instrument was calibrated using 0.5, 1.0 and 10 mg Fe l^{-1} in 0.026 M HNO_3 standards. Samples were diluted by 100x before analysis.

Sulfate analyses were performed by ion-chromatography, on Diomex 4508 I equipment with an AS4A column. The element was a $\text{NaHCO}_3/\text{Na}_2\text{CO}_3$ solution. The instrument was calibrated using 2, 10, 50 and 150 mg l^{-1} standards in 0.026 M HNO_3 . Samples were diluted 100x before elution to bring the concentration into the known range and reduce the effects of the nitrate peak.

5.3.5 SAMPLE CALCULATION

5.3.5.1 Calculation Evaluation

The basis of calculating iron and sulfate extractions evolved somewhat during the course of 30 months of testwork. Early in the program, all solids and liquids were collected and accounted for including the small amounts of solids which were accidentally collected in the liquid samples during the test. Calculations showed that these 'accidental' solids accounted for about 1% of iron and sulfate in the feed.

They were ignored beyond run S-4. The liquid samples themselves accounted for 4 - 5% of iron and sulfate in the feed. However, meticulously adding these samples back into the remnant liquids gave much the same answer as calculating that the samples represented all 1500 ml of liquid originally added. Table 5.3.5.1 compares the extractions using the two methods, for run S-4.

Table 5.3.5.1: Calculation Method Comparison S-4

| Time (mins) | Extractions Accounting for liquid samples | | Extractions Assuming Liquid Volume Constant | |
|-------------|---|-----------------------|---|-----------------------|
| | Fe (%) | SO ₄ = (%) | Fe (%) | SO ₄ = (%) |
| 5 | 20 | 12 | 20 | 12 |
| 10 | 56 | 45 | 55 | 45 |
| 20 | 71 | 70 | 71 | 70 |
| 30 | 92 | 85 | 92 | 86 |
| 45 | 97 | 86 | 98 | 87 |
| 60 | 99 | 86 | 98 | 90 |
| 90 | 99 | 91 | 98 | 92 |
| 120 | 98 | 95 | 97 | 96 |

The differences between the two methods were considered insignificant, especially in the light of later balance discrepancies, as discussed in the Supplemental Volume. Most calculations thereafter were based on the samples representing 1500 ml of liquid. Occasionally this assumption was checked with a more rigorous calculation. For the series using the attritioner, which showed appreciable evaporation losses, the more rigorous method was employed throughout, accounting for all liquids. Solids in samples were still insignificant.

5.3.5.2 Sample Calculations

A typical calculation, for sample S-32, is shown below. S-32 was chosen rather than the more complete S-4, because S-32 better typifies the limited sulfate assaying which was decided upon. It also typifies the less than perfect check balances which are discussed in the Supplemental Volume.

Leach Test S-32: 3.0000 g Gumeracha pyrite 90/125 μm , 80°C, 2.6 M HNO_3 , 280 rpm.

| Residue 0.2098 g | % by volume | Density | wt | % by wt |
|------------------|-------------|---------|-------|---------|
| FeS_2 | 4.5 | 4.5 | 20.3 | 9 |
| Gangue | 25 | 2.7 | 67.5 | 30 |
| S^0 | balance | 2.0 | 141 | 61 |
| | | | 228.8 | 100 |

$$\begin{aligned} \text{Fe in residue} &= 0.2098 \times 0.09 \times 0.465 \left(\frac{\text{Fe}}{\text{FeS}_2} \right) \\ &= 0.0086 \text{ g} \end{aligned}$$

$$\text{S}^0 \text{ in residue} = 0.2098 \times 0.09 \times 0.535 + 0.2098 \times 0.61 = 0.1381 \text{ g}$$

$$\text{SO}_4^{2-} \text{ in residue} = 0.1381 \times \frac{32.07 + 4(16)}{32.08} = 0.4135 \text{ g}$$

($\text{SO}_4^{2-}/\text{S}$)

Extractions based on **solids only**:

$$\text{Fe: } 1 - \frac{0.0086}{30 \times 0.465 \times 0.985 \text{ purity}} = 1 - 0.006 \rightarrow 99 \%$$

$$\text{SO}_4^{2-}: 1 - \frac{0.1381}{3.0 \times 0.535 \times 0.985} = 1 - 0.087 \rightarrow 91 \%$$

For **Calculated** extractions

Total species = species in solution + species in residue

$$\text{Fe: } 1.4891 = 1.4805 + 0.0086$$

$$\text{SO}_4^{2-}: 5.1760 = 4.7625 + 0.4135$$

Calculated extractions (Final)

$$\text{Fe: } 1.4805/1.4891 = 0.994 \rightarrow 99 \%$$

$$\text{SO}_4^{2-}: 4.7625/5.1760 = 0.920 \rightarrow 92 \%$$

For **check** extractions

Total species = species in feed solids

$$\text{Fe: } 3.000 \times \frac{0.465}{(\text{Fe}/\text{FeS}_2)} \times 0.985 = 1.3741 \text{ g Fe}$$

$$\text{S}^0: 3.000 \times \frac{0.535}{(\text{S}/\text{FeS}_2)} \times 0.985 = 1.5809 \text{ g S}^0$$

$$\text{SO}_4^- = 1.5809 \times \frac{32.07 + 4(16)}{32.07} = 12.5809 \times 2.99 = 4.7270 \text{ g SO}_4^-$$

(SO₄⁻/S)

Check extractions (final)

$$\text{Fe: } 1.4805/1.3741 = 1.077 \rightarrow 108\%$$

$$\text{SO}_4^-: 4.7625/4.7290 = 1.008 \rightarrow 101\%$$

Summing up consistency of test

| Final Extractions (%) | Fe | SO ₄ ⁻ |
|-------------------------------|-----|------------------------------|
| Solids only basis | 99 | 91 |
| (1 – residue) ÷ feed | | |
| Calculated | | |
| liquids ÷ (liquids + residue) | 99 | 92 |
| Check | | |
| liquids ÷ feed | 108 | 101 |

A consistent picture is shown, but the liquid assays are a little high, or perhaps for this test there was some evaporation loss. The standard method of calculating experimental data is to use solutions plus residues, or the **calculated** basis above. All extractions reported in this thesis are the calculated values.

5.4. TYPICAL LEACH TEST RESULTS AND DISCUSSION

5.4.1 NOTE ON GROUPING OF TESTS

Test results and discussion will be grouped into five areas. A 'typical' test will be described first

The second group of results presented will be those for which the variables tested are considered to be the classical kinetic variables. These are stirring rate, temperature, particle size and principal reagent concentration - in this case nitric acid.

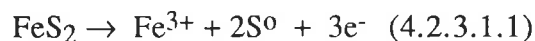
The third group of results is for those tests done to check experimental consistency. Results from duplicate runs to check the leach test consistency are followed by those tests used to check whether or not the solid pyrite had aged.

The fourth grouping is for those variables considered to be of industrial interest. This group includes five variables, with variations in sulfuric acid, ferric ion and chloride ion concentrations, followed by variations in percent solids in the slurry and then by blends of particle sizes.

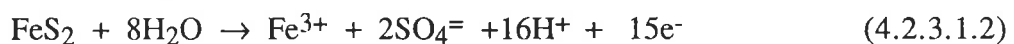
The fifth grouping of results includes experiments which demonstrate six additional effects. Three of these are variables which reading and discussion suggested were worth testing. They are attritioning, redox potential (Eh) and silver ion concentration. The next two sets are for effects observed during other tests. Two test runs were made to determine broadly whether other variable effects were additive; four results are presented to illustrate an observed time lag or induction period at the beginning of many tests. Finally, differences due to the source of pyrite are discussed briefly. The mathematical analysis of results is presented and discussed separately, in section 5.9. A separate section is employed because it is felt that this presents a more unified picture.

5.4.2 ELEMENTAL SULFUR FORMATION FROM PYRITE

It may be worthwhile reminding the reader that the oxidation of pyrite follows two parallel paths. In Chapter 4 these were shown to be:



and



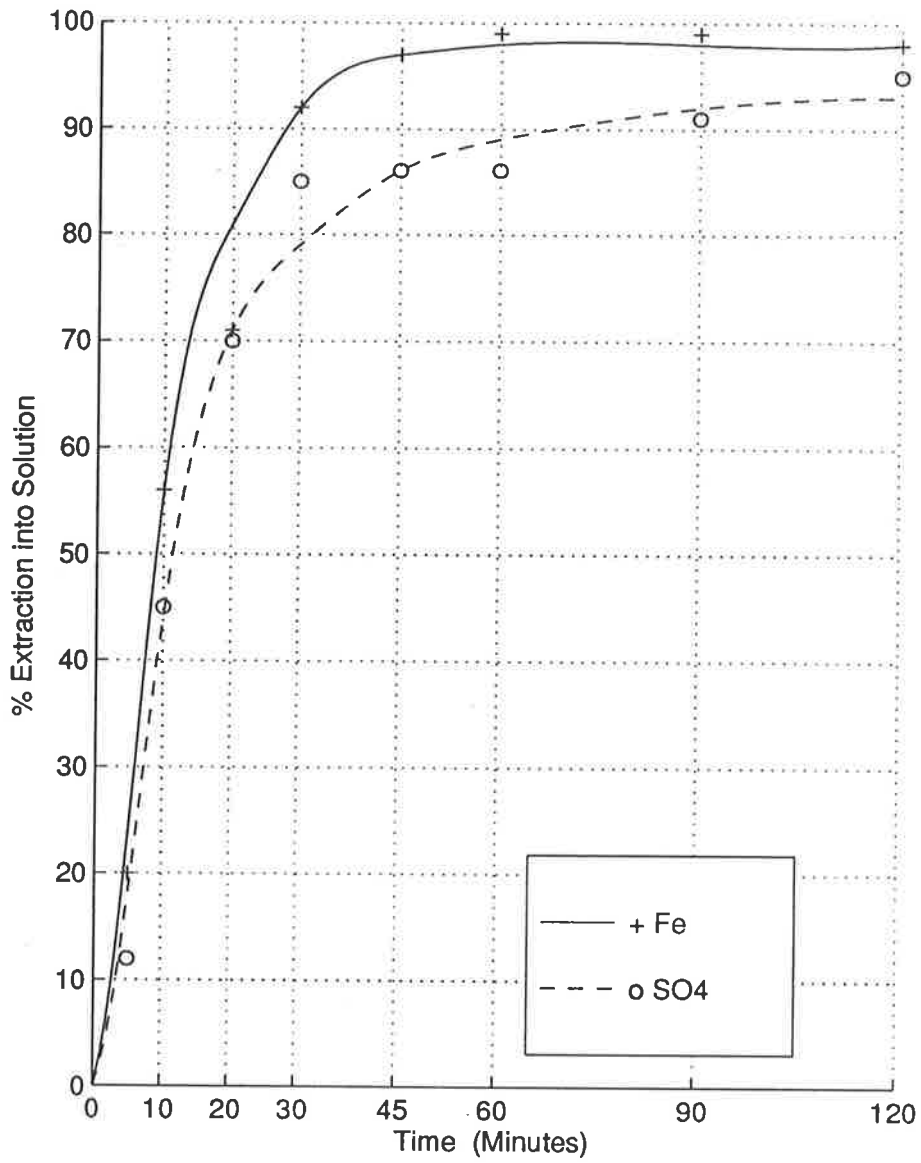


Figure 5.4.3.1 Typical Pyrite Leach Test in Nitric Acid

3.00g Gumeracha Pyrite +90 - 125 μm
 80° C 2.6 M HNO_3 1.5 litres

Nitric acid is an oxidant but is regenerated under conditions of the "Redox" process and so acts as a catalyst. In the leach tests of these experiments, the percentage concentration of pyrite is so low as to effectively maintain constant nitric acid concentration throughout a given test. (The exception being the percent solids series). Chapter 4 left open the question of whether the species formed was elemental sulfur or a sulfur rich lattice. The following "typical leach test" section answers this question, at least for macroscopic and practical purposes.

Two considerations are of interest throughout this chapter. The first is the effect of various variables in the kinetic oxidation rate of pyrite. That is the *sum* of the two parallel reactions above. This sum shows how fast the pyrite will react. The second consideration is the effect of the variables on the *difference* between the two reactions. This is elemental sulfur formation.

Given the experimental method, and the fact that elemental sulfur itself oxidises to sulfate, what can be obtained experimentally is the "sulfur gap". This is the amount of elemental sulfur *present* at various times. It remains to a mathematical analysis of results to estimate the oxidation rate of elemental sulfur *once it is formed*.

Two questions are of practical significance. One is how fast that elemental sulfur can be made to oxidise. The other is whether some conditions eliminate or reduce its formation in the first instance.

5.4.3 TYPICAL LEACH TEST - RESULTS

Figure 5.4.3.1. (opposite) is a typical leach test result, S-4. In this case Gumeracha pyrite 90/125 μm was leached at 0.2% solids in 2.6 M HNO_3 at 80°C. This test was one for which stirring speed was the key variable being tested.

It can be clearly seen that the rate of iron dissolution ($\text{FeS}_2 \rightarrow \text{Fe}^{3+}$) outpaces the sulfate dissolution ($\text{FeS}_2 \rightarrow \text{SO}_4^{2-}$). The difference is fairly constant - about 8% until the iron is virtually all dissolved, at about 60 minutes for S-4. After 60 minutes, the sulfate curve linearly approaches the iron curve to within 1-2% over the next hour.

For S-4 the accuracy of analysis can be judged as follows:

| <u>BASIS</u> (see 5.3.5.2) | <u>FINAL EXTRACTION</u> | |
|---------------------------------|-------------------------|------------------------------|
| | Fe ³⁺ | SO ₄ ⁼ |
| 'Calculated' extraction | 97% | 96% |
| Extraction based on solids only | 98% | 95% |
| 'Check' extraction | 93% | 105% |

For most other leach tests only three or four sulfate assays were obtained in order to limit analysis costs. A sulfate analysis cost more than double an iron analysis.

The figures which follow are generally summaries for a particular variable tested. For the sake of clarity, only iron extractions are shown in most cases.

5.4.4 DISCUSSION OF TYPICAL LEACH TEST

The curve for test S-4 (Fig 5.4.3.1) clearly shows that there is a 'gap' between iron and sulfate dissolution. That this 'gap' is due to elemental sulfur has been shown in several ways. First some of the early residues were dissolved in carbon disulfide, then tested with heavy liquids. The results showed S-4 residue to be 49% by weight soluble in CS₂. Visual analysis by microscope showed a waxy yellow 'flowerlet' morphology for most of the residue. This equated to 33% by weight sulfur. XRD and SEM analysis also confirmed that elemental sulfur is a major constituent of leach test residues.

Finally, the 'glue' which flocculated the pyrite particles during leach tests was identified as elemental sulfur by its now-familiar morphology under microscope. The frontpiece to this thesis shows such a floc, with elemental sulfur holding together partially-oxidised pyrite crystals.

Therefore, the 'gap' between the iron dissolution and sulfate dissolution curves is due to elemental sulfur. This 'sulfur gap' at about 8%, is considerably larger than that reported (3%) for nitric acid leaching of pyrite. The most likely reason is that other researchers reported only final, not intermediate values. After two hours, the 'sulfur gap' for S-4 has reduced to 2%.

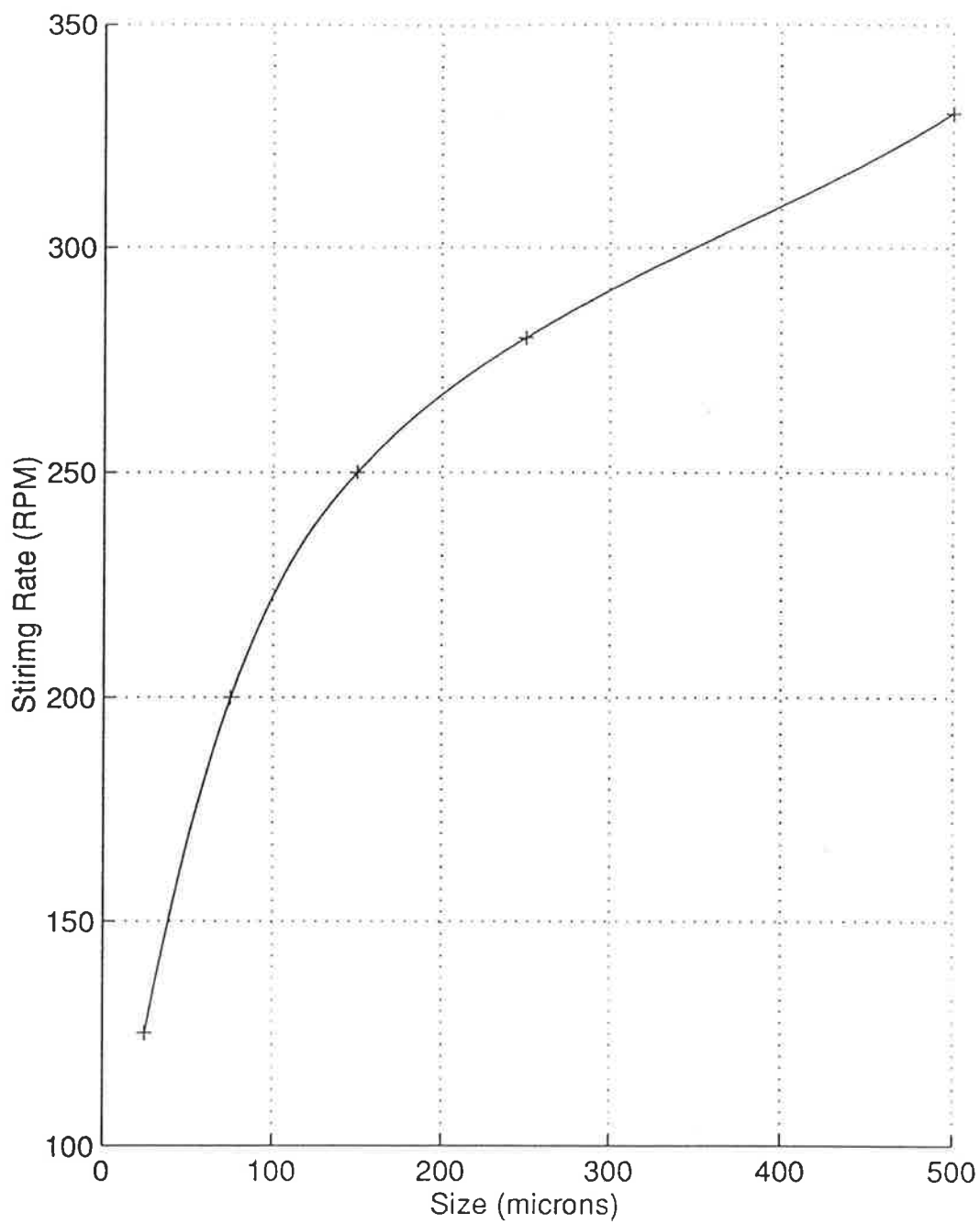


FIGURE 5.1.1.1. Minimum stirring speed to keep sand particles in suspension
180-250 μ m fraction

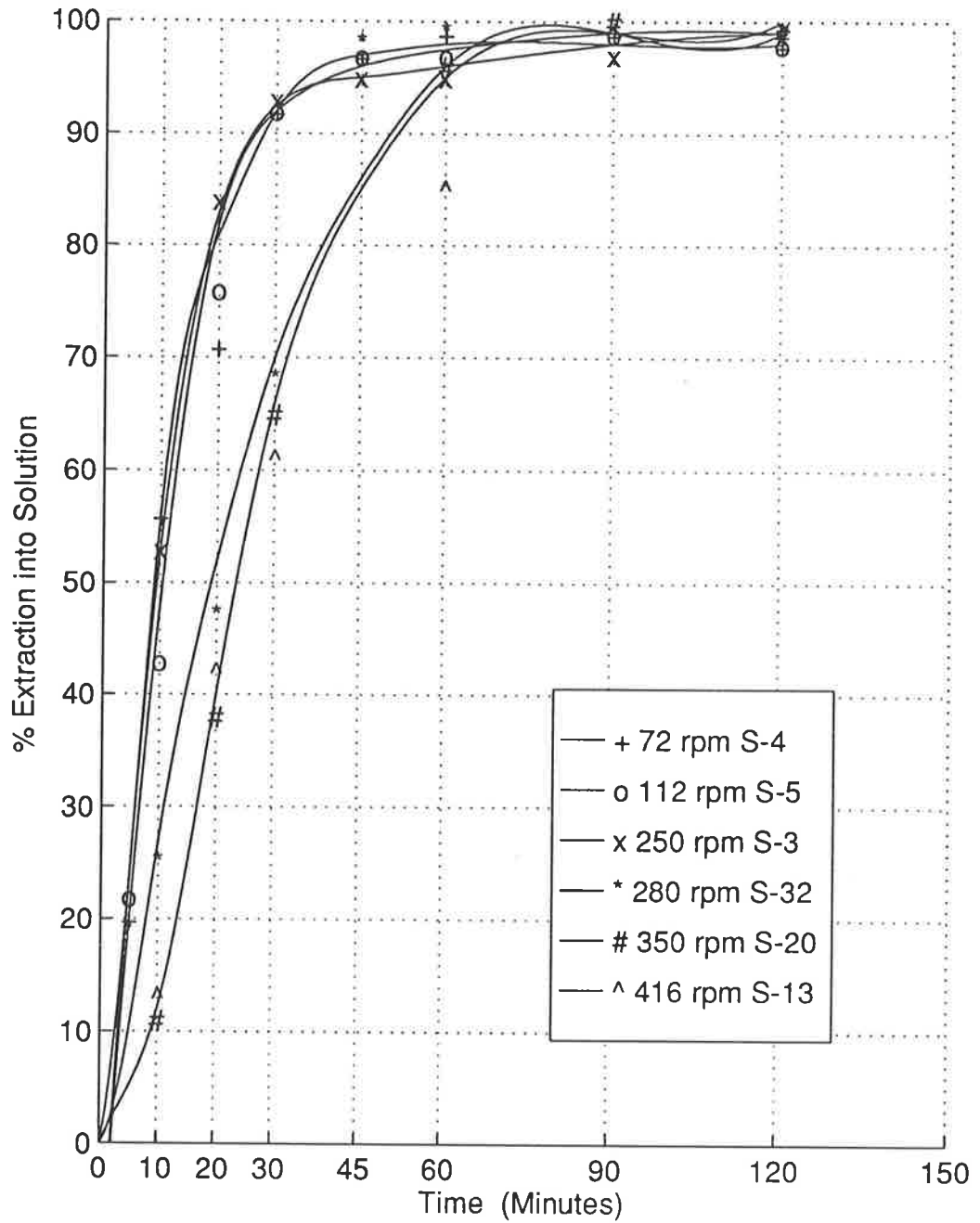


Figure 5.5.1.2

The Effect of Stirring Rate

Gumeracha Pyrite

+90 - 125 mm, 80° C, 2.6 M HNO₃ Iron Leaching Only

5.4.5 SECTION SUMMARY (TYPICAL LEACH TEST)

The typical leach test was discussed in some detail because the following sections are all summaries of series of such tests. Usually a series will include 3 -6 tests. The typical test was of rather better quality than some later tests but the pattern is similar. The ferric iron and sulfate curve and the 'sulfur gap' between them are typical. On a practical, macroscopic scale there is no question that the difference between the two curves is due to elemental sulfur, which in turn more slowly oxidises to sulfate. It may be useful to the reader to keep this typical test in mind when perusing subsequent sections in the present chapter.

5.5 CLASSICAL VARIABLES - RESULTS AND DISCUSSION

5.5.1 STIRRING RATE

5.5.1.1. Preliminary Suspension Test

Figure 5.5.1.1 (page 115) shows the results of the preliminary test, on screened sand, for the minimum speed required to suspend particles in the batch leach apparatus. The test using sand showed that all particles in the size ranges under consideration (45 - 250 μm) would be suspended at 280 rpm. Although this initial test was for sand (density 2.7 g cm^{-3}) the results turned out to be valid for pyrite (density 4.5 g cm^{-3}) as well. In fact, flocculating effects superseded these sand tests, allowing particles of oxidising pyrite to be suspended at lower stirring speeds.

5.5.1.2 Stirring Rate - Results

Figure 5.5.1.2 (opposite) summarises the seven tests performed on stirring rate. Results are shown for iron only. It is notable that the tests fall into three groups. From 72 to 250 rpm, the leaching rates are nearly identical. There is a significant decrease in leaching rate between 250 and 280 rpm, while the rate is much the same at 350 as at 280 rpm. At 416 rpm, the leaching rate has slowed again, at least in the range above 60% dissolution of iron.

5.5.1.3 Observations

In the glass apparatus, at the low % solids used, it was quite obvious that the appearance of the reacting pyrite particles mirrored the progress of the reaction. This effect is typified by table 5.5.1.1. describing run S-32 at 192 rpm with 90/125 μm Gumeracha Pyrite at 80°C in 2.6 M HNO_3 .

Table 5.5.1.1: Observations During Leach Test

| Time (min) | Fe Dissolution (by assay) % | Solids Appearance | NO _x generation |
|------------|-----------------------------|---|----------------------------|
| 1 | 1 | all pyrite suspended | none |
| 5 | 10 | all pyrite flocculated into 1 mm ϕ dark-green floccs | NO _x apparent |
| 10 | 25 | floccs 2-3 mm ϕ | |
| 15 | 40 | | copious NO _x |
| 20 | 52 | floccs reducing in size < 3 mm ϕ | |
| 30 | 68 | floccs smaller green | still generating |
| 40 | 86 | still green 2 mm ϕ | |
| 50 | 94 | light green 1 mm ϕ | decreasing |
| 75 | 98 (sulfate 84) | floccs greenish-yellow | little NO _x |
| 80 | 99 | floccs yellow - appear same density as liquid | |
| 90 | 99 | floccs yellow - transparent | none |

The colour change from green to yellow was consistent - it started at about 96% iron dissolution, which generally corresponded to about 85% sulfate conversion. The presence of an effective flocculant was also universal in these and all other low percent solids tests.

5.5.1.4 Stirring Rate - Discussion

Figure 5.5.1.2 deviates from the expected pattern. It is a common phenomenon that two-phase hydrometallurgical reactions are controlled by diffusion rates at the two-phase boundaries. In such cases, the leach rate could be expected to rise with stirring rate until the boundary layer reached its minimum. After that point, the leach rate would be constant (Cheng 1990).

For the data in Figure 5.5.1.2, stirring rates between suspension (70 rpm) and 250 rpm give rise to constant leach rates, within assay accuracy. This higher leach rate is associated with larger floc sizes up to 5 mm diameter. It is logical that large floccs would reduce leaching rate as surface area would be reduced. Therefore, the flocculation must be a result of the leaching reaction, not an unrelated phenomenon. The floccs appear, and logically are, open and porous as their size alone appears to have no effect on leach rate.

For the 416 rpm run, the solids, though still flocculated, became localised at the outer edges of the leach vessel. The space occupied by the solids was quite small,

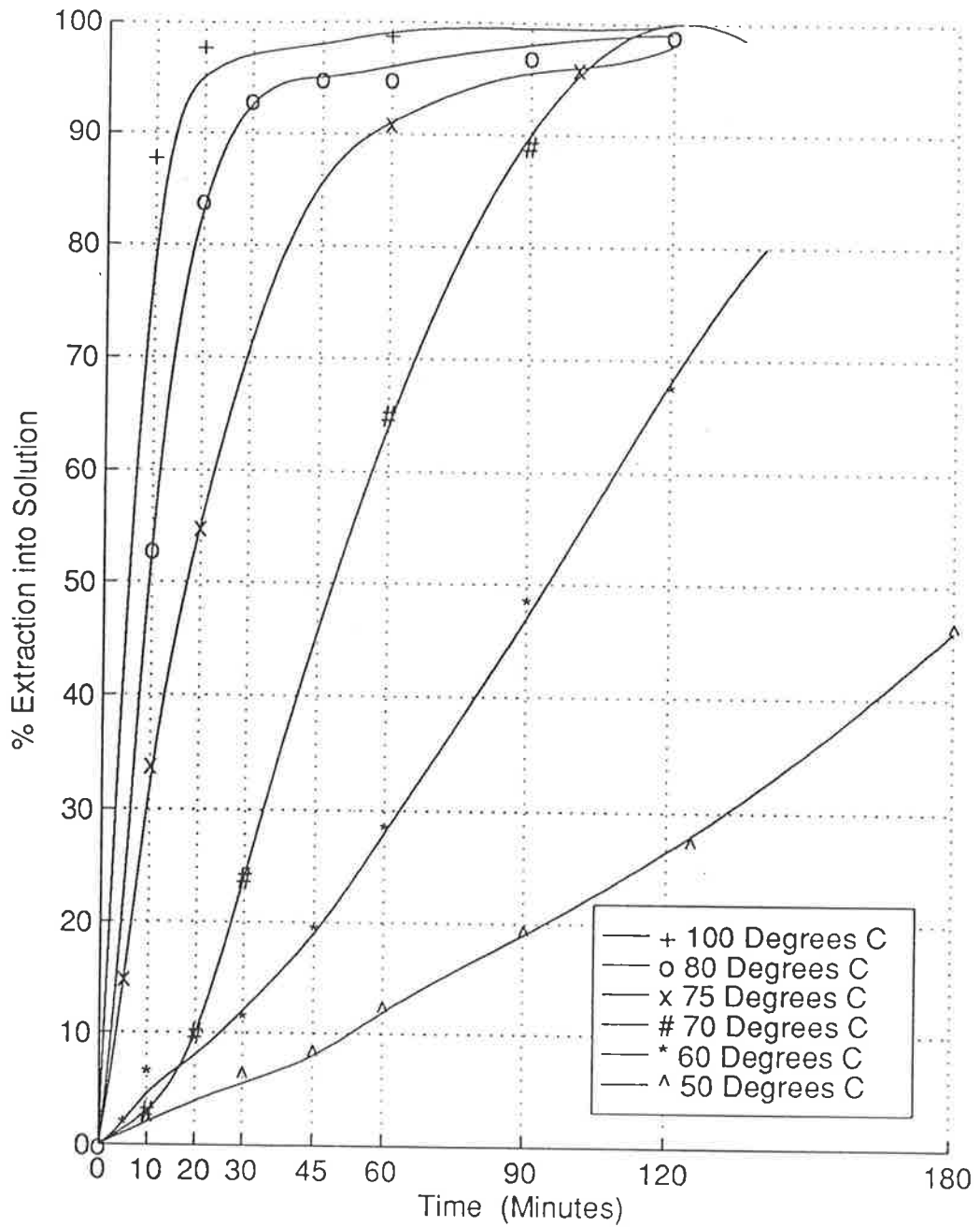


Figure 5.5.2.1 Effect of Temperature - Gummeracha Pyrite
 Gummeracha Pyrite
 Leaching 2.6 M HNO₃ +90-125 μm Curves for Iron
 Leaching Only

perhaps as small as 3 cm high by 2 cm thick. This could have led to a localised decrease in acid concentration which would account for the fall in leaching rate. This centrifuging effect arose because there were no baffles and represents a limiting condition for the experimental apparatus.

The results of these tests showed clearly the stirring speed should be kept constant for all further tests. A value of 280 rpm was selected. This speed could be expected to keep all particles in suspension, up to the anticipated maximum size of 250 μm . This was a consideration because there was less than 100 g of each size range of pyrite available.

5.5.1.5 Effect on 'Sulfur Gap'

Sulfur can only be measured during a test by the difference between the iron and sulfate assays in solution. In the present work, this difference will be referred to as the 'sulfur gap'. Stirring rate appears to have little effect on the 'sulfur gap'.

5.5.2. TEMPERATURE

5.5.2.1 Temperature Series - Results

Figure 5.5.2.1 (opposite) summarises the variation of leaching rate with temperature for Gumeracha pyrite (90/125 μm). This was actually the first test series run, before the effect of stirring rate was quantified. All tests except S-19 (70°C) were run at speeds below 250 rpm and so are comparable. S-19 should be slightly faster than the position shown for 70°C.

Figure 5.5.2.2 shows the variation in leaching rate for Huanzala pyrite with temperature. This material was the same size range as the Gumeracha pyrite but the fluid in the leach vessel turned black as soon as the pyrite was added. Microscopic inspection showed that the dry-screened Huanzala pyrite had adhering fines while the dry-screened Gumeracha pyrite was clean. For later series, Huanzala material was deslimed by washing on a 45 μm screen.

Table 5.5.2.1 shows the difference between the iron and the sulfate extractions for the Gumeracha Temperature test series of Figure 5.5.2.1. The difference must be due to that amount of pyrite sulfur ($\text{S}^{-\text{II}}$) which forms elemental sulfur (S^0) rather than sulfate ($\text{S}^{+\text{VI}}$). The "sulfur gap" decreases when the elemental sulfur itself oxidises to sulfate.

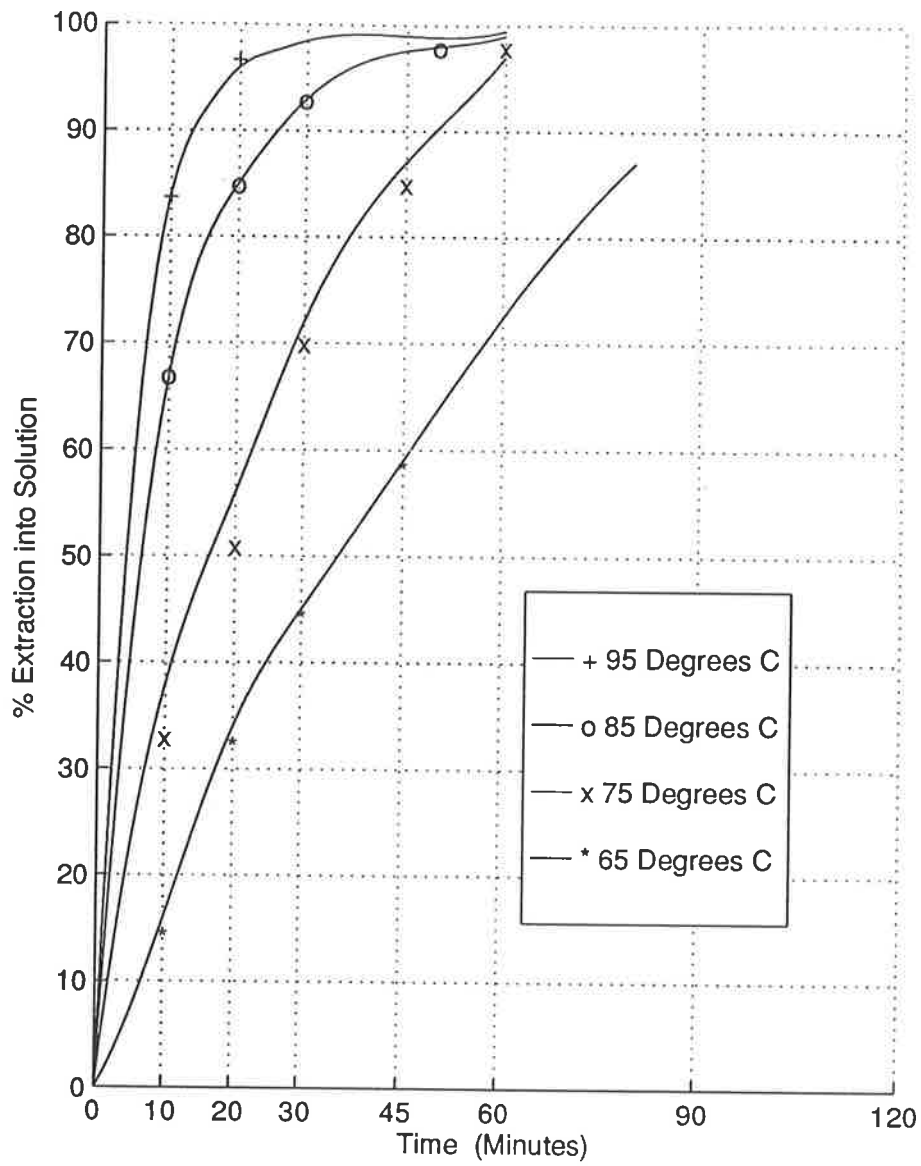


Figure 5.5.2.2 Effect of Temperature - Huanzala Pyrite
Huanzala Pyrite Leaching
 2.6 M HNO₃ +90 - 125 μm 296 rpm Curves for Iron Leaching Only

Table 5.5.2.1: "Sulfur Gap" for Gumeracha Pyrite Temperature Test Series

| Test No | Temp (°C) | "Sulfur Gap" (% S ⁰) at Fe Extractions % | | | | |
|---------|-----------|--|----|----|----|-------|
| | | 20 | 40 | 60 | 80 | Final |
| S-7 | 50 | 3 | 4 | 6 | — | 8 |
| S-6 | 60 | 3 | 5 | 8 | 6 | 4 |
| S-19 | 70 | 3 | 3 | 5 | 6 | 10 |
| S-9 | 75 | | | 8 | 8 | 5 |
| S-3 | 80 | | 5 | 10 | 14 | 3 |
| S-2 | 100 | | | | 7 | 5 |

Gumeracha pyrite 90/125 µm in 2.6 M HNO₃ @ 190 rpm (or equivalent)

Table 5.5.2.2 shows the "sulfur gap" for the Temperature test series using Huanzala pyrite.

Table 5.5.2.2: "Sulfur Gap" for Huanzala Pyrite Temperature Test Series

| Test No | Temp (°C) | "Sulfur Gap" (% S ⁰) at Fe Extractions % | | | | |
|---------|-----------|--|----|----|----|-------|
| | | 20 | 40 | 60 | 80 | Final |
| S-25 | 65 | 2 | 6 | 6 | — | 7 |
| S-28 | 75 | 3 | 1 | 3 | 2 | 4 |
| S-26 | 85 | 3 | 3 | 5 | 7 | 6 |
| S-27 | 95 | | | 43 | 5 | 4 |

Huanzala pyrite 90/125 µm in 2.6 Molar HNO₃ @ 296 rpm

5.5.2.2 Temperature Series - Discussion

Both series of tests show an expected increase in leaching rate with temperature. Temperatures below 70°C will be too slow for commercial leaching. Even H₂SO₄ leaching residence times seldom exceed two hours. Typically, the last 5% of iron extraction requires more than half of the time for reaction.

The Huanzala pyrite is more reactive than Gumeracha pyrite. That this is not merely due to the fines present in Huanzala was confirmed by comparing later individual results (S-48 to S-65).

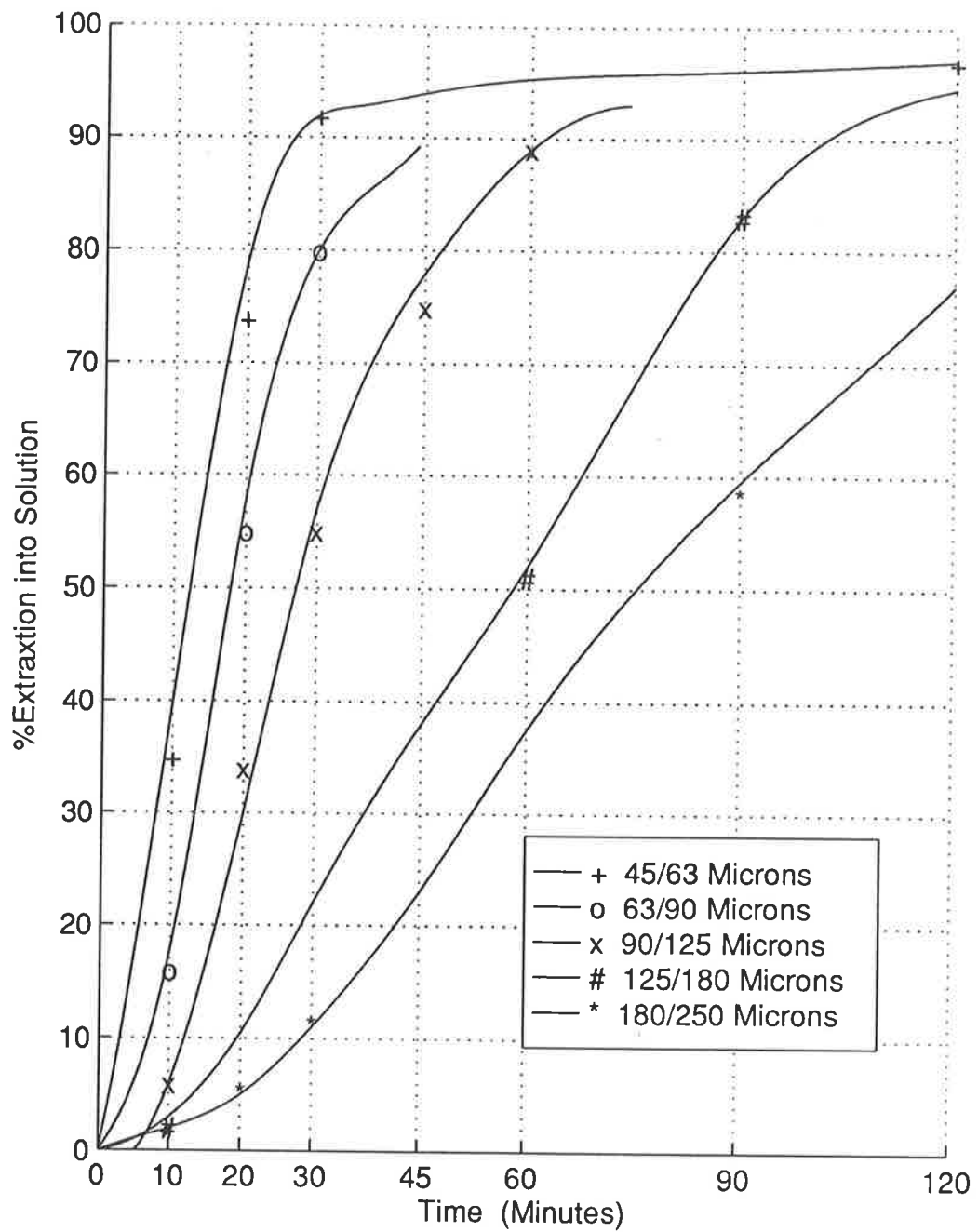


Figure 5.5.3.1 Effect of Particle Size

Gumeracha Pyrite, 75°C, 2.6 M HNO₃ 144 rpm

The 'sulfur gap' was not modified by temperature. At this particle size, Huanzala pyrite showed a smaller 'sulfur gap' (2 - 7%) than Gumeracha pyrite (3 - 14%).

5.5.3 PARTICLE SIZE

5.5.3.1 Series Results

Figure 5.5.3.1 (opposite) summarises the effect of pyrite particle size on the kinetics of leaching. Four of these tests were conducted at 75°C, in 2.6 M HNO₃ at 280 rpm. Test S-9 (90/125 µm) had been conducted at 144 rpm, so values plotted on Figure 5.5.3.1 for S-9 have been mathematically 'corrected' for the difference in stirring speed. Only iron dissolution is shown for simplicity.

5.5.3.2 Particle Size Series - Discussion

Reducing particle size increases the kinetics of leaching, as would be expected. Successively smaller screen fractions as tested have a mean particle dimension ratio of $1/\sqrt{2}$. Assuming all particles in a given size fraction are cubes of the mean dimension, the total pyrite surface area increases by a factor of $\sqrt{2}$ for the next finer fraction.

Table 5.5.3.1: Surface Area for different size fractions

| Fraction (µm) | Mean Size (µm) | For 1 cube | | For 3.0 g | |
|---------------|----------------|-------------------------|---------------------------|------------------|-------------------------|
| | | Area (cm) ² | Weight (gm) | No. of Particles | Area (cm ²) |
| 180/250 | 215 | 0.277x10 ⁻² | 0.0047 x 10 ⁻³ | 67,000 | 186 |
| 125/180 | 153 | 0.1404x10 ⁻² | 0.0161 x 10 ⁻³ | 186,000 | 261 |

It could be expected that doubling the surface area of pyrite available for reaction would double the reaction rate. In fact, over the size range tested, the first-order rate constants increase by a factor of 2.1 when the surface area is doubled (see section 5.9). For the limited number of tests performed, this slightly larger than expected increase in the rate constants may not be significant.

The curves for the coarse size fractions in Figure 5.5.3.1 also show a slow initiation part of the curve. The reaction does not seem to come up to speed until about 8-15% of the pyrite has reacted, requiring 30 minutes for the 180/250 µm fraction. This initiation section was included when calculating the rate constant but is discussed more fully in Section 5.8.

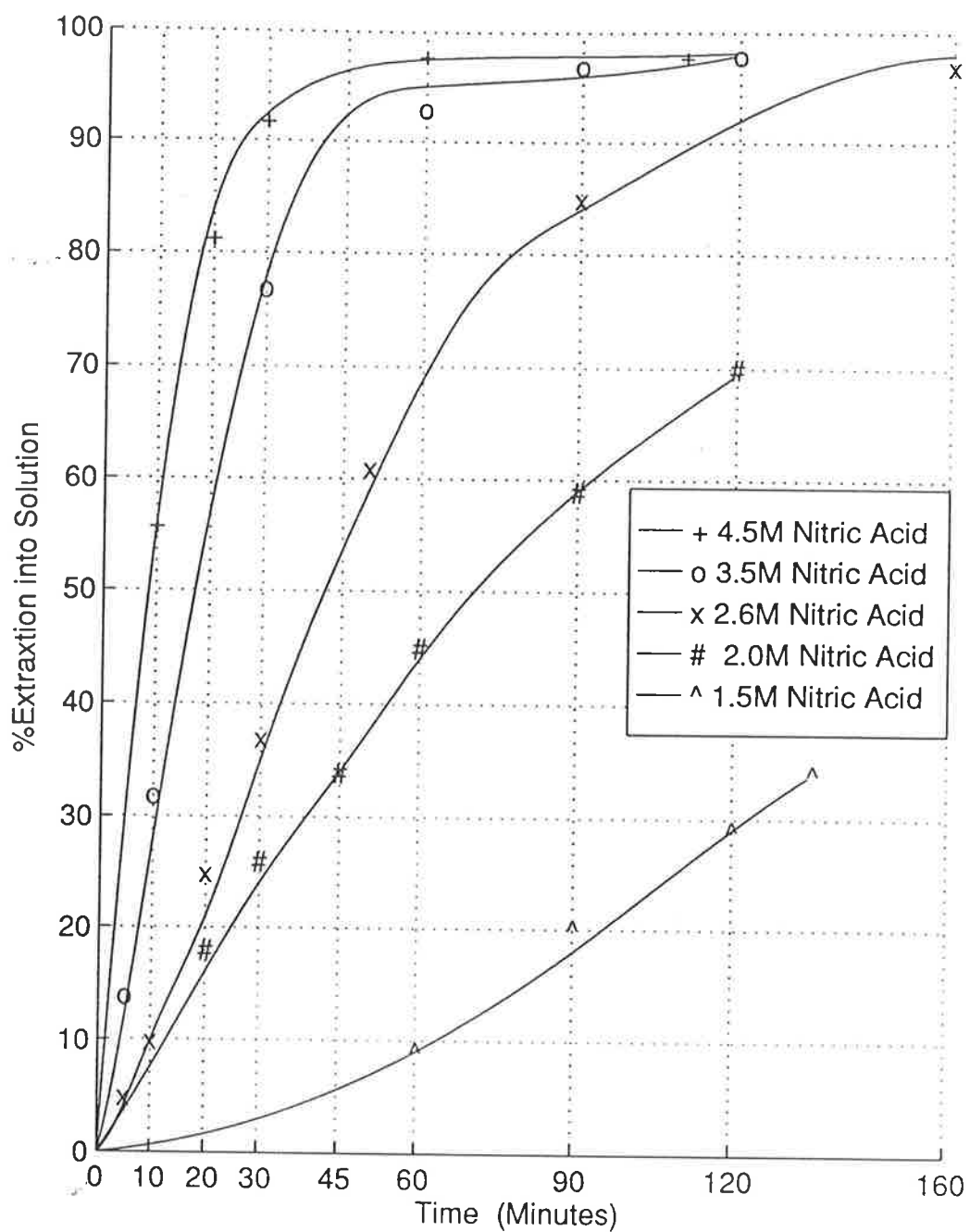


FIGURE 5.5.4.1 Effect of $[HNO_3]$
Gumeracha Pyrite 125-180 μm , 80°C

The 'sulfur gap' for this series of tests showed no surprises. The proportion of elemental sulfur was in the 6-12% range, much as for the temperature series of tests with Gumeracha pyrite. There was some indication that the maximum sulfur gap was lower at both coarse and fine ends of the size spectrum than in the middle 90/180 μm . This was one reason for performing subsequent series of tests on size fractions in the middle range.

5.5.4 NITRIC ACID CONCENTRATION

5.5.4.1 Series Results

Figure 5.5.4.1 summarises the effect of nitric acid concentration on leaching kinetics. The series, run on Gumeracha pyrite 125/180 μm at 80°C includes a 'corrected' curve for S-18.

Once again, only iron dissolution is shown on Figure 5.5.4.1, for simplicity.

For this series, there appears to be a tendency for the 'sulfur gap' to narrow at low acid strengths, particularly in the early stages of leaching. Table 5.5.4.1 gives an indication of the pattern.

Table 5.5.4.1: 'Sulfur Gap' for [HNO₃] Test Series

| Test No | [HNO ₃] moles litre | 'Sulfur Gap' (%) at Fe extractions of | | | | |
|---------------------|---------------------------------------|---------------------------------------|----|----|----|-------|
| | | 20% Fe | 40 | 60 | 80 | Final |
| S-51 | 1.5 | - 4% | 1 | * | * | 1* |
| S-18 (corrected) | 2 | - 1% | 3 | 4 | 6 | 8 |
| S-48 | 2.6 | 5% | 10 | 16 | 14 | 7 |
| S-49 | 3.5 | | 8 | 14 | 16 | 4 |
| S-50 | 4.5 | | | 6 | 5 | 3 |

* Test discontinued

5.5.4.1 Nitric Acid Concentration - Discussion

The series shows a very strong dependence of leach rate on the nitric acid strength. The corrected value for S-18 (63/90 μm) fits in well with the rest of the series (125/180 μm). The corrected values were obtained by using a first-order rate constant of 0.010 min^{-1} . The rate constant for the actual S-18 test was 0.022 min^{-1} .

Since the surface area should have been double that for the rest of the series, the rate constant should have been $0.022/2.1 = 0.010 \text{ min}^{-1}$ (See 5.5.3.1).

The 'sulfur gap' for this series, as shown in Table 5.5.4.1, was quite variable. The picture was incomplete and imprecise. This reflects economic constraints and assay accuracy. Nevertheless, there is a trend showing that less elemental sulfur results when lower nitric acid concentrations are used.

5.5.5 SECTION SUMMARY (CLASSICAL VARIABLES)

This summary will be qualitative in nature and will discuss trends. Quantification of leach variables effects will be found in Section 5.9, the Mathematical Analysis. The same pattern will be followed for sections 5.6 through 5.8.

A number of trends were established for the leach variables designated 'classical'. Leach rate appears independent of stirring rate. Some grouping of tests, attributed to flocculation effects and equipment limitations, was observed. Consequently, following tests series used a constant stirring speed of 280 rpm. Temperature had a strong effect on rate as expected. The 'sulfur gap' was independent of stirring speed and temperature. The leach rates varied with the initial surface area of the pyrite as determined on different screen fractions. There is some indication of larger 'sulfur gaps' for the mid-size particles. Leach rate showed a strong dependence on nitric acid concentration. Lower acid concentrations tended to show less elemental sulfur.

5.6 **EXPERIMENTAL CONSISTENCY - RESULTS AND DISCUSSION**

PURPOSE

The results in this section cover tests whose analysis served to check experimental consistency. Such checks were felt to be particularly important because part-time research meant that the leach tests were spread over some 30 months. It was possible the solid pyrite "aged" over that period.

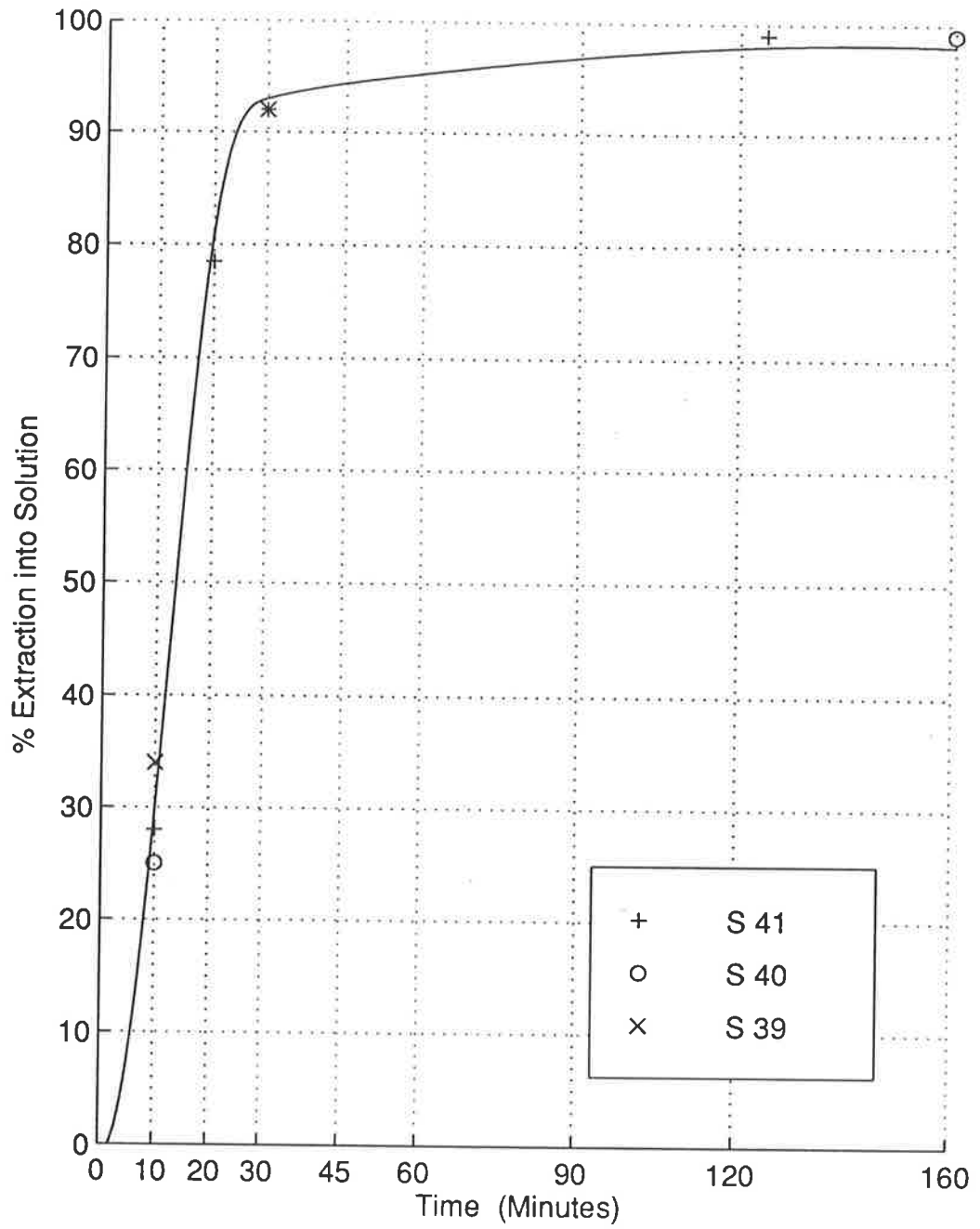


Figure 5.6.1.1 Checking Leach Test Method Consistency
Gumeracha Pyrite 63-90 μm
80°C, 2.6 M HNO_3 280 rpm

5.6.1 LEACH TEST METHOD

5.6.1.1. Series Results

Figure 5.6.1.1 (opposite) and Table 5.6.1.1 show the data for three leach tests run to check the repeatability of the method. All these tests used Gumeracha pyrite 63/90 μ m, at 280 rpm, 80°C in 2.6 Molar HNO₃.

Table 5.6.1.1: Leach Test Consistency

| Time Minutes | Iron Extraction % | | |
|---|-------------------|----------------------|-----------------|
| | S-39 19/3/95 | S-40 23/03/ 95 | S-41 28/3/95 |
| 10 | 25% | 33% | 28% |
| 20 | – | – | 78 |
| 30 | 92 | 92 | 92 |
| 60 | – | – | 105 |
| 120 | 97 | 97 | 98 |
| Final Fe Extraction (solids basis) % | 97 | 97 | 98 |
| Final SO₄⁼ extraction - (liquids basis) % | 92 | 92 | 91 |
| - solids basis | 92 | 91 | 90 |

5.6.1.2 Leach Test Method - Discussion

The values in Table 5.6.1.1 justify drawing a single curve for the three leach tests. The widest differences in the points assayed for is 8%, which occurs in a very steep section of the curve at 10 minutes. A one-minute difference in sample timing could easily account for the 8% extraction difference. At any rate 8% is within the assay accuracy quoted by Amdel ($\pm 10\%$). The 105% extraction value for S-41 at 60 minutes is spurious. It is 12% above the anticipated value from the curve, but could easily have been the result of an extra particle of pyrite included in the 60 minute sample. This series of tests were in error in that it was discovered that the laboratory assistant had forgotten to filter his samples. Thus any solid pyrite in the sample could dissolve over the several days before the assay was performed. This series therefore appears kinetically faster than (all other) series for which the solids were filtered out immediately. The surprising fact is how consistent this series is

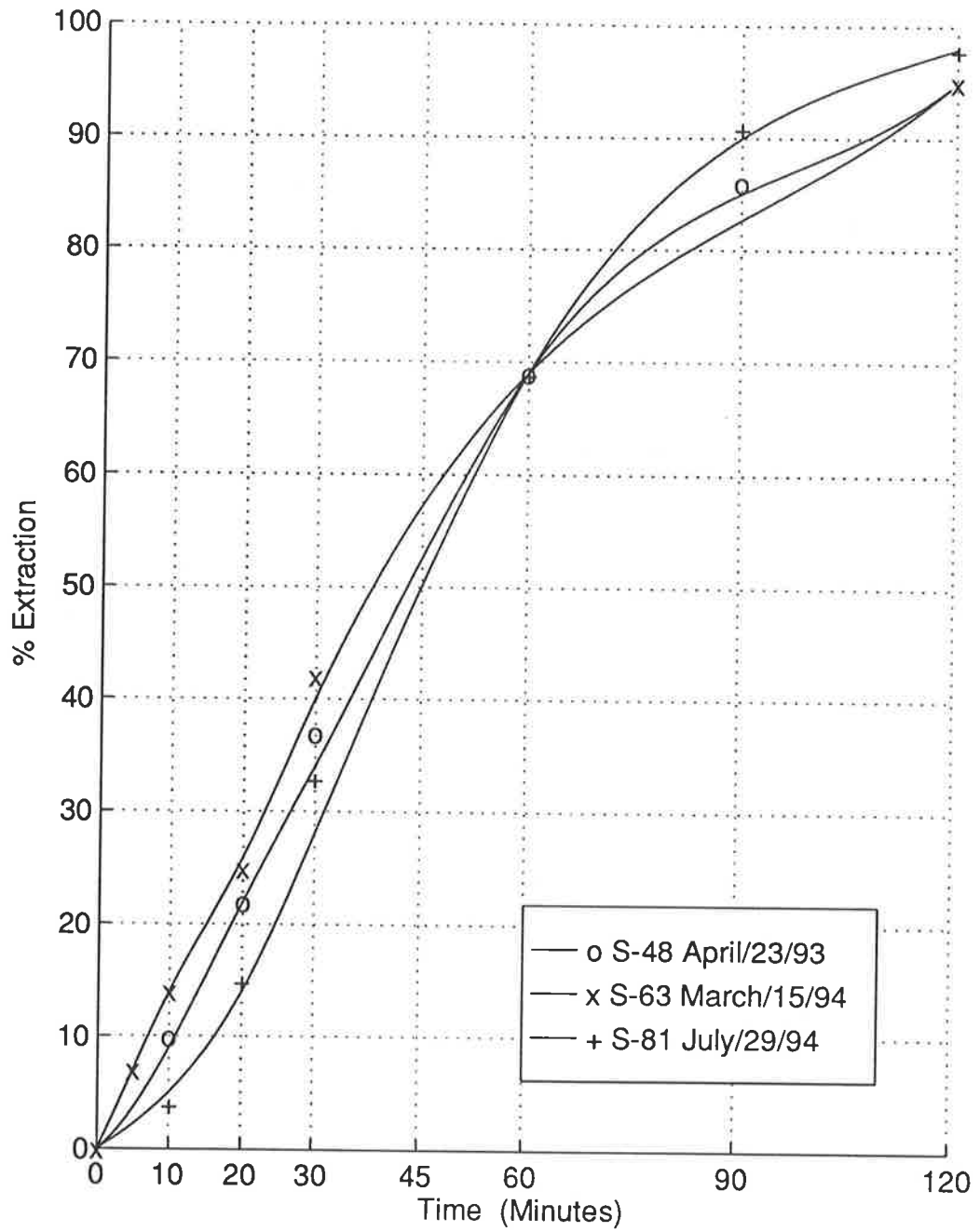


Figure 5.6.2.1 Aging of Pyrite Check
 125-180 μ m 80°C Gumeracha Pyrite 2.6 MHNO₃

within itself. It adequately demonstrates that the experimental leach method itself is consistent, at least in the hands of the same experimenter.

5.6.2 AGING OF PYRITE SAMPLES

The comparisons made to assess aging of pyrite samples are grouped as follows:

- 1) Gumeracha pyrite 125/180 μm - at 80°C
- 2) Gumeracha pyrite 125/180 μm - at 75°C
- 3) Gumeracha pyrite 90/125 μm
- 4) Gumeracha pyrite 63/90 μm
- 5) Huanzala pyrite 90/125 μm

The Gumeracha pyrite was crushed and screened on 13 May 1992. Huanzala pyrite was crushed and screened 4 June 1992, with the coarsest (+ 250 μm) fraction crushed again 28 July 1994.

5.6.2.1 Gumeracha Pyrite (125/180 rpm 80°C) - Results and Discussion

Figure 5.6.2.1 shows the iron leach results for 125/180 μm Gumeracha pyrite at 80°C, 280 rpm, 2.6 M HNO₃. The three tests were performed 4/3/93, 3/15/94, and 7/29/94 respectively. The time gaps between them were therefore eleven and four-and-a-half months.

Figure 5.6.2.1 could indicate a slight steepening of the curve as the pyrite ages; at the worst, however, the curves differ by 8% which is within assay error. Also, the three curves change their relative positions, S-63, the intermediate test, starts most quickly, matches the other two curves at 60 minutes and is in the intermediate position after 90 minutes. Such intermingling of the curves makes any trend, if it exists, less clear.

The feel of the experiments had the writer concerned that aging might be occurring as early as July 1992. It was decided that to run leach tests in batches or series, with a base case for each series. Thus a series, run over a month or two, would be valid for a given variable, even if the pyrite aged.

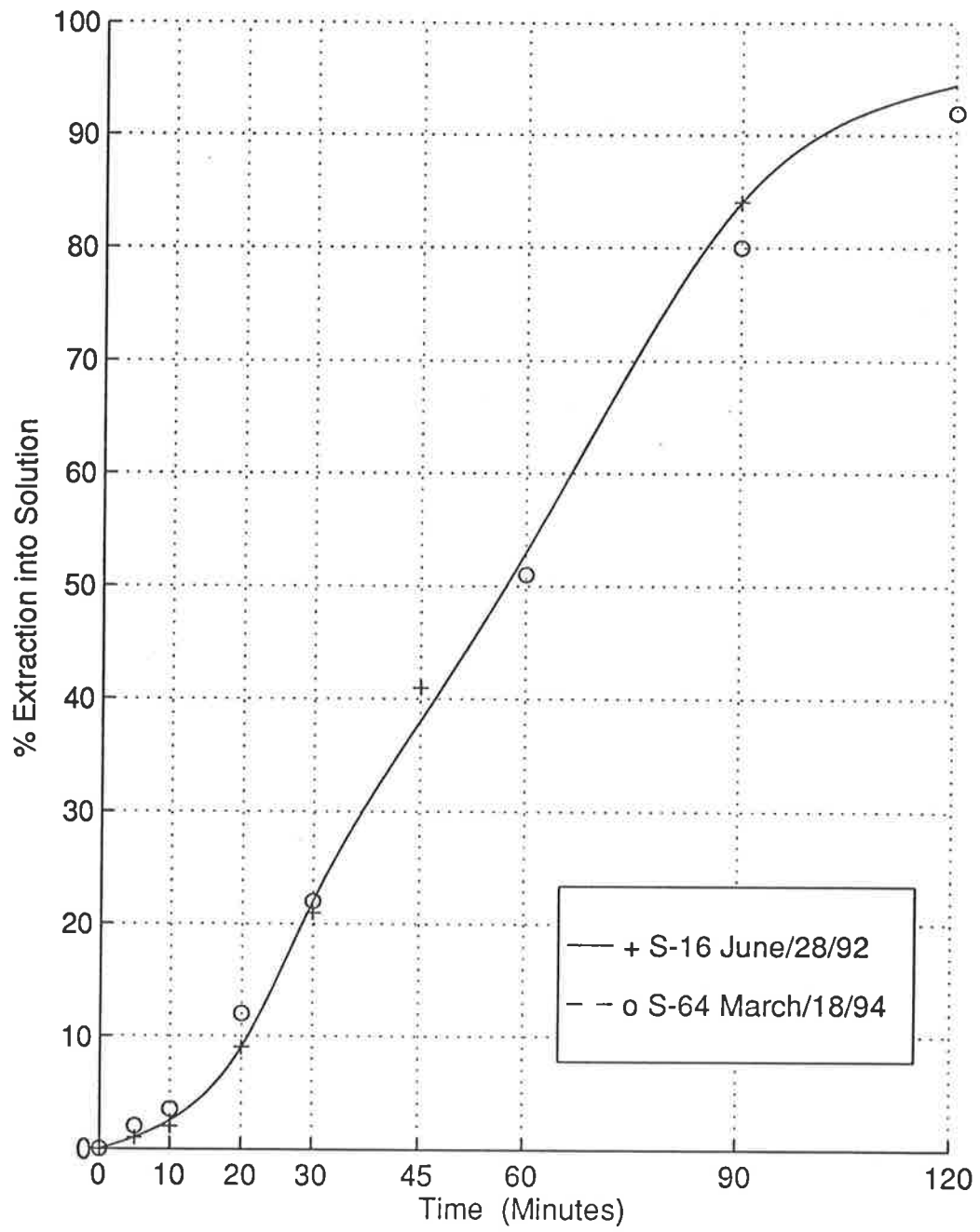


Figure 5.6.2.2 Aging of Pyrite Check

125-180 μm , 75°C, 2.6 M HNO_3 280 rpm

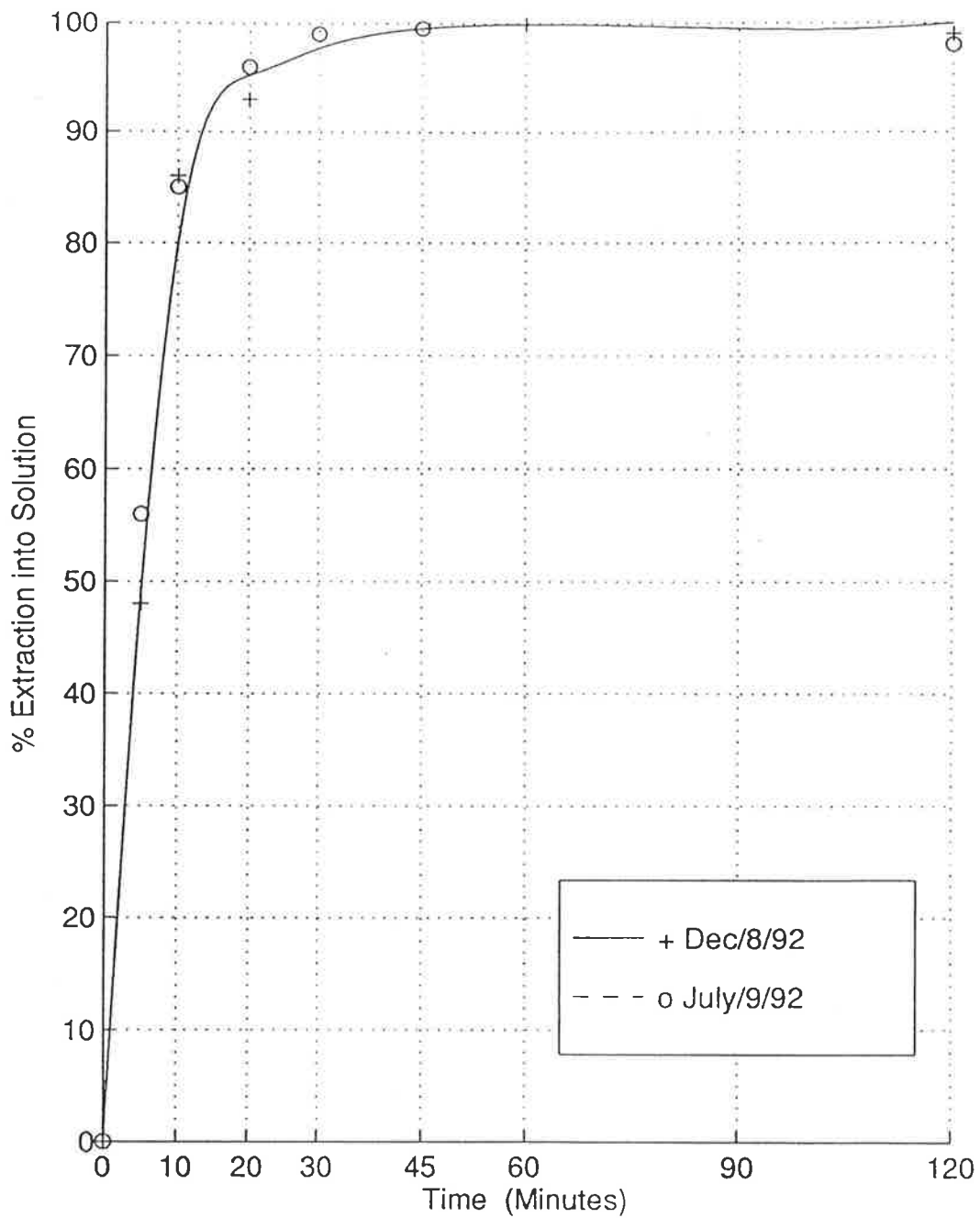


Figure 5.6.2.3: Aging of Pyrite Check
90-125 μm , 80°C, 2.6 M HNO_3 , H_2SO_4 , 280 rpm

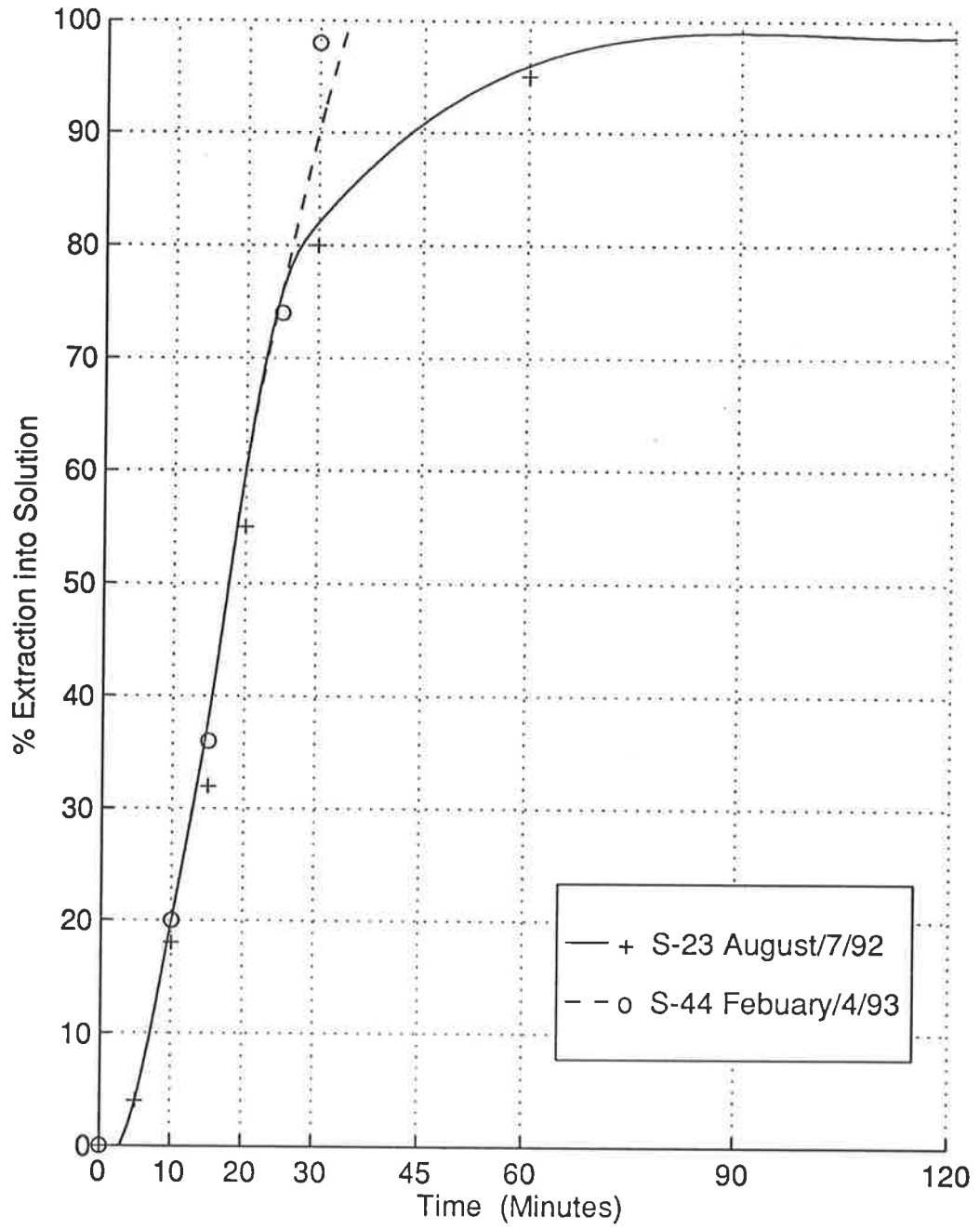


Figure 5.6.2.4 Aging Check of Pyrite Check Huanzala

63-90 μ m, 70°C, 280 rpm, 2.6 M HNO₃

5.6.2.2 Gumeracha Pyrite (125/180 μm 75°C) - Results and Discussion

Figure 5.6.2.2 shows iron leach results for 125/180 Gumeracha pyrite at 75°C, 280 rpm, 2.6 M HNO_3 . The tests were performed 6/28/92 and 3/18/94 or twenty months apart.

Figure 5.6.2.2 is the same size fraction (125/180 μm) as 5.6.2.1 but at 5°C lower temperature. With twenty months lapsed time, there is no evidence that the points fell on different curves for the two experiments. There is no indication of aging in this case.

5.6.2.3 Gumeracha Pyrite (90/125 μm) - Results and Discussion

Figure 5.6.2.3 is for Gumeracha pyrite sized between 90 and 125 μm . The other variables were 80°C, 280 rpm and 2.6 molar HNO_3 . In both cases sulfuric acid, 1.7 M, was also added. The tests, on 7/9/92 and 12/8/92 were four months apart. Again, only iron extractions are shown.

For the fraction 90/125 μm , the two experiments appear to be on the same curve. These two curves are only four months apart, and both had sulfuric acid added. At the end of the sulfuric acid series, the 90/125 μm Gumeracha fraction was exhausted. No later tests could be tried for aging. However, these two show no evidence for aging.

5.6.2.4 Gumeracha Pyrite (63/90 μm) - Results and Discussion

The iron leach results for Gumeracha pyrite at 63/90 μm are shown in Figure 5.6.2.4. These tests, performed on 7/8/92 and 4/2/93 were ten months apart. These tests were at 75°C, 280 rpm, in 2.6 M HNO_3 .

The points for the two experiments appear to be on identical curves up to 75% iron extraction. Above this, the S-44 curve appears to diverge from S-23. On the day of S-44 the laboratory had to be evacuated due to a fire in the building. Due to the confusion at the time, and the fact that the S-44 thirty minute result is totally atypical of all curves, the S-44 curve's divergence can be ignored. Given that, there is no evidence of aging in the 63/90 μm fraction Gumeracha pyrite.

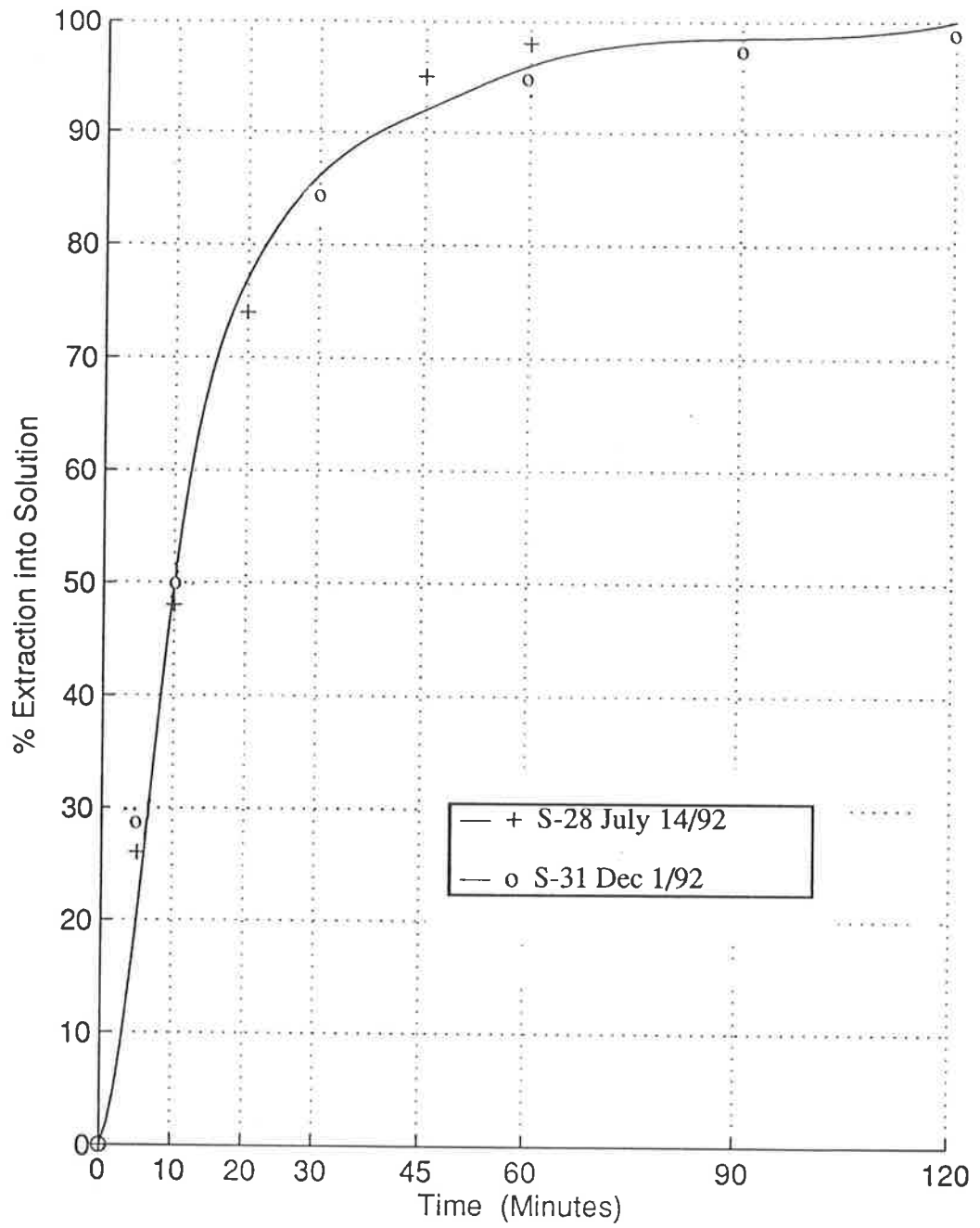


Figure 5.6.2.5 Aging of Pyrite Check
 Huanzala 90 - 125 μ m 75° C

5.6.2.5 Huanzala Pyrite

Figure 5.6.2.5 compares two runs with Huanzala pyrite four-and-a-half months apart. Both tests were run 2.6 M HNO₃, at equivalent speeds, 296 and 280 rpm. The former, at 75°C was mathematically corrected to 80°C for Figure 5.6.2.5

The two experiments for Huanzala pyrite 90/125 µm show equivalent results. The S-28 pyrite had not been deslimed. The experimental log failed to show whether S-31 had been deslimed or not. (This was one of very few examples when the log was incomplete.) However, the differences between S-31 and subsequent Huanzala tests indicated that S-31 was probably not deslimed. S-28 (corrected for temperature) figures exceed S-31 extraction by about 3% above 90% extraction. This is within assay and probably sampling error.

Later tests on Huanzala pyrite would be difficult to compare to S-31 because of the variables which were changed. For example, S-65 could not be compared mathematically because S-65 was coarser 125/180 µm and deslimed. Also, no tests had been done on Huanzala pyrite to quantify the effect of particle size. Thus, Figure 5.6.2.5 represents the only data on aging for Huanzala pyrite.

5.6.3 SULFUR GAP

5.6.3.1 Leach Test Method Series

The values for the sulfate curves have been left off the figures in this section for clarity. The leach test method results were calculated for the final filtrate sulfate values only. These were within 1% for the three experiments of Figure 5.6.1.1 and within 2% of the calculated values based on the original solids in the reactor.

5.6.3.2 Aging Series - "Sulfur Gap"

No particular pattern was evident for the sulfur gap from the aging analysis samples.

Unfortunately, there was not always close agreement between check and calculated extractions from all tests. In the aging series, sulfate data was less complete, for reasons of economy.

Occasionally the "sulfur gap" was negative (ie, SO₄⁼ extraction was greater than iron extraction for S-81). These cases corresponded to a poor correlation of data

for the balance in question. At the pH of these experiments (- 0.5) all iron remains in solution and it is not possible for the sulfate extraction figure to exceed the iron extraction figure for pyrite.

Those runs showing an anomalous sulfur gap such as S-81, had poor balances generally. For S-81 the extractions calculated by dividing the final filtrate species contents by that added as solid were lower by 10 and 13%, respectively for iron and sulfate, than those based on filtrate and residues. Suffice it to say that the "aging" series, anomalous "sulfur gap" values occurred only when the species balances were poor. Otherwise, the pattern for the sulfur gap was similar to previous work in this thesis. Maximum proportion of elemental sulfur during tests was from 6-16% for Gumeracha pyrite.

5.6.4. SECTION SUMMARY (EXPERIMENTAL CONSISTENCY SERIES)

The series showed that for tests run at about the same time, by the same experimenter, results could be in excellent agreement, as close as 2% and seldom worse than 8%. Over longer time periods, reproducibility appeared to become erratic. It had been suspected that the pyrite was aging, despite being stored in capped containers under nitrogen, in a freezer. The analyses of 5.6.2 refute this. There is little, if any evidence of aging. It would be expected that the finer size fractions would show more evidence than the coarse fractions. This did not occur, for the limited cases analysed. No evidence is available over the entire time span for the leach tests however (13/5/92 to 21/11/94 - thirty months.)

The strategy of doing tests in series - all within a month or so, covering the full range for a given variable, was adopted to overcome any aging problems. Aging has been shown not to be serious but the strategy has the side benefit of lessening variability due to other factors.

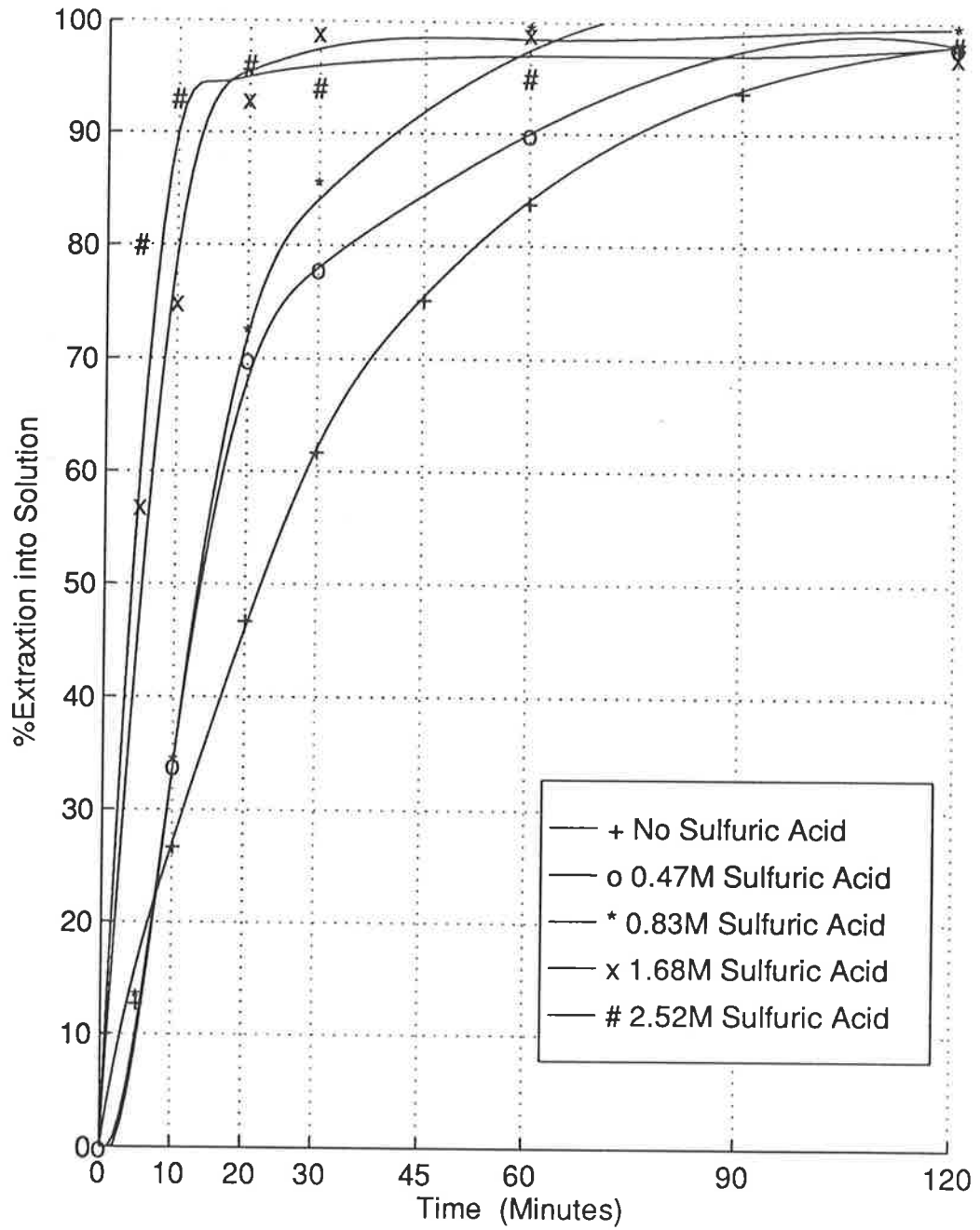


Figure 5.7.1.1 Effect of Sulfuric Acid Concentration

Gumeracha Pyrite 90-125 μm , 80°C, 2.2 M HNO_3 , 280 rpm
Curves are for Fe dissolution only

5.7 INDUSTRIAL VARIABLES - RESULTS AND DISCUSSION

This section covers summarised results for those variables which might be termed industrial. Both sulfuric acid and ferric iron are produced by the reaction of iron sulfides with nitric acid in the "Redox" process. Both of these may affect the reaction kinetics. Both will be present in recycled plant liquors. Chloride ion has been suggested as an oxidant. In many cases, it will be present if high total dissolved solids water is used in the plant. Plant equipment sizing and operating economics will be affected by the solids content of the feed stream. Feed ores or concentrates can normally be expected to have a wider size range than that used for experimental purposes.

5.7.1 SULFURIC ACID CONCENTRATION

5.7.1.1 Series Results

Figure 5.7.1.1 (opposite) summarises the effect of adding H_2SO_4 , at various concentrations, to the leach vessel before pyrite was introduced. This series was run on Gumeracha pyrite 90/125 μm at 80°C and 280 rpm. Nitric acid concentration was 2.2 molar for the series. Values for run S-32 were corrected for nitric acid concentration. Only iron extractions are shown.

No attempt was made to analyse solutions for sulfate ion, in this series, due to the very high background of sulfate ion in solutions (41,000 ppm @ 0.42 M H_2SO_4 and higher). For S-32 (no H_2SO_4 added) the "sulfur gap" was quite wide - 12% at 96% Fe extraction.

5.7.1.2 The Effect of Sulfuric Acid Concentration

It is obvious that sulfuric acid accelerates the oxidation of pyrite. The curves steepen regularly as $[\text{H}_2\text{SO}_4]$ increases. Some of the curves co-coincide at early times when extraction rates are highest. The 2.5 M H_2SO_4 curve reaches a ninety-four percent (94%) iron extraction as quickly as would be expected and then barely increases after 10 minutes, so that it appears to be overtaken by the 1.7 M and 0.83 M curves. The calculation of this section of the curve is very sensitive to the solids visual analysis. Inaccuracy here would explain the anomaly above 96% iron extraction, but the rest of the curve is still valid.

The sulfur gap for S-32 is in the range expected from the classical leach tests.

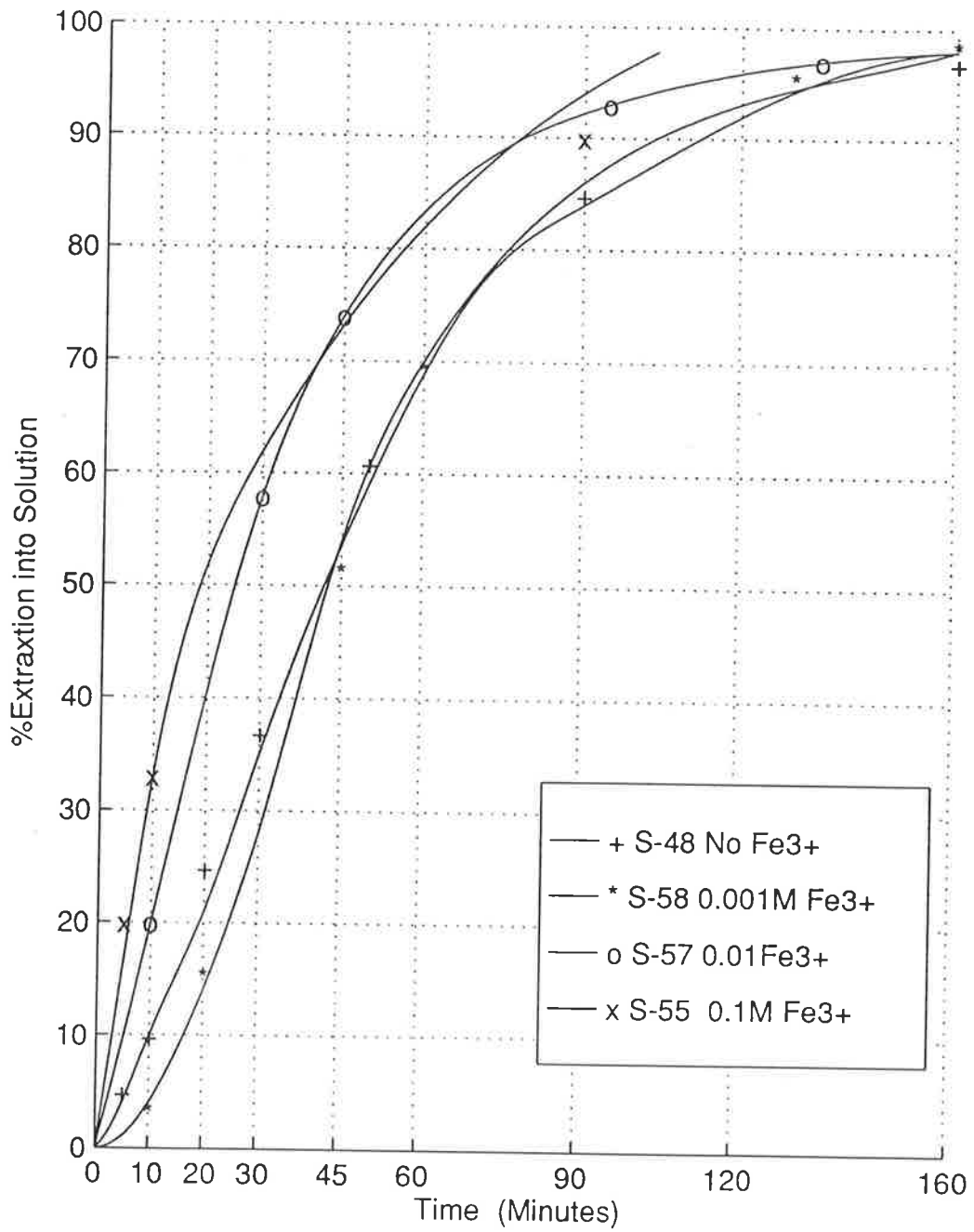


Figure 5.7.2.1: Effect of Adding Fe³⁺ (Fe dissolution only)
 Gumeracha Pyrite 125-180 μm , 80°C, 280 rpm, 2.6 M HNO₃

5.7.2 FERRIC ION CONCENTRATION

5.7.2.1 Series Results

Figure 5.7.2.1 (opposite) summarises the iron extractions for the series to which ferric ion was added. The curves are qualitative for 0.1 M Fe^{3+} and above. Iron analyses were difficult to distinguish from the background values of added iron (5,580 ppm for 0.1 M). Some confidence can be had in the iron curves, however, from the sulfate extraction curves of Figure 5.7.2.2. For this series, the sulfate curves are better than the iron extraction curves. The series was performed with Gumeracha pyrite (125/180 μm , at 80°C, 280 rpm in 2.6 M HNO_3).

Table 5.7.2.1 gives values for the difference between iron and sulfate extractions for the series. The accuracy of the "sulfur gap" is, of course, dependant on the accuracy of both the iron and sulfate curves. In the present series, the iron values are not as accurate as other series.

Table 5.7.2.1: "Sulfur Gap" For (Fe^{3+}) Series

| Test No | (Fe^{3+}) | "Sulfur Gap" at % Fe extraction (%) | | | | |
|---------|--------------------|-------------------------------------|-----|-----|-----|-------|
| | | 20% | 40% | 60% | 80% | Final |
| S-48 | nil | 4 | 10 | 16 | 13 | 7 |
| S-58 | 10^{-3} | – | 2 | 4 | 3 | 5 |
| S-57 | 10^{-2} | – | – | 3 | 4 | 7 |
| S-55 | 10^{-1} | Fe curve too questionable | | | | 6 |

5.7.2.2 The Effect of Ferric Ion Concentrations

Ferric ion acts as an oxidant in the nitric acid system as it does in most systems. The ferric ion concentrations tested were fairly low, because of the problems with iron assaying. An earlier test, S-8 at 70°C on 90/125 μm Gumeracha pyrite, suggested that the effect continues at 0.2 M [Fe^{3+}]. The oxidising effect of ferric ion is apparent at 10^{-3} M. This has applications to be discussed later in sub-section 5.8.5.

The iron curves placement becomes less certain as the added iron background increases. The balance for S-48 was quite good (within 4%) but at 10^{-2} M the balances were out by 14%. S-55 at 0.1 M, required some creative calculations, including the assumption that the stirrer shaft was dissolving at a linear rate with

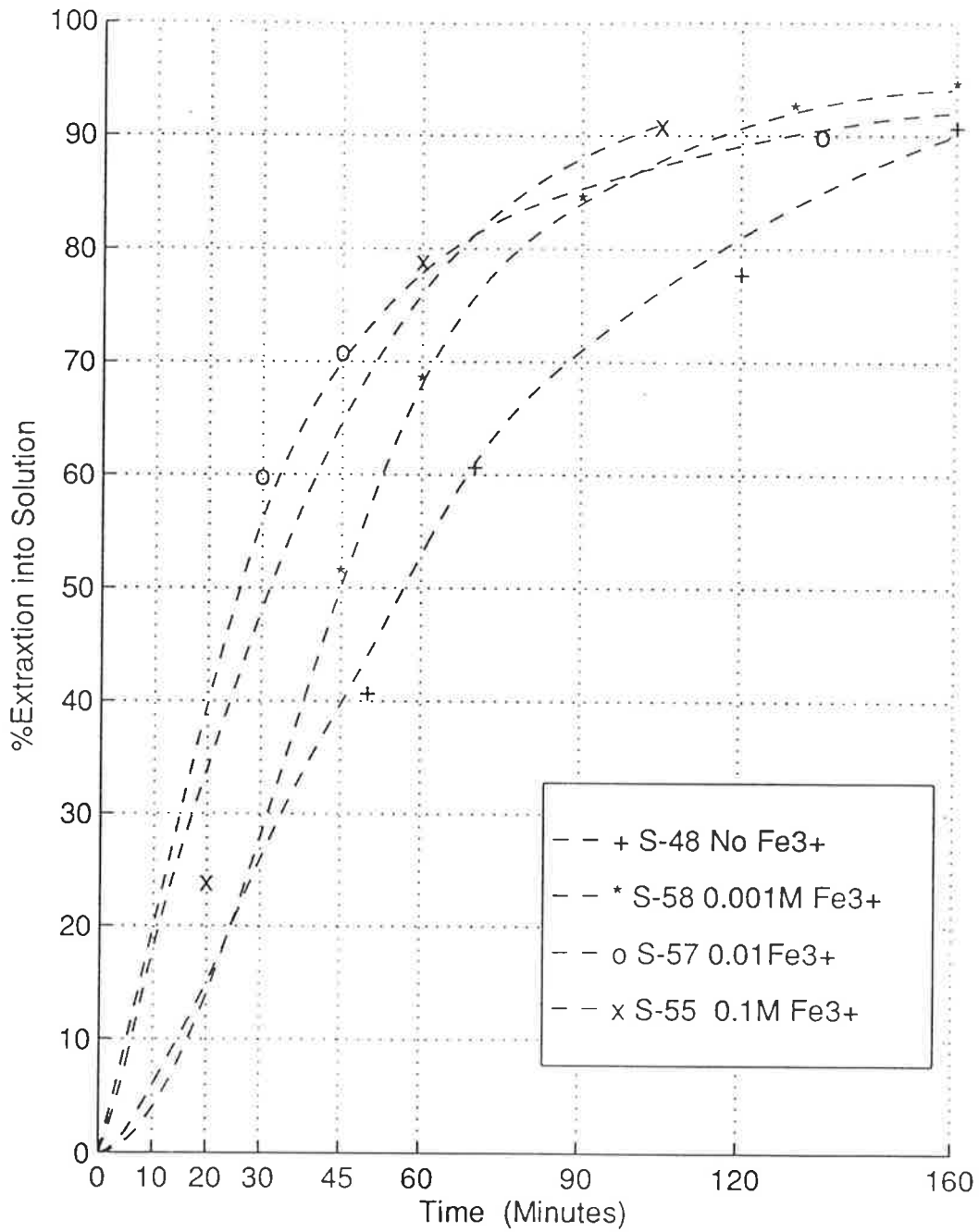


Figure 5.7.2.2: Effect of Adding Fe³⁺ (SO₄⁼ only)
 Gumeracha Pyrite 125-180 μ m, 80°C, 280 rpm, 2.6 MHNO₃

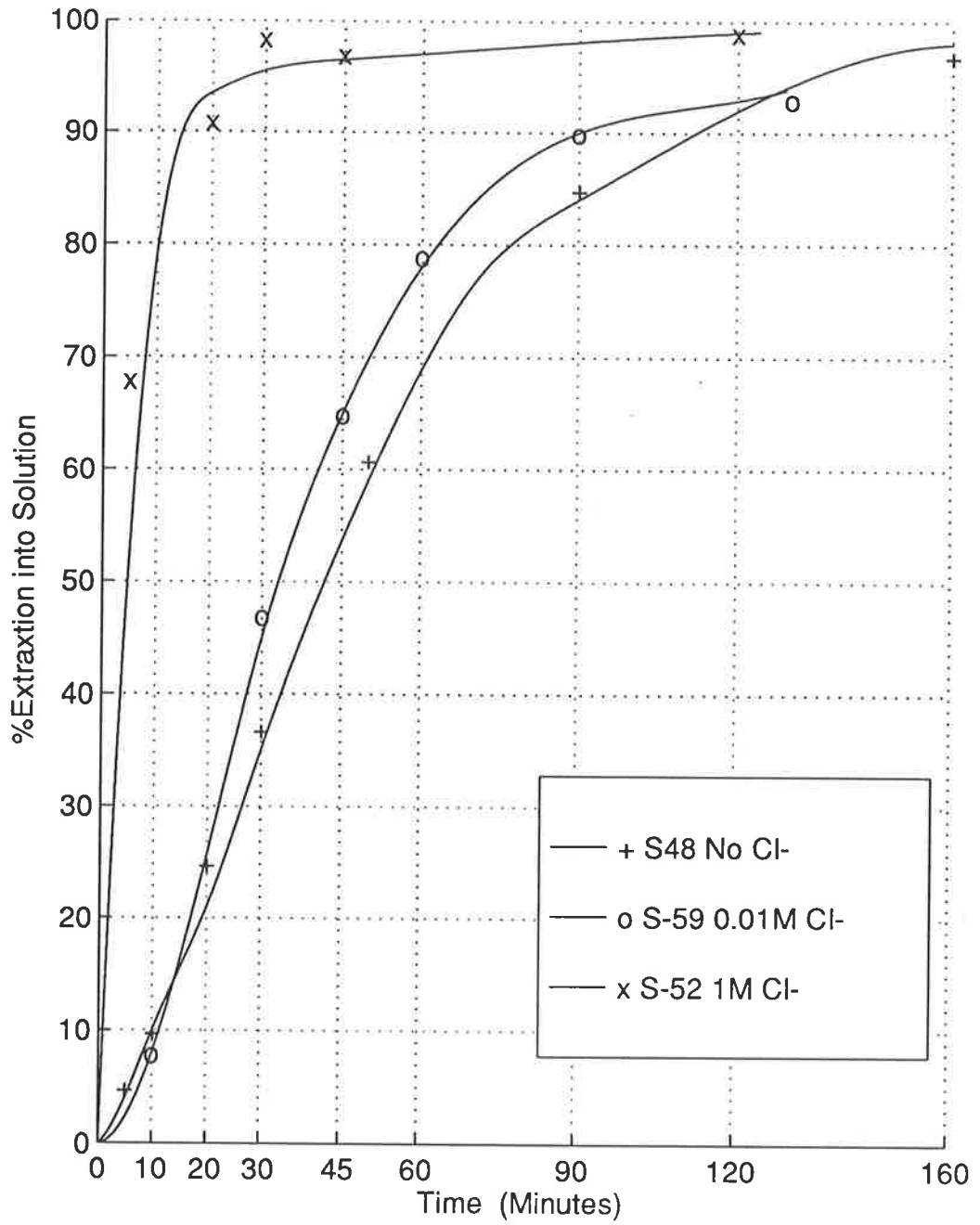


Figure 5.7.3.1 Effect of Cl⁻ Ion (Fe Dissolution only)

Gumeracha Pyrite, 125-180 μm, 80°C, 280 rpm, 2.6 M HNO₃

time. Without this assumption, the iron balance was 41% high. Sulfate balances were better, the worst being +13%.

Table 5.7.2.1 tends to indicate that ferric ion considerably decreases the sulfur gap at least up to 80% iron dissolution. Final sulfur gaps were similar for the series, however. Since this table is based on iron curves which are not very accurate, these sulfur gap numbers are also not accurate. The trend is quite marked, however. There is evidence that ferric iron reduced the sulfur gap.

5.7.3 CHLORIDE ION CONCENTRATION

5.7.3.1 Series Results

Figure 5.7.3.1 (opposite) summarises the effect of chloride ion on iron leach rate. The test (S-52) at 1.0 M KCl is qualitative, the stirrer shaft was attacked to such an extent that the solution turned dark. The iron curve is again given credence due to the sulfate curves for the same test (Figure 5.7.3.2). A test at 10^{-3} M Cl^- was unaccountably much slower than the run without any chloride ion. That test (10^{-3} M Cl^-) was not repeated and is not included in Figure 5.7.3.1. or 5.7.3.2.

Table 5.7.3.1 presents the data available on "sulfur gap" for the chloride ion series .

Table 5.7.3.1: "Sulfur Gap For $[Cl^-]$ Series

| Test No | $[Cl^-]$ | "Sulfur Gap" at % Fe Oxidation | | | | |
|---------|-----------|--------------------------------|----|--------------------|-----|-------|
| | | 20 | 40 | 60 | 80 | Final |
| | Molar | | | | | |
| S-48 | nil | 4 | 10 | 16 | 13 | 7 |
| S-60 | 10^{-3} | – | 2 | 3 | 7 | 6 |
| S-59 | 10^{-2} | – | –4 | 4 | 5 | 6 |
| S-52 | 1.0 | – | – | 24? qualitative | 28? | 1 |

5.7.3.2 The Effect of Chloride Ion Concentration

Chloride ion strongly enhances oxidation rate of the pyrite. Both iron and sulfate dissolution rates are accelerated at as little as 350 ppm Cl^- . Only two tests are available, and S-52 iron curve is qualitative. Again, some creative calculating assumed a linear dissolution rate of the stirrer shaft.

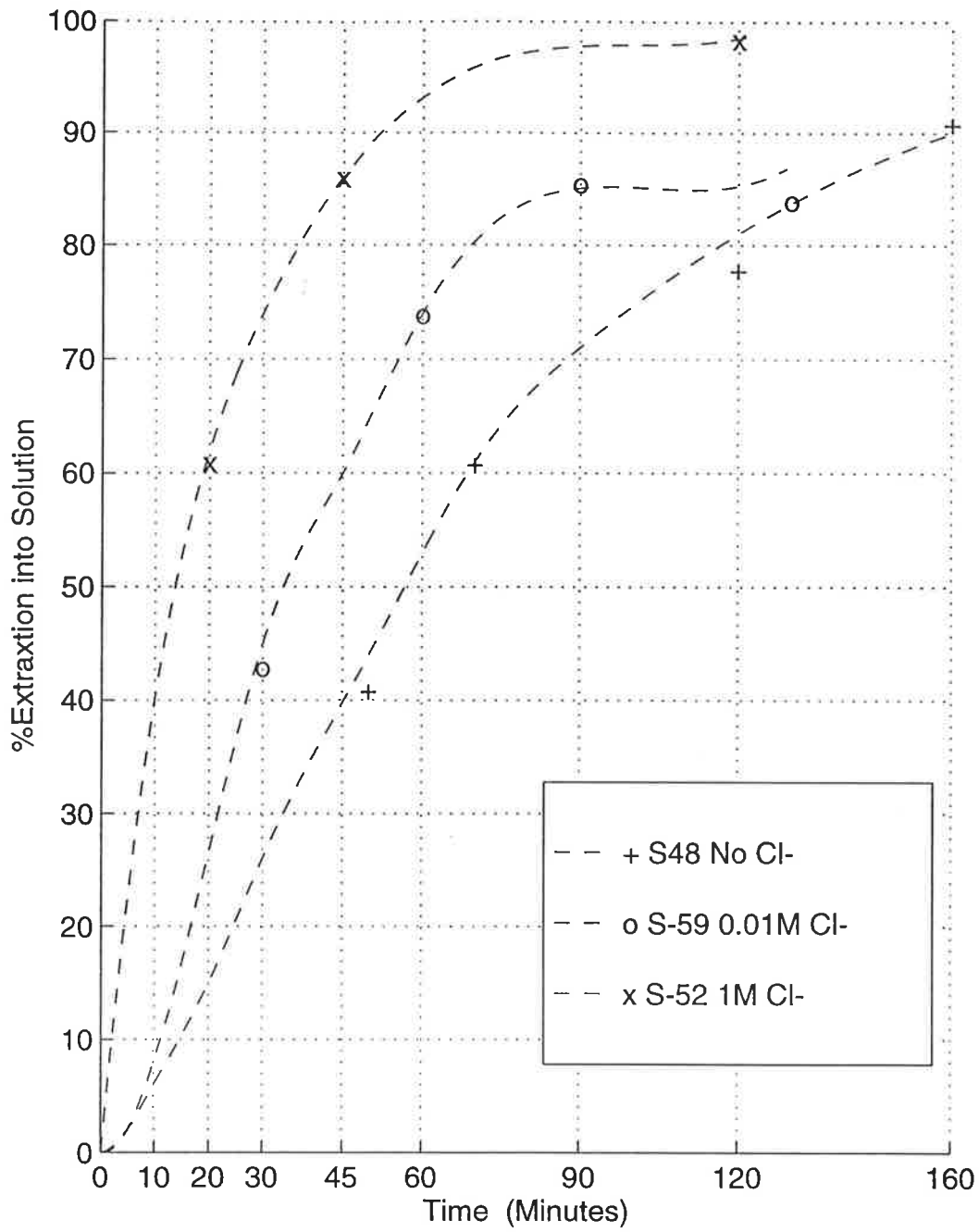


Figure 5.7.3.2 Effect of Cl Ion ($\text{SO}_4=$ only)
 Gumeracha Pyrite 125-180mm, 80°C, 280 rpm, 2.6 MHNO_3

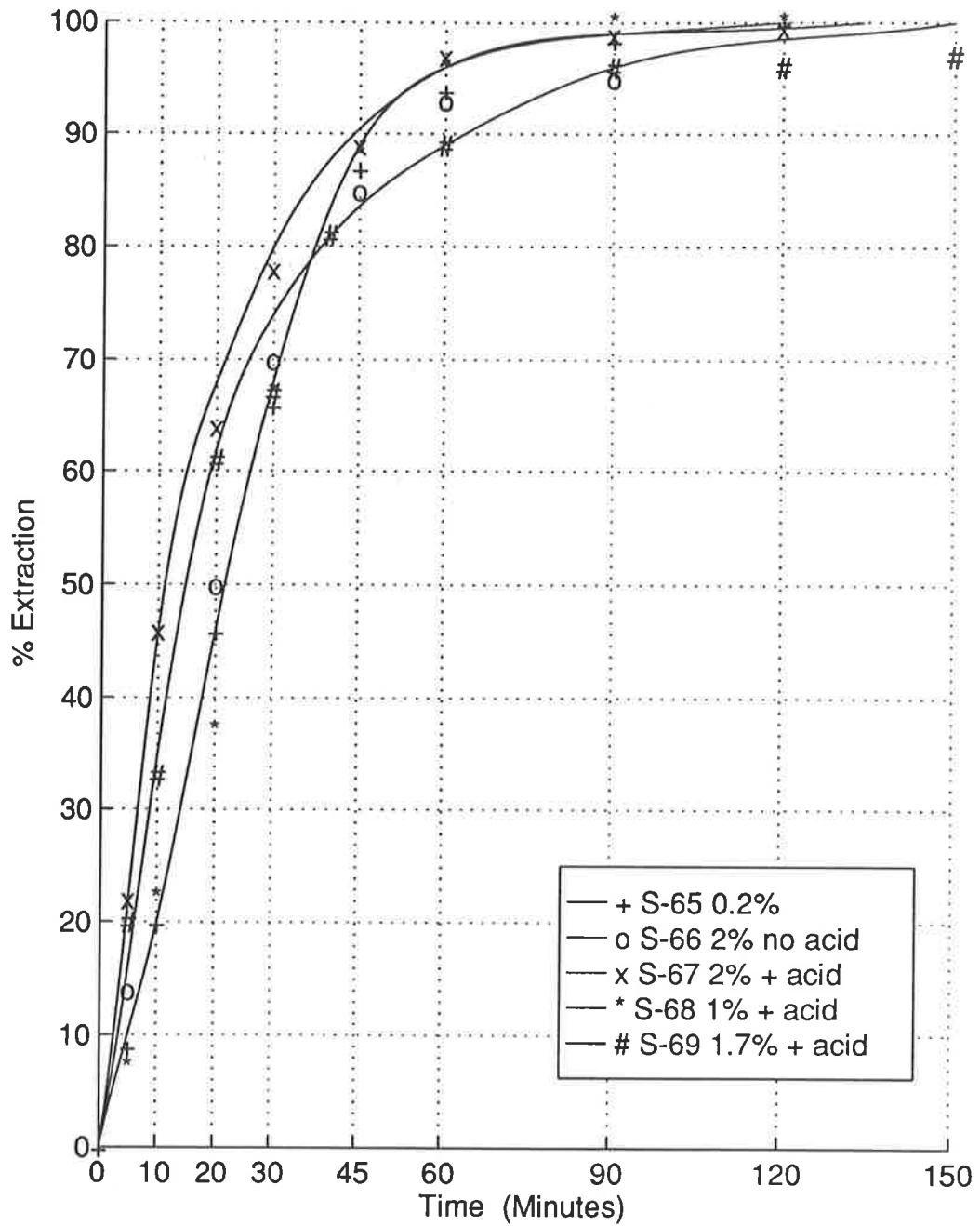


Figure 5.7.4.1: Effect of Pulp Density

Huanzala Pyrite, 125-180 μ m, 80°C (nominal) 2.6 M HNO₃ (initially)
280 rpm (Iron dissolution only)

The data of Table 5.7.3.1 might be the basis of a hypothetical reduction in the 'sulfur gap' due to presence of chloride ion. S-52 would seem to contradict this but the iron curve, and hence the "sulfur gap", for S-52 is qualitative at best. S-60 supports the hypothesis, but the overall kinetics of S-60 do not fit the expected pattern, so it is questionable. The best which can be said is that there is an indication that chloride ion reduces the "sulfur gap". More tests would be required for confirmation.

Most mine waters are saline, with 10% Cl⁻ being common in say, Kalgoorlie. Used with nitric acid such water could cause materials selection headaches for the "Redox" process for refractory gold ores. The attack on the stainless steel stirrer shaft illustrates this. In fact, water of low chloride content is usually specified for the "Redox" process, in order to avoid corrosion in the stainless steel reactors.

Another potential problem with chloride iron for a nitric acid-based refractory gold process could be the dissolution of the gold itself. This was not investigated in this series.

5.7.4 PULP DENSITY

5.7.4.1 Series Results

The iron extractions from the five tests in this series are summarised in Figure 5.7.4.1 (opposite). All tests used Huanzala pyrite 125/180 µm, which had been deslimed by wet screening at 45 rpm. As detailed in Section 5.3, these tests varied from 0.2% solids to 2.0% solids, with and without acid makeup. All tests were at 280 rpm, with 2.6 M HNO₃ initially and nominally at 80°C. A noteworthy observation on these series was the loss of temperature control. The base case (S-65 - 0.2% solids) remained within +2–1°C of target. At higher percent solids the temperature went to from 83 to 88°C - the worst case was S-67 which stayed at 87°C for 15 minutes at the beginning of the reaction.

Species balances were also poor for this series. The sulfate departments based on filtrate and feed disagree (from + 22% to –14%) with the departments based on filtrate and residues. (It is the latter which is reported as "calculated extraction". The former serves as a check.) Iron balances were slightly better, with two of the five tests outside the ± 10% figure.

5.7.4.2 The Effect of Pulp Density

The curves for iron extraction in this series overlap and intermingle. There are not really that far apart (the rate constant for S-67 is about 0.05 min^{-1} while that for S-65 is about 0.04 min^{-1} . This is for the most divergent curves, namely the outside curves on Figure 5.7.4.1).

Temperature control for the experimental apparatus was maintained by manual switching of the heater stirrer in the 10 l water bath. Since the heater itself had a variable output, this method, with a little care, sufficed to control the temperature on the 1.5 l reactor vessel to $\pm 1^\circ\text{C}$ for most tests. However, for this series, at high percent solids, the lack of a cooling coil in the reactor itself meant that the heat of the reaction raised the temperature in the reactor.

The series produced much higher concentrations (up to 10x) of iron and sulfate than normal. These high values seemed to be linked to the poorer iron, and especially sulfate, balances.

Given the narrow spread of data, the lack of temperature control, and the doubtful balances, it is difficult to say that there is any significant difference between the curves in the series. Accordingly, it can be said that for up to 2% solids, at 53% sulfur in feed, pulp density has little effect on pyrite leaching kinetics. This would apply to a whole ore, with 5% sulfur up to 21% solids.

The literature suggests that the values of sulfur in feed tested are close to the maximum used in industry. The amount of sample of a given screen fraction available, dictated against using higher pulp densities. Further, it is now evident that the lack of cooling coil would have made higher pulp densities of doubtful use.

Information on the proportion of elemental sulfur present is erratic, due to the poor balances, with many negative values. The only reliable figures seem to be those of the residues, weighed and inspected under the microscope. They fall in the range of 2-7% elemental sulfur after 120 minutes. This is in keeping with the sulfur gap for the "classical" variables. Pulp density has no discernible effect on the sulfur gap.

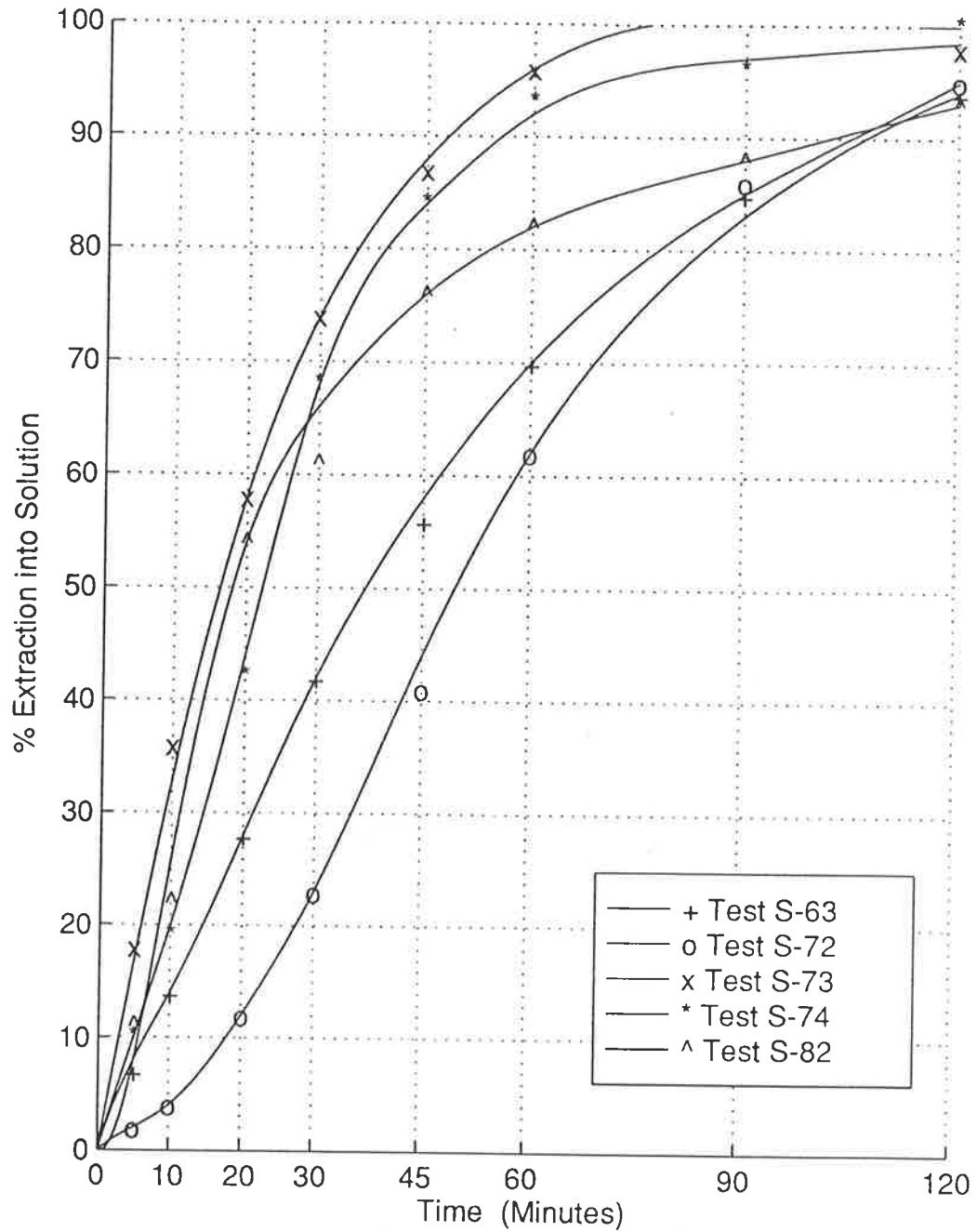


Figure 5.7.5.1

Effect of Blend of Sizes

(Adapted)

All samples Gumeracha Pyrite, 80°C, 2.6 M HNO₃, 272 rpm

+ 125 - 180 μm

o add coarse fraction

* add medium fraction (> 63 μm)

x add -45 μm

^ equal fractions -45 μm through +250 μm

5.7.5 BLEND OF FEED SIZES

5.7.5.1 Series Results

The iron extractions for this series are summarised in Figure 5.7.5.1 (opposite). For clarity, sulfate extractions have been omitted. Also, the curves have been adapted slightly. For this series, the amount of gangue (insoluble) seemed atypical, varying from 2 to 5% of the feed. An average value of 1.5% has been used for Gumeracha pyrite for all calculations up to this point, and a random selection of eight tests averaged 1.6% gangue in feed. For Figure 5.7.5.1 the simple expedient of ignoring the residues served to move all the curves up to 100% extraction and to separate overlapping curves which had presented a confusing picture. This was considered justified by the high gangue proportion in this series.

Table 5.7.5.1 presents the data for elemental sulfur proportion for this series.

With the exception of S-63, the iron and sulfate balances were satisfactory.

Table 5.7.5.1: Sulfur Gap for Blend of Sizes Series

| Sample | Sizes | "Sulfur Gap" % for Iron Extraction % | | | | |
|--------|------------------------------------|--------------------------------------|----|----|----|-------|
| | | 20 | 40 | 60 | 80 | Final |
| S-63 | Mono size 125/180 μm | – | 4 | 4 | 5 | 7 |
| S-72 | add coarse | –4 | – | –2 | 10 | 11 |
| S-73 | add slimes | – | – | – | 1% | 5 |
| S-74 | add medium to 63 μm | – | – | 1 | 4 | 4 |
| S-82 | Wide size range | 4 | – | 5 | 5 | 6 |

5.7.5.2 The Effect of Blend of Feed Sizes

The adapted curves of Figure 5.7.5.1 show a pattern which is generally to be expected. The addition of coarse material slows down the leaching rate, although not as much as expected. The curves for monosized particles and the coarse blend reach 90% extraction at the same time. The addition of 2/3 medium fine (to 63 μm) particles increase the leaching rate. The addition of 1/3 slime material (–45 μm median size unknown) increases the rate even more. The blend of nearly equal

amounts of all sizes produces a significantly different shape to the other curves. Initially, it is very fast, but the instantaneous leaching rate becomes the slowest of the series after about 80% iron extraction. This is rather surprising, considering two of the other samples had more coarse material (+ 125 μm initially). From Figure 5.9.2.3 (page 155 of the mathematical analysis) it would appear that the initial leaching rates are directly proportional to the initial surface area. This generally holds for extraction in the 10-60% Fe range. The first-order plots are not linear, either in the early stages or final stages of leaching.

The amount of elemental sulfur found appears slightly lower for this series than for the "classical" series. Also, the maximum occurs at the end of each run, with 4-11% elemental sulfur remaining. This may merely be a function of the coarse (125/180 μm) material which was the basis of this series. That pattern was followed for both S-63 in this series and S-16 in the classical "particle size" series.

In all, the blending of fines serves to speed up leaching rates, reflecting the increased surface area of the feed. Coarse pyrite (180 μm) slows down leaching rates and results in slightly more elemental sulfur.

5.7.6 SECTION SUMMARY (INDUSTRIAL VARIABLES)

Sulfuric acid accelerates leach rate, with no discernible effect on sulfur gap. Both ferric and chloride ion also increase rates. Both appear to reduce the sulfur gap somewhat, without eliminating it. Balances for ferric and chloride series were less certain due to high background levels and corrosion problems. Pulp density increases caused some loss of temperature control and exposed equipment limitations. Within the range tested pulp density itself did not affect leach parameters. Blending feed sizes altered the shape of the leach curves and coarse material tended to show a larger sulfur gap. Initial rate appeared to vary with initial surface area.

5.8 **ADDITIONAL FACTORS - RESULTS AND DISCUSSIONS**

This section presents summarised results for variables and phenomena which arose from contemplation of the literature, from talks with colleagues, or from consideration of the earlier detailed results themselves. Included here are tests on attritioning, attempts to increase Eh and the addition of silver ion. Two leach tests were run to assess whether the effects of variables were additive. The phenomena of acceleration of leaching rate at low extractions is examined. The differences in pyrite from three different sources (one from the literature) are examined.

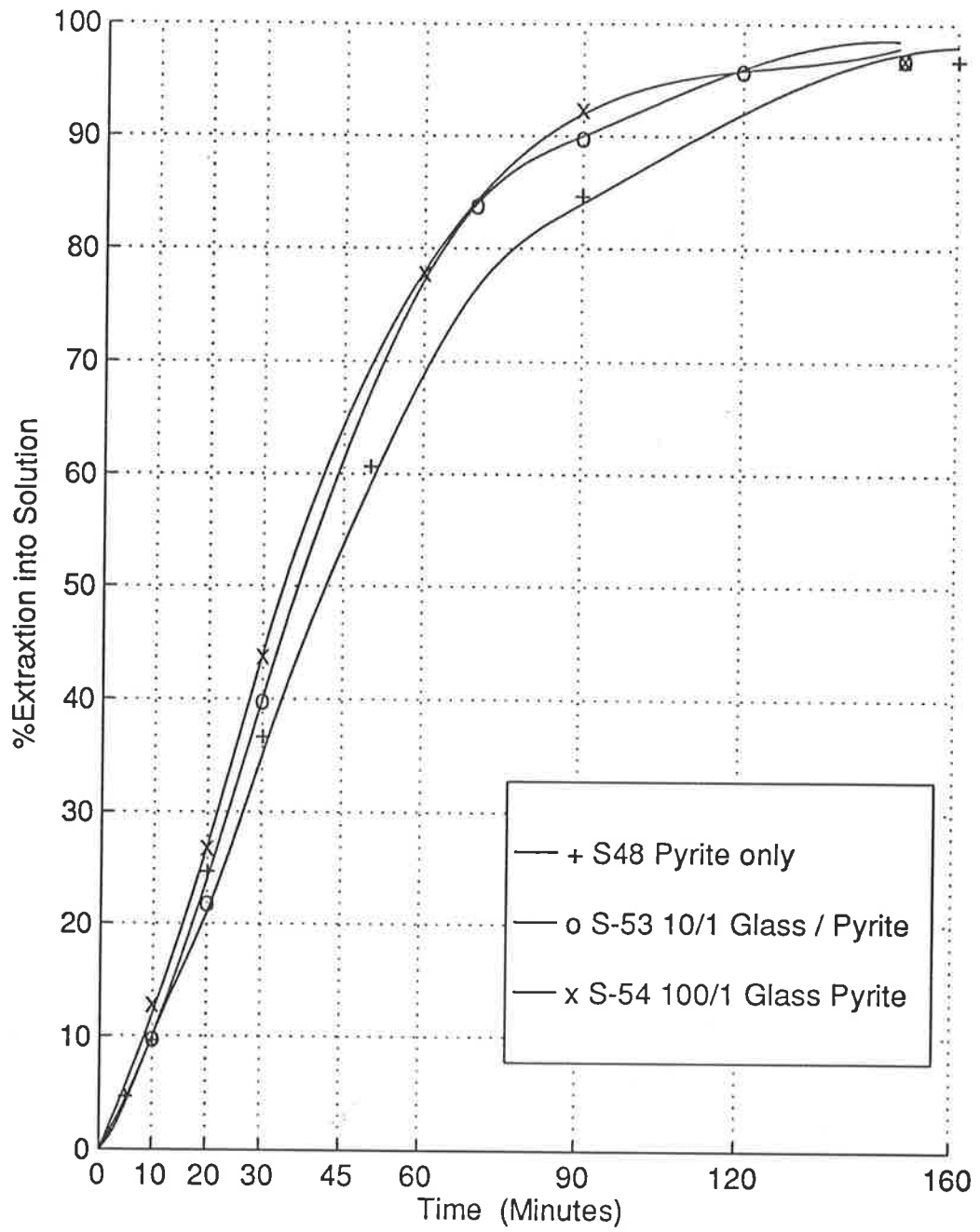


Figure 5.8.1.1 Effect of Scrubbing with Glass Balls (Iron dissolution only)

Gumeracha Pyrite, 125-80 μm , 80°C, 280 rpm, 2.6 M HNO_3

5.8.1 ATTRITIONING

5.8.1.1 Early Attempts - Results

The first attempts at a scrubbing treatment were with sand in the spherical glass reaction vessel. Several grains of the sand dissolved, despite the fact that it had been acid-washed earlier. This dissolution appeared to slow down the pyrite reaction and the tests were considered failures (S-11 and S-12 6/92).

The next attempts introduced soda lime glass balls, 3 mm in diameter to the spherical reactor. Figure 5.8.1.1 shows the results of these tests, compared to one without glass balls. Only iron dissolution is shown, for clarity. Table 5.8.1.1 compares the amounts of elemental sulfur (the "sulfur gap") for the tests. All tests were for Gumeracha pyrite, 125/180 μm , at 80°C and 280 rpm in 2.6 M HNO_3 .

Table 5.8.1.1: Sulfur Gap for Scrubbing Series

| Test No | Glass balls | "Sulfur Gap" at % Fe extraction (%) | | | | |
|---------|-------------|-------------------------------------|-----|-----|-----|-------|
| | | 20% | 40% | 60% | 80% | Final |
| S-48 | nil | 4 | 10 | 16 | 13 | 7 |
| S-53 | 2% | -10 | - | 4? | 8 | 6 |
| S-54 | 17% | - | -4 | -2 | 3 | 3 |

5.8.1.2 The Effect of Scrubbing- Early Attempts

The addition of glass balls to the spherical glass reaction vessel, with 280 rpm stirring, showed an appreciable effect on kinetics. Surprisingly, 2% of glass balls by weight, showed most of the increase, with 17% glass balls showing a further improvement only above 90% extraction. These tests used 10/1 balls/pyrite and 100/1 balls/pyrite ratios, respectively. Visually, the balls certainly broke up the flocs, which as was shown in section 5.4.4. were "glued" together by elemental sulfur.

The sulfur gap Table 5.8.1.1, imperfect as the data is, shows some reason to believe that scrubbing reduced the amount of elemental sulfur present at a given time. These tests provided the impetus to continue the scrubbing approach only using a proper attritioning apparatus and vessel.

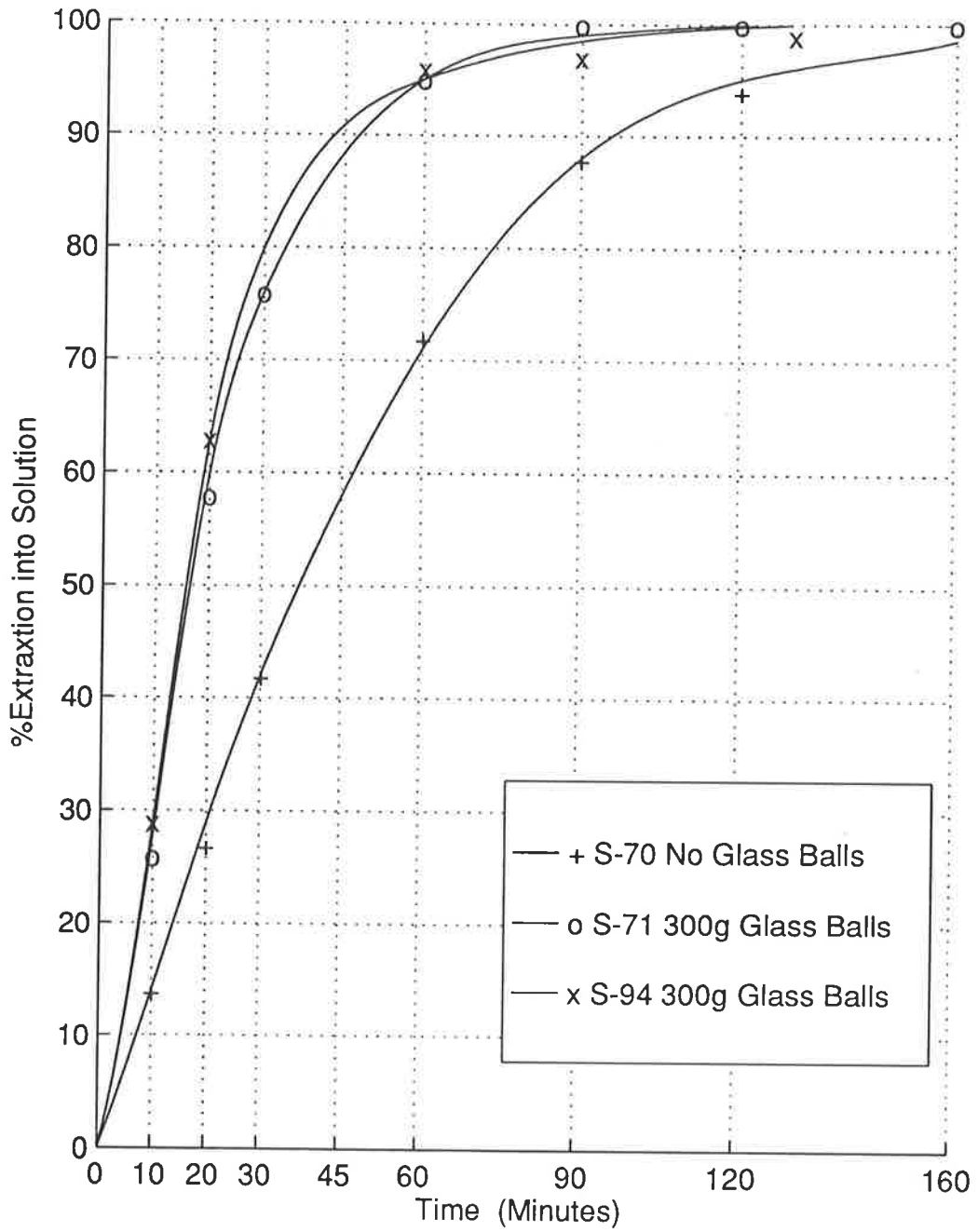


Figure 5.8.1.2 Effects of Attritioning

Huanzala Pyrite, 125-180 μm , in Attritioning Vessel,
900 rpm 80°C, 2.6 M HNO_3

5.8.1.3 Series Results for Attritioner Vessel

Figure 5.8.1.2 (opposite) summarises the iron extraction results for the series run with the high-speed attritioning mechanism. This series used Huanzala pyrite 180/250 μm deslimed at 45 μm . The tests were run at 80°C in 2.6 M HNO_3 . Tests S-75, S-94, S-98 were virtually duplications of S-71.

Calculations included corrections for samples, for any leakage and evaporation and for iron scoured from the attritioning vessel. A typical run, S-94, showed that leakage to the water bath from the attritioning vessel amounted to 29 ml or 4% of the original acid. This was determined by nitrate analysis of the bath. Scouring was determined from nickel analysis of the final filtrate, assuming that the attrition vessel was 8% Ni stainless steel. A typical value was 0.05 g Fe per run, or 7% of the iron in the pyrite feed. Evaporation losses, determined by difference, and assumed to be water only, amount to 76 ml for run S-94. It was not possible to seal the attritioner vessel completely, or to use a vapour condenser, as had been used for the majority of the leach tests in the spherical glass reactor. Typically the glass balls lost 5 g or 1.7% of their weight in a run. The mass balance for S-94 showed an unaccounted loss of 6 grams or 0.6%.

Residues for the series typically weighed 1-4 grams and were very different in appearance from the residues from the glass reactor. Microscopic inspection was no help - residues were extremely fine, black, with occasional large pieces of gangue recognisable. Table 5.8.1.2 gives values for those residues which were analysed.

Table 5.8.1.2: Residue from Attritioning Series

| Test | Conditions | Weight g | %S total | %S ^o | % of Original Feed S |
|------|------------|-------------|----------|-----------------|----------------------------|
| S-70 | no balls | 0.2311 | 5 | 4 | 1 |
| S-71 | 300g balls | 3.140 | 2 | n.d. | 8 |
| S-75 | 300g balls | 3.8481 | 0.85 | | 4 |
| S-94 | 300g balls | 1.0001 | 3.2 | n.d. | 4 |
| S-95 | 300g balls | 1.222 | 2.1 | 2.1 | 3 |
| S-90 | 300g balls | 1.3830 | 0.90 | n.d. | 1.5% |

Inspection of one attritioning residue sample by scanning electron microscope showed it to be rubber, glass and gangue, with perhaps 20% stainless steel.

5.8.1.4 The Effect of Attritioning in the Vessel

The data of Figure 5.8.1.2 shows that the addition of glass balls (200/1 balls/pyrite) to the attritioning vessel markedly increased the iron leaching rate. This is to be expected as the energy input of the attritioner is considerable, with the constant creation of fresh surface to be expected, by abrasion if not by actual comminution of the pyrite. Table 5.8.1.2 shows, however, that the sulfate species in solution still lagged behind the iron species. It has been hoped that the attritioning would scour elemental sulfur from the surface of the pyrite as fast as it was formed, thus oxidising the sulfur before it could form particles large enough to become stable. This was evidently not the case.

Table 5.8.1.3 presents the data for elemental sulfur present for the series.

Table 5.8.1.3: "Sulfur Gap" for Attritioning Series

| Samples | Balls used | "Sulfur Gap" (% S ^o) at Fe extraction (%) | | | | | |
|---------|------------|---|----|------|-----|-------|---------|
| | | 20 | 40 | 60 | 80 | Final | Comment |
| S-70 | none | – | 2 | 7 | (8) | 1 | |
| S-71 | 300 g | (5) | – | 3 | 6 | 5 | |
| S-75 | 300 g | – | – | – | – | 2 | * |
| S-94 | 300 g | – | – | 20 | 8 | 4 | |
| S-95 | 300 g | – | – | (11) | – | 4 | |

* Assumed 'typical' scouring Fe; balance on solids in feed basis only

Considerable difficulty was encountered over the data which makes up Table 5.8.1.3. There was a wide scatter of data particularly for sulfate assays. Microscopic analysis of the attritioned residues was of no assistance. It was thought that these residues could contain a significant proportion of abraded rubber and the rubber in the gaskets contained 2.2% sulfur. Gaskets were replaced with teflon and silicone. The materials balances were complex and metal scouring from the attrition vessel was difficult to pin down. As always, insufficient finance to get a complete set of analyses, which now required nitrate, chrome and nickel assays, as well as iron and sulfate, exacerbated the uncertainty. The end result was that another four attritioning tests were run, but were not assayed. A decision was made once it was considered there was sufficient evidence that the sulfur had not been eliminated.

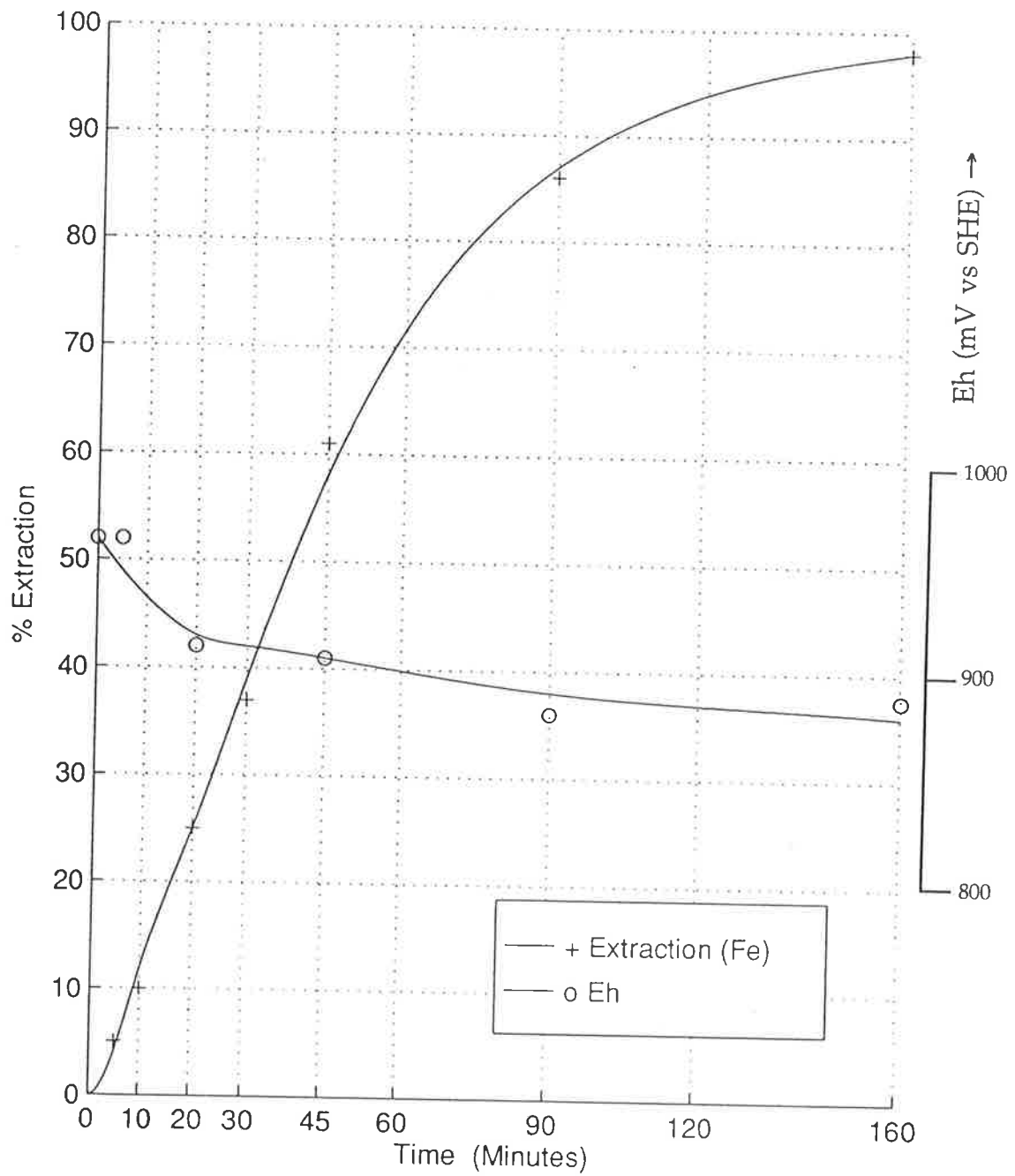


Figure 5.8.2.1: Variation of Eh with Time
 Gumeracha Pyrite 125-180 μm , 2.6 MHNO_3 80°C, 280 rpm

5.8.2 THE EFFECT OF Eh

5.8.2.1 Eh Variation During Tests

The redox potential (Eh) of the leach solutions varied with changes in the variables being tested. Table 5.8.2.1 summarises the Eh at the beginning of those tests which showed marked deviation from the Eh of 2.6 Molar nitric acid.

Although Eh was monitored throughout most leach tests, it generally steadied out after the first twenty minutes or so. Figure 5.8.2.1 shows the Eh trend against time and against percent iron extraction for a typical leach runs.

Table 5.8.2.1: Redox Potential Variation with Conditions

| Tests | Conditions | Eh Standard Solution | Adjustment mV | Intitial measured Value Ag/AgCl Electrode | Eh vs SHE |
|----------------------|-------------------------------------|----------------------|---------------|---|-----------|
| 17 tests S-48 etc | 2.6 MHNO ₃ 80°C | Light solution | + 10 | 0.927 ± 0.1 (S = 0.05) | 1.17 |
| S-8 | added Fe ³⁺ 0.2 Molar | Zobell | 0 | 0.942 | 1.18 |
| S-42 | H ₂ O ₂ added | Light | + 2 | 0.878 | 1.11 |
| S-46 | 50°C added KMnO ₄ | - | - | 1.204 | 1.44 |
| S-44 | 75°C | - | - | 0.922 | 1.16 |
| S-64 | 75°C | Light | 0 | 0.970 | 1.20 |
| S-45 | 60°C | - | - | 0.850 | 1.08 |
| S-94 | 20°C | Light | +7 | 0.609 | 0.82 |
| S-51 | 1.5 MHNO ₃ | Light | - 12 | 0.734 | 0.961 |
| S-49 | 3.5 MHNO ₃ | Light | - 13 | 0.932 | 1.15 |
| S-50 | 4.5 MHNO ₃ | Light | - 16 | 0.925 | 1.15 |
| S-58 | 10 ⁻³ M Fe ³⁺ | Light | - 37 | 0.927 | 1.18 |
| S-57 | 10 ⁻² M Fe ³⁺ | Light | - 13 | 1.088 | 1.31 |
| S-55 | 10 ⁻¹ M Fe ³⁺ | Light | + 17 | 0.968 | 1.22 |
| S-60 | 10 ⁻³ M Cl ⁻ | Light | + 7 | 0.970 | 1.21 |
| S-59 | 10 ⁻² M Cl ⁻ | Light | + 6 | 1.018 | 1.26 |
| S-52 | 10 ⁰ M Cl ⁻ | Light | - 9 | 0.850 | 1.08 |
| S-83 | Ag+ 10 ⁻² M | Light | - | 0.933 | 1.17 |

all values are suspect due to instrument drift.

Difficulty was encountered when trying to obtain stable readings for Eh at high temperatures and acid concentrations. After several attempts it was decided to merely check the Eh probe at room temperature against a standard solution and to accept whatever reading was obtained in the reaction vessel. Light solution or Zobell's solution were used for checking. A saturated KCl, platinum-silver/silver chloride, glass electrode was used throughout.

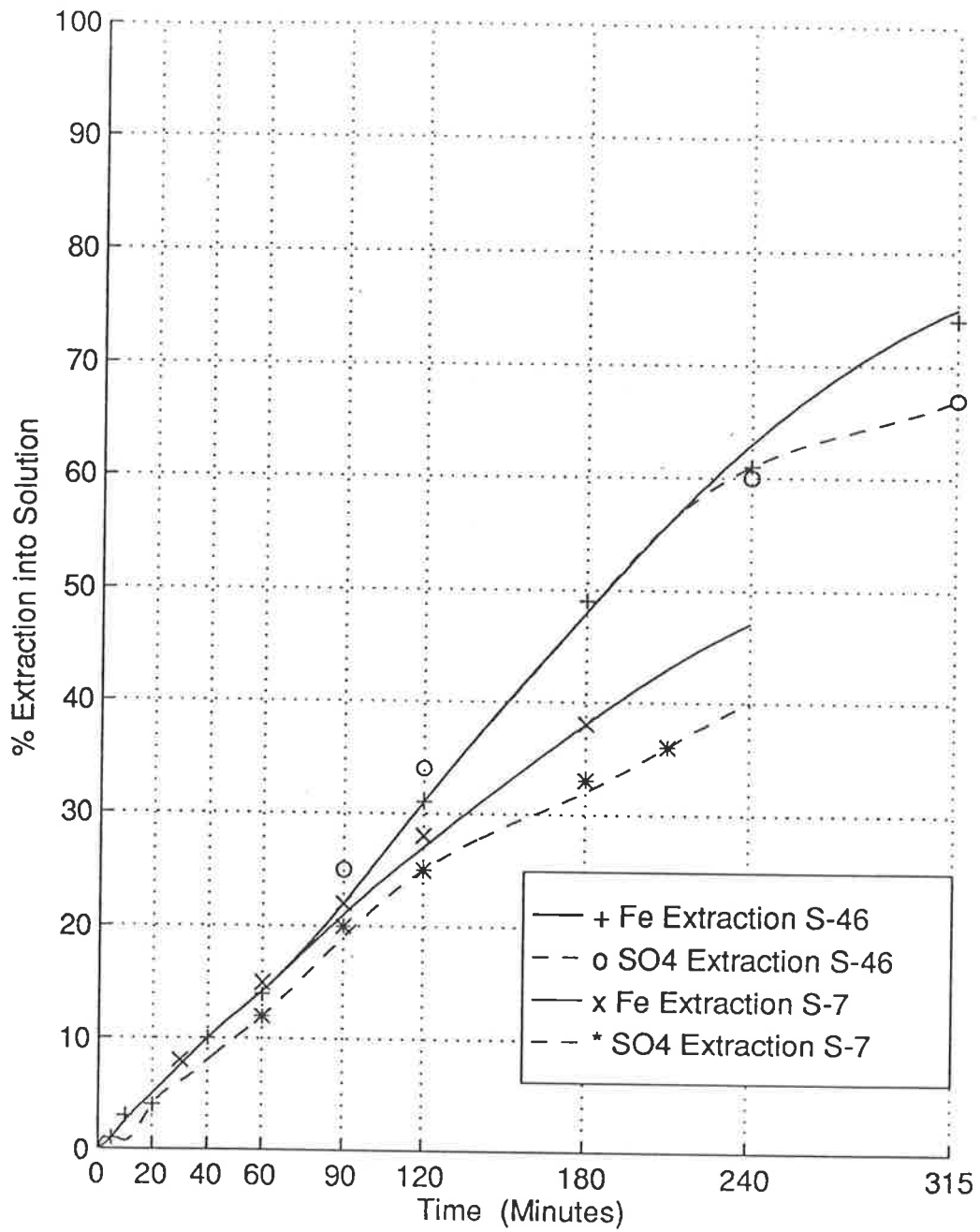


Figure 5.8.2.2: Effect of Increasing Eh
 Gumeracha Pyrite, 50°C, 2.6 M HNO₃
 S-7 Eh = 1.07 volts (SHE)
 S-46 Eh varied 1.07-1.37 volts

5.8.2.2 Discussion of Eh Measurements

Table 5.8.2.1 coupled with the difficulties in measuring Eh at high temperatures and acidities, indicates that there was not much to be gained by measuring Eh during the leach tests. Several days were spent seeing whether stable sensible Eh ratings could be obtained. It is considered that this in itself might be a worthwhile project, for a final year student in Chemical Technology for example.

Figure 5.8.2.1 shows that for these fairly typical runs, the Eh dropped approximately 100 mV in the first 10-20 minutes and then did not vary greatly. There was no particular pattern between Eh and iron dissolution either. Earlier test work had shown that changes of this magnitude could well be the Eh electrode drifting in the hot acid solution.

5.8.2.3 Higher Eh - Results

Two attempts were made to "artificially" raise the Eh of the 2.6 M HNO₃ solution. Test run S-42 employed hydrogen peroxide at 80°C, while run S-46 used potassium permanganate at 50°C. The standard (1 M) E⁰ of peroxide is 1.776 volts (versus 0.957 volts for NO₃⁻). That for KMnO₄ is 1.679 volts.

The leach kinetics visibly slowed down when hydrogen peroxide was added. Initial Eh was 1.10 volts (SHE). When the S-42 leach curve was compared to the appropriate test without peroxide (S-23), S-42 was found to be much slower despite being run at 5°C higher temperature. No reason was established for this.

When potassium permanganate was added to 2.6 molar nitric acid at 50°C (test S-46) the Eh jumped immediately to 1.370 volts vs SHE, but fell within a minute to 1.120 volts. This pattern was maintained by adding a pinch (perhaps 30 mg) of KMnO₄ every two or three minutes. The permanganate broke down within a minute. The purple colour disappeared and a black MnO₂ precipitate could be seen. No NO_x was observed at any time during the 5 hours of the run, nor were any floccs formed. Eh varied widely 1.07 - 1.37 volts but was consistently returned to the higher figure with KMnO₄. Permanganate added on its own (no pyrite) also broke down.

Figure 5.8.2.2 (opposite) compares the run with permanganate to its closest approximation, S-7. The S-7 curve has been mathematically adjusted to the coarser

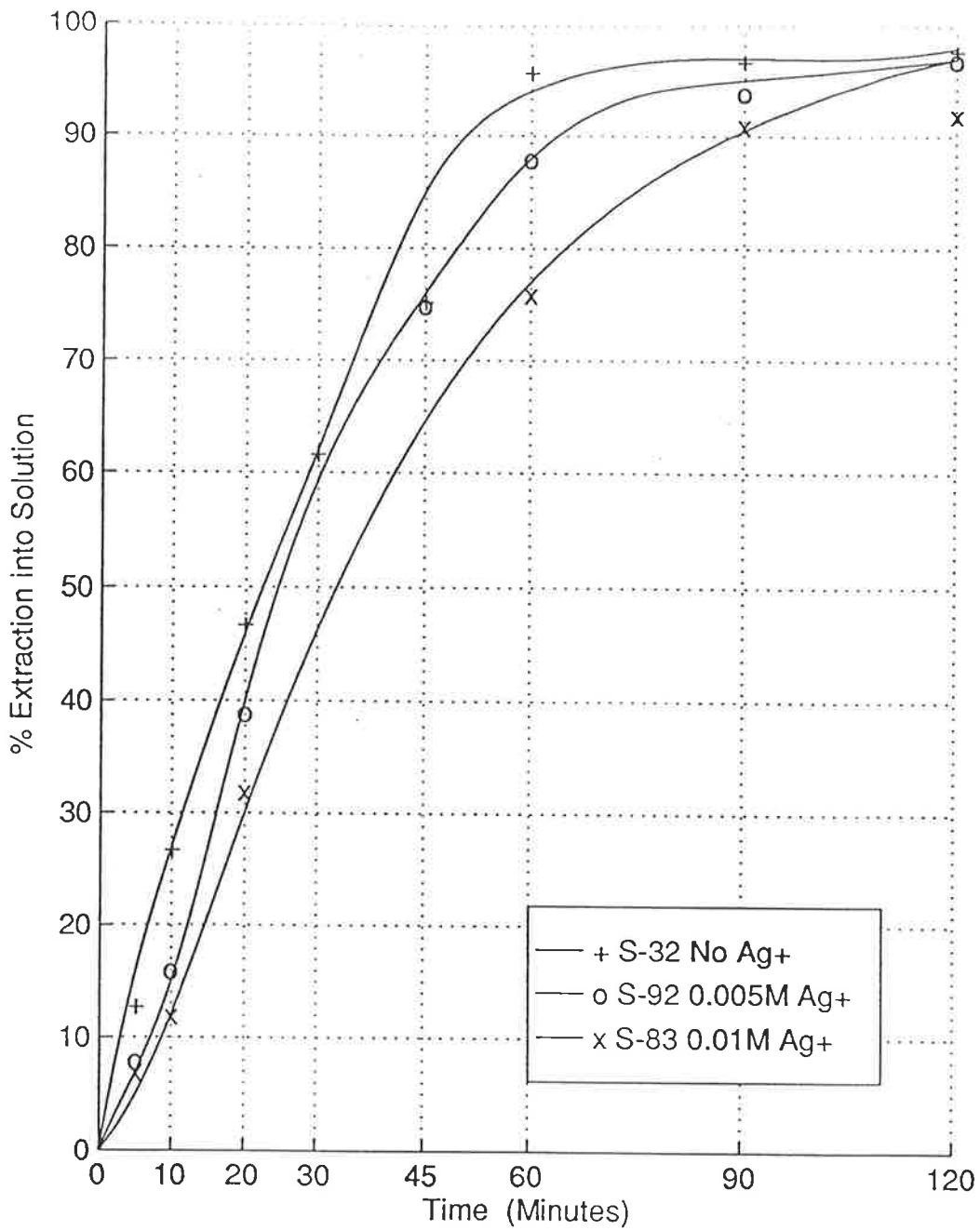


Figure 5.8.3.1: Effect of Ag⁺ Ion
 (Iron Extraction only)
 Gumeracha Pyrite, 90-125 μm, 80°C, 2.6 MHNO₃

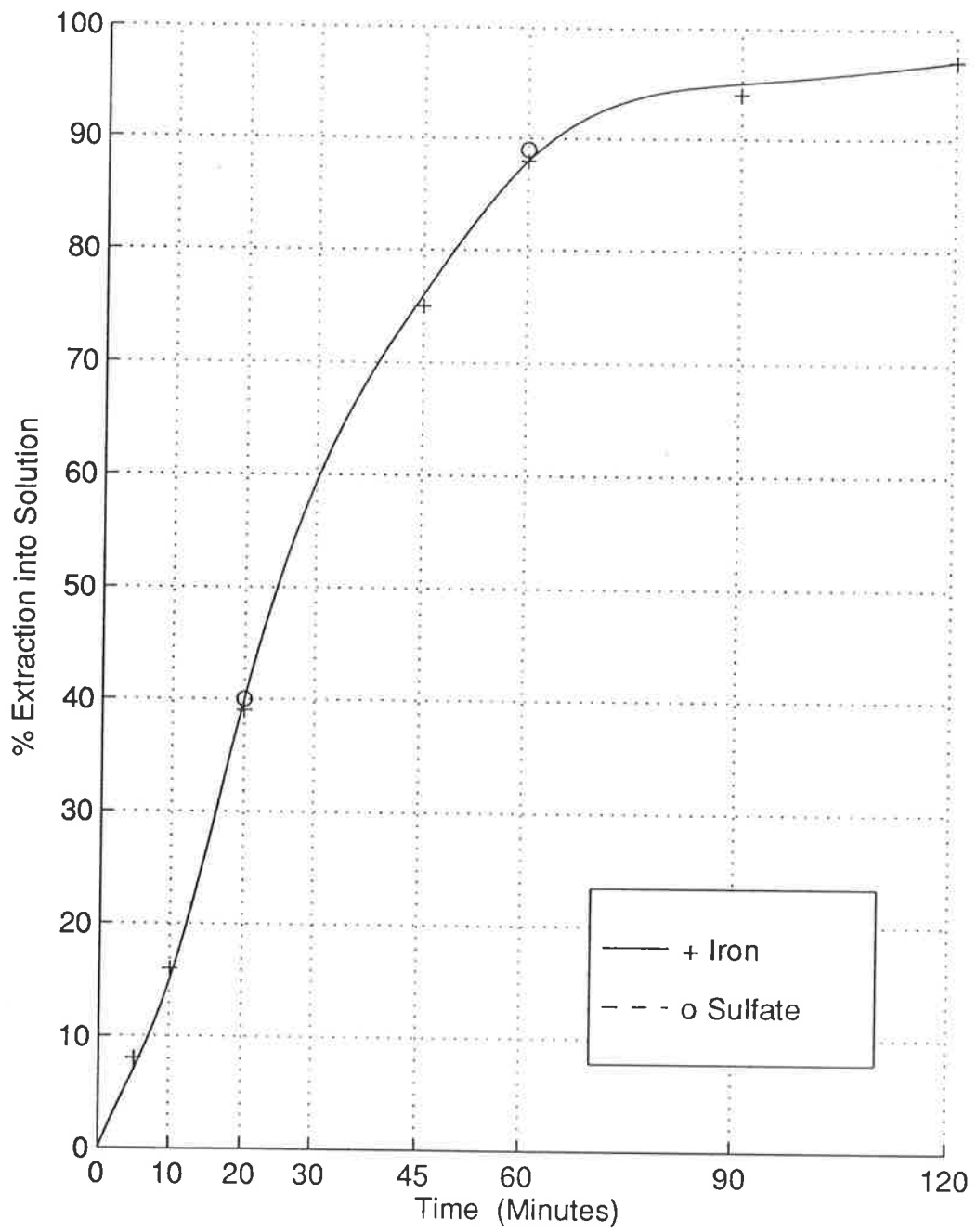


Figure 5.8.3.2: Iron and Sulfate Extractions at $5 \times 10^{-3} \text{ M Ag}^+$
Gumeracha Pyrite 90-125 μm , 80°C, 2.6 MHNO_3

grain size of S-46 (90/125 μm , adjusted to 125/180 μm). Using relationships established in Section 5.9.

5.8.2.4 Effect of Higher Eh

Figure 5.8.2.2 shows that the added KMnO_4 did in fact speed up the reaction kinetics. If the mathematical manipulation of test S-7 is valid, the permanganate increased the first-order rate constant by 67%. Both tests were run on Gumeracha pyrite at 50°C, in 2.6 M HNO_3 , at 280 rpm. S-42 was one screen size coarser, at 125/180 μm . The particularly interesting point of the graphs is that the permanganate suppressed the formation of elemental sulfur until an extraction of 60%. This was despite the Eh fluctuating between 1.37 volts and 1.07 volts (SHE). The higher value is that at which the electrochemical work in Chapter 4 predicted elemental sulfur would not form. While not conclusive, this test tends to indicate that if the Eh could be maintained at 1.4 volts (SHE), elemental sulfur could be eliminated. At the time of the experiment, the problem was thought to be to stop the permanganate decomposing. On reflection a stoichiometric excess may have had to be added, as the pyrite could be expected to reduce the permanganate before it reacted with nitric acid. Alternatively a leach test with only permanganate may have been controllable at a steady Eh of about 1.4 volts.

5.8.3 ADDITION OF SILVER ION

5.8.3.1 Series Results

Figure 5.8.3.1 summarises the effect of two levels of silver ion in the iron extraction rates. Figure 5.8.3.2 shows the details of both iron and sulfate extraction for one test, at 5×10^{-3} molar Ag^+ ion. All tests were run on Gumeracha pyrite (90/125 μm at 80°C, 280 rpm and 2.6 M HNO_3).

Test S-83 was visually obscured by a white precipitate, which probably was AgCl formed by reaction with the electrolyte from the Eh probe. Analyses showed that the depletion of silver ion in the solution was minor. Test S-92 was run without an Eh probe. Observations were normal including flocculation of pyrite.

5.8.3.2 Effect of Silver Ion

Figures 5.8.3.1 and 5.8.3.2 present an effect quite different from the other variables tested. Silver ion appears to slow down the kinetics of iron leaching appreciably. At the same time, the sulfate leaching curve has become

indistinguishable from the iron leaching curve. Increasing the silver ion concentration further to 10^{-2} molar slows down both iron and sulfate leaching rates. Again, however, an elemental sulfur gap cannot be distinguished from the data.

The problems of assay and sampling accuracies come into the question at this point. As discussed earlier, it is very difficult to state with certainty that the sulfur gap has been reduced to zero when the accuracy of the points on both iron and sulfate curves is $\pm 10\%$. For the tests concerned (S-83 and S-92) the iron balance based on liquids and the original solids in the pyrite was 14% higher than that based on the "calculated" (liquids and residue) balance. For sulfate, the corresponding figure was -8% . The direction of these mismatches tends to reinforce, if anything, the argument that silver ion has eliminated the formation of elemental sulfur.

While insufficient data is at hand to state with any statistical assurance that the sulfur gap has been eliminated, there is an indication that this is the case, from the assay results. On the other hand, the continued visual evidence of flocculation argues for some elemental sulfur present on the surface of the oxidising pyrite.

It seems reasonable to conclude from the literature that it will be the mixed potential of the system that will dictate whether silver ion will prevent elemental sulfur formation. Silver ion has not been tested before in nitric acid systems. If silver is indeed inhibiting elemental sulfur, it is probably through the formation of a silver sulfide layer. Such an Ag_2S layer would be consistent with the slower iron leaching rates observed.

Levels of silver in gold ores vary widely, but a quick review of Australian producers (Woodcock, 1980) indicated that 2-3 g/tonne of Ag was a reasonable average. This would give very low values of silver ion in leach solutions (10^{-5} molar). Certainly the Dickenson concentrate which was batch tested by Van Weert et al. (1988) had insufficient silver levels (1.3 g/tonne estimated from Pickett (1978)). When Van Weert's leach liquor was used to treat pyrite, 3% elemental sulfur resulted. However, if a sulfide concentrate was treated and if leach solutions were recycled, higher silver ion concentrations could be built up. Also, it is not beyond possibility that high silver feedstock could be purchased for the purpose of building up solution silver levels.

The most reasonable conclusion is that there is an indication that silver ion reduces elemental sulfur formation, but there is insufficient data to conclusively prove that sulfur is eliminated. Further work may be warranted but it would have to be statistically designed. It would be worthwhile trying to improve accuracy of the

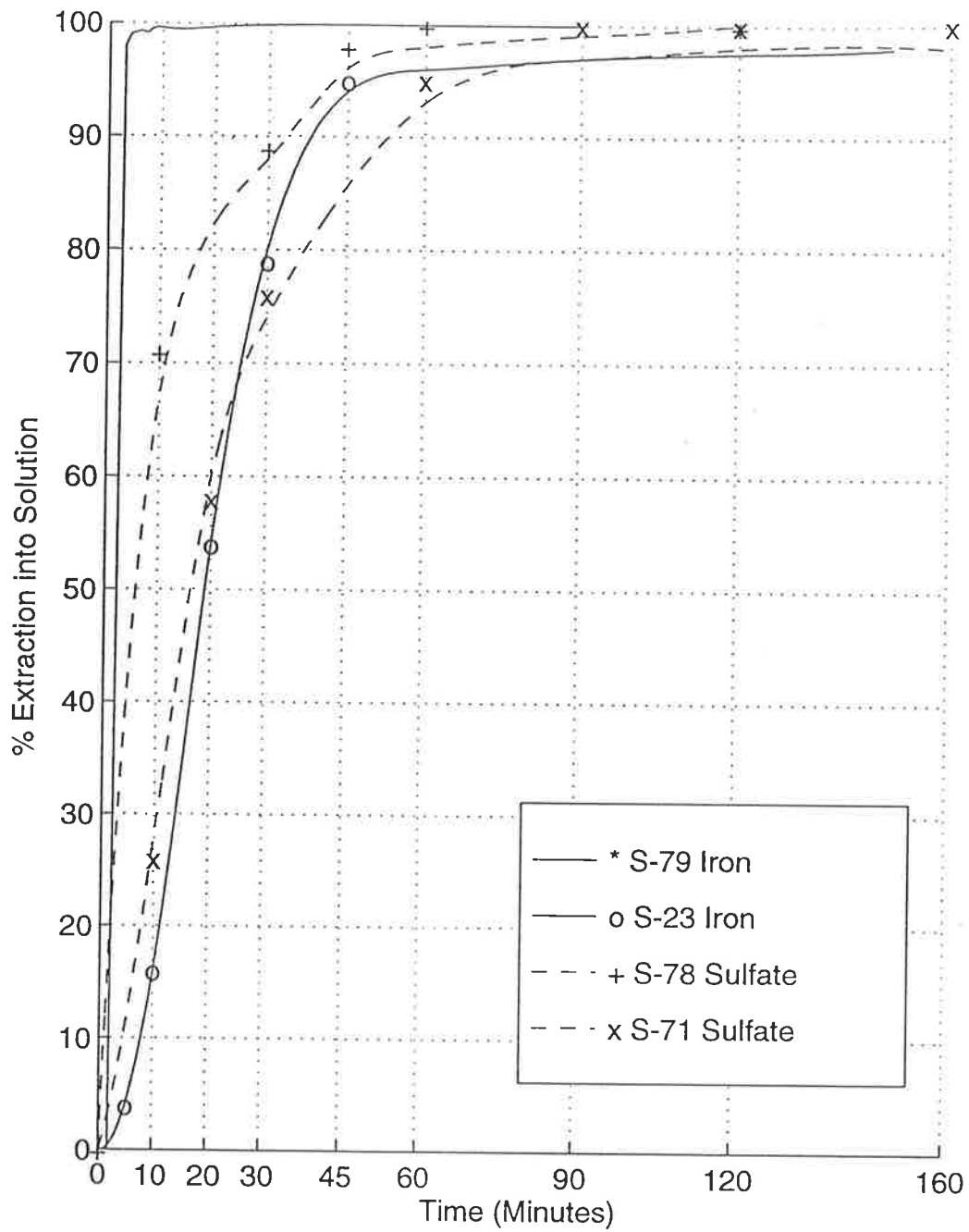


Figure 5.8.4.1: Additive Effect of Variables

- x S-71 Huanzala Pyrite, 180-250 μm , 80°C, 900 rpm, 2.6 MHNO_3
- o S-23 Gumeracha Pyrite, 63-90 μm , 75°C, 280 rpm, 2.6 MHNO_3
- + S-78 Huanzala Pyrite, 180-250 μm , 90-C, 900 rpm, 2.6 MHNO_3
- * S-79 Gumeracha Pyrite, 63-90 μm , 90°C, 900 rpm, 3.5 MHNO_3
2.0 MH_2SO_4

iron and sulfate assays; even carbon disulfide sulfur extraction may be worth the considerable extra work. Liaison with industrial developers should be included, to better bracket the silver ion concentration range which is industrially realistic to test.

5.8.4 ADDITIVE EFFECTS OF VARIABLES

5.8.4.1 Series Results

Two leach tests were performed with a combination of variables, to determine, at least qualitatively, whether the variables' effects were additive. Test S-78 used Huanzala pyrite, 180/250 μm (deslimed at 45 μm) in the attritioning apparatus with 300 g of glass balls. 2.6 Molar HNO_3 was used, but the temperature was increased to 90°C and ferric iron was added at an initial concentration of 0.07 Molar. The sulfate extraction assays are plotted on Figure 5.8.4.1 (opposite). The comparative run S-71 is also plotted.

Test S-79 used Gumeracha pyrite, again in the attrition with 300 g of glass balls. Figure 5.8.4.1 also plots the iron extraction for S-79 against those for S-23 for the same size fraction. Test S-79 used equally fine pyrite (63/90 μm), higher temperature (90°C), higher nitric acid concentration (3.5 M), added sulfuric acid (2.0 M) and attritioning.

5.8.4.2 Discussion of Additive Effects

It is obvious that changing a number of variables at once considerably speeds up the leaching rates. Attritioning at 90°C and adding ferric ion causes the Huanzala pyrite to be completely oxidised to sulfate in 60 minutes. It is estimated that the iron dissolution was complete in 45 minutes. Finer pyrite (Gumeracha 63/90 μm) and increased temperature and acids concentrations accelerated S-79 to complete iron oxidation in about 5 minutes. The sulfate assays for this test made very little sense initially, indicating very rapid sulfate production to 80% dissolution (5 minutes) with perhaps a slowing down beyond that. Reasons for this apparent anomaly are discussed in Section 5.9 - The Mathematical Analysis.

Thus the variable effects are at least partially additive. Quantitative analysis may be found in 5.9.2.5. (page 158).

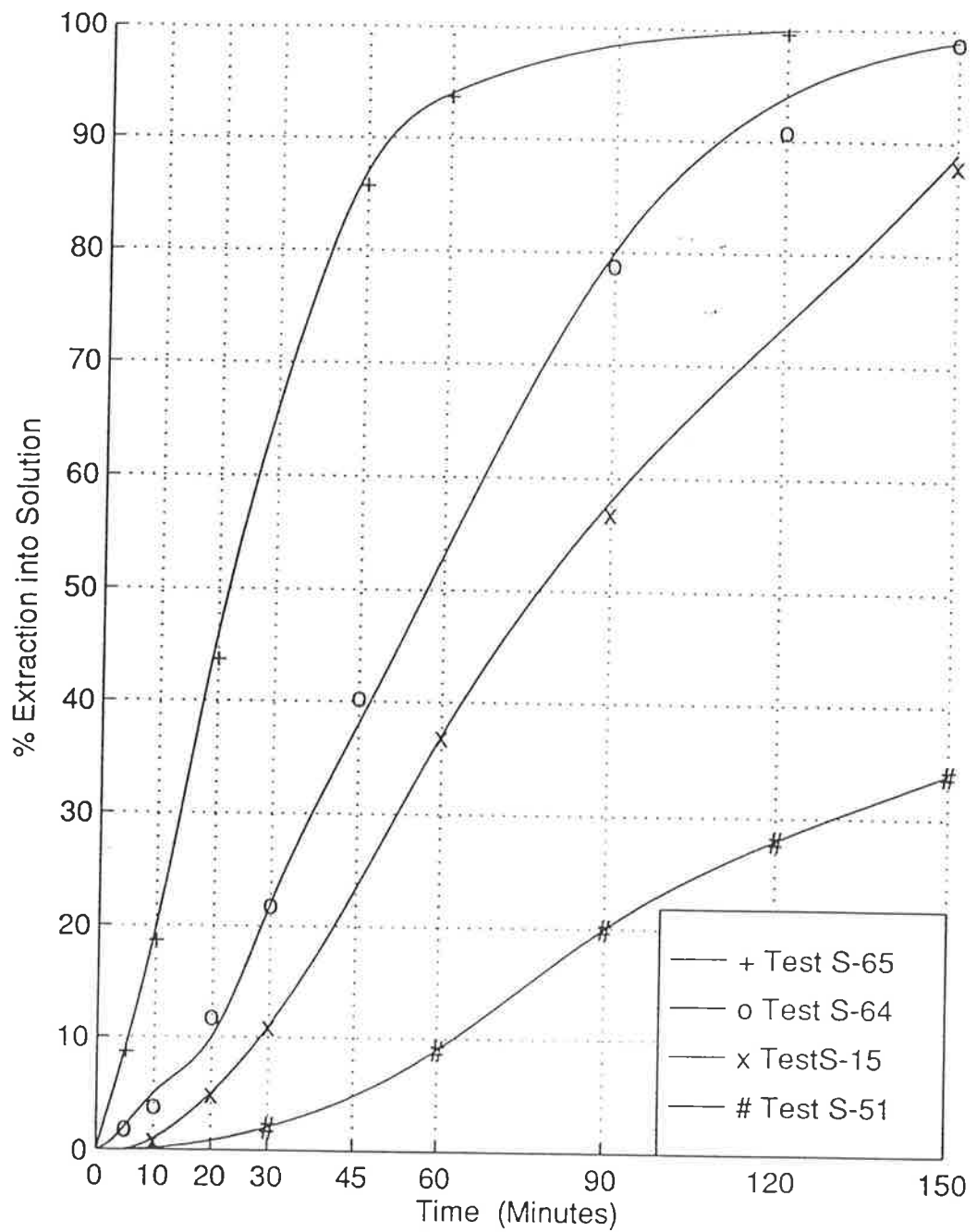


Figure 5.8.5.1 Range of Tests showing Lag Periods

- S-51 Gumeracha Pyrite 125-180 μ m, 80°C, 280 rpm, 1.5 MHNO₃
- S-15 Gumeracha Pyrite 180-250 μ m, 75°C, 280 rpm, 2.6 MHNO₃
- S-64 Gumeracha Pyrite 125-180 μ m, 75°C, 272 rpm, 2.6 MHNO₃
- S-65 Huanzala Pyrite 125-180 μ m, 80°C, 280 rpm, 2.6 MHNO₃

5.8.5 LAG TIME IN PYRITE DISSOLUTION

5.8.5.1 Observed Lag Time

A pattern is observed whereby the reaction rate of the pyrite is slow initially, but then speeds up after a lag time. Lag time is an observed phenomenon of this pyrite-nitric acid investigation, rather than a deliberately chosen variable. Nevertheless, it is considered worth discussing here. The pattern is particularly evident in those test runs at low temperatures or large grain size. It can be seen at low acid concentrations and is arguably evident for most conditions with first-order reaction constants below about 0.02 min^{-1} . Figure 5.8.5.1 displays four such curves, with iron extraction plotted. The presence of a lag time for Huanzala pyrite is debatable. S-65 is the second slowest of the Huanzala deslimed tests and has a rate constant of 0.04 min^{-1} . Sulfate extractions follows much the same pattern as iron. Lag time seems to have little effect on the proportion of elemental sulfur formed.

5.8.5.2 Discussion of Pyrite Reaction Lag Time

From Figure 5.8.5.1, the lag time increases for those reactions which are slower. At 50°C (not shown) the lag time lasted 3 hours. As a general rule, however, the lag time finishes at about 10% iron extraction. Initial mathematical modelling showed that the pyrite-nitric acid reaction was probably first-order for both iron and sulfate extraction. The fit was noticeably better for the faster reactions; the slower reactions did not fit the first-order straight line in the lower regions. Consideration of the lag time phenomenon led to a second round of calculations. Results of both sets of calculations are presented in Section 5.9.

Lag times are well recognised in chemical reactions. They can result from a number of reasons:

- A protective or passivating layer which is slow to remove;
- the reaction produces a product which speeds up further reaction (autocatalysis);
- the reaction produces more surface area on an initially smooth particle.

5.8.5.3 Passivating Layer Possibility

A protective or passivating layer could be present but it is most likely to be an oxide of some sort. The pyrite was crushed some days before testing began. However, as discussed in section 5.6.2, there is no conclusive proof of samples aging. In

fact, on two occasions fresh crushed (ie the day previously) samples were compared to pyrite which had been in the freezer for months. In both cases, the fresh crushed pyrite showed slower kinetics.

It is possible that such a protective layer forms within minutes or hours. In that case there will likely be such a layer on sulfides which are treated for pre-oxidation in a refractory gold plant. Oxidation by dissolved oxygen in mill pulps during grinding is a well-known phenomenon.

5.8.5.4 Autocatalysis Possibility

For autocatalysis to cause a speeding up of the reaction (thereby giving the appearance of a lag time earlier), one of the reaction products must accelerate the dissolution of pyrite. This can only be iron as ferric ion, or sulfates as sulfuric acid. The products from HNO_3 reduction are gaseous (NO) or water. The gas escapes during the process and/or comes back as HNO_3 .

At 10% iron extraction from pyrite, there should be 0.093 g l^{-1} iron in the reaction vessel. This is $1.7 \times 10^{-3} \text{ M Fe}^{3+}$. Test S-58 at $1 \times 10^{-3} \text{ M}$ showed an increase in overall kinetics over no initial Fe^{3+} , although it also showed a longer lag time. The effect is quantified in Section 5.9. Sulfuric acid is also produced - $3 \times 10^{-3} \text{ M}$ at 10% extraction. This seems too low to affect leaching rate. The lowest level of sulfuric acid addition tested was 0.42 M.

5.8.5.5 Surface Area Increase Possibility

Microscopic examination of the pyrite samples and residue has shown that the pyrite surface is altered. Although pyrite is basically a competent crystalline form, during nitric acid oxidation it takes on a burnished, then "burnt" appearance. Many new facets result, if not exactly corrosion pits. It would seem that attack takes place unevenly over the surface, as is to be expected from different crystallographic planes, ridges and crevices at the surface.

While this aspect has not been quantified, it is certainly possible from simple observations, that the pyrite surface area has been increased.

In summary, the lag-time phenomenon definitely occurs during leaching of the pyrite with nitric acid. To a large extent, the lag time accounts for differences in behaviour between pyrite of different origins (see Section 5.9). The cause of the

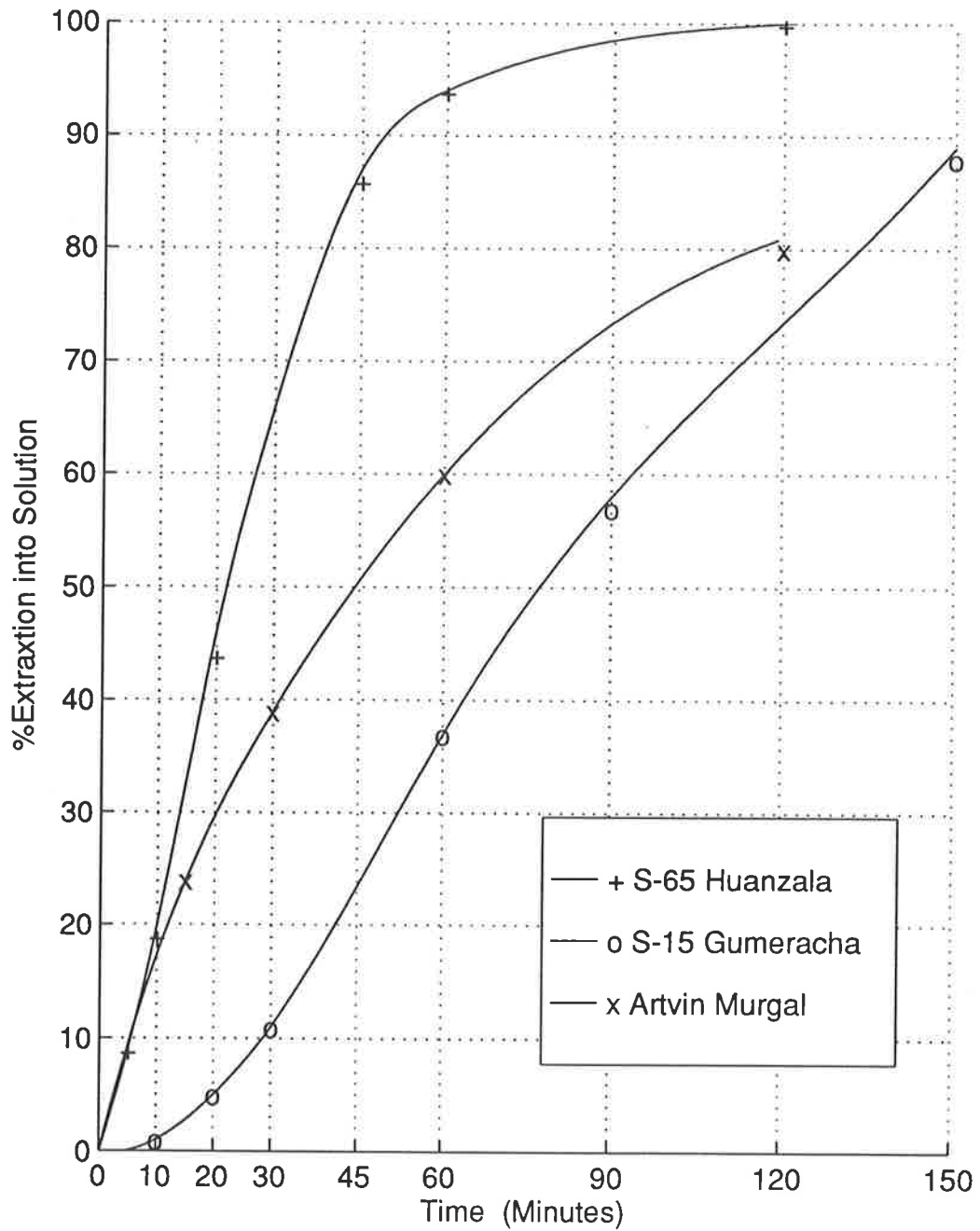


Figure 5.8.6.1 Comparison of Pyrites from Three Sources

180-250 μ m, pyrite, 26 MNHO 3, 80°C

Literature source adjusted to same basis as experimental

lag period for this experimental work has not been fully established. If a protective layer exists on the pyrite, it forms quickly.

5.8.6 PYRITE SOURCE EFFECTS

Figure 5.8.6.1. compares the raw data for the most closely comparable tests from pyrite from three sources. Only iron extractions are shown for clarity. The three sources are Gumeracha (South Australia) and Huanzala (Peru) as tested in the present work and Artvin Murgul (Turkey) as reported in Kadioglu et al. (1995). The raw results are not strictly comparable as the test conditions varied slightly as shown in Table 5.8.6.1 below. The experimental program of this thesis had been completed by the time the Kadioglu paper was published.

Table 5.8.6.1: Raw Data for Leach Tests on Pyrite from Three Different Sources

| Source | Gumeracha | Huanzala | Artvin Murgul |
|---|-----------|----------|---------------|
| Test No | S-15 | S-65 | Literature |
| Stirring Speed (rpm) | 280 | 280 | 800 |
| Size (μm) | 180/250 | 125/180 | 180/250 |
| [HNO ₃] concentration (Molar) | 2.6 | 2.6 | 2.4 |
| Temperature ($^{\circ}\text{C}$) | 80 | 80 | 70 |

Comparison of pyrites by source was not originally intended for the present work. However, these three tests were considered worthwhile analysing, if they could be mathematically manipulated to the same basis. This is done and the results discussed in the Mathematical Analysis (Subsection 5.9.5).

5.8.7 SECTION SUMMARY (ADDITIONAL FACTORS)

The addition of inert solids to 'scrub' or attrition element sulfur from the surface of oxidising pyrite showed promise initially. Practical and statistical difficulties were encountered with this series. These difficulties were largely overcome but the initial promise of attritioning proved unfulfilled. Redox potential (Eh) proved impractical to measure at test conditions. Attempts to introduce reagents to increase the Eh of the nitric acid system showed limited success. Silver ion slowed the kinetics of pyrite leaching but gave promise of eliminating elemental sulfur. If the economics of adding silver warrant it, this route should be investigated further.

The various variables are additive in their effects, at least qualitatively. Gumeracha pyrite shows a marked lag period before it achieves its maximum leaching rate.

This is probably contributed to by a combination of factors. Raw data was compared for pyrite from three different sources. It will be necessary to mathematically adapt the raw data to the same experimental conditions basis to allow a more meaningful interpretation of the difference between sources.

This last sentence applies to a greater or lesser extent to all the variables in Section 5.5 through 5.8.

5.9 MATHEMATICAL ANALYSIS OF LEACH TESTS

5.9.1 PREAMBLE

The mathematical analysis is presented separately from the main results and discussion because it is considered that a separate section will give a better overview of the quantitative effects of the numerous test variables. This section is very much a summary. The calculations evolved as the overall picture emerged. Certainly there is scope for further mathematical analysis of the experimental data.

Rate constants are summarised in subsection 5.9.2 for the majority of the variables. These results are for the tests as conducted. Those tests which exhibited appreciable lag periods have the range for which the rate constants apply specified. Apparent relationships between the rate constants and the variables are described and discussed.

The shrinking core model has been put forward by recent authors (Kadioglu et al. 1995) as fitting pyrite oxidation data. Applicability of this model to the author's leach data is described in Subsection 5.9.3.

Summaries of the variables tested in Section 5.4 through 5.8 were qualitative, with quantitative findings being considered in the present section 5.9. Accordingly, this summary should be read with the appropriate Results and Discussion section in mind. The grouping will follow that of Sections 5.4 through 5.8.

A more rigorous analysis, with the lag period excluded, was applied to selected data. This analysis is discussed in Subsection 5.9.4. The rate constants for pyrite from three different sources (one from the literature) are described in Subsection 5.9.5. The activation energy for pyrite oxidation is calculated in Subsection 5.9.6.

Subsection 5.9.7. addresses the question of the rate of oxidation of elemental sulfur, once it is formed, to sulfate. Sample calculations for the rate constants may be found there.

5.9.2. SUMMARY OF KINETIC DATA

5.9.2.1 Rate Constant Summary

Table 5.9.2.1 summarises the first-order rate constants for the test variables, by series as described in Sections 5.4-5.8. First-order kinetics were found to give the best fit, as described in Subsection 5.9.3. The data of Table 5.9.2.1 includes the extraction range over which first-order kinetics appear to apply. The statistical correlation coefficients over the range are also given. This data is considered to reflect the practical kinetics of pyrite oxidation better than the more sophisticated analysis of 5.9.4.

Table 5.9.2.1: First-Order Rate Constant for Pyrite-HNO₃ Leach Tests

A - Classical Variables

| Series | Conditions | Variable Value | Applies Over Extraction Range % Fe | Correlation Coefficient r | Rate Constant k (min ⁻¹) |
|--------------------------------|--|---|------------------------------------|---------------------------|--------------------------------------|
| Stirring Rate | Gumeracha Pyrite 90/125 µm, 80°C, 2.6 M HNO ₃ | 72, 112, 192, and 250 rpm 280 and 350 rpm | 0 - 95 | 0.9795 | 0.076 |
| | | | 10-98 | 0.9887 | 0.051 |
| Temperature | Gumeracha Pyrite 90/125 µm 2.6 M HNO ₃ < 250 rpm | 50°C 60°C ≠ 70°C 75°C 80°C 100°C | 5-38* | 0.9882 | 0.003 |
| | | | 10-77* | 0.9790 | 0.013 |
| | | | 10-99 | 0.9891 | 0.040 |
| | | | 10-90 | 0.9981 | 0.044 |
| | | | 0-95 | 0.9736 | 0.075 |
| | | | 0-90 | 0.9240 | 0.150 |
| Particle Size | Gumeracha Pyrite 75°C 280 rpm 2.6 M HNO ₃ | 180/250 µm 125/180 µm ≠ 90/125 µm 63/90 µm 45/63 µm | 1 - 80* | 0.9804 | 0.013 |
| | | | 2 - 85 % | 0.9580 | 0.021 |
| | | | 6 - 90 % | 0.9986 | 0.030 |
| | | | 1 - 97 % | 0.9711 | 0.044 |
| | | | 1 - 96 % | 0.9537 | 0.057 |
| HNO ₃ Concentration | Gumeracha Pyrite 125/180 µm 80°C 280 rpm | 1.5 Molar ≠ 2.0 Molar 2.6 Molar 3.5 Molar 4.5 Molar | 5 - 35* | 0.9877 | 0.0041 |
| | | | 0 - 70* | 0.9999 | 0.010 |
| | | | 10-97 | 0.9978 | 0.023 |
| | | | 0-95 | 0.9818 | 0.041 |
| | | | 0-99 % | 0.9914 | 0.076 |

* test terminated at higher value

≠ values adjusted for one other variable different from main test series

B - Industrial Variables

| Series | Conditions | Variable Value | Applies Over Extraction Range | Correlation Coefficient | Rate Constant (min ⁻¹) |
|--|---|------------------------------------|-------------------------------|-------------------------|------------------------------------|
| H ₂ SO ₄ Concentration | Gumeracha Pyrite 90/125 μm, 80°C, 280 rpm 2.2 M HNO ₃ | Nil H ₂ SO ₄ | 0 - 85 % Fe | 0.9950 | 0.049 |
| | | 0.42 M | 0 - 80 % Fe | 0.9875 | 0.057 |
| | | 0.83 M | 10 - 90 % Fe | 0.9902 | 0.064 |
| | | 1.68 M | 0 - 96 % Fe | 0.9924 | 0.10 |
| | | 2.52 M | 0 - 96 % Fe | 0.9563 | 0.22 |
| Fe ³⁺ Concentration (Sulfate Figures) | Gumeracha Pyrite 125/180 μm, 80°C 280 rpm 2.6 M HNO ₃ | nil Fe ³⁺ | 14 - 81% SO ₄ = | 0.9971 | 0.015 |
| | | 10 ⁻³ M | 14 - 89% SO ₄ = | 0.9958 | 0.021 |
| | | 10 ⁻² M | 4 - 88 % SO ₄ = | 0.9976 | 0.023 |
| | | 10 ⁻¹ M | 4 - 87 % SO ₄ = | 0.9913 | 0.025 |
| | | ≈2 x 10 ⁻¹ M | 4 - 91 % SO ₄ = | 0.9923 | 0.047 |
| Cl ⁻ Concentration (Sulfate Figures) | Gumeracha Pyrite 125/180 μm 80°C 280 rpm 2.6 M HNO ₃ | nil Cl ⁻ | 0 - 85 % SO ₄ = | 0.9971 | 0.015 |
| | | 10 ⁻² M | 0 - 90 % SO ₄ = | 0.9964 | 0.028 |
| | | 1.0 M | 0 - 97 % SO ₄ = | 0.9956 | 0.040 |
| Blend Sizes | Gumeracha Pyrite 80°C 280 rpm 2.6 M HNO ₃ | Mono Size | 7 - 85 % Fe | 0.9989 | 0.022 |
| | | 125/180 μm | 2 - 62 % Fe | 0.9792 | 0.018 |
| | | add coarse | 10 - 42 % Fe | 0.9959 | 0.029 |
| | | add medium | 18 - 88 % Fe | 0.9995 | 0.045 |
| | | add - 45 μm | 10 - 76 % Fe | 0.9729 | 0.035 |
| Range - 45 + 250 μm | | | | | |

C - Additional Factors

| Series | Conditions | Variable Value | Applies Over Extraction Range | Correlation Coefficient | Rate Constant (min ⁻¹) |
|-------------------------------|--|---|-------------------------------|-------------------------|------------------------------------|
| Attritioning | Huanzala Pyrite 180/250 μm 80°C 2.6 M HNO ₃ | no glass balls in attritioner | 10 - 99 % Fe | 0.9940 | 0.027 |
| | | 30% glass balls | 0 - 99 % Fe | 0.9944 | 0.033 |
| Eh | Gumeracha Pyrite 50°C 125/180 μm 2.6 M HNO ₃ | φ Eh 1.06 (SHE) | 0 - 26 % Fe | 0.9937 | 0.0018 |
| | | Eh 1.07 -1.37 | 0.- 30 % Fe | 0.9965 | 0.0030 |
| Ag ⁺ Concentration | Gumeracha Pyrite 90/125 μm 80°C 280 rpm 2.6 M HNO ₃ | nil Ag ⁺ | 0 - 85 % Fe | 0.9950 | 0.049 |
| | | 5 x 10 ⁻³ M | 0 - 98 % Fe | 0.9980 | 0.035 |
| | | 10 ⁻² M | 0 - 97 % Fe | 0.9961 | 0.029 |
| Additive Effects | Huanzala Pyrite 180/250 μm 2.6 M HNO ₃ attr. - 30% balls | 80°C | 0 - 93 % SO ₄ = | 0.9712 | 0.030 |
| | | 90°C | 0 - 99 % SO ₄ = | 0.9855 | 0.075 actual 0.101 predicted |
| | Gumeracha Pyrite 63/90 μm | 75°C 2.6 M HNO ₃ , 280 rpm | 10 - 95 % Fe | 0.9934 | 0.044 |
| | | 90°C 3.5 M HNO ₃ 2 M H ₂ SO ₄ attr. 30% balls | 0 - 98 % Fe | 0.9360 | 1.10 actual 0.82 predicted |

φ Rate constant adjusted from 90/125 μm

5.9.2.2. Rate Constant Variation with Stirring, Temperature, Size and Nitric Acid Size Blends - Classical Variables

As described in section 5.6, the data on kinetic variation with stirring speed falls into two groups. In the range from suspension to 250 rpm, the first-order rate constant is 0.076 min^{-1} as per Table 5.9.2.1. Independence of stirring is typical of processes controlled by surface chemical reactions (Flatt and O'Neill, 1995). The grouping of results is perhaps related to the flocculation which is obvious during leaching. For Gumeracha pyrite, the relationship between temperature and the first-order kinetic rate constant is shown on Figure 5.9.2.1 (below). For this graph $\ln k \propto 1/T \text{ } ^\circ\text{K}$. While the fit for this relationship is only fair (r , the correlation coefficient, = 0.9644) the lack of fit stems from the lag times of the lower-temperature leach tests. When these lagtimes are excluded (see 5.9.4) a much better fit is obtained.

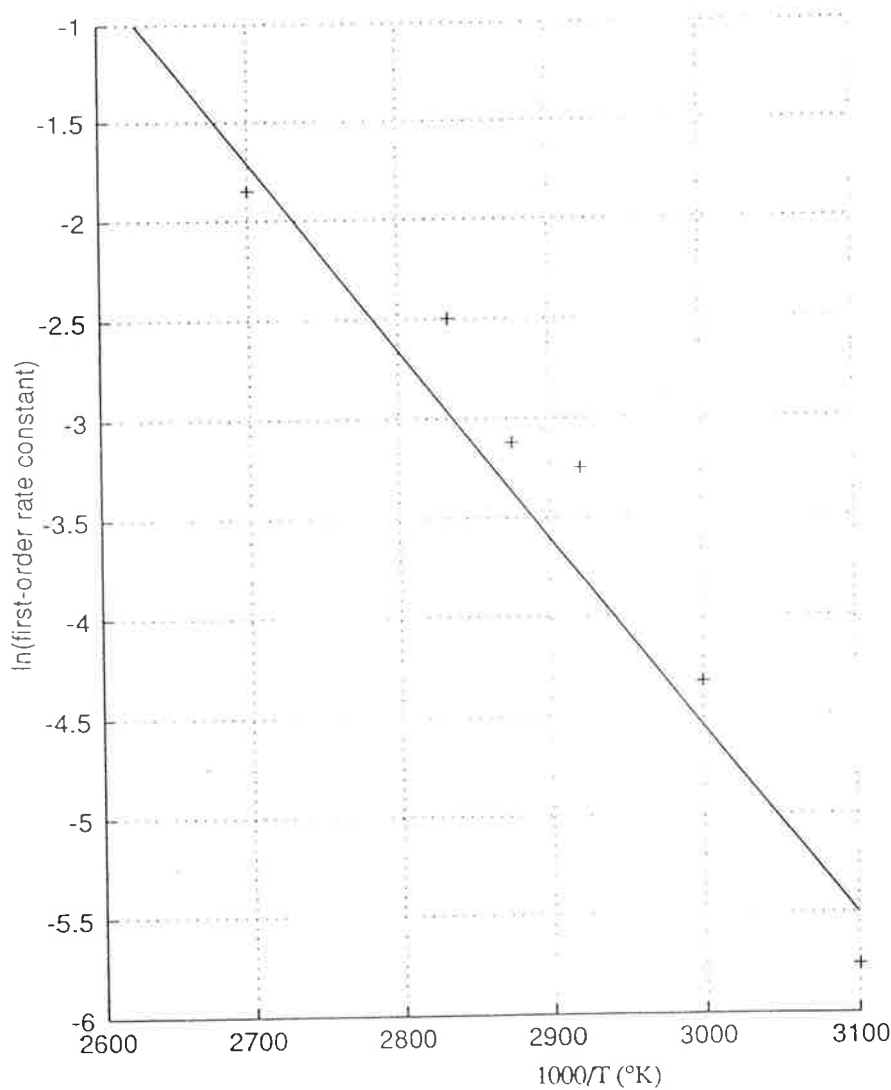


Figure 5.9.2.1 Arrhenius Plot
Rate Constant Variation with Temperature
Gumeracha Pyrite 90-125 μm < 250 rpm
2.6 MHNO_3 - Raw Data

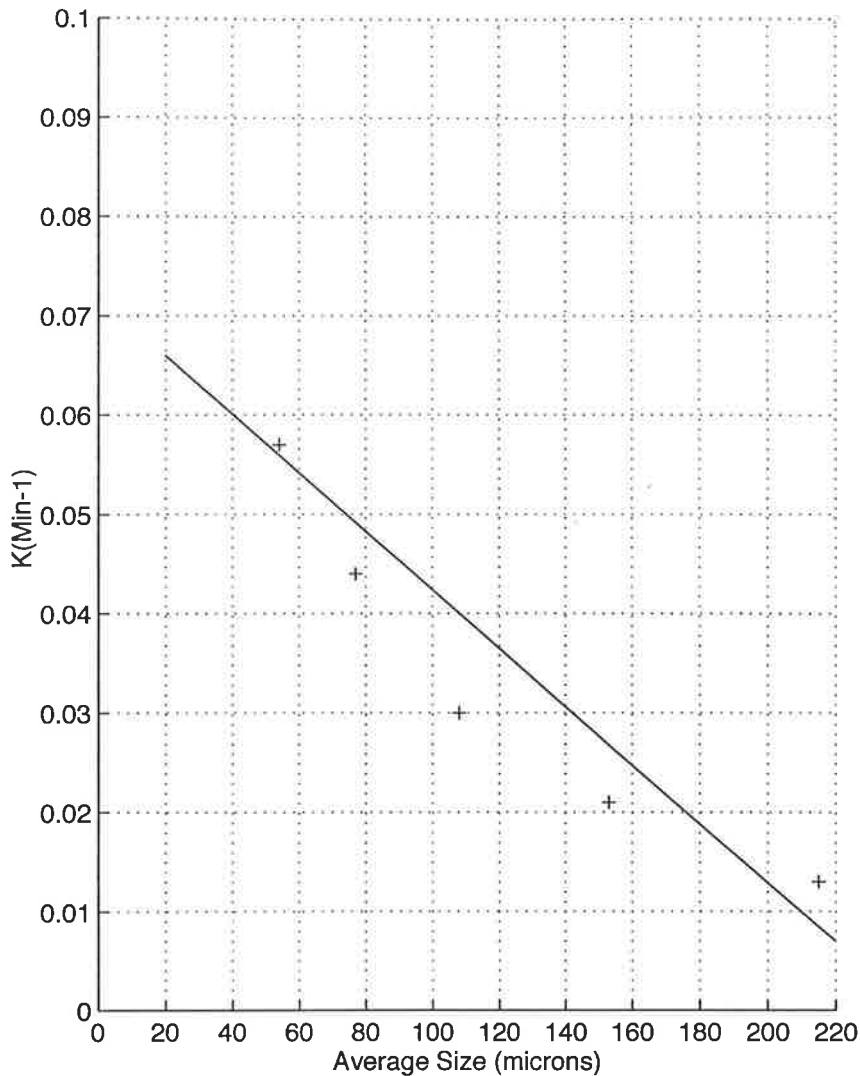


Figure 5.9.2.2 Variation of Rate Constant with Particle Size

Gumeracha Pyrite 75°C 280 rpm 2.6 MHNO₃

Figure 5.9.2.2 shows the relationship between the first-order rate constant of Table 5.9.2.1 and particle size. Again the linearity of the first-order rate curves is only fair ($r = 0.9572$) but the values chosen for Table 5.9.2.1 give a slope for Figure 5.9.2.2 which is reasonable. For Figure 5.9.2.2 a decrease in one screen size will increase the rate constant by a factor of 1.46. For cubic pyrite particles, a decrease in one screen size would increase the initial surface area by a factor of $\sqrt{2}$ or 1.41. Thus the rate constant varies very nearly directly with the expected surface area.

The effect of surface area on rate constant is linear for blends of sizes at least as far as initial surface area. These curves are discussed in Section 5.7.5.2. Figure 5.9.2.3 plots initial surface area against initial rate constant for this series of tests. The surface area of the blends containing -45 μm slimes is open to question. If the average particle size of the -45 μm is assumed to be 38 μm (one screen size smaller than the -63 + 45 μm fraction) the solid line of Figure 5.9.2.3 results. This line gives a correlation coefficient of 0.9569. For it, the rate constant very nearly

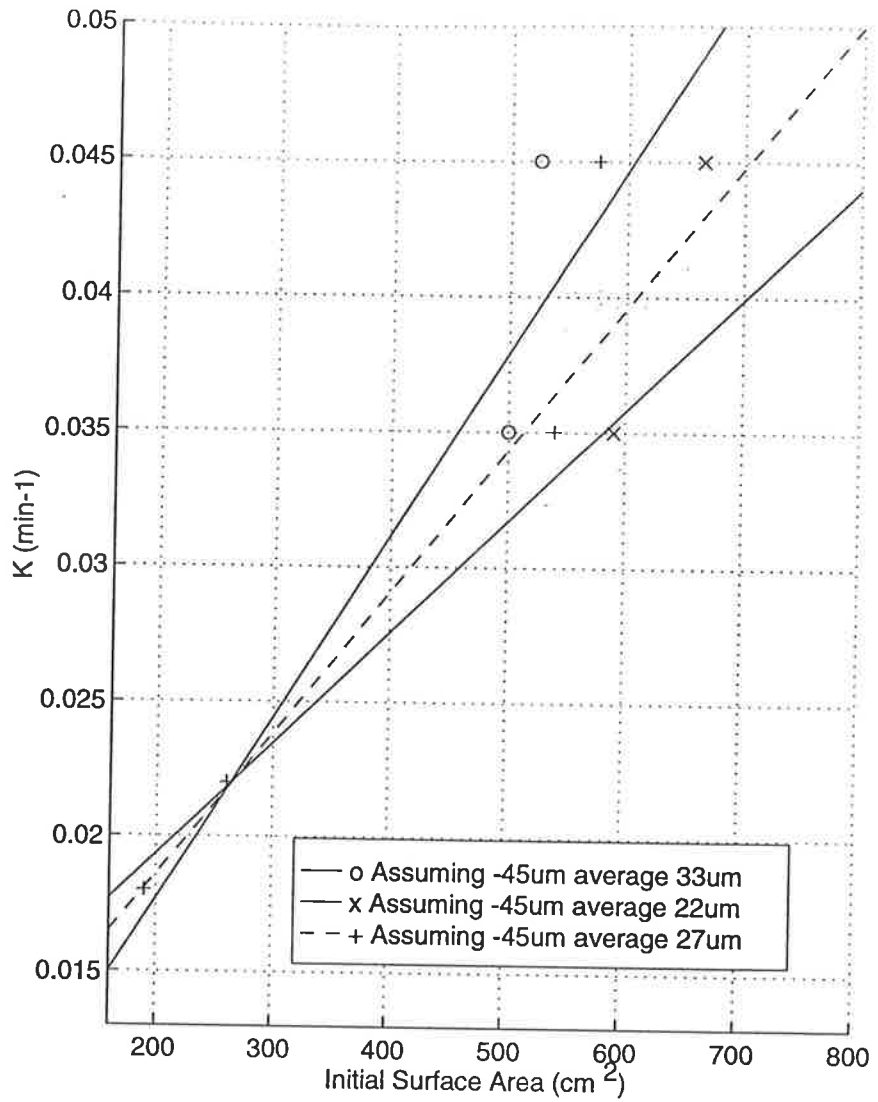


Figure 5.9.2.3: Variation of Rate Constant with Size Blends
 Gumeracha Pyrite, 80°C, 272 rpm, 2.6 MHNO₃

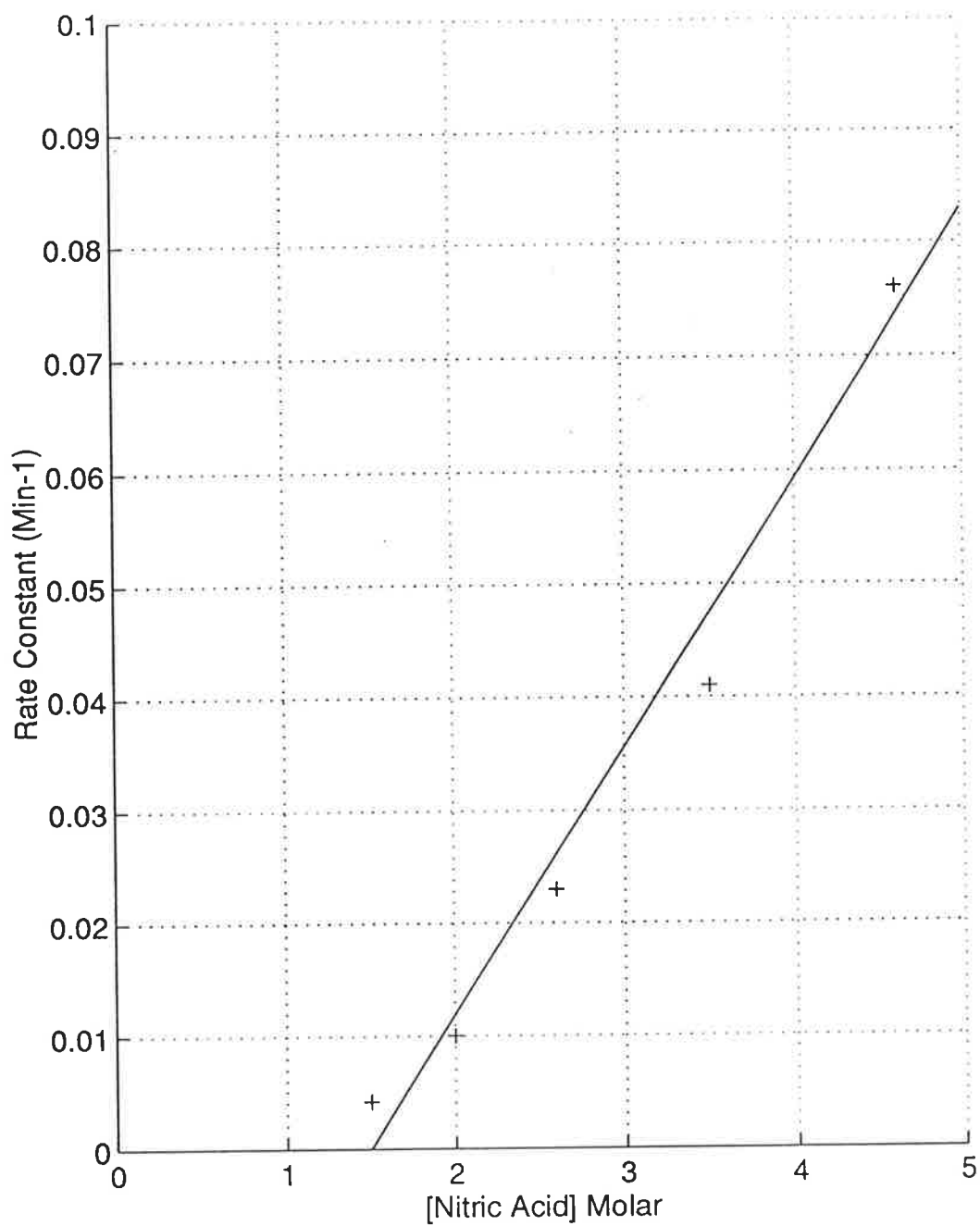


Figure 5.9.2.4 Variation of Rate Constant with Nitric Acid Concentration
Gumeracha Pyrite 125-180 μm , 80°C, 280 rpm

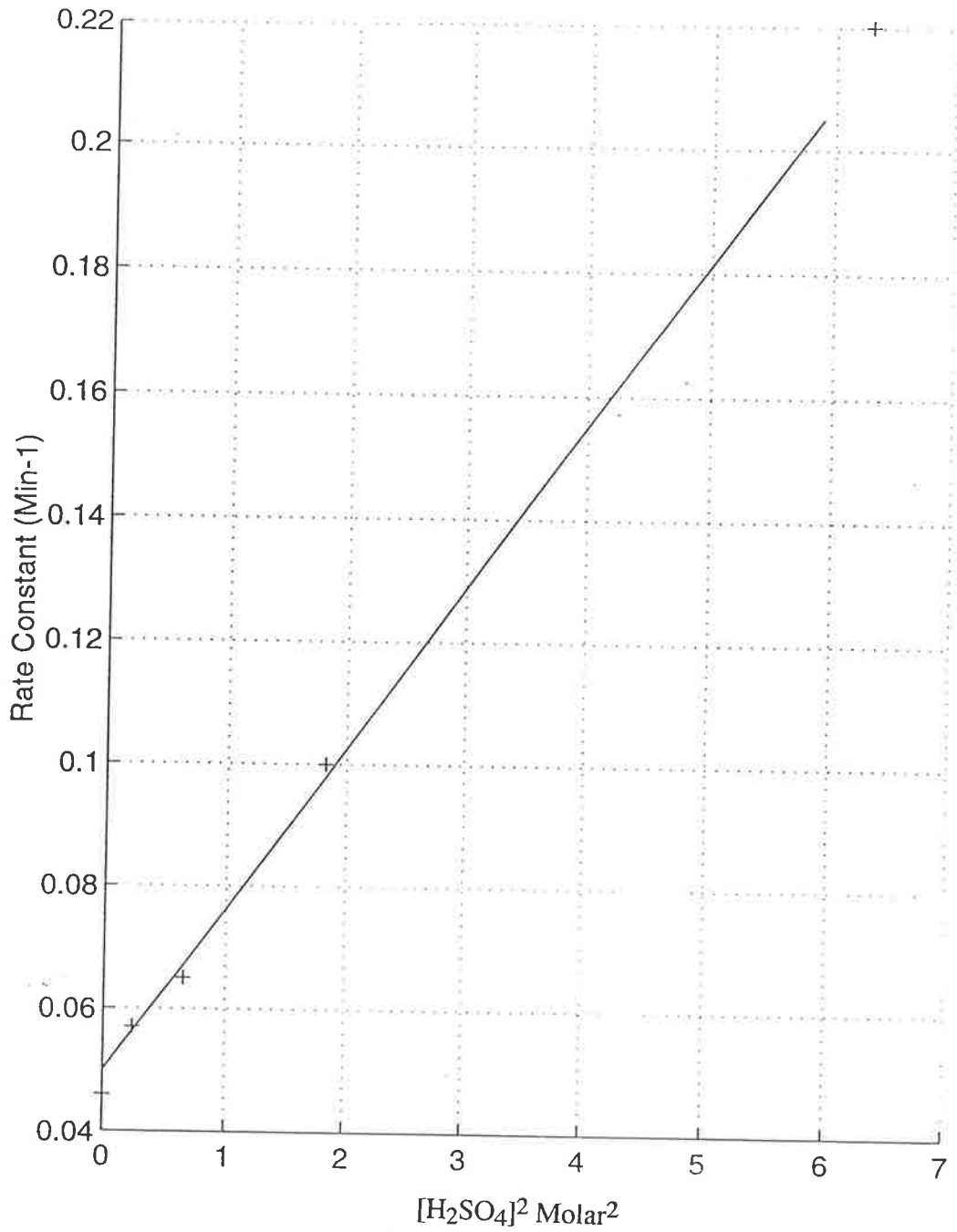


Figure 5.9.2.5

Variation of Rate constant with Sulfuric Acid Concentration

Gumeracha Pyrite 90-125 μm , 80°C, 280 rpm, 2.2 M HNO₃

doubles (1.84) when the initial surface area doubles. If the surface area of the – 45 μm fraction is higher, as seems likely, then a shallower slope results. If an average size of 27 μm is assumed (two screen fractions down) the dashed line of Figure 5.9.2.3 results. This line has a better correlation coefficient 0.9785 but a lower slope. For this line, if the initial surface area doubles, the rate constant increases by 60%. Resolution of the matter would require an accurate surface area determination, which was not performed. While the linear relationship would appear to hold for blends of sizes, the rate constant does not appear to increase quite as fast as the surface area. Also, in the later stages of leaching (high extraction) the shape of the curve is flattened by the coarse size fractions.

Figure 5.9.2.4 shows the variation of rate constant with nitric acid concentration. The variation is close to linear and the fit is quite good ($r = 0.9865$). Again the slower tests (low acid concentration) show a lag period.

5.9.2.3 Rate Constant variation with added Reagents H_2SO_4 , Fe^{3+} , Cl^- , Ag^+

Figure 5.9.2.5 shows the variation of the rate constant with sulfuric acid concentration. Again, the figures are from Table 5.9.2.1. The variation is second-order. The reason for this dependence is not obvious, as sulfuric acid is not a reactant. The statistical correlation coefficient for Figure 5.9.2.5 is 0.9893.

Data for the analysis of the variation of rate constant with iron concentration are shown in Table 5.9.2.2. The concentrations chosen made mathematical analysis difficult. However, the lack of confidence in iron assays (due to background iron added) makes analysis difficult as well. Given that none of the correlation coefficients for Table 5.9.2.2 is particularly good, potential users of the data may as well assume the leach rate is linear with ferric ion concentration.

Table 5.9.2.2: Variations of Rate Constant with Ferric Ion Concentration

| Data Points (From Table 5.9.2.1) | Correlation Coefficient | Slope | Intercept @ [Fe^{3+}] = 0 | k varies as |
|-------------------------------------|----------------------------|--------|---|-----------------------------------|
| | r | b | | |
| 5 | 0.9343 | 0.1301 | 0.018 | [Fe^{3+}] |
| 5 | 0.9694 | 0.6842 | 0.019 | [Fe^{3+}] ² |
| 5 | 0.9680 | 3.385 | 0.020 | [Fe^{3+}] ³ |

For Gumeracha Pyrite, 125/180 μm , 80°C, 280 rpm, 2.6 M HNO_3

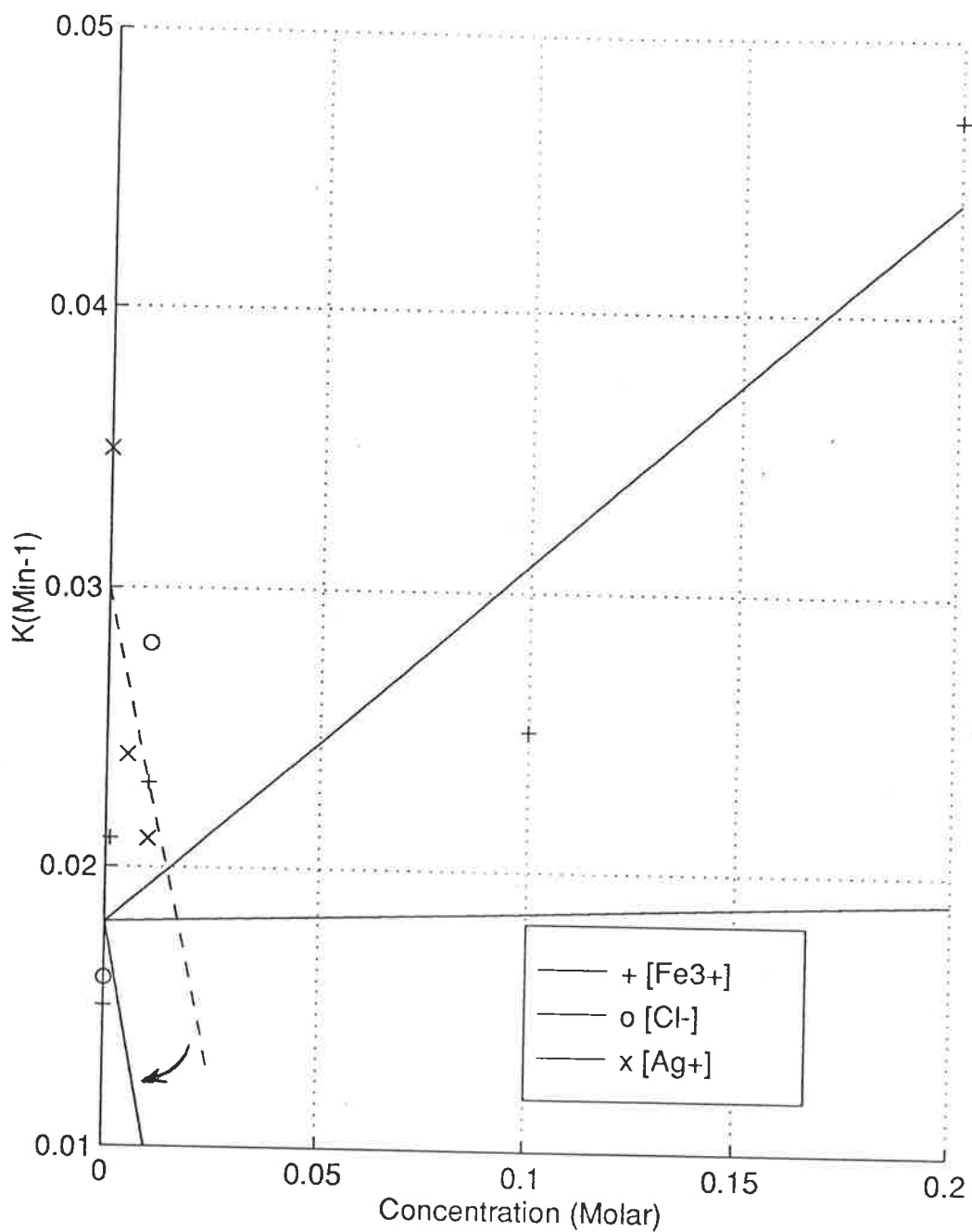


Figure 5.9.2.6 Variation of Rate Constant with (Fe^{3+}), (Cl^-), (Ag^+)
 (All lines normalized to $k = 0.018$)
 (Fe^{3+}) Series Gumeracha Pyrite 125-180 μm , 80°C, 280 rpm, 2.6 MHNO_3
 (Cl^-) Series Gumeracha Pyrite 125-180 μm , 80°C, 280 rpm, 2.6 MHNO_3
 (Ag^+) Series Gumeracha Pyrite 90-125 μm , 80°C, 280 rpm, 2.6 MHNO_3

The data for variation of rate constant with chloride ion suffers from the same shortcomings as the ferric ion data. Further, there are only three valid data points. There are also only three data points for the addition of silver ion. While it is obvious that chloride ion increases pyrite leaching rate, and silver ion decreases it, statistical analysis of the variation, from these data points, is not very meaningful. Accordingly, linear relationships have been assumed and the correlation coefficients are given in Table 5.9.2.3

Table 5.9.2.3. Assumed Variation of Rate Constant with:

- a) Chloride Ion Concentration
- b) Silver Ion Concentrations

| Data Points (Table 5.9.2.1) | Correlation Coefficient | Slope b | Intercept @ [ion] = 0 | k varies as |
|--------------------------------|----------------------------|---------|--------------------------|-----------------------|
| 3 | 0.873 | 0.018 | 0.022 | a) [Cl ⁻] |
| 3 | 0.963 | - 1.95 | 0.047 | b) [Ag ⁺] |

Gumeracha Pyrite a) 125/180 μm b) 90/125 μm all 80°C, 280 rpm, 2.6 M HNO₃

In the hope that it may be useful, the data for iron, chloride and silver ion additions of Tables 5.9.2.2 and 5.9.2.3 is shown on Figure 5.9.2.6. All three sets of data were 'normalised' to the same k values at zero addition of their particular reagents.

5.9.2.4 Rate Constant Variation with Additional Factors: Attritioning and Eh

From Table 5.9.2.1 attritioning speeds up pyrite leaching rate. Coarse pyrite (180/250 μm) displayed a significant rate constant increase when glass balls were added to the attritioning vessel. The first-order rate constant increased from 0.027 to 0.033 min^{-1} or 22%.

The crude attempt at increasing Eh (S-46) also showed promise for increasing leaching rate. When compared to S-7 (itself adjusted for particle size) there was a first-order rate constant increase of 67%. The Eh of S-46 fluctuated wildly from 1.07 - 1.37 V (SHE) as KMnO₄ was added. As stated previously, Eh measurement was questionable at best, so other runs were not statistically comparable on the basis of measured Eh.

5.9.2.5 Additivity of Effects

Two runs were analysed and compared to earlier tests to see if the various factors gave additive improvements to the rate constants. The result for S-78 is compared in Table 5.9.2.4 to its predicted rate constant using S-71 as a basis.

Table 5.9.2.4: Comparing Additive Rate Constants

| Condition | S-71 | S-78 | Adjustment Factor (to S-71) | Comparison Basis | Comments |
|---------------------|-----------------------|-----------------------|-----------------------------|------------------|--------------------------|
| Pyrite source | Huanzala | Huanzala | 1.0 | – | |
| size | 180/250 μm | 180/250 μm | 1.0 | – | |
| Temperature | 80°C | 90°C | 2.11 | Fig 5.9.2.1 | Gumeracha data |
| [HNO ₃] | 2.6 M | 2.6 M | 1.0 | | |
| [Fe ³⁺] | – | 0.07 M | $\frac{.035}{.022}$ | Fig 5.9.2.6 | Sulfate assays Gumeracha |
| Attritioning | yes | yes | 1.0 | | |

∴ Predicted Rate Constant for S-78

$$= 0.030 \times 2.11 \times \frac{0.035}{0.022} = 0.101 \text{ min}^{-1}$$

(S-71) (10C°) [0.07 Fe³⁺]

Actual S-78 rate constant 0.075 min⁻¹ (sulfate)

The result for S-79 is compared in Tables 5.9.2.5 to its predicted value using test S-23 as a basis.

Table 5.9.2.5: Comparing Additive Rate Constants

| Condition | S-23 | S-79 | Adjustment Factor (to S-23) | Comparison Basis | Comment |
|-----------------------------------|---------------------|---------------------|-----------------------------|------------------|---------|
| Pyrite source | Gumeracha | Gumeracha | 1.0 | – | |
| size | 63/90 μm | 63/90 μm | 1.0 | – | |
| Temperature | 75°C | 90°C | 3.31 | Fig 5.9.2.1 | |
| [HNO ₃] | 2.6 M | 3.5 M | $\frac{0.047}{0.023}$ | Fig 5.9.2.4 | |
| [H ₂ SO ₄] | – | 2.0 M | $\frac{0.10}{0.044}$ | Fig 5.9.2.5 | |
| [Fe ³⁺] | – | – | 1.0 | | |
| Attritioning | No | yes | 1.22 | Text 5.9.2.4 | |

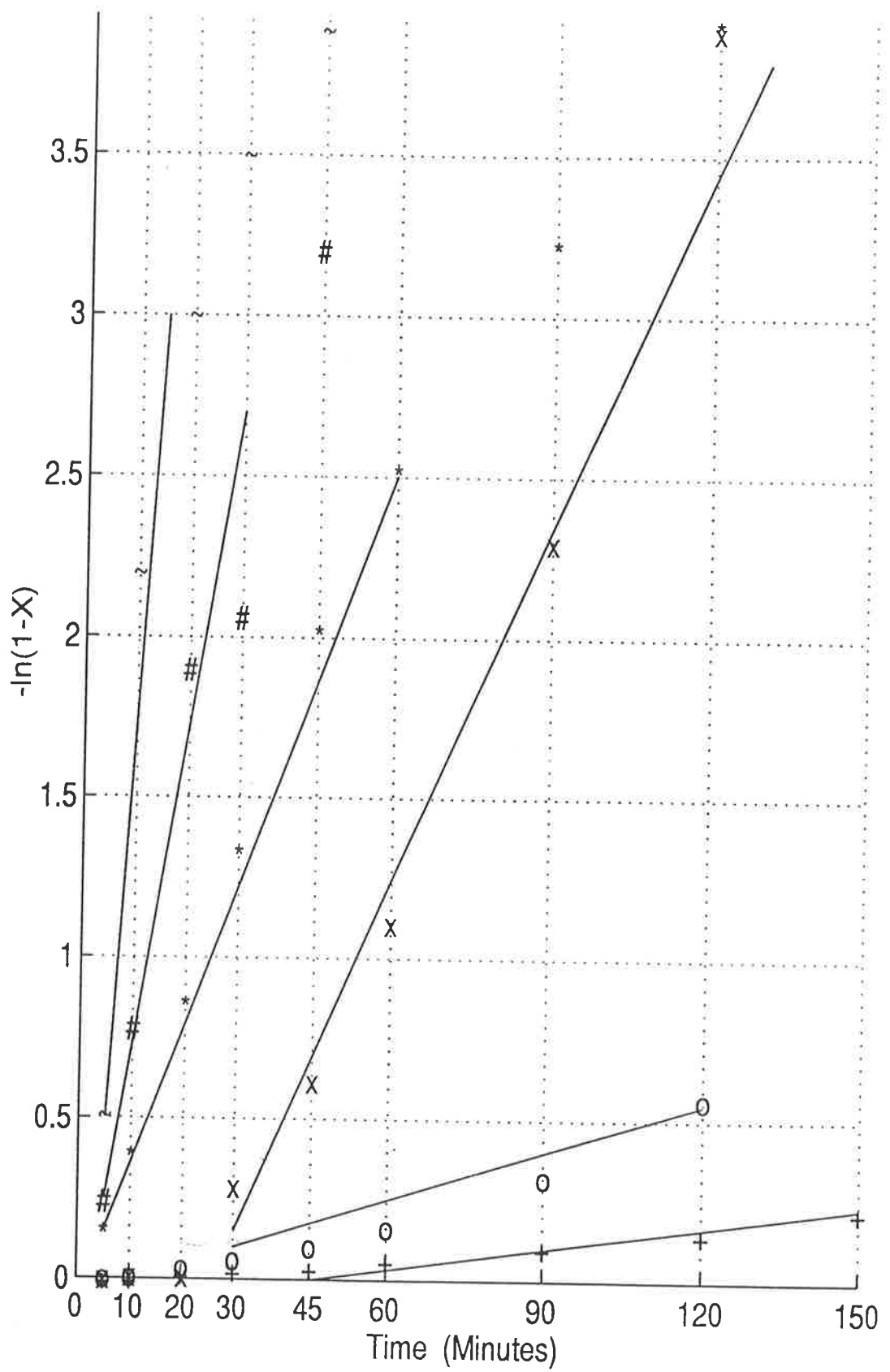


Figure 5.9.3.1 Fit of Temperature Series Data (Raw Data) to First Order Model
 Gumeracha Pyrite 90-125 μm 2.6 MHNO_3
 + 50°C, o 60°C, x 70°C, * 75°C, # 80°C, ^ 100°C

$$\begin{aligned}
&\therefore \text{Predicted rate constant for S-79} \\
&= 0.044 \times 3.31 \times \frac{0.047}{0.023} \times \frac{0.10}{0.044} \times 1.22 \\
&\quad [S-23] \quad [15^\circ\text{C}] \quad [0.9 \text{ MHNO}_3] \quad [2 \text{ M H}_2\text{SO}_4] \quad (\text{Attr}) \\
&= 0.044 \times 3.31 \times 2.04 \times 2.27 \times 1.22 \\
&= 0.82 \text{ min}^{-1} \\
&\text{S-79 Rate Constant actual} - 1.10 \text{ min}^{-1}
\end{aligned}$$

Of the two values checked, one predicted value is high, the second low. The differences between predicted and actual are about 30% which can be considered quite good for this type of work. Given that the k values themselves are sensitive to the size picked (see 5.9.4) it can be suggested that the k values are additive. More tests and a more rigorous analysis might improve the confidence in this statement.

5.9.3 FIRST-ORDER KINETICS VERSUS SHRINKING CORE MODEL

5.9.3.1 Background

Various researchers in the literature (Bailey and Peters, 1976; Kadioglu et al. 1995) have provided evidence that pyrite leaching follows the shrinking core model. In this model

$$1 - (1 - x)^{1/3} = k t \quad (5.9.3.1)$$

where x is the extraction (fraction dissolved)

For first-order rate kinetics, however,

$$\ln(1 - x) = k t \quad (5.9.3.2)$$

5.9.3.2 Model Fitting - Gumeracha Temperature Series - Raw Data

Early on in the mathematical analysis of results, attempts were made to fit the experimental data to the shrinking core model. Similar attempts were made as the analysis progressed.

Figure 5.9.3.1 compares the raw data fit to the first-order model. Figure 5.9.3.2 compares the same data to the shrinking-core model. It can be seen that both models fit the data, if the extraction ranges are limited. This is quite common for first-order data (O'Neill, 1994) which involves a lag time and non-linearity at high

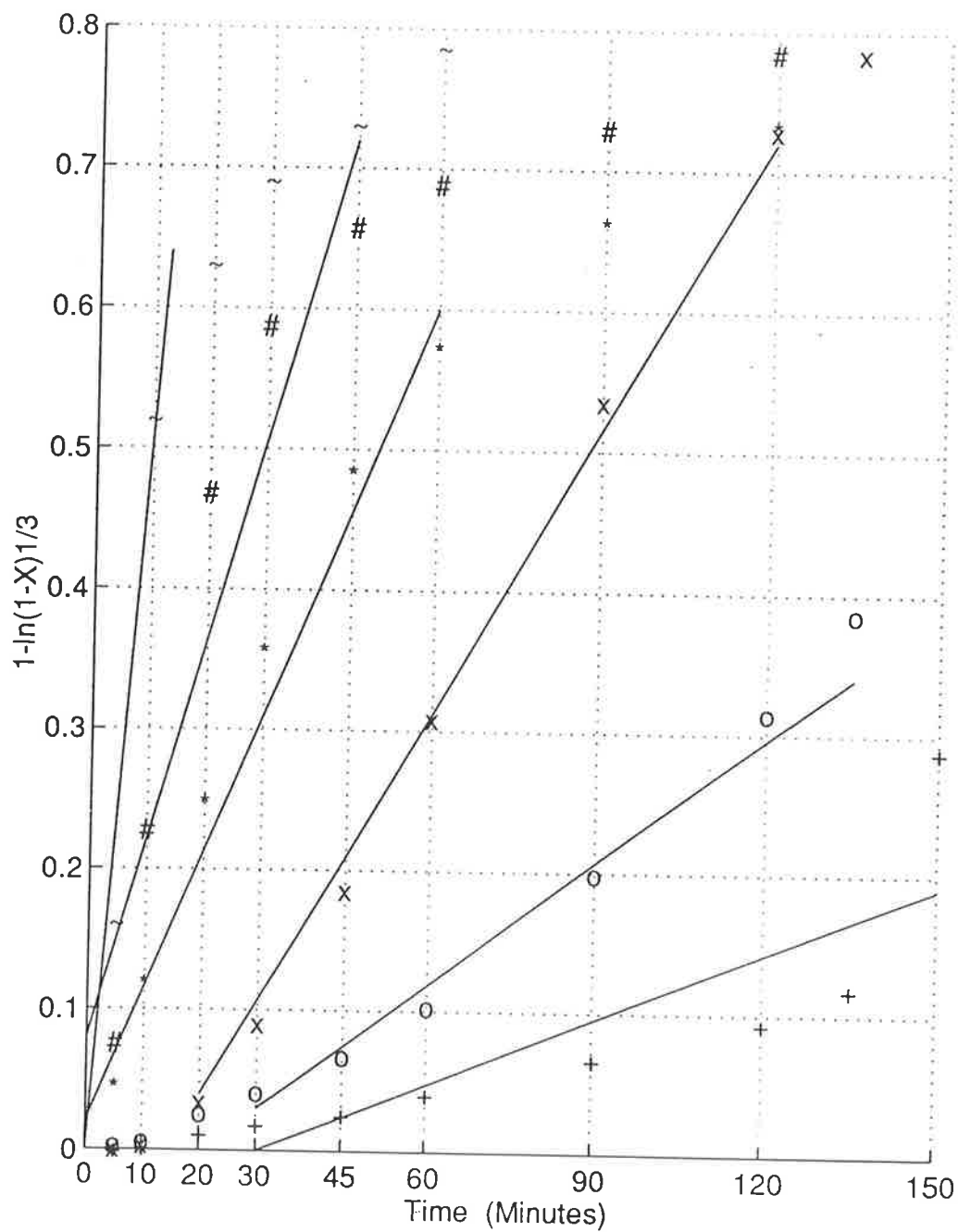


Figure 5.9.3.2: Fit of Temperature Series Data (Raw Data) to Shrinking-Core Model

Gumeracha Pyrite 90-125 μ m, 2.6 MHNO₃
 + 50°C, o 60°C, x 70°C, * 75°C, # 80°C, ^ 100°C

extractions. It is generally not allowed for in shrinking-core models. Therefore Figure 5.9.3.2 has shown the full range of data. However, it seems only reasonable to compare the same range for both models. Data for the same range is also included in Table 5.9.3.1.

Table 5.9.3.1: Rate Constant Fitting for Raw Temperature Series Data (Gumeracha)

| Temp (°C) | Limited Fe Extraction Range | | | | Full Range of Data | | | | |
|-----------|-----------------------------|-------------------|-------|----------------------|--------------------|----------------|--------|---------|----|
| | | First-order Model | | Shrinking-Core Model | | Shrinking-Core | | | |
| | Range | r | k | r | k | r | k | Range | n |
| 50 | 5 - 36 % | 0.9882 | 0.003 | 0.8780 | 0.0018 | 0.8697 | 0.0014 | 0 - 36% | 11 |
| 60 | 10 - 77 % | 0.9790 | 0.013 | 0.9910 | 0.0031 | 0.9839 | 0.0028 | 0 - 77 | 10 |
| 70 | 10 - 99 % | 0.9891 | 0.040 | 0.9991 | 0.0071 | 0.9940 | 0.0063 | 0 - 99 | 10 |
| 75 | 10 - 90 % | 0.9981 | 0.044 | 0.9882 | 0.0096 | 0.9496 | 0.0063 | 0 - 98 | 9 |
| 80 | 0 - 95 % | 0.9736 | 0.075 | 0.9436 | 0.0144 | 0.8136 | 0.0058 | 0 - 99 | 9 |
| 100 | 0 - 90 % | 0.9240 | 0.150 | 0.8552 | 0.0367 | 0.8291 | 0.0125 | 0 - 99 | 7 |

Table 5.9.3.1 shows that the raw data shows a slightly better fit for first-order kinetics than the shrinking-core model over the same restricted range. If the full range is considered, (as is normal for the shrinking core model) the poorer fit of the shrinking-core model is emphasised. Both models fit reasonably well in the 60-70°C range. The first-order model fits the data slightly better at 50°C and 80-100°C than the shrinking-core model.

5.9.3.3. Model Fitting when Excluding Lag Time

Further analysis, considering the lag time (see Section 5.9.4) reinforced the conclusion that first-order kinetics gave a better fit than shrinking core. Table 5.9.3.2 shows the data with lag periods excluded.

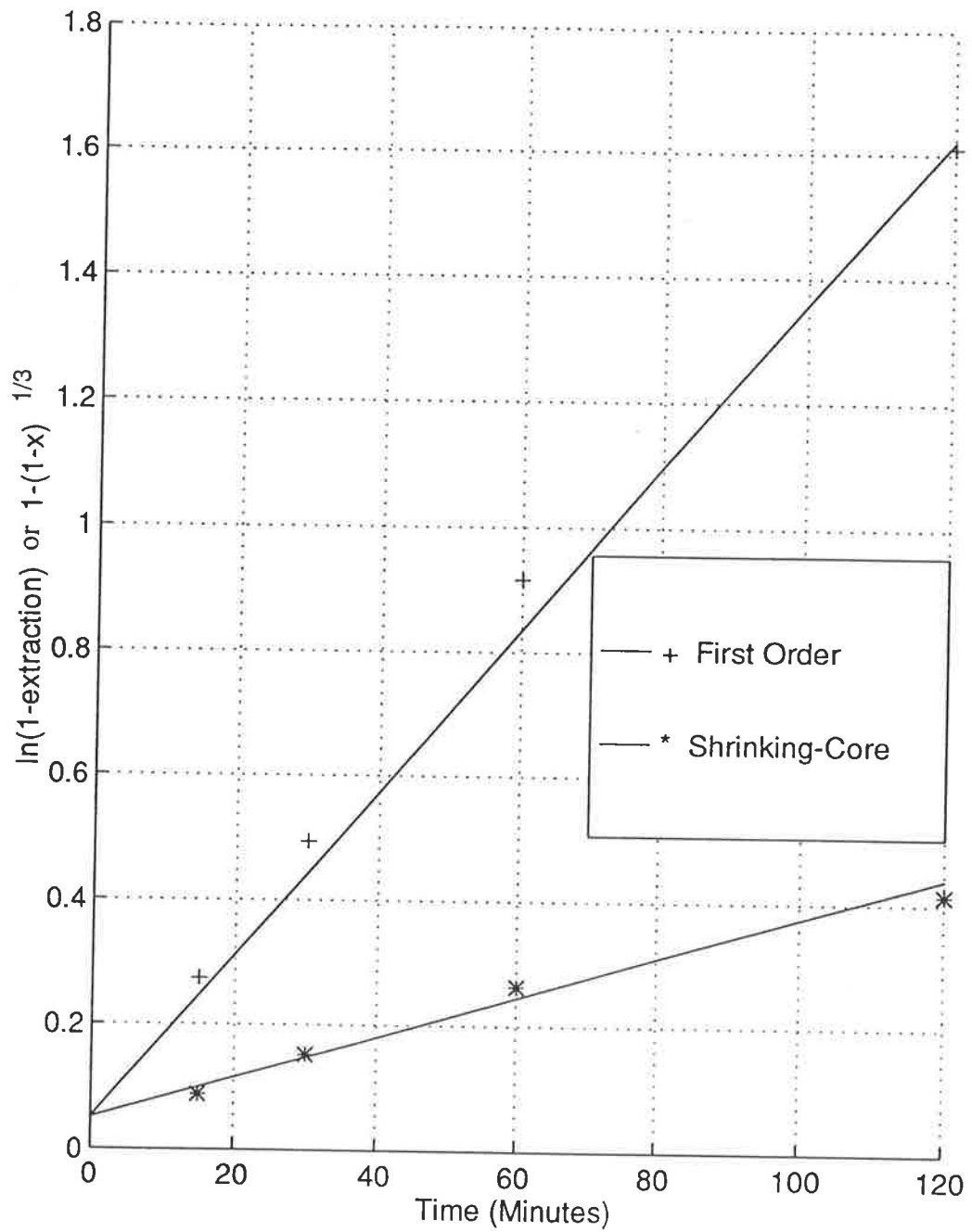


Figure 5.9.3.3 Fit of Data from Literature to Models

First-order model $r = 0.9967$

Shrinking-core model $r = 0.9870$

Kadioglu et al (1995), Artvin-Murgal 180-250 μm ,
70°C, 800 rpm, 2.4 M HNO_3

Table 5.9.3.2: Rate Constant Fitting for Temperature Series with Lag Periods Excluded

| Temp °C | Fe Extraction Range | Lag Time minutes @ a % | First-Order Model | | Shrinking-Core Model | |
|---------|---------------------|------------------------|-------------------|--------|----------------------|---------|
| | | | r | k | r | k |
| 50°C | 2 - 38% | 55 @ 10% | 0.9897 | 0.0039 | 0.9820 | 0.00075 |
| 60°C | 20 - 63 | 45 @ 19% | 0.9902 | 0.0114 | 0.9933 | 0.0032 |
| 70°C | 10 - 96 | 20 @ 10% | 0.9881 | 0.033 | 0.9790 | 0.0049 |
| 75°C | 10 - 85 | 3 @ 10% | 0.9983 | 0.039 | 0.9413 | 0.0093 |
| 80°C | 0 - 90 | 0 @ 0 | 0.9970 | 0.091 | 0.9208 | 0.011 |
| 100°C | 0 - 90 | 0 @ 0 | 0.9860 | 0.26 | 0.9398 | 0.0135 |

Normalised, ie $\left(x' = \frac{x - a}{100 - a}\right)$ where a is lag %

The normalised first-order rate constants of Table 5.9.3.2 were plotted against $1000/T^{\circ}k$ as before (Figure 5.9.2.1 page 153). This data gave $\ln k$ vs $1000/T$ with $r = 0.9914$ and $k = -10.28$. This was the best fit of a number of combinations attempted. The shrinking core model for the data with lag time removed gave a poor fit $r = 0.9140$ with slope -6.88 .

5.9.3.4 Model Fitting Data from Literature

Because the literature favours the shrinking core model, it was decided to plot some of the data from Kadioglu et al. (1995) to see whether it might also fit a first-order model. Figure 5.9.3.3 displays one of Kadioglu's tests on pyrite from Artvin-Murgul (Turkey) at 70°C, 800 rpm in 2.4 M HNO₃ (15%). The size range of this test was 180/250 μm and the pyrite had been ground in a ceramic ball mill. This particular test was selected as the closest to those conditions typical of the majority of the present work. The raw data is shown on Figure 5.8.6.1 (page 149).

It can be seen that this particular test actually fits a first-order curve slightly better than the shrinking-core model ($r = 0.9967$ vs $r = 0.9870$ respectively) although both could be said to fit well. The Turkish pyrite, moreover, did not display a lag period. This finding reinforces the point that some data will fit either model. The range of data encountered in the present work would seem to fit first-order kinetics best. Also there is evidence of a lag period, at least for Gumeracha pyrite, on which the majority of leach tests were performed. This lag period is dealt with in subsection 5.9.4.

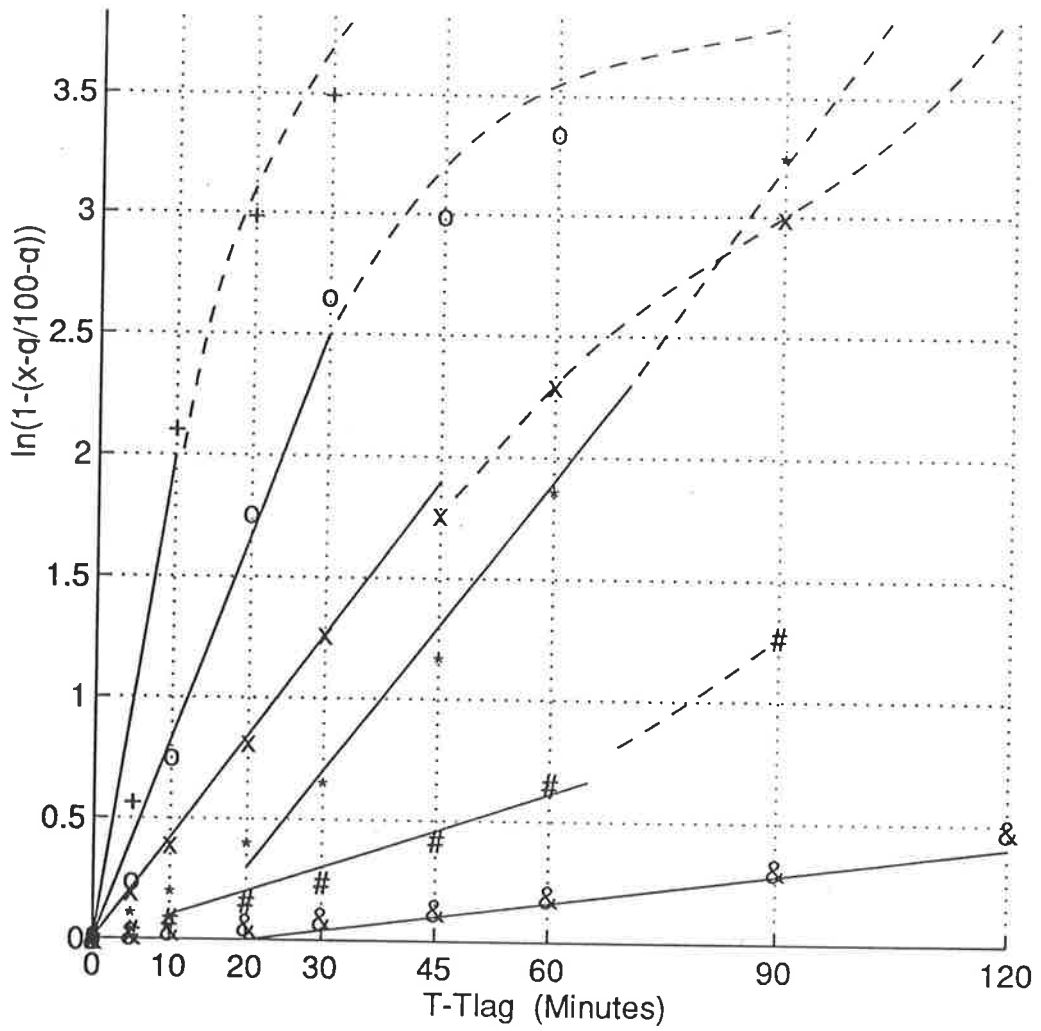


Figure 5.9.4.1: "Normalised" First-Order Temperature Series Data (Lag period removed)

Gumeracha Pyrite Temperature Series 90-125 μm , 2.6 MHNO_3 , < 250 rpm

Note: $-\ln(1 - \text{extraction}) = 2.0$ corresponds to 90-96% actual extraction

& - 50°C, # - 60°C, * - 70°C, x - 75°C, o - 80°C, + - 100°C

The first-order kinetic rate constants of Table 5.9.2.1 include the lag period and are considered to be the most representative for the tests conducted. If the pyrite's lag period is a function of a surface oxidation layer, then that layer is likely to exist on pyrite milled for refractory gold ores. The evidence suggests that if such a layer is responsible for lag time, the layer forms in hours or minutes. Oxygen in grinding mill pulps would be likely to form such a layer during grinding. Thus the rate constants of Table 5.9.2.1 are considered practical.

5.9.4 LAG PERIOD CONSIDERATION

5.9.4.1 Basis for Analysis

As described in Section 5.8, many of the Gumeracha tests display a marked lag period (Figure 5.8.5.1 page 147). Those tests tended to be the slower ones anyway - those with low temperatures, low acid strength or large grain sizes. They were dealt with by arbitrarily excluding from the first-order plots data which did not fit the straight-line portion of the curve - as in Figure 5.9.3.1. While this is accepted practice, it was considered worthwhile analysing the lag period on a more rigorous basis.

5.9.4.2 Gumeracha Temperature Series

The original leach curves were reviewed again and lag periods excluded entirely from the data which was then used to calculate first-order correspondence. This data was 'normalised' - that is the portions of the pyrite which reacted during the lag period were removed from the analysis. Thus, for Figure 5.9.4.1 $\ln(1 - x')$ is plotted against time, where $x' = \frac{x - a}{1.00 - a}$ and a is the fraction of pyrite dissolved at the end of the lag period. The time plotted was $t' = t - \text{lag time}$.

Table 5.9.4.1 gives the statistical data for Figure 5.9.4.1

Table 5.9.4.1: Gumeracha Pyrite Temperature Series

| Temp °C | r | k | n | Range % Fe Extraction | Lag period Min |
|---------|--------|--------|---|-----------------------|----------------|
| 50°C | 0.9897 | 0.0039 | 8 | 2 - 38% | 55 |
| 60°C | 0.9902 | 0.0114 | 5 | 19 - 63% | 45 |
| 70°C | 0.9881 | 0.0332 | 5 | 10 - 96% | 20 |
| 75°C | 0.9983 | 0.0393 | 7 | 10 - 85% | 3 |
| 80°C | 0.9970 | 0.091 | 5 | 0 - 90% | 0 |
| 100°C | 0.9860 | 0.26 | 4 | 0 - 90% | 0 |

When plotted ($\ln k$ vs $1000/T$) similarly to Figure 5.9.2.1, the data from Table 5.9.4.1 gives an improved fit. These results are compared in Table 5.9.4.2 below.

Table 5.9.4.2: Arrhenius Plot Fitting - Gumeracha Temperature Series

| Statistical parameters | Data with lag time excluded (Table 5.9.4.1) | Data with lag time not excluded (Table 5.9.2.1) |
|------------------------|--|--|
| n= | 6 | 6 |
| r= | 0.9914 | 0.9644 |
| k= | - 10.3 | - 9.2 |

5.9.4.3 Gumeracha Iron Series

Original data for this series was treated in the same fashion, as for 5.9.4.2. Results are given in Table 5.9.4.3.

Table 5.9.4.3: Statistical Data For Gumeracha [Fe^{3+}] Series

(based on Iron Extractions)

| [Fe^{3+}] Molar | r | k | n | Range Fe extraction | Lag period (mins) |
|-------------------------------|--------|-------|---|------------------------|----------------------|
| 0 | 0.9993 | 0.023 | 9 | 12 - 97% | 10 |
| 10^{-3} | 0.9981 | 0.025 | 8 | 12 - 95% | 17 |
| 10^{-2} | 0.9985 | 0.029 | 8 | 10 - 94% | 7 |
| 10^{-1} | 0.9838 | 0.030 | 8 | 10 - 94% | 4 |
| 2×10^{-1} | 0.9954 | 0.053 | 5 | 10 - 80% | 2 |

When this data is compared to Table 5.9.2.1 (which does not exclude lag time) it can be seen that the main effect of the normalising calculation is to widen the range over which the first-order rate constant applies. The model fit is still very good. The rate constants increase because the 'normalised' extraction figures are effectively 11% higher, with $a = 0.10$ or 0.12 for Table 5.9.4.3.

5.9.4.4 Causes and Ramifications of Lag Time

The data from Table 5.9.4.3 was used to estimate the extent to which iron might be autocatalytic in pyrite oxidation. Most lag periods appear to be completed at about 10% iron extraction. At this point the solution in the leach vessel would be 0.093 gl^{-1} or about $1.7 \times 10^{-3} \text{ M}$ in Fe^{3+} . According to the values on Table 5.9.4.3 the first-order rate constant should be increased by about $0.026/0.023$ or about 13% due to that concentration of ferric ion.

Two tests which showed the lag period very clearly are examined more closely in Table 5.9.4.4. Their lag periods are described in terms of a succession of first-order rate constants.

Table 5.9.4.4: Lag Period Described as Changing Rate Constant

| Test S-15 Gumeracha Pyrite 180/250 μm @ 75°C | | | Test S-64 Gumeracha Pyrite 125/180 μm @ 75°C | | |
|--|---------------|------------------------|--|---------------|------------------------|
| Time (min) | Fe Extraction | k (min ⁻¹) | Time (min) | Fe Extraction | k (min ⁻¹) |
| 0 - 15 | 0 - 5% | 0.00064 | 0 - 25 | 0 - 13% | 0.0057 |
| 15 - 30 | 5 - 10% | 0.0051 | | | |
| 15 - 30 | 10 - 22% | 0.0086 | 25 - 65 | 13 - 54% | 0.0165 |
| 30 - 110 | 22 - 74% | 0.0092 | > 65 | 54 - 90% | 0.031 |
| > 110 | 74 - 93% | 0.0164 | | | |

The increase for S-15 (at about 10% extraction is 0.0086-0.0051/0.0051 or about 70%. The increase for S-64 at about 10% extraction is 0.0105 - 0.0057/0.0057 or about 190%. Since the ferric ion present at 10% extraction could only account for about a 13% increase in rate constant, ferric ion is not the main reason for the increase in rate.

No attempt has been made to quantify the increase in surface area of the pyrite as it oxidises.

The analyses excluding lag period are encouraging for modelling purposes and theoretical understanding. While there is certainly scope for more rigorous analysis of the remaining experimental data, it has not been attempted. It is felt that the data including the lag period is more likely to be realistic in practice.

5.9.5 VARIATION OF PYRITE WITH SOURCE

While the majority of the leach testwork, and all the electrochemical tests, were performed using Gumeracha pyrite, it is worthwhile analysing the data to compare pyrites. Gumeracha pyrite (South Australia) contained 1.5% impurities, while that sourced from Huanzala contained 0.5%. The data for the Artvin-Murgul (Turkey) pyrite (Kadioglu et al. 1995) was compared as well. This material was stated to be 98% FeS₂.

The data from Figure 5.9.3.3 was used to give a first-order rate constant for one test on the Turkish pyrite. This run was the one closest to the conditions of much of the present work, being run on 180/250 μm pyrite at 70°C, 800 rpm in 2.4 M

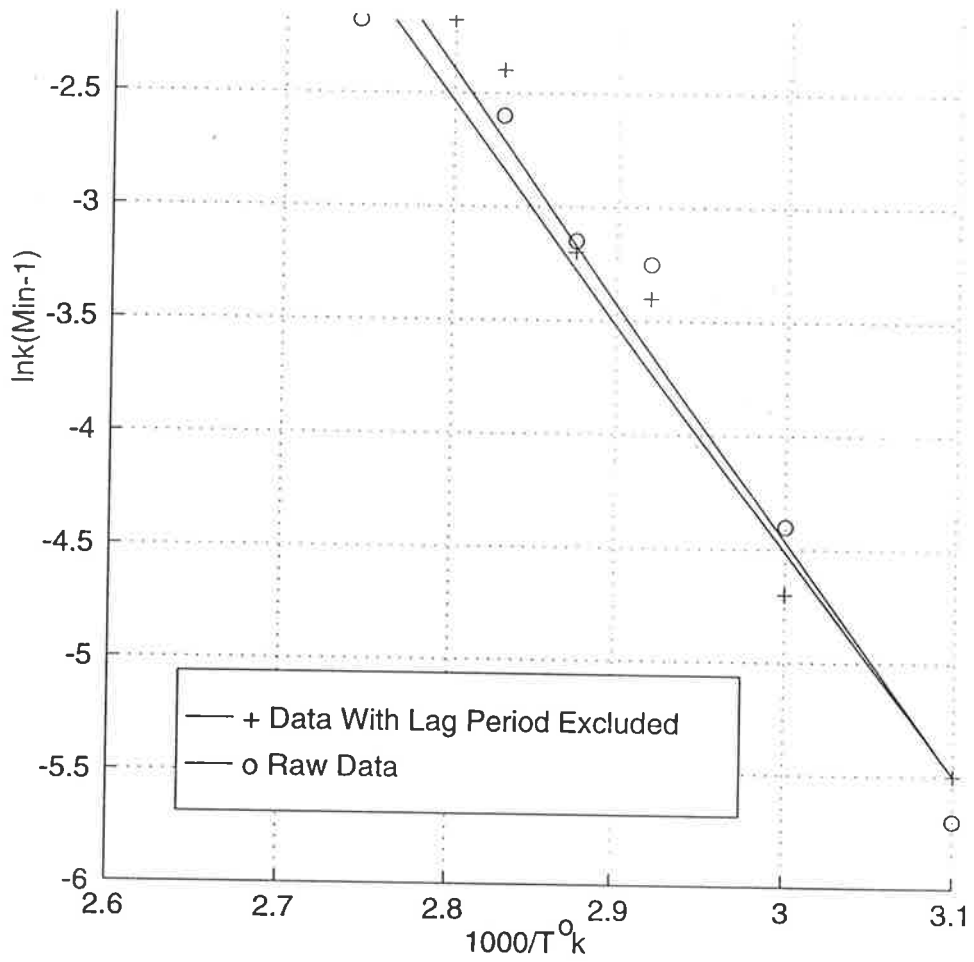


Figure 5.9.6.1 Arrhenius Plots for Gumeracha Pyrite
 Gumeracha Pyrite 90 - 125 μm , 2.6 MHNO₃ < 250 rpm

HNO₃. For Table 5.9.5.1 test S-15 (Gumeracha pyrite, 180/250µm, 80°C, 2.6 M HNO₃, 280 rpm) was adjusted mathematically. The experimental rate constant was adjusted downwards for 10°C and 0.2 M HNO₃ using the relationships in 5.9.2. The data from test S-65 (Huanzala pyrite, 125/180µm, 80°C, 2.6 M HNO₃, 280 rpm) was adjusted as well. The experimental rate constant was reduced for 10°C, for 0.2 M HNO₃, and for one screen fraction. Thus all rate constants are first-order adjusted to the same conditions of the Turkish test. It was not possible to adjust for the different reactors or stirring speeds.

Data is given in Table 5.9.5.1 with and without exclusion of the lag period. Huanzala pyrite generally showed a much smaller lag period than Gumeracha pyrite. While the data for the Artvin-Mugul pyrite only started at 15 minutes, there did not appear to be a lag period.

Table 5.9.5.1: Comparison of Pyrite Sources

| Source | Lag Period included in data | | Lag Period excluded | |
|---------------|-----------------------------|---------------------|------------------------|---------------------|
| | k(min ⁻¹) | Range Fe Extraction | k (min ⁻¹) | Range Fe Extraction |
| Gumeracha | 0.0093 | 10 - 85% | 0.014 | 24 - 90% |
| Huanzala | 0.015 | 9 - 99% | 0.016 | 20 - 90% |
| Artvin-Murgul | 0.013 | 0 - 80% | 0.013? | 23 - 80% |

All values adjust to 180/250 µm, 70°C, 2.4 Molar HNO₃

It is clear from Table 5.9.3.3 that the main difference between the three pyrites is the lag period. The k values with lag periods excluded all fall within 20%.

5.9.6 CALCULATION OF ACTIVATION ENERGIES

5.9.6.1 Data Source

The data used was the Gumeracha temperature series, as plotted on Figure 5.9.2.1. Added to it is the data for the same series, but with the lag period excluded and the data 'normalised' as per Figure 5.9.4.1. These give two Arrhenius plots on Figure 5.9.6.1 (opposite). Huanzala data was not plotted as the only temperature range tests for Huanzala had not been deslimed.

5.9.6.2 Calculation

The two sets of data give very similar lines although the data fit is improved by excluding the lag period. The slope of the raw data line of best fit is -9.2×10^{-3} (K^{-1}); that with the lag period excluded is -10.3×10^{-3} (K^{-1}).

Since R , the gas constant, is $8.314 \text{ J g-mole}^{-1} \text{ K}^{-1}$ and $-\frac{E_{\text{activation}}}{R} = \text{slope of Arrhenius plot (Hiller and Herber 1960)}$

Then for the raw data

$$\frac{-E_{\text{act}}}{8.314} = -9.2 \times 10^3$$

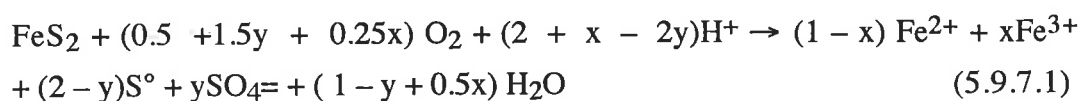
$$E_{\text{act}} = 77 \text{ kJ mol}^{-1}$$

This value is probably more realistic, based as it is on the data included the lag periods. This is the rate reported previously (Flatt, and O'Neill, 1995). The data with the lag periods excluded gives 86 kJ mol^{-1} . The literature reports a range of values (see Table 5.2.3.1) for a variety of mediums. The reported range (Hiskey and Schlitt, 1982) is 39.6 to 83.7 kJ mol^{-1} . Kadioglu et al (1985) reported two values 52 kJ mol^{-1} for 3.8 M HNO_3 and $25\text{-}28 \text{ kJ mol}^{-1}$ for 1.6 M HNO_3 .

5.9.7 OXIDATION RATE OF ELEMENTAL SULFUR

5.9.7.1 Background Chemistry

It may be worth reviewing the reactions taking place which yield the experimental leach curves. As originally noted in Chapter 4, pyrite reacts to form both sulfate (directly) and elemental sulfur, as well as ferric ion. Bailey and Peters (1976) gave the best single equation for this as:



Although under the conditions of the present leach tests no Fe^{2+} (Equation 5.9.7.1) is produced, this is still a cumbersome equation. It is convenient to consider a series of related partial reactions.

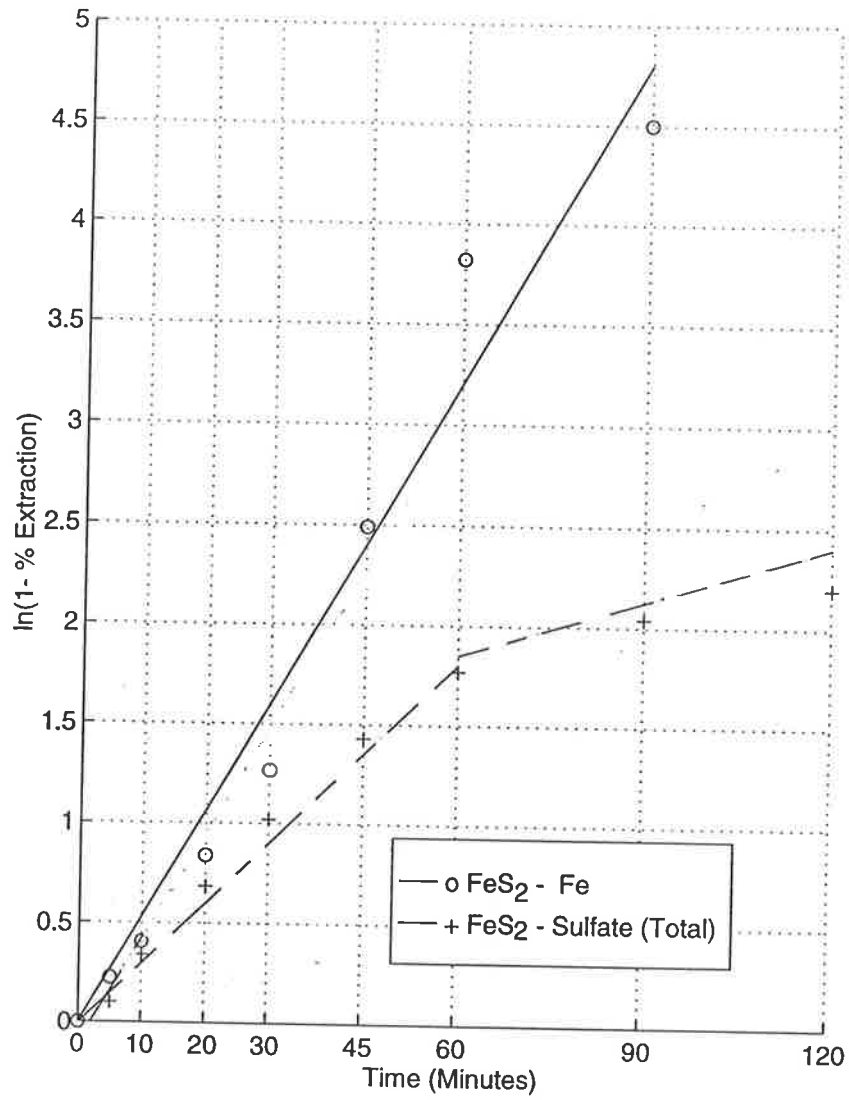


Figure 5.9.7.1: Iron and Sulfate First-Order Plots
 (S-20 + S-32 combined)
 Gumeracha Pyrite, 90-125 μm , 80°C, 280 rpm, 2.6 MHNO_3

| | <u>Partial Reaction</u> | <u>First Order Rate Constant</u> |
|----|---|----------------------------------|
| a) | $\text{FeS}_2 \rightarrow \text{Fe}^{3+}$ | k_a |
| b) | $\text{FeS}_2 \rightarrow \text{SO}_4^{\text{=direct}}$ | k_b |
| c) | $\text{FeS}_2 \rightarrow \text{S}^\circ$ | k_c |

The amount of Fe^{3+} produced must equal the sum of b) + c) but the quantification of the relative rates of b) and c) is one object of this investigation. Further, the elemental sulfur can react to sulfate as well. The total amount of sulfate present can be quantified as that produced directly from pyrite plus that produced from sulfur oxidation.

| | <u>Partial Reaction</u> | <u>Rate Constant</u> | |
|----|--|----------------------|---------|
| d) | $\text{S}^\circ \rightarrow \text{SO}_4^{\text{=}} \text{ from } \text{S}^\circ$ | k_d | |
| e) | $\text{S}^\circ + \text{FeS}_2 \rightarrow \text{SO}_4^{\text{=Total}}$ | k_e | 5.9.7.2 |

Two practicalities are evident. All that are measurable with this experimental method are the total sulfate present and the total iron in solution at a given time. Secondly, in the absence of a mechanism, there is no firm way of relating the rates of a) to b) since oxygen uptake was not measured.

The result of these practicalities is that the proportion of elemental sulfur formed, plus its rate of oxidation to sulfate, are indeterminate. Some speculation may be made however, hopefully intelligently. Such speculation is the subject of the remainder of Subsection 5.9.7.

5.9.7.2 Data Selection

The data selection for this part of the study was that for which the most sulfate analyses were available. As mentioned previously, financial constraints restricted sulfate analyses to three or four per leach test, while nine or ten iron analyses per test were performed. Four data sets were selected for analysis of elemental sulfur oxidation rate. Two of these sets were combinations of tests which had been done as duplicates to check possible aging of the pyrite.

The Fe^{3+} and $\text{SO}_4^{\text{=Total}}$ extraction data for these data sets were analysed as first-order plots. A typical results is given in Figure 5.9.7.1.

The outstanding feature of Figure 5.9.7.1 is the sharp change in the sulfate production rate slope at $t = 60$ minutes. Both segments of the sulfate rate plot show

Table 5.9.7.1: First-Order Plot Results (Lag Periods Excluded)

| Data Set | Conditions | First Segment | Second Segment |
|-------------------------|---|---|---|
| S-(20 + 32) Combined | Gumeracha 90/125 μ m 80°C 2.6 M HNO ₃ 280 rpm | Fe: $k_a = 0.053$ $r = 0.9844$ valid 10 - 98% Fe SO ₄ ^{=total} $k_e = 0.033$ $r = 0.9974$ valid 7 - 84% SO ₄ ⁼ | $k_a = 0.048$ $r = 0.9306$ 92 -- 100% Fe $k_d = 0.007$ $r = 0.9892$ valid 84 - 90% SO ₄ ⁼ |
| S-4 | Gumeracha 90/125 μ m 75°C 2.6 M HNO ₃ 72 rpm | Fe: $k_a = 0.086$ $r = 0.9567$ valid 10 - 99% Fe SO ₄ ^{=total} $k_e = 0.070$ $r = 0.9985$ valid 10 - 82% SO ₄ ⁼ | none discerned $k_d = 0.0125$ $r = 0.9997$ valid 86 - 95% SO ₄ ⁼ |
| S-48 | Gumeracha 125/180 μ m 80°C 2.6 M HNO ₃ 280 rpm | Fe: $k_a = 0.023$ $r = 0.9985$ valid 10 - 95% Fe SO ₄ ^{=total} $k_e = 0.015$ $r = 0.9984$ valid 8 - 84% SO ₄ ⁼ | none discerned none discerned |
| S-(16 + 64) Combined | Gumeracha 125/180 μ m 75°C 2.6 M HNO ₃ 280 rpm | Fe: $k_a = 0.0211$ $r = 0.9817$ valid 15 - 80% Fe SO ₄ ^{=total} $k_e = 0.0186$ $r = 0.9971$ valid 10 - 83% SO ₄ ⁼ | $k_a = 0.051$ $r = 0.9954$ valid 69 - 99% Fe $k_e = 0.017$ $r = 0.9996$ valid 83 - 94% SO ₄ ⁼ (debatable) |

reasonable first-order correlation. ($r = 0.9974$, $n = 6$ for 60 minutes and below, and $r = 0.9892$, $n = 3$ for 60 minutes and above.) All four data sets showed some inflection in the curves, all at about the same point (see Table 5.9.7.1). There is an additional indication for this in the experimental observations typified by run S-32 in Table 5.5.1.1. (page 117) of this thesis. It is at the inflection point that the solid floccs change colour to yellow. Iron extraction was 98% for S-32, sulfate extraction was 84%. Combined, these findings indicate that at this point, the pyrite is virtually all reacted. The first segment of the curve results from sulfate being produced by the oxidation of both pyrite and sulfur. The second segment must be due to sulfur alone oxidising. Accordingly, the slope of the second segment of the plot should be the rate constant for the oxidation of elemental sulfur alone. This change in first-order slope is masked for some leach tests. When pyrite oxidation is slow it masks the change to predominantly sulfur oxidation. The slope change tends to show more clearly for faster tests. In the fastest test conducted (S-79 Additive Effects) the iron was all oxidised in four minutes. The sulfate was 80% extracted in five minutes. However the 20% remaining sulfur, which must have been in the elemental form, required an additional seventy minutes to oxidise completely.

Table 5.9.7.1 shows the data for the first-order plots for the four data sets selected. In most cases, sulfate oxidation did not reach 100%.

5.9.7.3 Modelling

It is recognised that there are dangers in too much manipulation of data. It may be difficult to discern whether problems observed originate from genuine phenomena or from the manipulation. The literature is of little help in providing a possible mechanism for pyrite oxidation, as already noted. Parametric modelling is common for leaching systems, for example, see Frazer and Zachariades. The present work is, therefore, restricted to a parametric approach.

Results of parametric modelling were checked constantly against the original leach curves. The entire original curve was considered for S-4 and gave a fairly good ($r = 0.9952$) correlation to first-order kinetics. However, when the derived rate constant was used in a first-order model ($e^{-kat} = (1 - \text{extraction})$) the model showed poor fit with the original curve. Earlier work on a range of leach curves had shown that the lag period was not linear with the main curve, particularly for slower tests. Accordingly for all work on modelling, data with the lag period excluded was employed. Resulting models were still compared with the complete original curves, however.

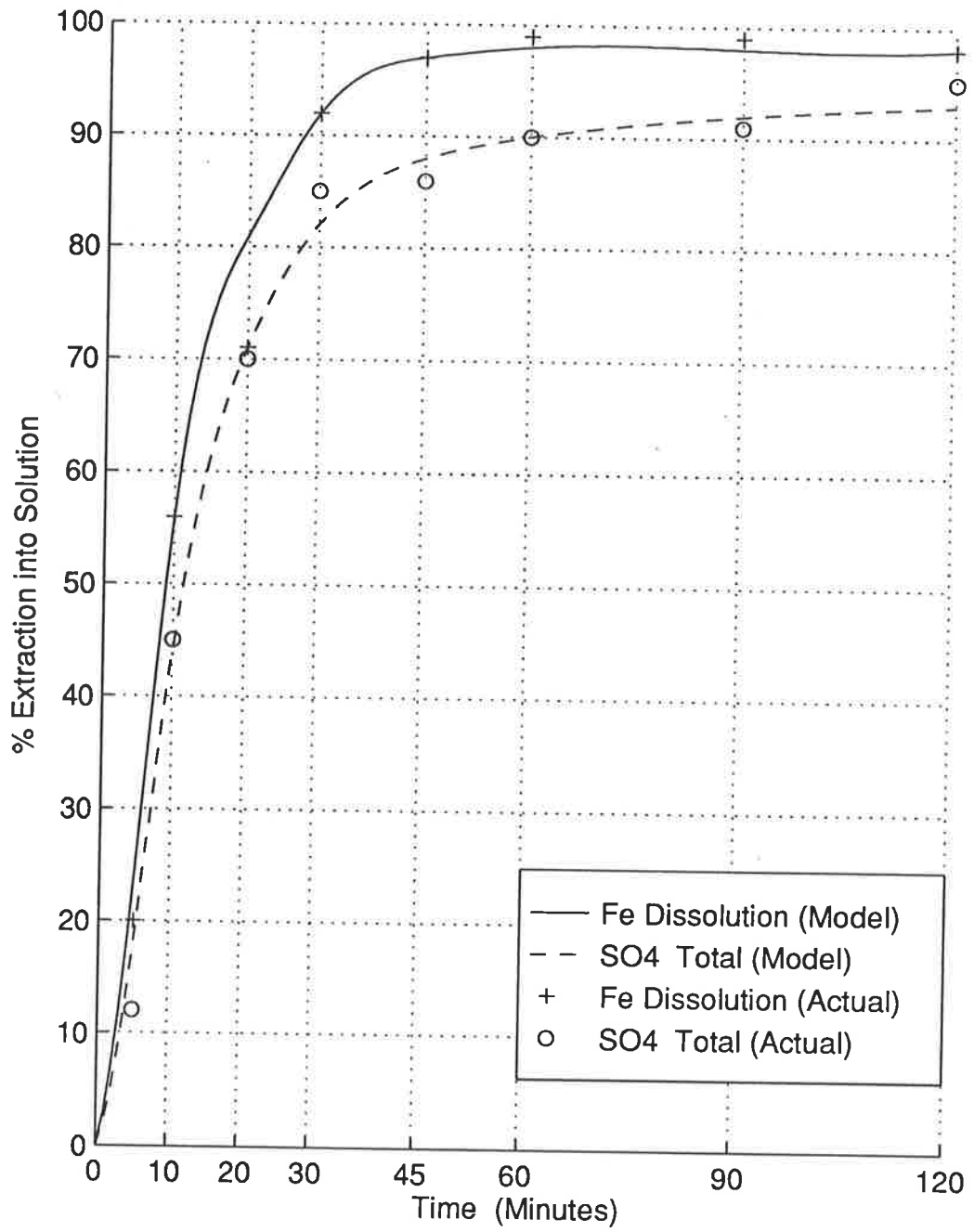


Figure 5.9.7.2 Iron and Sulfate Extraction Plots (S-4)
 Gumeracha Pyrite 90-125 μ m, 80°C, 72 rpm, 2.6 MHNO₃

Figure 5.9.7.2. shows a comparison of a model for test S-4 with the original data. For the model, the iron extractions were calculated from $e^{-0.086t}$ and the sulfate (total) extractions were calculated from $e^{-0.070t}$. Lag periods, plotted from experimental data rather than the model, were 4 minutes at 10% extraction for Fe and 5 minutes at 10% extraction for sulfate (total). In some cases, the lag periods were adjusted, from the values originally chosen by eye, to those values indicated by the zero extraction intersection of the best-fit first-order rate plots.

5.9.7.4 Bases for Sulfur Oxidation Rate Calculations

It was considered that the models were a valid basis for further calculations. These calculations attempt to quantify the reaction rates for sulfur production and oxidation. While it is recognised that the solution is indeterminate, there are some good indications as to what a reasonable speculation might be.

According to the results of the linear sweep voltammetry, an Eh of 1.17 volts should result in an elemental sulfur yield of 10-20% from pyrite oxidation (see Figure 4.6.4.3 page 76). There is strong evidence that the Eh measurements of the leach tests were high due to electrode instability at 80°C, 2.6 N acid. Although the data is not conclusive, there is an indication that a more accurate Eh figure for 2.6 M HNO₃ would be about 1.07 volts (SHE) compared to the impressed voltage of the electrochemical tests. This lower figure would, in turn, suggest 18-30% S⁰ from Figure 4.6.4.3.

Second, there is the inflection in the first-order sulfate curve. This inflection point was first noted in 5.9.7.2. It occurs consistently in the region of 84% sulfate extraction. If a low rate of elemental sulfur oxidation were expected, 84% total sulfate extraction would fit well with 20% elemental sulfur formation plus 4% elemental sulfur oxidation. Table 5.9.7.2 indicates the consistency of this pattern of inflection points.

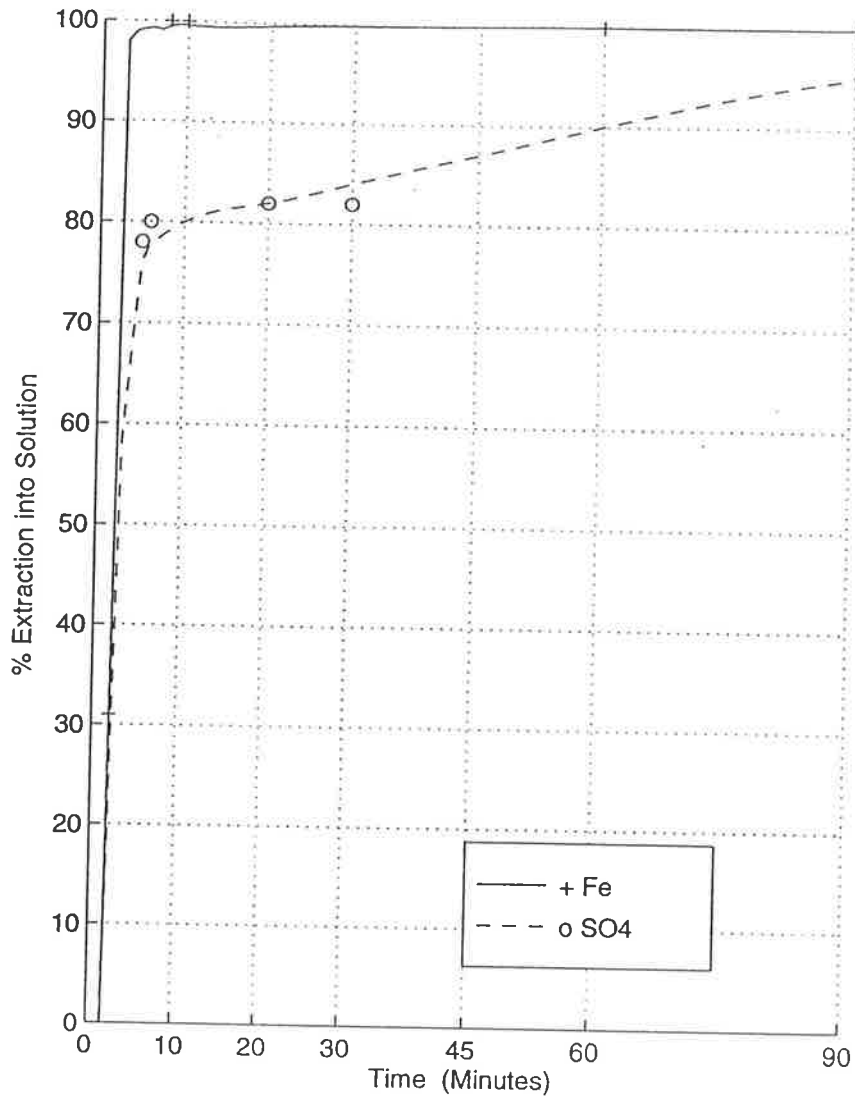


Figure 5.9.7.3: Leach Test for Additive Factors
 S-79 Gumeracha Pyrite, 63-90 μm , 90°C, 3.5 MHNO_3 ,
 2.0 MH_2SO_4 , Attritioning

| Data Set | S(20 + 32) | S-4 | S-48 | S(16 + 64) |
|--|---|-----|------|------------|
| Inflection point (last point on lower segment) | SO ₄ ⁻ total 84% | 86% | 84% | 83% |
| | Fe ³⁺ 98% | 93% | 94% | 91% |
| Change in colour of flocs to yellow at this point | | | | |
| Second point on upper segment | SO ₄ ⁻ total 88% | 89% | 91% | 90% |
| | Fe ³⁺ 99% | 97% | 97% | 98% |

Table 5.9.7.2: Inflection Point Data-Extractions (From First- Order Rate Plots)

Figure 5.9.7.1 (page 167) may be consulted as a typical example.

Third there is the evidence of test S-79, cited earlier. It is presented as Figure 5.9.7.3. The first-order plot (not shown) of this test gives a k_e value for total sulfate extraction of 0.34 min^{-1} . The second part of the sulfate plot has a slope (k_d) of 0.018 min^{-1} . This test had extremely fast rate of iron oxidation. If the sulfur oxidation rate is comparatively slow, the point at which the pyrite disappears might be expected to correspond very nearly to the total amount of elemental sulfur formed. And the inflection point for test S-79?. It is at 80% sulfate, 20% elemental sulfur.

Considering the evidence of the electrochemical tests, the known inaccuracy of leach test Eh measurements, the inflection points in the first-order sulfate curves, and test S-79, a figure of 20% elemental sulfur formation was decided upon for 2.6 M HNO₃. If it is granted that 20% S⁰ is a reasonable proportion of elemental sulfur formation at 2.6 M HNO₃, values for the oxidation rate of the elemental sulfur can be calculated.

The approach taken for this work was to assume 20% S⁰ formation and use k_d values, (first-order rate constants for S⁰ → SO₄⁼) from the inflection point data of Table 5.9.7.1. The total sulfate leach curves can then be simulated from the models. If these simulated curves approximate the experimental curves, that supports the assumptions. A typical calculation follows.

5.9.7.5 Typical Calculation - S⁰ Oxidation

The model for test S-4 has already been displayed as Figure 5.9.7.2 (Page 169) From the iron curve of the model, the extraction values from pyrite for sulfate and

sulfur were calculated. The value for k_d used was 0.0125 min^{-1} from Table 5.9.7.1.

At $t = 60 \text{ mins}$ Fe extraction (Model) = 0.99 (as a fraction)
 ($t' = t - t_{lag} = 56 \text{ mins}$) SO_4^- direct = $0.8 \times 0.99 = 0.792$ reaction b)
 $\text{S}^0 = 0.2 \times 0.99 = 0.198$ reaction c)

(These are cumulative values)

Time interval = 15 mins (since last sample)

$$d \frac{\text{S}^0 \rightarrow \text{SO}_4^-}{d t} = k_d \times (\text{S}^0 \text{ present})$$

S^0 present at start of period = 0.128

S^0 formed during period = 0.004

$\text{S}^0 \rightarrow \text{SO}_4^-$ oxidation:

from that already present $0.128 \times 0.0125 \times 15 = 0.0241$

from that formed this period $\frac{0.004 \times 0.0125}{2} \times 15 = 0.004$

Total $\text{S}^0 \rightarrow \text{SO}_4^-$ This period $0.004 + 0.0241 = 0.0245$

Total sulfate present at end of period

= $\text{S}^0 \rightarrow \text{SO}_4^-$ this period + cumulative $\text{S}^0 \rightarrow \text{SO}_4^-$ + cumulative Fe $\text{S}^0 \rightarrow \text{SO}_4^-$

= $0.0245 + 0.0656 + 0.792 = 0.882$ (model)

Sulfur gap at end of period (Model)

= $0.99 - 0.802 = 0.108$

Check values against original graph (Figure 5.4.3.1 Page 113)

| at $t = 60 \text{ mins}$ | Original graph | Calculation above |
|--------------------------|----------------|-------------------|
| Total sulfate present | 0.90 | 0.882 |
| Sulfur gap | 0.08 | 0.108 |

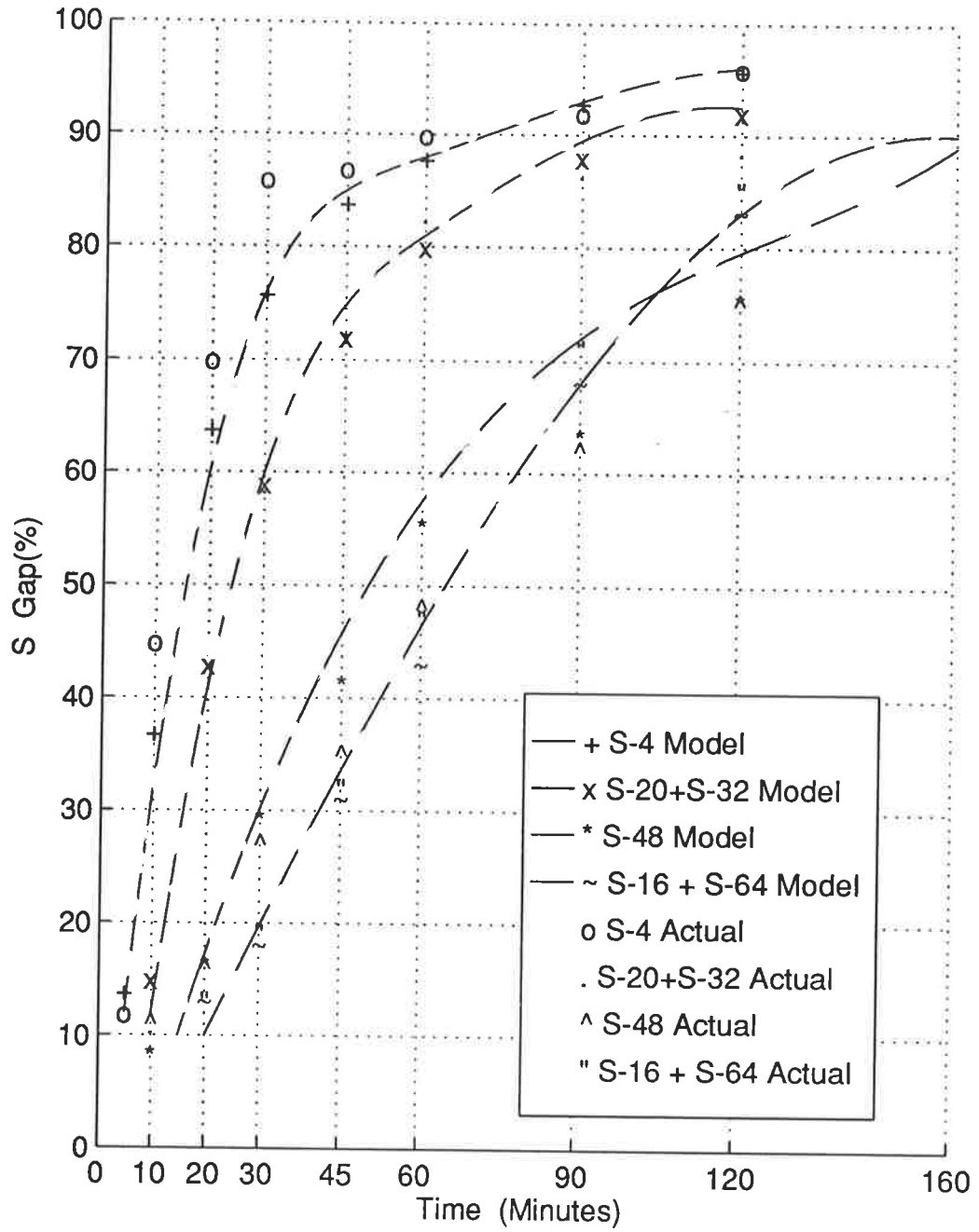


Figure 5.9.7.4 Sulfate Curves - Model vs Actual

See Table 5.9.7.3. (opposite) for data

5.9.7.6. Results

Table 5.9.7.3 shows the calculated first-order rate constants for the four data sets. Also shown are the regression coefficients for the best-fit first-rate linear plots. This data is based on the models.

Table 5.9.7.3. Rate Constants for Oxidation Reactions

| Data Set | Partial Reaction | Constant (min ⁻¹) | Correlation Coefficient (r) | k Relative to Range |
|---|--|-------------------------------|-----------------------------|--|
| S(20 + 32) 90/125 μm 80°C 280 rpm | a) FeS ₂ → Fe ³⁺ | 0.053 | 0.9974 | FeS ₂ 10-99% Fe ³⁺ |
| | b) FeS ₂ → SO ₄ ⁼ | 0.054 | 0.9845 | 0.8 Fe ³⁺ 10-99% Fe ³⁺ |
| | c) FeS ₂ → S ⁰ | 0.054 | 0.9994 | 0.2 Fe ³⁺ 10-99% Fe ³⁺ |
| | d) S ⁰ → SO ₄ ⁼ | 0.007 | 0.9886 | 20% S ⁰ 10-99% Fe ³⁺ |
| S4 90/125 μm 75°C 72 rpm | a) FeS ₂ → Fe ³⁺ | 0.086 | 0.9967 | FeS ₂ 10-99% Fe ³⁺ |
| | b) FeS ₂ → SO ₄ ⁼ | 0.084 | 0.9943 | 0.8 Fe ³⁺ 8-98% Fe ³⁺ |
| | c) FeS ₂ → S ⁰ | 0.084 | 0.9943 | 0.2 Fe ³⁺ 8-98% Fe ³⁺ |
| | d) S ⁰ → SO ₄ ⁼ | 0.0125 | 0.9997 | 20% S ⁰ 0-20% S ⁰ |
| S-48 125/180 μm 80°C 280 rpm | a) FeS ₂ → Fe ³⁺ | 0.023 | 0.9985 | FeS ₂ 15-94% Fe ³⁺ |
| | b) FeS ₂ → SO ₄ ⁼ | 0.0234 | 0.9998 | 0.8 Fe ³⁺ 15-94% Fe ³⁺ |
| | c) FeS ₂ → S ⁰ | 0.0234 | 0.9998 | 0.2 Fe ³⁺ 15-94% Fe ³⁺ |
| | d) S ⁰ → SO ₄ ⁼ | 0.007 | not calculated | 20% S ⁰ 0 - 20% S ⁰ |
| S(16 + 64) 125/180 μm 75°C 280 rpm | a) FeS ₂ → Fe ³⁺ | 0.0211 | 0.9817 | FeS ₂ 15-80% Fe ³⁺ |
| | b) FeS ₂ → SO ₄ ⁼ | 0.021 | not calculated | not calculated |
| | c) FeS ₂ → S ⁰ | 0.021 | not calculated | not calculated |
| | d) S ⁰ → SO ₄ ⁼ | 0.007 | not calculated | not calculated |

The correlation coefficients of Table 5.9.7.3 serve to check only the internal consistency of calculations, as they are based on the model. In the two figures following, calculated results are compared to the original leach test data. Figure 5.9.7.4 compares the original sulfate extraction curves for four data sets to the sulfate curves built up from the model. These latter are calculated from reactions b) FeS₂ → SO₄⁼ direct plus d) S⁰ → SO₄⁼. Figure 5.9.7.5 compares the original data for the 'sulfur gap' (which is the difference between the ferric iron curve and the total sulfate curve) to the calculated results from the models. In this case sulfate from reactions (b) plus d)) were subtracted from reaction (a) FeS₂ → Fe³⁺.

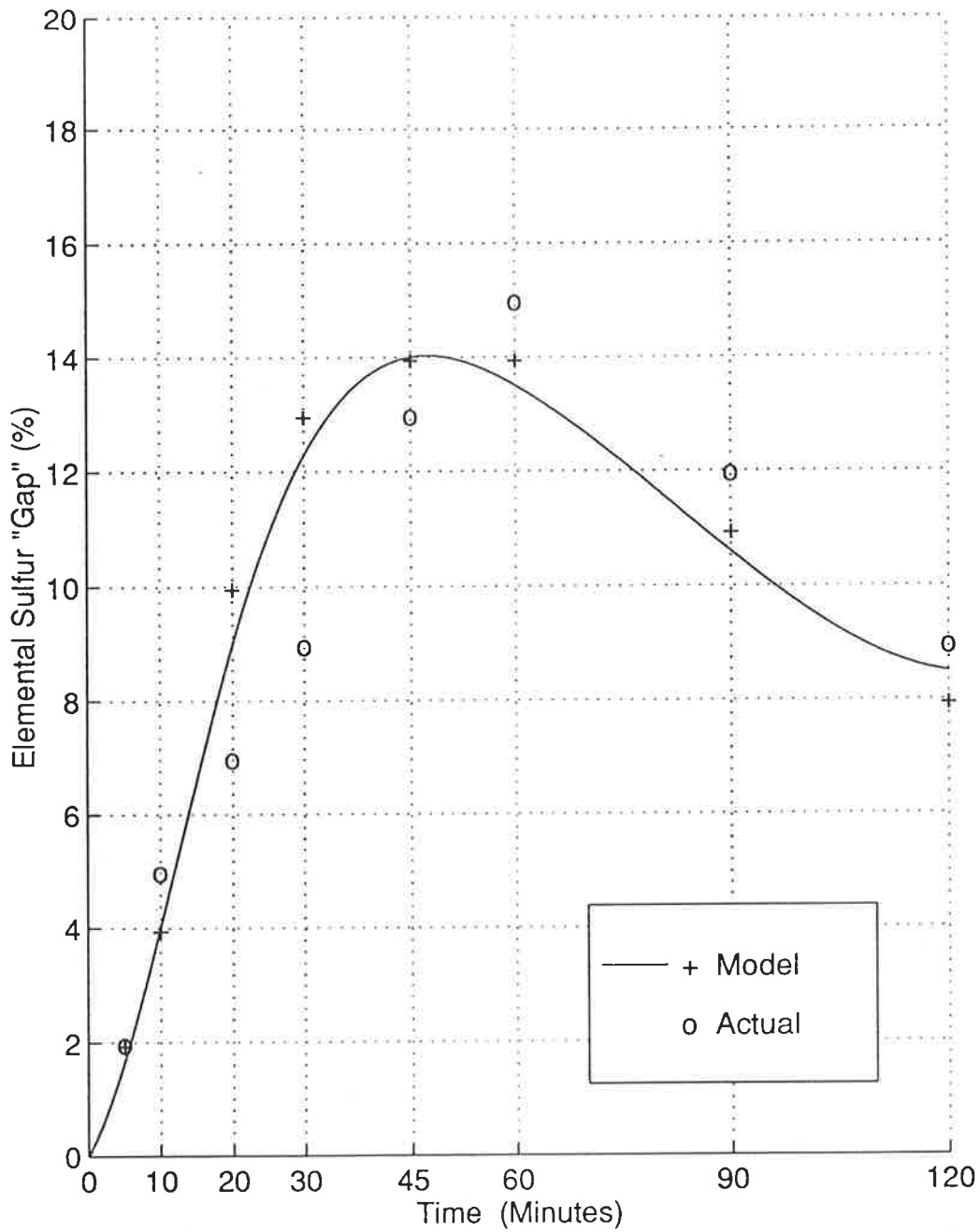


Figure 5.9.7.5 a)

Sulfur Gap Model Compared to Actual Results

S^0 gap model from S^0 proportions and K_d for $S^0 \rightarrow SO_4^{=}$)

S^0 gap measured as Fe^{3+} minus $SO_4^{=}$ total

S-(20 + 32) Gumeracha Pyrite 90-125 μm , 80°C, 280 rpm, 2.6 M HNO_3

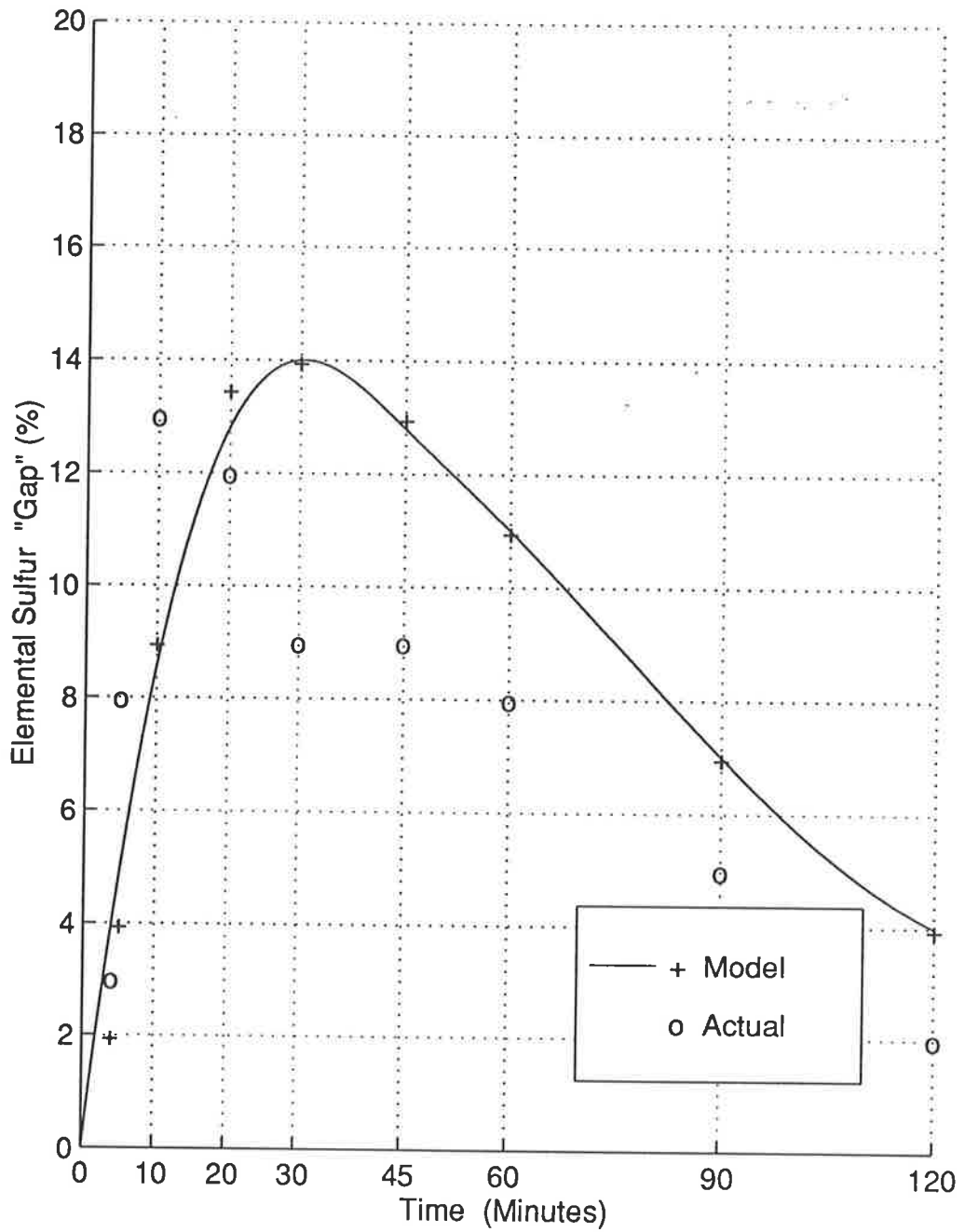


Figure 5.9.7.5 b)

Sulfur Gap Model Compared to Actual Results

S-4 Gumeracha Pyrite, 90-125 μm , 80°C, 72 rpm, 2.6 M HNO_3

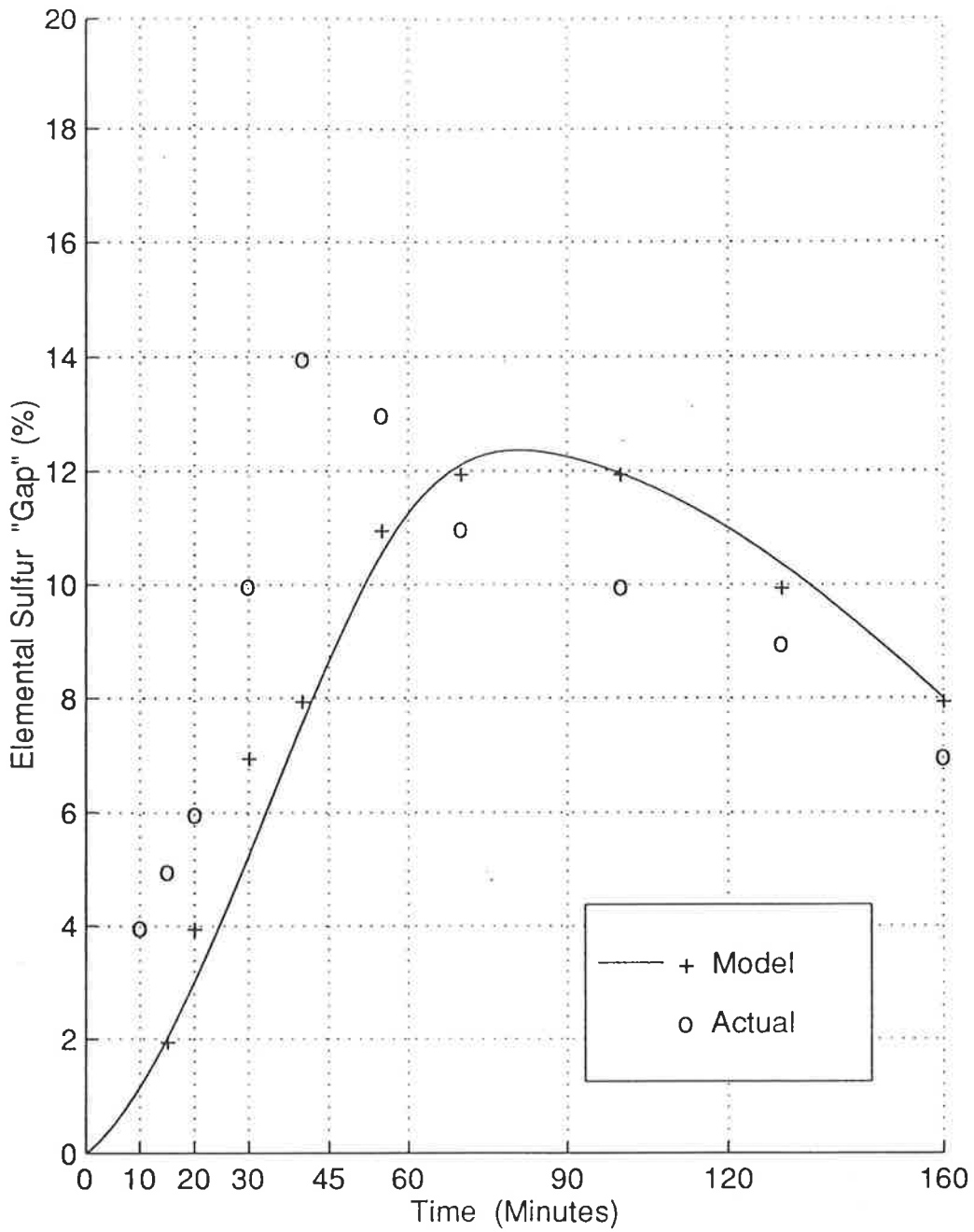


Figure 5.9.7.5 c). Sulfur Gap Model Compared to Actual Results

S-48 Gumeracha Pyrite, 125-180 μm , 80°C, 280 rpm, 2.6 M HNO_3

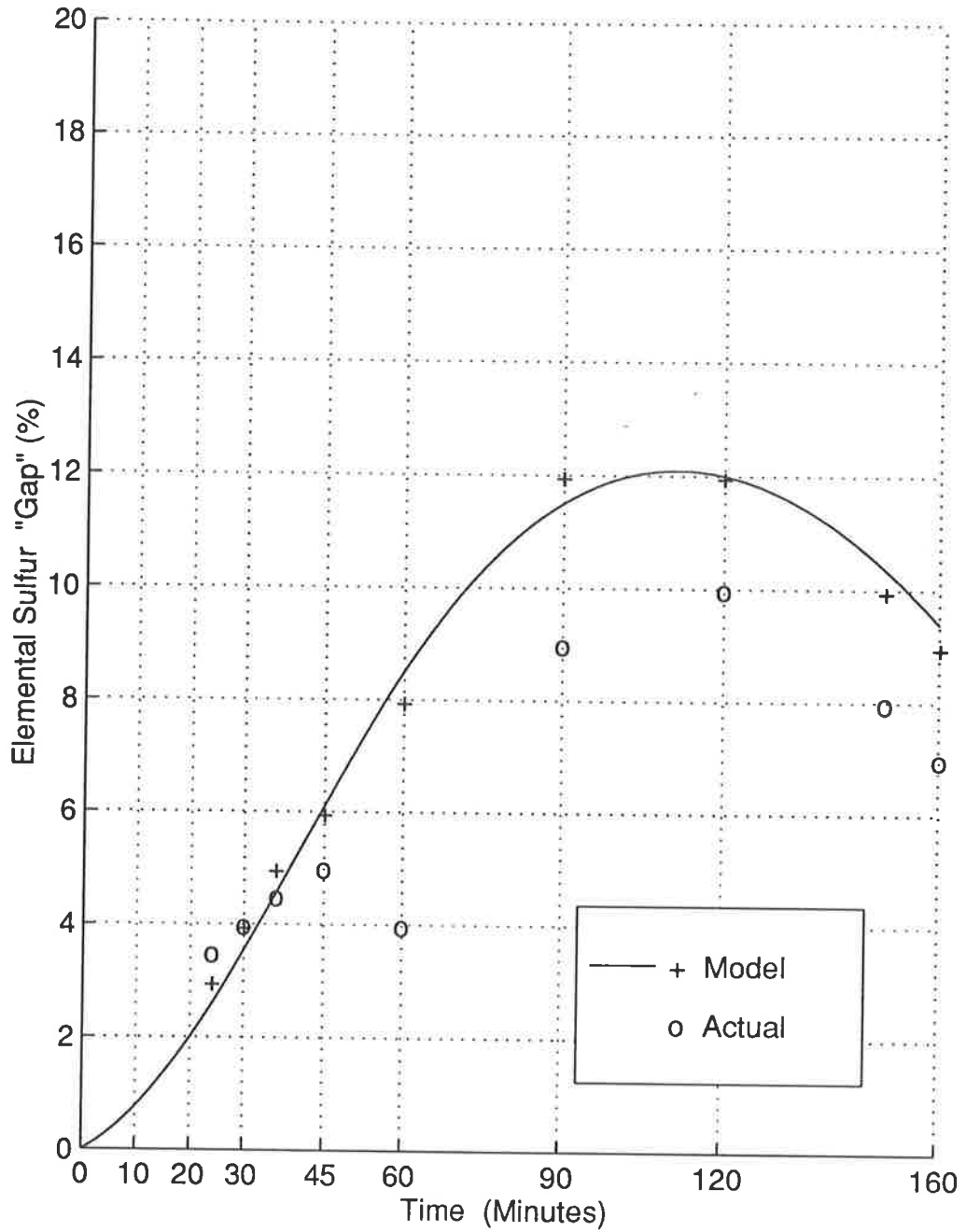


Figure 5.9.7.5 d) Sulfur Gap Model Compared to Actual

S^0 gap model from S proportion to K_d for $S^0 \rightarrow SO_4^{2-}$

S^0 gap Measured as Fe^{3+} minus SO_4^{2-} total

S-(16- + 64) Gumeracha Pyrite 125-180 μm , 75°C, 280 rpm,
2.6 M HNO_3

5.9.7.7 Discussion of Results

Both the 'model' and 'actual' results of the previous section are based on imperfect information. The leach test data was manipulated for the models in that the lag periods were excluded. The proportion of elemental sulfur originally formed was postulated from electrochemical tests, and Eh measurements of the leach tests themselves were highly imperfect although the conditions were carefully controlled. The 'actual' data is imperfect as well. The sulfate extraction curves was less certain (fewer points) than the iron curves. Both are based on assays which were stated to be accurate to $\pm 10\%$. This last factor shows most dramatically in the actual 'sulfur gap' data which is the difference between the two extraction curves and is of the same order of magnitude (0-20%) as the stated assay accuracy from which it was derived.

Despite the manipulation and the imperfect information, the picture generated is surprisingly consistent. The data of Table 5.9.7.3 (page 172) covers a reasonable range of rate constants - 0.021 min^{-1} to 0.086 for k_a . The correlation coefficients show the models to be internally consistent.

Figure 5.9.7.4 (page 172) shows a very reasonable fit between the total sulfate extraction curves generated from the models and the actual total sulfate extraction curves of the leach tests.

The discrepancies between the models and the actual data show more strongly in Figures 5.9.7.5a) through 5.9.7.5d). So also does the imperfection in the data for the actual sulfur gap. For the data set for S(20+32) combined, the model appears to fit the scattered actual data. For test S-4, the sulfur gap of the model rises more slowly and persists for longer times than the 'actual' data would indicate. Both follow roughly the same trend however (Figure 5.9.7.5b). This pattern holds for S-48, while for S(16+64) combined, the model fits the experimental data within that data scatter. (Different combinations of assumptions would alter the models; for example 30% S^0 formation and $k_d = 0.018$ for S-48 gave a model for which the sulfur gap decayed more quickly than that of the actual data. There is no basis for these assumptions from the electrochemical work however.)

Overall, the fit between the models (with k_d as per Table 5.9.7.3 and S^0 proportion 20%) and the actual data is reasonable. Certainly, the fit is within the accuracy of the original assay data.

5.9.7.8 Summary - Oxidation of Elemental Sulfur

The parametric picture which emerges is that the S^0 proportion formed from pyrite is in keeping with electrochemical work, but considerably higher than that referred to by developers of nitric acid process. The proportion of elemental sulfur formed is about 20% for 2.6 M HNO_3 . The electrochemical results of chapter 4 give as good an indication of expected S^0 proportion as can be predicted from the present work.

A possible mechanism involving an activated sulfur complex is consistent with the data. Given the system's complexity and the fact that other writers avoid mechanistic pronouncements, no further attempt is made here.

The oxidation rate of this elemental sulfur, as reflected by the k_d values, is low. The analysis which has been done indicates a value in the vicinity of 0.007 min^{-1} . Preliminary indications are that k_d is much less sensitive to conditions than k_a for ferric iron oxidation. The variation of k_d for sulfur oxidation with leach variables is touched upon further in 5.10.3.5. The effect of elemental sulfur's slow oxidation rate was shown most dramatically by Figure 5.9.7.3 (page 170). The combination of variables has succeeded in speeding up the pyrite reaction to complete iron dissolution within five minutes. The sulfur is not completely oxidised until ninety minutes. If zero elemental sulfur is required, its oxidation will govern the required residence time of reactions for low-temperature ($< 100^\circ\text{C}$) nitric acid processes.

5.9.8. SECTION SUMMARY (Mathematical Analysis)

5.9.8.1 General

The leach kinetics were found to best fit a parametric first-order kinetic model. The rate constants for pyrite dissolution ($FeS_2 \rightarrow Fe^{3+}$) were detailed in Table 5.9.2.1.

5.9.8.2 Classical Kinetic Variables

The rate constants for the stirring speed series fell into two main groups, attributed to flocculation by elemental sulfur. The difference between the two groups was significant - 50% and sudden - between 250 and 280 rpm. The practical consequence was that all following series were run at 280 rpm. The overall impression was independence of stirring speed, within the ranges.

The series at different temperatures gave fair correlation ($r = 0.9644$) with an Arrhenius-type plot, as expected from the literature. Subsequent calculations gave an Activation Energy value of 77 kJ mole^{-1} , which is within the range reported in the literature for pyrite oxidation.

The rate constants for the particle size series varied directly with surface area (or inversely with mean screen dimension). This was later found to apply to blends of sizes for initial rates and initial surface areas.

The pyrite dissolution rate varies directly with nitric acid concentration. The rate is negligible below about 1.0 Molar HNO_3 .

5.9.8.3 Industrial Kinetic Variables

The rate constant displays second-order variation with sulfuric acid concentrations. Within the restrictions of the mathematical analysis and the test conditions, the first-order rate constants for pyrite dissolution vary directly with ferric ion and chloride ion concentration and inversely with silver ion concentration. Silver ion shows evidence of eliminating the elemental sulfur, however. No mathematical analysis was performed for the pulp density series of tests. Any change in the rate constant with pulp density was indistinguishable due to equipment-limited loss of control of the experiments. Wide blends of sizes altered the shape of the leach curves; fines speed up initial leach rates and coarse material slowed down the final sections. Initial leach rates varied directly with initial surface areas.

5.9.8.4 Additional Factors

Attritioning at about 30% by weight of glass balls increased pyrite leach rate by 22%.

An Eh increase to the range of 1.01 - 1.37 volts SHE increased the first-order rate constant by 67%. It proved difficult to achieve a reasonable increase in Eh of the nitric acid system. There is an indication that increased Eh reduces elemental sulfur formation.

Variables are certainly additive to an extent. Only two tests were run combining variables. Both showed variables effects to be additive within 30%. More tests would be required to establish quantitative additivity.

Autocatalysis by ferric ion probably contributes a small proportion (5 - 20%) of the rate increase after the lag period. Change in surface area may also contribute but the two pyrites tested differ markedly in the extent of their lag periods. It is considered that oxidised surface layers, which form within hours or minutes, probably account for most of the lag periods.

The lag period was the main difference between the two tested pyrites and one detailed in the literature. With the lag period removed, pyrites from the three sources show rate constants within 20% of each other. ($k = 0.013 - 0.016 \text{ min}^{-1}$ for $180/250 \mu\text{m}$ @ 70°C , 2.4 M HNO_3 .)

5.9.8.5 Model Fitting

The temperature series of tests were analysed against the shrinking core model, favoured by some sources in the literature. The raw data showed a better fit to first-order kinetics. When the lag periods were excluded, the first-order fit improved even more over the shrinking core model. Correlation coefficients were 0.9914 for first-order and 0.9140 for shrinking core. The test from the literature (Kadioglu et al. 1995) was analysed and proved not inconsistent with first-order kinetics.

Two series of Gumeracha pyrite tests were analysed with lag periods excluded. Model fitting improved, but not enough to justify recalculating all series. The data with the lag period included is considered more practical.

5.9.8.6 Oxidation of Elemental Sulfur

This was summarised in section 5.5.7.8. Elemental sulfur, once formed, oxidises very slowly. The rate constant is not only much lower than that for pyrite dissolution it is much less sensitive to increase by the various variables tested. This has implications for reactor residence times, which are discussed in Sub-section 5.10.3.

5.10. RELATION OF LEACH TEST FINDINGS TO THE LITERATURE, ELECTROCHEMICAL RESULTS, AND REFRACTORY GOLD ORE TREATMENT

5.10.1 RELATION OF LEACH TESTS TO THE LITERATURE

5.10.1.1 Species Formed and Thermodynamic Relevance

Section 5.2 pointed out the importance of specifying conditions when discussing leaching of sulfides. Much of the literature reported results which were apparently conflicting due to different experimental conditions. The current findings certainly underline the necessity for specifying conditions. Pyrite oxidizes to ferric iron and both sulfate and metastable sulfur and the amount of the products depends not only on most variables but also on the time at which products are measured. Thermodynamics can set boundary conditions but does not predict elemental sulfur formation. While thermodynamically metastable, this species is, in practice, stable. XRD tests showed the sulfur in leach residues was orthorhombic (see Appendix A). This is the most stable form of sulfur and was found to exist one hour after leaching. (The sample was frozen in liquid nitrogen).

Finally, classical thermodynamics is of little assistance because it employs conditions which are irrelevant to industrial conditions necessary to achieve commercial kinetics.

5.10.1.2 Earlier Kinetic Studies

Numerous kinetic studies have been reported, but each covered only a small portion of a large multidimensional picture. The present work may well be as comprehensive a study as may be found and yet it covers only part of the system - pyrite-nitric acid. Chemical control of the leach rate is indicated, agreeing with the majority of authors surveyed. Linear kinetics were found, agreeing with Mishra (1973) and King and Lewis (1980 (both in Hiskey and Schlitt (1982))). Those researchers who found the kinetics fit the shrinking core model, namely Bailey and Peters (1976) and Kadioglu et al. (1995), were not necessarily incorrect. Some of Kadioglu's data fit linear kinetics equally well, under nearly identical conditions to the present work.

5.10.1.3 Recent Kinetic Study of Kadioglu et al. (1955)

This work is the most relevant to the present findings being the only other study on pyrite-nitric acid. The Turkish researchers studied what has been termed here the

'classical' kinetic variables. The present study generally confirmed their results although larger amounts of elemental sulfur were found in the present work (often up to 12% versus 7% for Kadioglu et al.) This higher proportion of S^0 formed may well have been because the conditions employed in the present work generally gave faster pyrite leach rates. The elemental sulfur oxidises independently and slowly, and would have had more time to do so in the Turkish tests. Typically the present tests were complete (at least as far as pyrite oxidation) in 1 - 2 hours, while the Turkish tests required 2 - 6 hours for pyrite dissolution.

The current study analysed an additional eleven industrial and other variables' effects on the leaching kinetics of pyrite, beyond the Turkish publication. The Kadioglu et al. pyrite showed no lag period, whereas the lag period for the slower Gumeracha pyrite tests was appreciable. With the lag period removed, the Gumeracha pyrite, the Turkish Artvin-Morgul pyrite and the Peruvian Huanzala pyrite all had rate constants within 20%, for those tests using comparable conditions.

5.10.1.4 Relevance of Current Findings to other Variables in the Literature

The current study found leach rates to be independent of stirring speeds. However, grouping of results was found, which was attributed to flocculation by elemental sulfur.

Leach rates were found to be proportional to surface area of the pyrite as noted by Bailey and Peters (1976) among others.

Kinetics of the present work were accelerated by both ferric ion and chloride ion. This was qualitatively in keeping with limited findings by other workers, King and Lewis and Ichikuni (in Hiskey and Schlitt 1982).

Silver ion was found to slow kinetics in keeping with the findings of Buckley et al. 1989. In addition there was an indication that silver reduces or eliminates elemental sulfur formation. This was the only experimental condition to do so and more work should be performed in this area if it is of commercial interest.

The present study found that a considerable lag period is evident for Gumeracha pyrite. The rate of leaching is partially autocatalysed by ferric ion produced by the reaction. Shashi et al. (1987) indicated that such acceleration would occur. In the present work, however, ferric ion would account for a first-order rate constant increase of only about 13%. For two cases analysed the rate constant increased

70% and 190% after the lag period. Thus the autocatalytic effect is small. Increasing surface roughness as the reaction proceeds could also have an effect.

Lag period accounted for the main practical kinetic differences between the Gumeracha, Huanzala and Artvin-Morgul pyrites. Huanzala displayed small lag periods and the Turkish figures showed none for the Artvin-Morgul pyrite. This, along with the findings of the previous paragraph, would argue that the major contributing factor to lag period is the presence of inhibiting surface layers.

5.10.2 RELATION OF LEACH TESTS TO ELECTROCHEMICAL FINDINGS

The electrochemical work in Chapter 4 of the present work pointed the way to a number of the findings of the pyrite leach tests. In general, the correspondence between the two modes of experimentation has been very encouraging.

5.10.2.1 Oxidation Rates

Predicted rates for pyrite oxidation, from the electrochemical work, were compared to the measured initial leach rates for two cases. These results are compared in Table 5.10.2.1.

Table 5.10.2.1: Actual vs Predicted Pyrite Oxidation Rates

| | | |
|---|--|---|
| Electro Chemical Tests (80°C) | | |
| upper sweep limited (volts) | 1.02 | 1.32 |
| weighted average (volts) | 0.95 | 1.20 |
| Predicted rate $10^{-8} \text{ g cm}^{-2} \text{ sec}^{-1}$ | 91 | 385 |
| <u>Leach Tests</u> | | |
| Test No. Conditions | S-51 80°C 1.5 M HNO ₃ | 4 tests S48, S20, S32, S81 2.6 M HNO ₃ 80°C |
| Measured Eh | 0.96 | 1.13 - 1.20 |
| Oxidation Rates ($10^{-8} \text{ g cm}^{-2} \text{ sec}^{-1}$ in lag period) | 13 | avg 150 |
| Initial after lag | 102 | avg 340 |

All voltages are vs SHE

The level of agreement is very good for the two quite different techniques. It should be remembered, however, that the measured leach tests Eh values are only approximate. The four tests examined were all at the most common nitric acid concentration of 2.6 M and should have had similar Eh values. Estimation of the initial leach rates is not very accurate, either; the standard deviation for the leach rates for the four tests was $65 \text{ g cm}^{-2} \text{ sec}^{-1}$.

Nevertheless, the predictive value of the voltammetric sweep tests appears good. In comparing different techniques, an order of magnitude agreement is generally considered satisfactory. The pronounced effect of the lag period for Gumeracha pyrite is also demonstrated.

5.10.2.2 Temperature Independence

The temperature series on Gumeracha pyrite confirms the electrochemical findings on elemental sulfur proportion. Table 5.5.2.1 (page 119) shows this independence for Gumeracha pyrite. Table 5.2.2.2 shows a similar pattern for Huanzala pyrite. In both cases the sulfur gap is fairly constant across the temperature range for a given iron extraction. Since the results are compared at the same pyrite dissolution values, and elemental sulfur oxidation is relatively slow, the sulfur gap is indicative of the proportion of elemental sulfur formed.

5.10.2.3 Effect of Eh on S⁰ Proportion

The pattern from the Chapter 4 whereby the elemental sulfur proportion was expected to disappear at Eh 1.4-1.5 volts SHE remains unconfirmed. The [HNO₃] series showed if anything an increasing sulfur gap with nitric acid concentration (Table 5.5.4.1 page 121). This may simply reflect higher iron extraction rates, which allow less time for a fixed proportion of S⁰ to oxidise. While this data might benefit from mathematical analysis of the sulfate curves, time and a paucity of data points have precluded such analysis.

Attempts to increase Eh artificially were of limited success. Hydrogen peroxide decomposed at the conditions tested, with no pyrite added. Adding KMnO₄ to test S-46 did increase the Eh. Though it fluctuated widely the Eh reached 1.37 volts. While this markedly increased the oxidation rate of pyrite, no conclusion can be drawn about elemental sulfur. No sulfur gap was apparent until iron extraction reached 60%. However, the test was very slow due to its temperature and pyrite size (50°C, 125/180 μm). A quick calculation showed that even if 5% S⁰ were

generated at the Eh of the experiment, over four hours it would all be converted to sulfate given a k_d value of 0.007 min^{-1} . The test was too slow and the Eh too erratic to be certain. In any event, about 7% S^0 had appeared after six hours.

It is worth recalling that Eh measurement during the leach tests is only the roughest of guides. As discussed in 5.8.2.2, the Ag-Ag Cl probe drifted badly at high temperatures and acid strengths. Stronger nitric acid solutions gave lower Eh readings. Most leach tests at 2.6 M HNO_3 averaged 1.18 volts SHE (Table 5.8.2.1 page 141). According to the data generated during several days of quantifying Eh probe drift in 2.6 N HNO_3 at 80°C , this reading should be reduced by at least 0.1 volts. The resultant Eh of 1.08 volts would give about 20% elemental sulfur proportion according to electrochemical predictive work in Chapter 4.

The calculations of section 5.9.7 are based largely on this figure of twenty percent (20%) elemental sulfur formation. To these are applied sulfur oxidation rate constants as indicated by late sections of the leach curves, when the pyrite can no longer contribute to $\text{SO}_4^{=}$ formation. The resultant models give reasonable agreement to measured sulfate (total) values. This, albeit circumstantial evidence, is one more correlation between the electrochemical work and leach test findings.

5.10.2.4 Nature of Oxidizing Surface

The electrochemical work suggested that a change in the nature of the sulfur product was occurring. Some authors have attributed this to a metal-deficient sulfide. The rate-constant data of the leach tests is not inconsistent with an activated-species mechanism. This in turn could be a metal-deficient sulfide lattice. A very limited supporting investigation, using XPS surface analysis of a pyrite crystal leached for five minutes was undertaken. The XPS findings were interpreted by the technical expert as being a metal-deficient sulfide. While this could well be the transition state, there is ample evidence that elemental sulfur itself is formed and makes up the bulk of the non-sulfate product. Microscopic observation, carbon disulfide dissolution, SEM results and the flocculating action observed also point to appreciable quantities of S^0 throughout the leach tests.

5.10.3 RELATION OF LEACH TEST FINDINGS TO REFRACTORY GOLD ORE TREATMENT

5.10.3.1 Leach Test Targets

The philosophy behind the extensive leach tests was to investigate the kinetics of pre-oxidation. They were intended to find ways to improve the kinetics of pyrite oxidation. It was expected that the leach tests would define the extent to which elemental sulfur was a kinetic problem. It was hoped that the tests would provide answers as to how to avoid elemental sulfur formation or else how to speed its oxidation, thereby eliminating it. These points, the problem for overall pre-oxidation kinetics, the avoidance of elemental sulfur, or the oxidation of it, will be dealt with in turn.

5.10.3.2 Effect of Elemental Sulfur on Pre-oxidation Kinetics

The testwork has shown that for the pyrite nitric acid system, elemental sulfur has a major effect on pre-oxidation kinetics. This will very much apply to the low-temperature version of the "Redox" process.

Firstly, the proportion of elemental sulfur formed from pyrite is much larger than that generally reported by developers of nitric acid processes. Sulfur formation was known to be appreciable for arsenopyrite-nitric acid, and it was known that 80% of the reactor residence time was necessary to eliminate S^0 for the high temperature "Redox" process, working on arsenopyrite or pyrrhotite feeds (Leonard et al. 1990). What was not known is that the same can apply to pyrite-nitric acid for certain conditions. In fact, for conditions typical of the commercial "Redox" process (2.6 M HNO_3) about twenty percent of the sulfide sulfur oxidizes to the elemental form. Over a wide range of conditions, the oxidation of this sulfur, once formed, is slow. The effect of this on reactor residence time is more dramatic for those conditions displaying the fastest pyrite oxidation kinetics.

Figure 5.10.3.1 and Table 5.10.3.1 show the effect of the elemental sulfur on leach times for four sets of conditions. The four cases were analysed from mathematical models but the models check well with original leach tests.

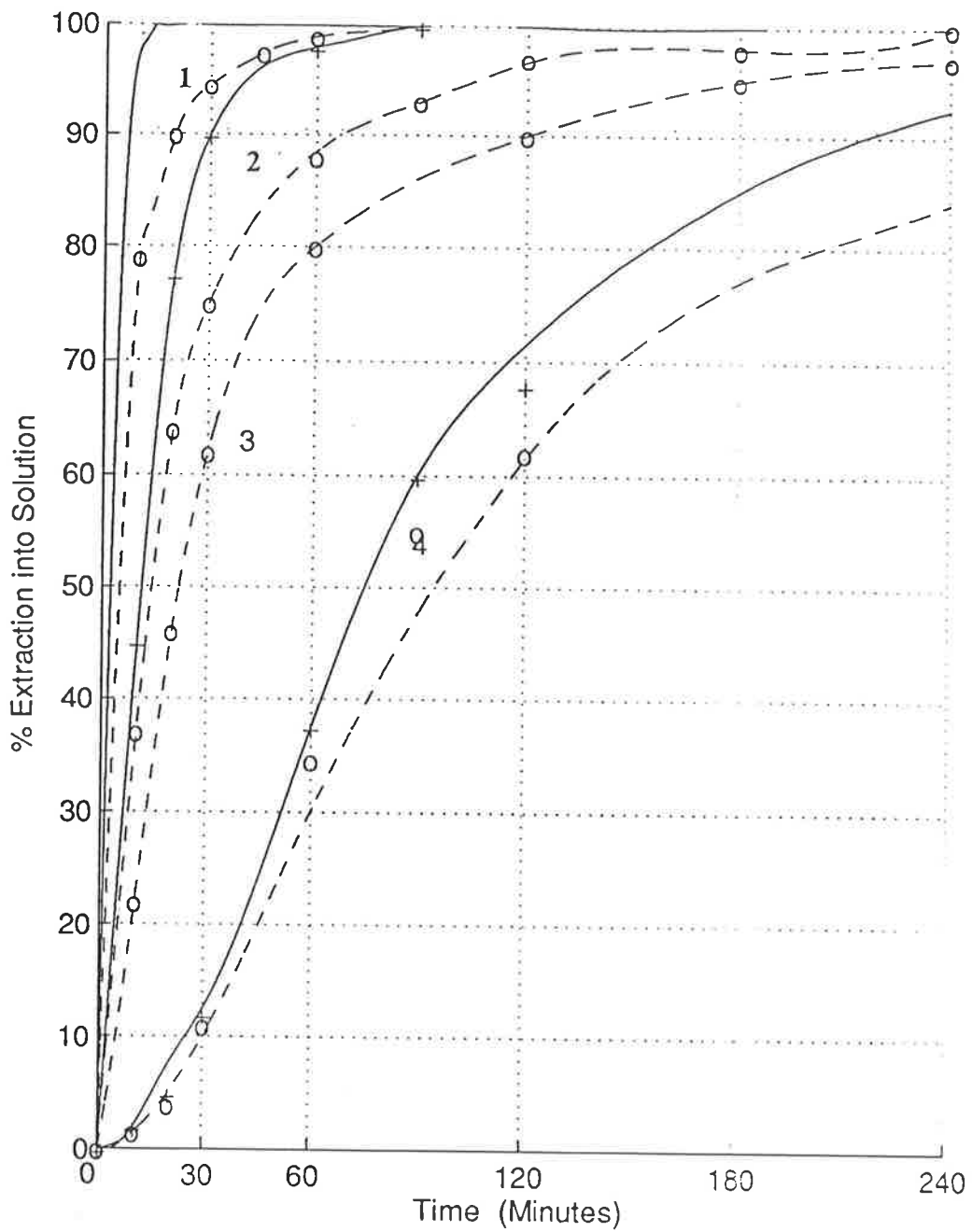


Figure 5.10.3.1. Effect of S^0 Oxidation on Leach Reactor Residence Time



Cases 1-4 as per Table 5.10.3.1

Table 5.10.3.1: Reaction Leach Times for Four Cases

| Case | 1 | 2 | 3 | 4 |
|---|---|------------------------|------------------------|-------------------------|
| Test Run | S-79 | S-4 | S(20+32) | S-15 |
| Pyrite | Gum. 63/90 μ m | Gum. 90/125 μ m | Gum. 90/125 μ m | Gum. 180/250 μ m |
| [HNO ₃] | 3.5 M | 2.6 M | 2.6 M | 2.6 M |
| Temp °C | 90 | 80 | 80 | 75 |
| Other | H ₂ SO ₄ 2.0 M | 72 rpm | | |
| Conditions | Attritioning | | | |
| k _a (min ⁻¹) | 1.10 | 0.086 | 0.053 | 0.013 |
| k _d (min ⁻¹) | 0.04 | 0.0125 | 0.007 | 0.005 |
| Times for FeS ₂ →Fe ³⁺ (0.995 completion) | 5 min | 1 $\frac{1}{3}$ hours | 1 $\frac{3}{4}$ hours | 7 hours |
| for SO ₄ ⁼ total (0.97 completion) | $\frac{3}{4}$ hour | 2 $\frac{1}{3}$ hours | 4 $\frac{1}{2}$ hours | 7 $\frac{1}{2}$ hours |
| for SO ₄ ⁼ total (0.995 completion) | 1 $\frac{1}{4}$ hours | 4 hours | 9 hours | 12 hours |
| Sulfur Gap at FeS ₂ →Fe ³⁺ (0.995) | 21% | 10% | 11% | 3 $\frac{1}{2}$ % |

From Figure 5.10.3.1 the effect of the requirement to oxidise the elemental sulfur is seen clearly. The extent of S⁰ oxidation is important. Table 5.10.3.1 includes benchmarks at 3% of elemental sulfur (0.97 SO₄⁼ completion) and 0.5% S⁰. One hundred percent of elemental sulfur oxidation is completely impractical. The 3% figure is benchmarked because that is the figure nitric acid developers are familiar with. This figure is for "pure" pyrite and would be much reduced for most whole ores. The extent to which elemental sulfur at those levels is still a problem in discussed in Chapter 6. The 0.5% figure is considered a realistic target for sulfur elimination. As can be seen from Table 5.10.3.1 even this level adds considerably to reactor residence times. Commercial pilot tests of the low-temperature variants of the "Redox" process have used 1-2 hours residence times. For this range, severe conditions (such as case 1) must be used, or higher levels of elemental sulfur accepted. The point is that the elemental sulfur has an inordinately strong effect in increasing the residence time required for oxidation.

5.10.3.3 Avoidance of S⁰ Formation - Eh

Only two variables of the range tested show any promise of avoiding the formation of elemental sulfur. They are Eh and silver ion addition. Eh-redox potential-is discussed first. Due to the practical problems of measuring high acid-high temperature Eh, the only tests for which high Eh can be reasonably assured are

those using stronger nitric acid. (Test S-46 using KMnO_4 was not carried far enough to warrant further analysis.) Three tests at different nitric acid concentration are listed in Table 5.10.3.2. The first-order kinetic plots (not shown) tests showed inflection points which indicated the amounts of elemental sulfur formed and its oxidation rate constants.

Table 5.10.3.2: Sulfur Formation and Oxidation; (High Eh Tests)

| Test | S-48 | S-49 | S-50 |
|---|-------|--------|-------|
| [HNO_3] | 2.6 M | 3.5 M | 4.5 M |
| Eh (measured) volts - unreliable | 1.172 | 1.153 | 1.143 |
| k_a ($\text{FeS}_2 \rightarrow \text{Fe}^{3+}$) | 0.024 | 0.039 | 0.076 |
| k_d ($\text{S}^0 \rightarrow \text{SO}_4^{2-}$) | 0.007 | 0.013 | 0.014 |
| k_e ($\text{FeS}_2 + \text{S}^0 \rightarrow \text{SO}_4^{2-}$ total) | 0.015 | 0.036 | 0.052 |
| Inflection Points in first-order Plots | | | |
| Fe^{3+} conversion | 0.94 | 0.92 | 0.96 |
| SO_4^{2-} conversion | 0.84 | 0.87 | 0.90 |
| Estimated fraction of S^0 formed | 0.20 | 0.15 ? | 0.12 |

The figures for elemental sulfur formed are very much estimates - model simulation and iteration was not undertaken. The first-order plots give a strong hint there was less S^0 formed, with stronger nitric acid concentration, and this would be in keeping with higher Eh, as discussed in Chapter 4. As noted, the measured Eh values are no help at all and are included only for completeness. Increased Eh vs nitric acid concentration may reduce the formation of elemental sulfur but does not eliminate it, at least up to the concentration tested.

In an earlier publication (Flatt and O'Neill, 1995) the author stated that high nitric acid concentration appeared to increase the "sulfur gap". This is not inconsistent with lower elemental sulfur formation. The effect of k_a (iron dissolution) simply outpaces the effect on k_d (S^0 oxidation) so that a larger sulfur gap is apparent at some times even though a lower proportion of elemental sulfur is formed initially.

5.10.3.4 Avoidance of S^0 Formation - Ag^+ Ion

The addition of silver ion shows promise towards eliminating elemental sulfur formation. More testwork needs to be done to confirm this promise. The present work was limited by finance and the peculiarities of part-time research; the potential of silver ion, investigated late in the test program, was not quantified until after the test program was completed. Table 5.10.3.3 gives the relevant data. The first-

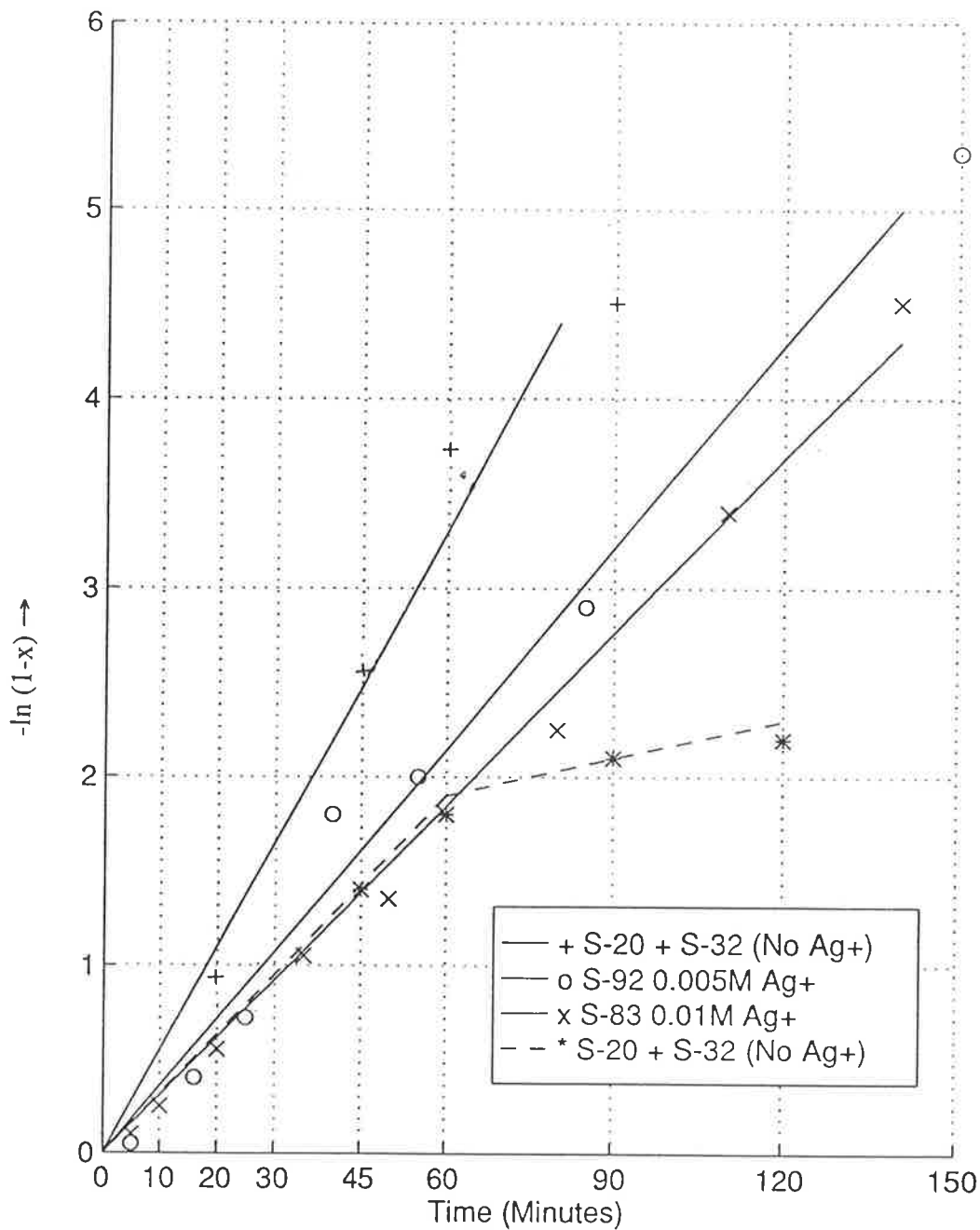


Figure 5.10.3.2 Iron and Sulfate First-Order Plots
 (Ag^+ Addition Tests)
 Gumeracha Pyrite 90-125 μm , 80°C , 2.6M HNO_3 , 280 rpm

— Iron - - - - sulfate

order plots (Figure 5.10.3.2) display neither a sulfur gap nor inflection in the sulfate curves.

Table 5.10.3.3: Sulfur Formation and Oxidation; Ag⁺ Addition Tests

| Test | S-(20 + 32) | S-92 | S-83 |
|---|-----------------------|-----------------------|-----------------------|
| [Ag ⁺] | nil | 5x10 ⁻³ M | 10 ⁻² M |
| k _a (min ⁻¹) | 0.053 | 0.034 | 0.031 |
| k _d (min ⁻¹) | 0.007 | 0.034 | 0.031 |
| Times for FeS ₂ → Fe ³⁺ (0.995 conversion) | 1 $\frac{3}{4}$ hours | 2 $\frac{1}{2}$ hours | 2 $\frac{3}{4}$ hours |
| SO ₄ ⁼ total 0.97 conversion | 4 $\frac{1}{2}$ hours | 1 $\frac{2}{3}$ hours | 2 hours |
| SO ₄ ⁼ total 0.995 conversion | 9 hours | 2 $\frac{1}{2}$ hours | 2 $\frac{3}{4}$ hours |

Table 5.10.3.3 indicates that silver ion slows down the pyrite leach kinetics, but eliminates elemental sulfur formation. The resultant reaction residence times are considerably reduced. In this case elemental sulfur may not govern leach time. For some ores a 3% elemental sulfur in residue may be acceptable while 3% pyrite in residue may not be acceptable.

5.10.3.5 Oxidation Rates for Elemental Sulfur

The mathematical analysis of elemental sulfur oxidation proved to be an involved, iterative process, the validity of which was made less certain by the need to manipulate the lag period data. Nevertheless, it is broadly evident that the variables which affect pyrite oxidation rate (Fe³⁺) also affect the elemental sulfur oxidation rate. This means all the variables tested. However, the effect is much less pronounced for elemental sulfur; it oxidises comparatively slowly compared to pyrite. This may be appreciated from Table 5.10.3.4, which compares the extremes of the test program. Test S-79 combined a number of rate-increasing variables (see Table 5.10.3.1) and was the most rapid of all tests. Test S-15 used a very coarse pyrite and was one of the slowest tests.

Table 5.10.3.4: Effect of Variables on Kinetics of FeS₂ and S⁰ Oxidation

| Test | S-79 | S-15 | Factor |
|---|------|-------|-------------|
| Status | Fast | Slow | (Fast/Slow) |
| k _a (min ⁻¹) FeS ₂ → Fe ³⁺ | 1.10 | 0.013 | 84 |
| k _d (min ⁻¹) S ⁰ → SO ₄ ⁼ | 0.04 | 0.005 | 8 |

first-order
rate
constant

Broadly then, elemental sulfur oxidation rate is an order of magnitude less sensitive to the variables tested than is pyrite oxidation rate.

5.10.3.6 Sub-Section Summary

The findings of the leach tests should be quantitatively useful for developers of nitric acid pre-oxidation routes for refractory gold. In particular, Table 5.9.2.1 (pages 151-152) gives kinetic rate constants for pyrite oxidation, and shows the likely effects of twelve controllable variables at least nine of which are independent.

The oxidation rate of pyrite itself may not govern required reaction residence times. It is more than likely that elemental sulfur may be the governing consideration. Of the variables tested, only Eh and silver ion showed any potential to reduce elemental sulfur formation. Both of these need more work. Elemental sulfur, once it is formed, oxidises very slowly compared to pyrite. Its oxidation rate does vary with the variables tested, but in an order of magnitude less sensitive to the variables than the pyrite.

Whether the elemental sulfur is governing will depend on the acceptable conversion of elemental sulfur to sulfate. The industry has generally tolerated 3% of elemental sulfur in residues. Even at this level elemental sulfur will generally govern the required residence times. This may not have been recognised for low-temperature nitric acid preoxidation, which usually processes whole ores. Those whole ores given low sulfur in residues, which nevertheless could exceed 3% of the pyrite sulfur in the feed. Whether incomplete elemental sulfur oxidation is a problem for gold recovery will depend on the ore. This will be addressed further in Chapter 6.

5.11 CHAPTER SUMMARY

5.11.1 FULFILMENT OF AIMS

The extensive leach tests described in this chapter have quantified the effects of a wide range of variables on the pyrite-nitric acid system. The variables, and their values, were chosen so as to be relevant to pre-oxidation of refractory gold deposits.

The wide range of variables in the present study has led to a large chapter and limited the depth of some aspects of the mathematical analysis of data. The leach tests themselves were at atmospheric pressure, in keeping with their relevance to low-temperature variants of commercial pre-oxidation with nitric acid. Nevertheless, the present work is perhaps the most comprehensive study of pyrite oxidation to date.

Most of the variables tested failed to show significant effects on the proportion of elemental sulfur formed when pyrite oxidises in nitric acid. Eh may have an effect but the Eh attainable in nitric acid systems is limited by oxygen reduction. Attempts to increase Eh were of limited success. Silver ion appeared to reduce or eliminate elemental sulfur formation but its use is questionable commercially. Both variables require more work.

The alternative of eliminating elemental sulfur formation is unproven. A high enough Eh is one possibility but is probably not obtainable in nitric acid. Silver ion additive needs further experimental and financial evaluation.

5.11.2 OXIDATION KINETICS

Classical thermodynamics has been shown to be of limited practical use for the pyrite-nitric acid system. This is because of the importance of metastable sulfur, which means that the present study is a kinetic one.

The quantification of the kinetics of pyrite oxidation to ferric iron yielded results which were in keeping with what might be expected for a kinetic study. The fit of the data was best for first-order kinetics when considered over the whole range of variables tested. Segments of the data fit the shrinking-core model, but then portions of other researchers data, regarded as fitting the shrinking-core model, also fit the first-order model. The dependence of first-order rate constants upon individual isolated variables yielded few surprises. These dependencies are probably additive, although tests to determine additively were not extensive.

The quantification of the kinetics of pyritic sulfur oxidation was shown to be more complex. The pyritic sulfur proceeds by parallel paths to sulfate and elemental sulfur. The elemental sulfur itself oxidises to sulfate. The difference between the ferric iron and sulfate curves is what is experimentally determined. This is the sulfur gap. Apparent inconsistencies were found in the sulfur gap. These are explainable in forms of the variation of rates of direct sulfate and sulfate from elemental sulfur formation. Elemental sulfur oxidation rates were found to be

relatively slow. Further, the first-order rate constants were an order of magnitude less sensitive to change in variables than were the rate constants for pyrite oxidation.

The alternative of eliminating elemental sulfur by increasing its oxidation rate after it has formed does not appear viable.

5.11.3 RELEVANCE OF FINDINGS

The literature on sulfide oxidation presents a complex picture. This has been likened to a giant multi-dimensional crossword puzzle. The fact that so many variables produce measurable effects is significant. It explains why previously-reported test results often appeared to conflict. Conditions selected may well have been relevant to the particular researchers' situation at the time but differed enough from other researchers' conditions, so that the overall patchy picture was confusing. Different parts of the crossword puzzle were being illuminated and the puzzle was multi-dimensional.

The leach test results compared well with the preliminary electrochemical findings of Chapter 4. Leach oxidation rates of the pyrite after the lag period were acceptably close to those predicted. As shown in Chapter 4, the proportion of elemental sulfur was independent of temperature. The Eh of the nitric acid system did not prove amenable to manipulation, hence leach tests were unable to confirm the dependence of sulfur proportion on Eh. Elemental sulfur forms on a macroscale although a metal deficient lattice could be a precursor. Amorphous elemental sulfur is present in the residues and forms during leaching in quantities sufficient to cause flocculation of pyrite.

The test results should be useful to those developing nitric acid systems for refractory gold ore pre-oxidation. Much more elemental sulfur forms from pyrite than that which has been measured at the end of developmental nitric acid tests. Acceleration of S^0 oxidation by combinations of variables is possible, but not nearly to the extent that the pyrite oxidation can be accelerated. It is not practical to eliminate all residual elemental sulfur in a low-temperature nitric acid process. Whether residual elemental sulfur level will govern the process will depend upon the elemental sulfur's effect on gold recovery. While the effect on gold recovery may be a function of a given ore, the quantified effects shown in the body of this chapter should be valid for most pyrite sources. Accordingly, the data on pyrite and elemental sulfur kinetics established in this chapter should be valuable to the gold industry.

5.12 REFERENCES

- Bailey, L.K. and Peters, E., 1976, See chapter 4.
- Beattie, M.J.V. and Ismay, A., 1990, See Chapter 2.
- Berezowski, R.M.G.S., Collins, M.J., Kerfoot, D.G.E. and Torres, N., 1991. The commercial status of pressure leaching technology, *J.Mines.*, Feb. pp 9-15.
- Buckley, A.N., Wouterlood, H.V. and Woods, R., 1989, The interaction of pyrite with solutions containing silver ions, *J. Applied Electrochemistry*, **19**, pp 744-751.
- Chander, S. and Briceno, A., 1987, Kinetics of pyrite oxidation, SME-AIME Annual Meeting, Denver, Colorado, Feb 23-27, Soc. of Mining Engineers.
- Cheng, C.Y. 1990, The leaching of copper sulphide in acidic oxygenated sulphate-chloride solutions, PhD Thesis, Dept of Chemical Engineering, Monash University, pp 51.
- Fair, K.J. and Van Weert, G., 1989, See chapter 2.
- Ferreira, R.C.H., 1975, High temperature E-pH diagrams for the systems S-H₂O, Cu-S-H₂O and Fe-S-H₂O, from Barkin, A.A. "*Leaching and Reduction in Hydrometallurgy*", I.M.M., pp 67-83.
- Flatt, J.R. and O'Neill, B.K., 1995, The pyrite-nitric acid system in refractory gold ore treatment - A study of kinetics and elemental sulfur formation. *CHEMECA '95*, Adelaide, pp 192-197.
- Fraser, D.M. Zacharaides, J.C., "A comparison of alternative models for non-linear leaching kinetics", pp 365-372.
- Hiller, L.A. and Herber, R.H., 1960, *Principles of Chemistry* McGraw-Hill, Toronto, pp 640.
- Hiskey, J.B. and Schlitt, W.J., 1982, See chapter 2.
- House, C.I., (1987) Potential -pH diagrams and their application to Hydrometallurgical Systems in Davies C.A. (Editor), *Separation Processes in Hydrometallurgy*, Ellis Horwood, Chichester, pp 3-19.

- Kadioglu, Y., Karaca, S. and Bayakceken, S., 1995, See chapter 2.
- Leonard, R.C. Christenson, K.C. and Dawson, P.A. 1990, See chapter 2.
- O'Neill, B.K., 1994, verbal communication.
- Peters, E. and Majima, H., 1968, See chapter 4.
- Peters, E., 1981, Metastable diagrams and extended phase stabilities, unpublished lecture notes.
- Peters, E., 1984, Electrochemical mechanisms for decomposing sulphide minerals, *Proc. Int. Symp. on Electrochemistry in Mineral and Metal Processing*. The Electrochemical Society Pennington, N.J., 10: pp 343-361.
- Peters, E., 1991, Private communication.
- Pickett, D.E., 1978, *Milling practice in Canada*, CIM, Montreal, pp 58.
- Raudsepp, R., Peters, E. and Beattie, M.J.V., (1987), see Chapter 2.
- Sato, M., 1960, Oxidation of sulfide ore bodies II. Oxidation mechanisms of sulfide minerals at 25°C", *Economic Geology*, 55, pp 1202-1231.
- Shashi, B, Lalvani, M., Shami, I., 1987, Passivation of pyrite oxidation with metal cations, *J. Materials Science*, 22, 3503-3507.
- Van Weert, G., Fair, K.J., and Aprahamian, V.H. (1988), see Chapter 2.
- Wadsley, M., (1990), Private communication.
- Wong, P., (1991), Private communication.
- Woodcock, J.T. (Ed), 1980, Mining and metallurgical practice in Australasia, *Monograph 10*, Aus.I.M.M., Melbourne.
- Woods, R., Yoon, R.,H. and Young, C.A., 1987, Eh-pH Diagram for stable and metastable phases in the copper-sulphur-water system, *International Journal of Mineral Processing*, 20, 1987, pp 109-120.

6 CONCLUSIONS AND RECOMMENDATIONS

6.1 PREAMBLE

The reader has crossed a massive tract of data. Hopefully, the path has been illuminated by short summaries acting as lampposts, placed throughout the data. With the same idea of easing the reader's voyage, the writer will begin this final chapter with a review of what has gone before. This will be an attempt to place the earlier chapters in perspective.

The key specific findings will be listed in Section 6.2. General patterns which have emerged from the work will be discussed in Section 6.3. Section 6.4 will outline recommendations for further work and Section 6.5 will be a final summary.

6.1.1 CHAPTER 1 - INTRODUCTION

Chapter 1 set the tone of the thesis. The work was intended to be of practical relevance. The fundamental study is the kinetics of pyrite-nitric acid system and conditions have been chosen in ranges which should be useful to developers of nitric acid processes.

The Chapter foreshadowed the usefulness and attraction of nitric acid processes for treating refractory gold deposits. It pointed out that elemental sulfur is a problem for such processes.

6.1.2 CHAPTER 2 - BACKGROUND TO STUDY

This chapter expanded on reasons why the study is worthwhile. The importance of refractory gold deposits to Australia and overseas was described. The attraction of nitric acid processes was outlined. Their favourable kinetics and their history were described. The low-temperature variant of the "Redox" process promises a 40% capital cost reduction over the higher-temperature variant. Typical conditions for the former were given. These were the conditions used as a basis for testwork in Chapter 5.

The experience of developers of nitric acid processes with elemental sulfur was described. Elemental sulfur caused the developers to opt for the more expensive higher-temperature (185°C) process for Snow Lake. The "Nitrox" process, similar to the low-temperature "Redox" variant, ran into flowsheet complications due to elemental sulfur formed from the mixed pyrite-arsenopyrite Dickenson concentrate. It is safe to conclude that elemental sulfur was a major factor in the demise of the "Nitrox" process.

The literature on nitric acid oxidation of sulfides showed that limited fundamentals had been studied. Those studies that existed had different goals from the present work. Contacts among developers also confirmed that no fundamental study of elemental sulfur formation during sulfide leaching existed.

6.1.3 CHAPTER 3 - AUTOCLAVE AND CYANIDATIONS TESTS

The tests summarised in this chapter do not constitute a kinetic study. Rather, they were preliminary tests to develop a feel for the field, while searching for a niche of original research. Four different refractory materials were tested. These materials gave conventional cyanidation recoveries of from 48 to 68% Au. Pre-oxidation with nitric acid improved recoveries of all four materials to an average figure of 93%. Average cyanide requirements were reduced from 4.5 to 1.9 kg/tonne ore. Average base requirements were reduced from 4.5 to 2.2 kg/tonne ore as well. These figures are hopefully useful confirmation for the sponsors of the work. Follow-up enquiries have resulted in consulting work on one material.

The four refractory gold-bearing materials tested were quite different from one another. As far as any such pattern can be determined from four cases, the mineralogy may give an indication of the amount of elemental sulfur likely to be found in pre-oxidation residues. On the other hand, the limited mineralogy conducted gave little indication of cyanicides or likely reagent consumptions. Certainly the four refractory materials showed individual problems in assaying and metal balances.

The question of elemental sulfur in residues' effect on gold losses was followed up. Table 6.1.3.1 gives what data is available for the four materials, plus more recent data from two Stawell Gold ore bodies. The "Wonga" concentrate is several years deeper into the ore-body than the original "Wonga" test ore.

Table 6.1.3.1: Relationship Between Elemental Sulfur in Pre-oxidation Residue and Gold Loss in Cyanidation

| Material | Sulfur in Feed S ⁼ (%) | S ^o in Residue (%) | Proportion of S ⁼ as S ^o (%) | Gold Loss (%) |
|------------------------------------|-----------------------------------|-------------------------------|--|---------------|
| Bougainville Pyrite | 43.9 | 1.3 | 3.0 | 3-6 |
| Stawell Wonga Ore 1989 | 3.0 | 0.05 | 1.7 | 6 |
| Stawell Wonga Spiral concentrate ‡ | 2.5 | 0.5 | 19 | 10 |
| Stawell Wonga Ore [#] | 0.62 | 0.38 | 55 | 8 |
| Stawell Central Ore [#] | 3.7 | 1.25 | 30 | 4 |
| Cinola Ore | 2.1 | 0.1 | 4.7 | 7-14 |
| Tonkin Springs Ore | 1.4 | 0.1 | 7.1 | 6-9 |

[#] Figures from consulting testwork by the author 1994

[‡] Figures from N. Thiel, student project 1995

There is no pattern evident which fits the data from the different sources. The three tests on Stawell "Wonga" material show a relationship ($r = 0.966$) whereby gold loss increases linearly with S^o in pre-oxidation residue. However, these are only three points. Otherwise gold losses follow neither S^o in residue nor S^o proportion of S⁼ in feed. In retrospect, this was a simple-minded attempt at correlation. A sensible approach would require the proportions of the minerals (arsenopyrite, pyrite and pyrrhotite) in each feed, plus the usual grade of gold these minerals carry individually. (Arsenopyrite is usually the richest). This last data was not available. It is likely that the sulfur forming from a given mineral would encapsulate gold in the matrix of that mineral. This might well also be a function of the size of the gold associated with a given mineral.

To summarize this issue, there remains a suspicion that elemental sulfur in residues could account for some of the gold losses, but it is only a suspicion. A separate investigation would be required to answer the question.

6.1.4 CHAPTER 4 - ELECTROCHEMISTRY

The purpose of the electrochemical investigation was to become familiar with the behaviour of the pyrite-nitric acid leaching system. In particular, the emphasis of linear potential-sweep voltammetry is on Eh and it was expected that elemental sulfur formation and oxidation could be studied.

The literature for this chapter necessarily overlapped that of Chapter 5. It pointed out the parallel reactions by which pyrite can oxidise, to sulfate or to elemental sulfur. The voltammetry confirmed these parallel paths. It showed that the

proportion of elemental sulfur formed was independent of temperature. It predicted that no elemental sulfur would be formed from pyrite in nitric acid above Eh 1.40 volts (SHE).

Calculations at the end of the chapter predicted oxidation rates in nitric acid leaching. The importance of quantification of the rate of oxidation of the elemental sulfur itself to sulfate was foreshadowed.

In retrospect, the predictions made about leaching rates from the electrochemistry work were possibly very good - the two checked were within 12% of experimental rates found in Chapter 5. If similar work was to follow this thesis, and funds and geography permitted, more use would be made of electrochemistry. Electrochemical results require a lot of interpretation and the technique is fussy. However, experiments, once set up, are quick and easy, and are repeatable.

6.1.5 CHAPTER 5 - PYRITE LEACH TESTS

The literature review of Chapter 5 pointed out the apparent conflict of much of the research and development work to date. In particular, some laboratory researchers seemed to be finding considerably more elemental sulfur present than developers were reporting. Thermodynamics was shown to be of little help, since elemental sulfur is metastable. Eminent researchers such as Peters and Woods considered elemental sulfur to be effectively stable. Peters proposed an overvoltage of at least + 0.5 V before S^0 oxidation became appreciable. The literature sparked ideas for testing such as attritioning and silver ion addition. The literature almost uniformly agreed that the mechanism for pyrite oxidation is complex and obscure.

The experimental results of the kinetic study produced few surprises. Variables affected leach rates as could be expected from a consideration of kinetic principles. One surprise was that the sulfur gap was larger than anticipated - 8% S^0 being quite normal during a leach test, falling to about 3% by about two hours. A suspected aging problem with the pyrite proved unfounded. Ferric and chloride ions reduced the sulfur gap but did not eliminate it. A higher Eh value did show promise of eliminating S^0 but this remains unproven. Further, much higher Ehs than 1.1 volts (SHE) may be unobtainable in the nitric acid system. Silver ion addition also appeared to stop S^0 formation, but more tests would be required to prove this statistically.

Chemical analyses accuracy and Eh measurement are both areas for improvements in technique.

The mathematical analysis of Section 5.9 succeeded in quantifying many of the trends in the experimental results. The analysis could have been both more extensive and more sophisticated. This was resisted because it was felt that the value of results decreases as they are manipulated. The experimentally determined first-order rate constants are detailed in Table 5.9.2.1 (pages 151-152). The rate constants for pyrite producing ferric ion varied in the range of 0.003 - 1.10 min⁻¹.

Further analysis and modelling suggested that the S⁰ → SO₄⁼ first-order rate constants were in the range of 0.005 - 0.04 min⁻¹. The solution is actually indeterminate, as the proportion of S⁰ originally formed, and its subsequent oxidation rate, both affect the sulfur gap which is the measured variable. However, the original sulfur proportion was postulated from the electrochemical results, there is strong evidence supporting the sulfur oxidation rate constant values used, and the resultant calculated models are quite close to the actual leach test data. Further, there are physical colour changes observable which correlate well with the elimination of pyrite in the leach tests.

The kinetic data showed a better fit to first-order kinetics than to the shrinking-core model. Typical regression analysis coefficients were 0.961 for first-order as opposed to 0.914 for shrinking-core. If the lag period was removed, the first-order model fit improved to r = 0.991 for the same data. It is interesting to note that some tests from the literature at conditions close to those employed in the present study, fit both first-order and shrinking-core models (r = 0.997 and 0.987 respectively).

The effects of various variables on the dissolution rate of pyrite appears to be additive. Two tests conducted gave predicted versus actual results within 30%. Calculations gave an Arrhenius activation energy of 77 kJ mol⁻¹ for the data with the lag time incorporated.

Very limited computer simulation of the data was attempted by a colleague (Ross Frick of University of South Australia, a statistician). In order to obtain a good fit of a curve with an appreciable lag time (S-19, 70°C) an inhibiting phenomena must exist, with a half-life of 360 minutes. This could be an elemental sulfur layer on the pyrite surface. The work warrants further investigation.

The proportion of elemental sulfur formed, as calculated from the modelling of subsection 5.9.7, is even larger than anticipated. Twenty percent (one atom of S⁼ in

five) is a justifiable proportion for 2.6 M nitric acid. Subsequent oxidation of this sulfur to sulfate is fast enough to reduce the sulfur gap to 3%, as reported by some developers. However, it is too slow to eliminate elemental sulfur, once formed, at temperatures below boiling.

Given the fact that elemental sulfur cannot be prevented from forming in appreciable proportions (Ag^+ and Eh being possible exceptions) and the further fact that once liquid, S^0 causes even more problems - the only way to eliminate it is high temperatures, about 190°C . The developers of nitric acid processes had it right some years ago.

For a glimpse of how much elemental sulfur is acceptable in residues, the reader is invited to return to Table 6.1.3.1. There is a suspicion, particularly from the Stawell concentrates, that elemental sulfur in residues is contributing to gold losses. This is unproven but worthy of further work.

6.2 SPECIFIC FINDINGS

6.2.1 PYRITE OXIDATION KINETICS

The fundamental kinetics of the pyrite-nitric acid system has been studied. The kinetics fit a first-order model, with an initiation (lag) period, and reduced rates above 95-99% pyrite dissolution. First-order kinetic rate constants for twelve variables have been evaluated. The rate is chemically controlled, with an activation energy of about 77 kJ mol^{-1} .

6.2.2 ELEMENTAL SULFUR FORMATION

The parallel routes by which pyrite oxidises to form sulfate and elemental sulfur are confirmed by both the electrochemical and leach tests of the present work. The **proportion** of elemental sulfur formed is larger than limited reporting has suggested. For 2.6 M nitric acid, the proportion of S^0 is about twenty percent. No variable tested proved able to eliminate elemental sulfur formation, although Eh and silver ion are worthy of further evaluation.

6.2.3 ELEMENTAL SULFUR OXIDATION

Oxidation of elemental sulfur, once formed, is slow but appreciable. For typical conditions tests of 2.6 M nitric acid at 80°C, the first-order rate constant (k_d) for S^0 oxidation is 0.007 min^{-1} , compared to k_a for iron dissolution of 0.048 min^{-1} . These comparative rates account for much of the discrepancy in reporting elemental sulfur proportions measured. The measurable amount depends not only on the detailed experimental conditions but also on when the measurements are taken.

The rate constant for elemental sulfur oxidation is itself affected by experimental conditions. However, its sensitivity appears to be an order of magnitude less than that of the rate constant for pyrite oxidation. The overall pyrite oxidation picture is perhaps best understood from Figure 5.9.7.6 (page 176).

6.2.4 ELEMENTAL SULFUR PROPORTION SENSITIVITY

The electrochemical work found that elemental sulfur proportion was independent of temperature. This was supported by the leach tests. The electrochemical work suggested no S^0 would be formed at redox potentials above 1.4 volts (SHE). This remains unproven from the leach tests. Chemically increasing the Eh of nitric acid leaching above about 1.2 volts may not be possible.

6.2.5 LAG TIME PHENOMENON

The Gumeracha pyrite used for the majority of the tests displayed a lag period before maximum leaching rates were obtained. This proved to be the major difference between Gumeracha material, another pyrite tested, and a third from the literature. With lag period removed from the analysis, the three pyrites displayed first-order rate constants within 20%.

6.2.6 Eh MEASUREMENTS

Measurement of Eh at high acid strengths and temperatures proved unreliable. Probe drift in 2.6 HNO_3 was temperature dependent and heating rate dependent. Attempts to reduce drift using a remote leg were unsuccessful.

6.3. GENERAL PATTERNS FOUND

6.3.1 IMPROVED VIABILITY OF LOW TEMPERATURE 'REDOX' VARIANTS

The hope that the present work would allow sufficient improvement in kinetics for the low-temperature "Redox" variant to be applicable to high-sulfur feedstocks has proved unfounded. If enough elemental sulfur is produced to be a problem, the high-temperature variant remains the sole solution.

There is an unconfirmed suspicion that residual S^0 reduces gold recovery to a small extent, even for low-sulfur feeds. Confirmation of this suspicion, and commercial assessment of any reduction, are beyond the scope of this work.

6.3.2 PREDICTIVE ABILITY OF ELECTROCHEMICAL TESTWORK

The electrochemical tests may be quite good for predicting oxidation rates in the pyrite-nitric acid system. This would be consistent with kinetics which are controlled, at the liquid-solid interface, by chemical reaction rate. This should apply at various degrees of oxidation. Two predictions of oxidation rate from the electrochemical tests proved to be within 12% of actual leach rates (after the lag period). This is very encouraging, although more comparisons need to be made.

6.3.3 UNIQUE NATURE OF CURRENT STUDY

The limitations of previous studies have been discussed. The current study is one of only two studies on pyrite-nitric acid. The current study is more comprehensive. The use of electrochemistry to study the pyrite nitric acid system is new. No evaluation of the additive effect of variables has been attempted before.

Elemental sulfur figures reported have been limited and in apparent conflict. Sulfur was noted only by most developers, and when it was measured, that was done only at the end of leach tests (ie, in residues).

6.3.4 USEFULNESS OF CURRENT STUDY

The present study is a fundamental one, though with the range of variables chosen as to be industrially realistic. No breakthrough was found which allowed the elimination of elemental sulfur. However, it is hoped that a better understanding of the fundamental kinetic of pyrite in nitric acid may be useful to developers and

operators of nitric acid pre-oxidation systems. At the very least, the quantification of variables' effects should be useful.

6.3.5 SULFIDE OXIDATION PUZZLE

The analogy has already been drawn that sulfide oxidation is a massive, multidimensional crossword puzzle, with only a few of the white squares pencilled in. The current work fills in quite a few squares, but only for the pyrite-nitric acid corner of the puzzle. What it does highlight is just how much the picture is influenced by the experimental variables chosen, and by the magnitude of those variables. **Everything affects sulfide oxidation rates.** It is quite understandable how early investigators appeared to get conflicting results - they were looking at different parts of the puzzle.

6.3.6 TIME AS AN ADDITIONAL DIMENSION

In developing the beginnings of comprehension for the aforementioned jigsaw puzzle, the author has an instinctive feeling that time has been left out as a variable. In particular, time affects the sulfur gap for any experiment. This is obvious when the two rate constants ($\text{FeS}_2 \rightarrow \text{Fe}^{3+}$ and $\text{S}^0 \rightarrow \text{SO}_4^{2-}$) are quantified for a given experiment. What is not so obvious is that while change in experimental conditions may radically speed up iron dissolution (and hence direct SO_4^{2-} production), the $\text{S}^0 \rightarrow \text{SO}_4^{2-}$ reaction rate constant is much less affected by the changed conditions and **hence the sulfur gap is increased for a time even though the sulfur proportion formed is unchanged.** Thus the sulfur gap depends not only on the experimental conditions, but also on when it is measured. The writer believes this is the source of much apparent contradiction in reported experimental findings. The amount of sulfur reported has been a function of when the particular experiment was stopped. Developers reporting pilot plant results have found low amounts of elemental sulfur from pyrite because they were looking at points where the pyrite had disappeared and most of the elemental sulfur had oxidised as well.

6.4 **RECOMMENDATIONS**

It is to be expected that a number of questions remain unanswered or could be answered better after such an investigation as this one. The following recommendations fall into two groups. The first five follow more or less directly from the present work. The last four are interesting side issues which arose during the work but were set aside at the time.

6.4.1 PURSUE THE SILVER ION AND Eh TRAILS

Silver ion was the only variable tested which shows promise of eliminating elemental sulfur formation. It was not pursued further because that pursuit would require several parallel tests to prove statistically that elemental sulfur had not formed. (It is not enough to prove there is no S^0 in the residue.) A similar pursuit with attritioning had been very expensive.

The question needs to be discussed on a commercial basis first. If silver can be built up in recycled liquors, then feedstocks fairly high in silver may provide enough. The question is tied up with the amount of gold tied up in elemental sulfur - see subsection 6.4.6.

It would appear that an Eh of 1.4 volts, at which elemental sulfur should not form according to the electrochemical work, is not obtainable in nitric acid systems. However, it would be intellectually satisfying to verify the elimination of S^0 at that potential. This could probably be done in potassium permanganate solution without nitric acid.

The pursuit of both questions could probably be satisfied by ten leach tests. If the minimum level of silver ion required needed to be established, perhaps another ten runs would be required. For twenty tests, about five thousand dollars (\$5,000) would be required, mostly for assays.

6.4.2 TEST OTHER MINERALS

Since this program has been done once for pyrite, the study of another mineral should prove smoother. Arsenopyrite is the logical next choice. This could be a good PhD program, supervised by this writer.

6.4.3 ADDITIONAL MATHEMATICAL ANALYSIS OF CURRENT RESULTS

The modelling and mathematical analysis could be pursued further. This has a number of possibilities.

- further analysis of sulfur gap as a function of S^0 proportion and oxidation rates.
- quantify effect of the various variables on k_d , the rate constant for elemental sulfur oxidation.

- parametric computer curve fitting to see whether understanding of kinetic factors can be improved, in particular, lag time incorporation.

6.4.4 MORE SPECIFIC EXPERIMENTS FOLLOWING S⁰

The oxidation of elemental sulfur was inferred from models incorporating estimates for both S⁰ proportion and k_d. A more specific experimental method could determine S⁰ directly. One possibility would be stopping a given experiment at four or five progressive times and analysing for S⁰. Some quenching techniques would be required.

6.4.5 ELIMINATE LAG TIME

Better correlation of data is obtained when lag periods are mathematically removed from the analysis. One group of experimenters have apparently been able to eliminate lag time (by such techniques as washing with HCl) or else used a pyrite which did not display a lag period. This may not be realistic commercially.

6.4.6 EVALUATE EXTENT TO WHICH S⁰ TIES UP GOLD

Fairly large beaker tests should suffice to produce enough residue to recover elemental sulfur by, for example, flotation. This could then be analysed for gold. The extent to which elemental sulfur contributes to gold loss may be ore-dependent. Sulfur may also contribute by forming pellets of unreacted sulfides, and this will have to be tracked.

6.4.7 FURTHER ELECTROCHEMICAL INVESTIGATIONS

A number of questions could be investigated. The techniques are faster than leach tests and can establish the basis for them. Chronopotentiometry is one technique which may provide answers about inhibiting layers.

6.4.8 Eh MEASUREMENT

None of the writer's contacts could provide an answer to the problem of Eh probe drift in strong nitric acid at high temperatures. The problem may well be insoluble, but at least the drift could be quantified in terms of conditions. This would be a good final-year student project.

6.4.9 REFRACTORY GOLD ORE METAL BALANCE PROBLEMS

It is possible that a publication of the writer's problems with metal balances might save another researcher similar frustration. Such a publication would ideally include the location of a suitable package for varying the assays within limits, or the writing of a specific program for the task.

6.5 SUMMARY

The study has confirmed the parallel reactions by which pyrite oxidises in nitric acid. A fair amount of quantified knowledge has been contributed to the understanding of sulfide leaching. Rate constants for pyrite oxidation have been established. Rate constant for elemental sulfur oxidation have been postulated.

Elemental sulfur formation cannot be avoided during nitric acid leaching of pyrite. The proportion of elemental sulfur which forms is larger than has been reported for pyrite. The effect on residence time for low-temperature variant of the "Redox" process is such that if elemental sulfur causes unacceptable gold losses, the high-temperature variant must be resorted to. There is an indication that elemental sulfur in residue may be responsible for part of the unrecovered gold, usually about 7%, in cyanide residues. This is worthy of further investigation.

Further investigation may also be warranted on various questions, the most notable being the effect of adding silver to the leach. It may be worthwhile working to improve analytical techniques and to test other minerals of interest to companies with refractory gold deposits.

The oxidation of sulfides is a tremendous, complex puzzle. If the small portion of the puzzle illuminated by the writer's eight years of research proves useful to the gold industry, then the writer will be satisfied.

NOMENCLATURE

This list excludes standard chemical symbols and standard dimensional abbreviations

Latin

| | |
|-------------------|---|
| a | fraction of pyrite dissolved at the end of the lag period |
| E_{act} | Arrhenius activation energy, kJ mol^{-1} |
| Eh | reduction - oxidation potential of a solution (usually a mixed potential) volts |
| k | generalised rate constant, min^{-1} |
| k_a | first-order rate constant for iron dissolution $\text{Fe S}_2 \rightarrow \text{Fe}^{3+}$, min^{-1} |
| k_b | first-order rate constant for sulfate produced directly from pyrite $\text{FeS}_2 \rightarrow \text{SO}_4^{\text{direct}}$, min^{-1} |
| k_c | first order rate constant for elemental sulfur formation $\text{FeS}_2 \rightarrow \text{S}^0$, min^{-1} |
| k_d | first order rate constant for S^0 oxidation $\text{S}^0 \rightarrow \text{SO}_4^{\text{=}}$, min^{-1} |
| k_e | apparent first-order rate constant for total sulfate formation $\text{S}^0 + \text{FeS}_2 \rightarrow \text{SO}_4^{\text{total}}$, min^{-1} |
| Me | generalised symbol for metal |
| n | number of data points |
| O^{18} | isotope of oxygen |
| ppm | parts per million (generally by weight or mg l^{-1} for solutions) |
| R | ideal gas constant, $\text{J mol}^{-1} \text{ } ^\circ\text{K}^{-1}$ |
| r | correlation coefficient for regression analysis (1.0000 implies perfect fit) |
| rpm | revolutions per minute |
| S | sulfur as determined by chemical analysis - usually total sulfur as $\text{S}^{\text{=}}$ and S^0 |
| $\text{S}^{\#}$ | activated sulfur species |
| S-n | test number designation S-4, S-20, etc |
| S_8 | elemental sulfur - most stable polymer ring, but crystal form still unspecified |
| S_α | elemental sulfur, rhombic crystal form |
| SHE | Standard Hydrogen Electrode |
| S^0 | elemental sulfur - allotropic crystal form unspecified |
| t | time, min |
| t' | time minus the lag period, mins |

t_{lag} time at the end of the lag period, min
tpd tonnes per day
x extraction of a species from the solid (% or fraction)
x' normalised extraction (lag period removed)

Greek

μm metres x 10^{-6}

Acronyms

CRA Conzinc Riotinto Australia - major mining company
AMDEL Australian Mineral Development Laboratories
CSIRO Commonwealth Scientific and Industrial Research Organisation
AAS Atomic Absorption Spectrometry
PAR Princeton Applied Research
UBC University of British Columbia (Vancouver)
XRD X-Ray Diffraction
XPS X-Ray Photoelectron Spectroscopy

LIST OF FIGURES

Legend: 1 (Chapter)
 1.2. (Section)
 1.2.3 (Subsection)
 1.2.3.4 (Figure No.)

| Number | Title | Page |
|--------------|--|------|
| Frontispiece | Pyrite During Nitric Acid Leach | iii |
| 2.2.5.1 | Generalised Flowsheet for Pre-Oxidation and Cyanidation | 8 |
| 2.3.4.1 | Rates of Pyrite and Arsenopyrite Oxidation in Nitric Acid (from Fair et al. 1987) | 14 |
| 2.3.5.1 | Low Temperature Redox Process Flow Sheet (from Canterford 1994b) | 15 |
| 2.3.5.2 | High Temperature Redox Typical Process Flow Sheet (From Canterford 1994b) | 16 |
| 2.3.5.3 | Elemental Sulfur Formation and Oxidation in Pipe Reactor (from Leonard et al. 1990) | 16 |
| 2.4.3.1 | S ₈ Ring Structure (from Powell and Timms, 1974) | 22 |
| 3.4.1.1 | Typical Whole Ore Gold Balance | 33 |
| 3.4.1.2 | Typical Sulfide Concentrate Iron Balance | 34 |
| 3.4.3.1 | Typical Effect of Pre-oxidation on Gold Recovery | 37 |
| 3.4.3.2 | Typical Effect of Pre-oxidation on Reagent Consumptions | 38 |
| 4.2.1.1 | Voltammograms for a stationary pyrite electrode at pH4.6 (from Hamilton and Woods 1981) | 51 |
| 4.2.3.1 | Sulfide conversion to Sulfate as Found by Various Researchers (from Hiskey and Schlitt 1982) | 54 |
| 4.3.1.1 | Schematic of Equipment Arrangement | 57 |
| 4.3.1.2 | Schematic of Electrode Polishing | 59 |
| 4.4.1.1 | Test "A" from Manual | 60 |
| 4.4.1.2 | Duplication of test "A" | 60 |
| 4.4.1.3 | Test "B" from Manual | 61 |
| 4.4.1.4 | Duplication of test "B" | 61 |
| 4.4.2.1 | Hamilton and Woods Experiment Result | 63 |
| 4.4.2.2 | Duplication of Hamilton and Woods Experiment | 63 |
| 4.5.2.1 | Voltammetric sweep for pyrite electrode + 1.7., - 0.75 volts in 0.5 M H ₂ SO ₄ | 66 |

| Number | Title | Page |
|---------------|---|-------------|
| 4.5.2.2 | Voltammetric sweep for pyrite electrode + 1.7, - 0.75 volts in 0.22 M HNO ₃ | 66 |
| 4.5.3.1 | Voltammetric sweeps for pyrite electrode + 0.97, - 0.28 volts in 0.5 M H ₂ SO ₄ and 0.22 M HNO ₃ | 68 |
| 4.6.2.1 | Typical voltammetric scan Main Test Series | 70 |
| 4.6.3.1 | Resolution of area under anodic curve | 71 |
| 4.6.3.2 | Resolution of area under cathodic curve | 72 |
| 4.6.4.1 | Anodic portions of voltammograms for pyrite electrode in 0.22 M HNO ₃ at different temperatures | 74 |
| 4.6.4.2 | Cathodic portions at voltammograms for pyrite electrode at 60°C, reversed at different anodic potentials | 75 |
| 4.6.4.3 | Dependence of Proportion of pyrite sulfur oxidised to Sulfate as a function of the upper potential limit of the scan | 76 |
| 4.6.4.4 | Comparison of experimental Sulfate Yield to literature | 78 |
| 5.2.2.1 | Equilibrium Eh-pH diagrams for Fe-S-H ₂ O systems at 25°C and 100°C, 1 atm (from Ferreira, 1995) | 91 |
| 5.2.3.1 | Eh-pH diagram at the Fe-S-H ₂ O system with extended metastable zones (from Peters 1984) | 93 |
| 5.2.3.2 | Extent of Elemental Sulfur formed as a function of Nitric Acid concentration and time at 70°C (from Kadioglu et al. 1995) | 95 |
| 5.2.4.1 | Correlation of Pyrite Dissolution data with surface reaction rate equation (from King and Lewis 1980) | 97 |
| 5.2.4.2 | Electrolytic current at constant voltage (from Shashi et al. 1987) | 99 |
| 5.3.2.1 | Schematic of Leach Test Apparatus | 104 |
| 5.3.3.1 | Schematic of Attritioning Apparatus | 107 |
| 5.4.3.1 | Typical pyrite leach test in nitric acid | 113 |
| 5.5.1.1 | Minimum Stirring Speed to keep sand particles in suspension | 115 |
| 5.5.1.2 | The effect of stirring rate | 116 |
| 5.5.2.1 | Effect of temperature - Gumeracha pyrite | 118 |
| 5.5.2.2 | Effect of temperature - Huanzala pyrite | 119 |
| 5.5.3.1 | Effect of Particle Size | 120 |
| 5.5.4.1 | Effect of [HNO ₃] | 121 |
| 5.6.1.1 | Checking leach test Method Consistency | 123 |

| Number | Title | Page |
|---------------|--|-------------|
| 5.6.2.1 | Aging of pyrite check 125-180 μm 80°C | 124 |
| 5.6.2.2 | Aging of pyrite check 125-180 μm 75°C | 125 |
| 5.6.2.3 | Aging of pyrite check 90-125 μm 80°C | 125 |
| 5.6.2.4 | Aging of pyrite check 63-90 μm 75°C | 126 |
| 5.6.2.5 | Aging of pyrite check Huanzala 90-125 μm 75°C | 127 |
| 5.7.1.1 | Effect of $[\text{H}_2\text{SO}_4]$ | 129 |
| 5.7.2.1 | Effect of adding Fe^{3+} (Fe dissolution only) | 130 |
| 5.7.2.2 | Effect of adding Fe^{3+} ($\text{S}^{=}$ \rightarrow $\text{SO}_4^{=}$ only) | 131 |
| 5.7.3.1 | Effect of Cl^- Ion (Fe dissolution only) | 132 |
| 5.7.3.2 | Effect of Cl^- Ion ($\text{S}^{=}$ \rightarrow $\text{SO}_4^{=}$ only) | 133 |
| 5.7.4.1 | Effect of Pulp Density | 134 |
| 5.7.5.1 | Effect of Blend of Sizes (adapted) | 136 |
| 5.8.1.1 | Effect of Scrubbing with glass balls | 138 |
| 5.8.1.2 | Effect of Attritioning | 139 |
| 5.8.2.1 | Variation of Eh with Time and FeS_2 oxidation | 141 |
| 5.8.2.2 | Effect of increasing Eh (1.1. - 1.37 volts SHE) | 142 |
| 5.8.3.1 | Effect of Ag^+ Ion | 143 |
| 5.8.3.2 | Iron and Sulfate Extractions at 5×10^{-3} M Ag^+ | 144 |
| 5.8.4.1 | Additive effect of variables | 146 |
| 5.8.5.1 | Range of tests showing Lag Periods | 147 |
| 5.8.6.1 | Comparison of Pyrites from Three Sources | 149 |
| 5.9.2.1 | Rate Constant Variation with Temperature - Arrhenius Plot | 153 |
| 5.9.2.2 | Variation of Rate Constant with Particle Size | 154 |
| 5.9.2.3 | Variation of Rate Constant with Size Blends | 155 |
| 5.9.2.4 | Variation of Rate Constant with Nitric Acid Concentration | 155 |
| 5.9.2.5 | Variation of rate constant with Sulfuric Acid Concentration | 156 |

| Number | Title | Page |
|---------------|---|-------------|
| 5.9.2.6 | Estimated Variation of Rate Constant with Fe ³⁺ , Cl ⁻ , and Ag ⁺ addition | 157 |
| 5.9.3.1 | Fit of Raw Temperature series data to First-Order Model | 159 |
| 5.9.3.2 | Fit of Raw Temperature series data to shrinking-core model | 160 |
| 5.9.3.3 | Fit of Data from Literature to Models | 161 |
| 5.9.4.1 | "Normalised" First-Order temperature series data (lag period removed) | 162 |
| 5.9.6.1 | Arrhenius plots for Gumeracha pyrite | 165 |
| 5.9.7.1 | Iron and sulfate First-Order Plots (S-20 plus S-32 combined) | 167 |
| 5.9.7.2 | Iron and sulfate Extraction Plots (S-4) | 169 |
| 5.9.7.3 | Leach test for Additive Factors (S-79) | 170 |
| 5.9.7.4 | Sulfate curve Models vs Actual | 172 |
| 5.9.7.5 | "Sulfur Gap" comparison Model vs Actual | 173-175 |
| | a) (S-20 + S-32) combined | |
| | b) S-4 | |
| | c) S-48 | |
| | d) (S-16 + S-64) combined | |
| 5.9.7.6 | Relative Oxidation Reaction rates for Pyrite in 2.6 M HNO ₃ | 176 |
| 5.10.3.1 | Effect of S ⁰ Oxidation on Leach Reaction Residence Time | 186 |
| 5.10.3.2 | Iron and Sulfate First-Order Plots (Ag ⁺ addition tests) | 188 |

LIST OF TABLES

Legend: 1 (Chapter)
 1.2. (Section)
 1.2.3 (Subsection)
 1.2.3.4 (Table No.)

| Number | Title | Page |
|---------|---|------|
| 2.3.3.1 | Relative reactivity and elemental sulfur yield of pure minerals leached with nitric acid (from Prater et al. 1973) | 12 |
| 2.3.3.2 | Effect of temperature and concentration on elemental sulfur formation (from Prater et al. 1973) | 12 |
| 2.3.3.3 | Results of HNO ₃ -H ₂ SO ₄ -H ₂ O interaction with elemental sulfur (from Prater et al. 1973) | 12 |
| 2.3.5.1 | Relative costs for pre-oxidation processes (from Canterford 1994b) | 17 |
| 2.3.6.1 | Previous experimental conditions tested | 18 |
| 3.2.1.1 | Chemical analyses of feedstocks | 29 |
| 3.4.1.1 | Typical rolling bottle log | 35 |
| 3.4.2.1 | Approximate mineralogy of gold bearing materials | 35 |
| 3.4.2.2 | Grinding data for cyanide and autoclave test feeds | 36 |
| 3.4.2.3 | Amalgamation test data | 36 |
| 3.4.2.4 | Variability of feed samples for gold content | 36 |
| 3.4.3.1 | The effect of pre-oxidation with nitric acid on cyanidation of four gold bearing materials | 37 |
| 3.4.4.1 | Gold and silver departments | 38 |
| 3.4.4.2 | Iron, Copper, Arsenic and Antimony departments for autoclave and cyanidation tests | 39 |
| 3.4.5.1 | Autoclave test on elemental sulfur | 40 |
| 3.4.5.2 | Elemental sulfur in autoclave residues | 40 |
| 3.5.5.1 | Predicted elemental sulfur in autoclave residues | 44 |
| 4.6.1.1 | Anodic Settings for Main Test Series | 69 |
| 4.6.4.1 | Moles of sulfur and sulfate produced by electrochemical oxidation of pyrite in nitric acid on potential scans at 20 mV s ⁻¹ | 76 |
| 4.6.4.2 | Calculation - moles of S ⁰ oxidised cm ⁻² | 77 |
| 5.2.2.1 | Limitations of classical Eh-pH diagrams | 90 |

| Number | Title | Page |
|---------|---|---------|
| 5.2.3.1 | Summary of the kinetics of aqueous oxidation of pyrite (from Hiskey and Schlitt 1982) | 92 |
| 5.3.1.1 | Pyrite assays | 103 |
| 5.3.5.1 | Calculation method comparison S-4 | 109 |
| 5.5.1.1 | Observations during leach test | 117 |
| 5.5.2.1 | "Sulfur gap" for Gumeracha pyrite temperature test series | 119 |
| 5.5.2.2 | "Sulfur gap" for Haunzala temperature test series | 119 |
| 5.5.3.1 | Surface area for different size fractions | 120 |
| 5.5.4.1 | "Sulfur gap" for [HNO ₃] test series | 121 |
| 5.6.1.1 | Leach test consistency | 123 |
| 5.7.2.1 | "Sulfur gap" for [Fe ³⁺] series | 130 |
| 5.7.3.1 | "Sulfur gap" for [Cl ⁻] series | 132 |
| 5.7.5.1 | "Sulfur gap" for blend of sizes series | 136 |
| 5.8.1.1 | "Sulfur gap" for scrubbing series | 138 |
| 5.8.1.2 | Residues from attritioning series | 139 |
| 5.8.1.3 | "Sulfur gap" for attritioning series | 140 |
| 5.8.2.1 | Redox potential (Eh) variation with conditions | 141 |
| 5.8.3.1 | Effect of Ag ⁺ Ion | 143 |
| 5.8.6.1 | Raw data for leach tests on pyrite from three different sources | 149 |
| 5.9.2.1 | First-order rate constant for pyrite HNO ₃ leach tests a) classical variables b) industrial variables c) additional factors | 151-152 |
| 5.9.2.2 | Variation of rate constant with ferric ion concentration | 156 |
| 5.9.2.3 | Assumed variation of rate constant with chloride ion and silver ion concentrations | 157 |
| 5.9.2.4 | Comparing additive rate constants S-71 to S-78 | 158 |
| 5.9.2.5 | Comparing additive rate constants S-23 to S-79 | 158 |
| 5.9.3.1 | Rate Constant Fitting for raw temperature series data | 160 |
| 5.9.3.2 | Rate Constant Fitting for raw temperature series with Lag Periods Excluded | 161 |
| 5.9.4.1 | Gumeracha pyrite temperature series "Normalised" | 162 |

| Number | Title | Page |
|---------------|---|-------------|
| 5.9.4.2 | Arrhenius plot fitting - Gumeracha temperature series | 163 |
| 5.9.4.3 | Statistical data for Gumeracha [Fe ³⁺] series | 163 |
| 5.9.4.4 | Lag period described as changing rate constant | 164 |
| 5.9.5.1 | Comparison of pyrite sources | 165 |
| 5.9.7.1 | First-order plot results (Lag period excluded) | 168 |
| 5.9.7.2 | Inflection point data - extraction | 170 |
| 5.9.7.3 | Rate constants for oxidation reactions | 172 |
| 5.10.2.1 | Actual vs predicted pyrite oxidation rates | 182 |
| 5.10.3.1 | Reaction leach times for four cases | 186 |
| 5.10.3.2 | Sulfur formation and oxidation (High Eh tests) | 187 |
| 5.10.3.3 | Sulfur formation and oxidation (Ag ⁺ addition tests) | 188 |
| 5.10.3.4 | Effect of variables on kinetics of FeS ₂ and S ⁰ oxidation | 188 |
| 6.1.3.1 | Relationship between elemental sulfur in pre-oxidation residue and gold loss on cyanidation | 196 |

APPENDIX

Supporting Investigations

This appendix provides evidence, mainly scanning electron microscope (SEM) microphotographs and Xray Diffraction Analyses (XRD), which supports various points made in the thesis. The actual analysis were done by experienced technicians, and only a few of the typical results are given here.

Figure A-1: SEM Microphotograph (50X) Huanzala Pyrite plus SEM elemental analysis graph

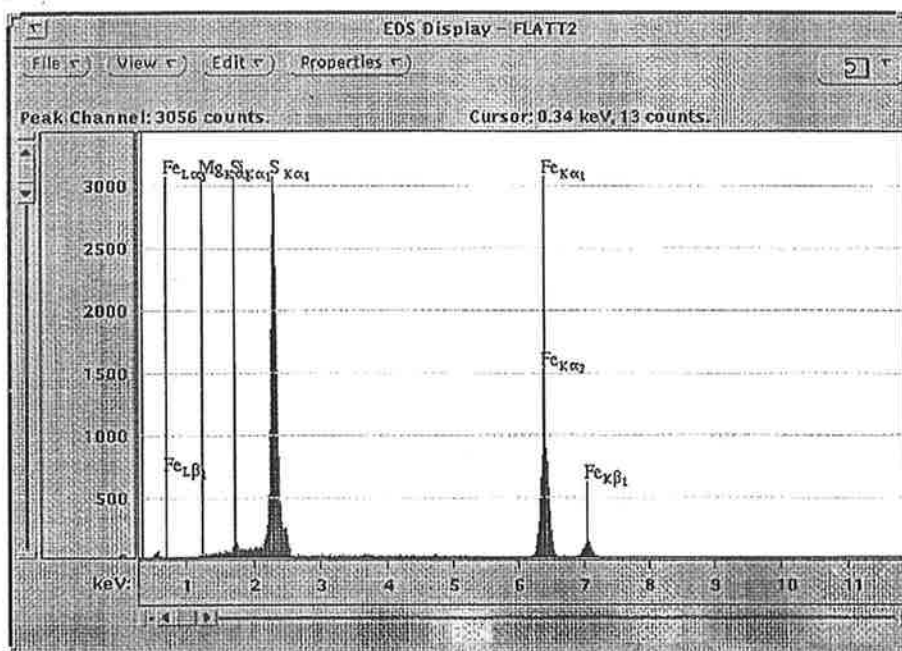
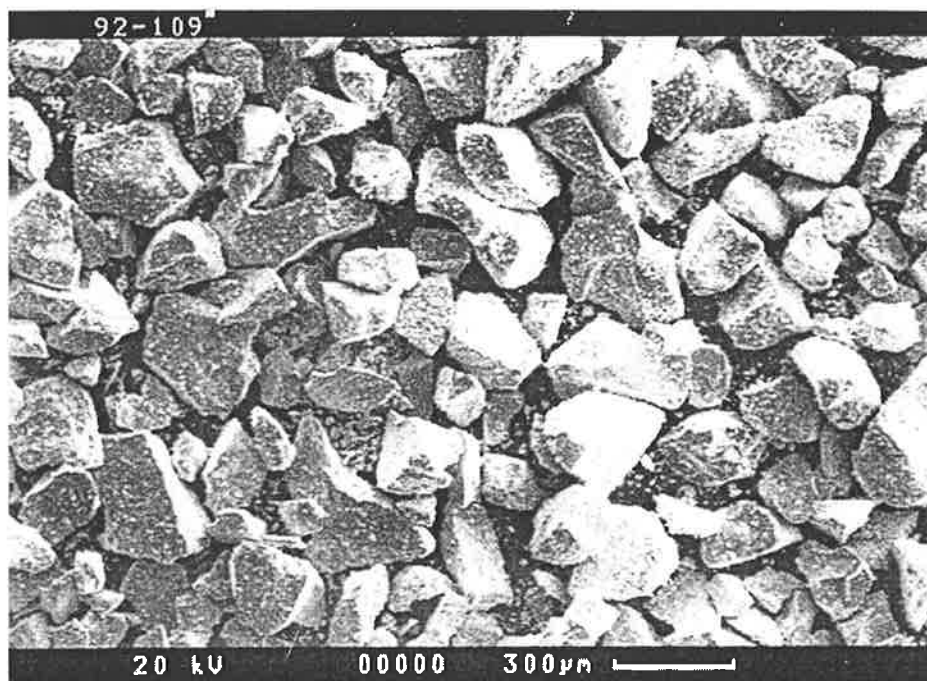
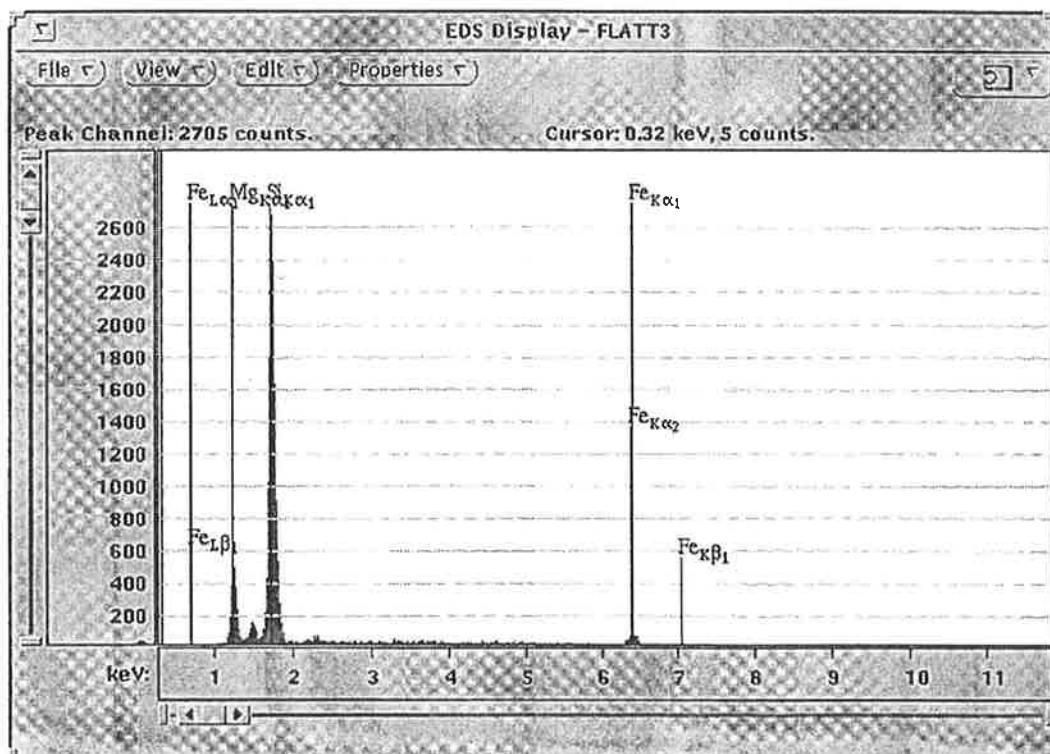
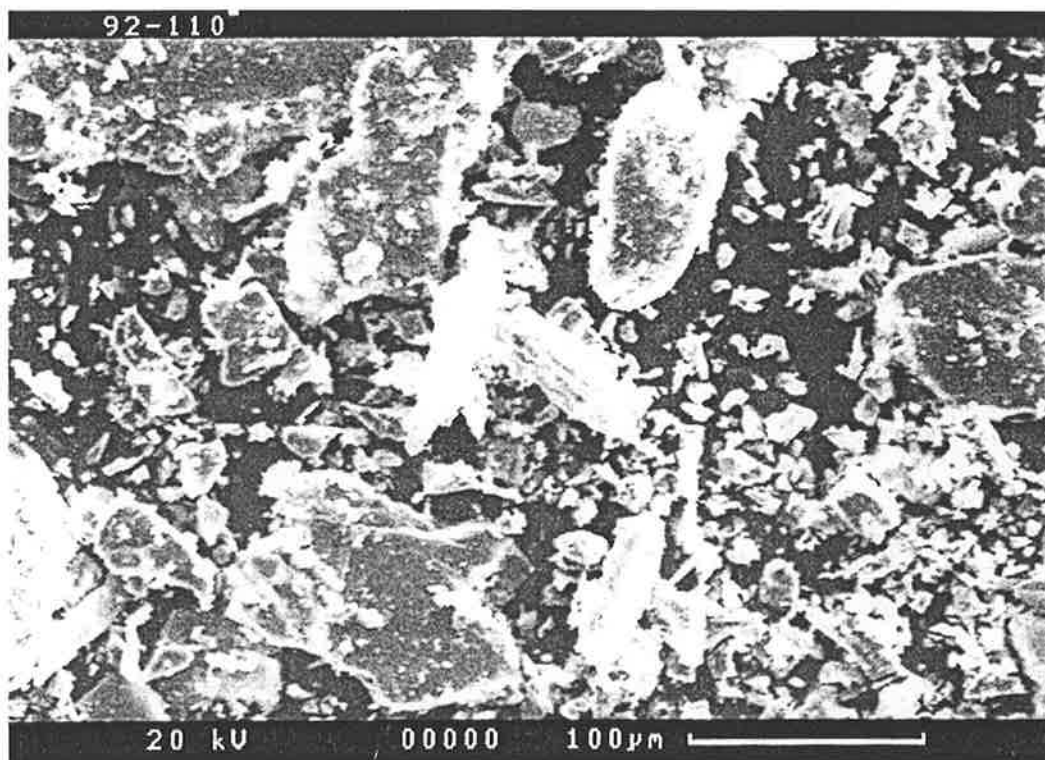


Figure A-1 shows a typical feed material for the nitric acid leach tests. Iron and sulfur are identified, plus minor magnesium and silicon. XRD analysis of the same sample identified only pyrite, so no other component makes up as much as 5%.

Figure A-2: SEM Microphotograph (250x) of HNO₃ Leach Residue (Heavy liquid float fraction after Soxhlet dissolution of S⁰) plus SEM elemental analysis graph



The material in Figure A-2 is the majority of the HNO₃ leach residue from run S-8 (Gumeracha pyrite, 90.125 mm, 2.6 M HNO₃, 70°C, 200 rpm, plus 0.2 M Fe³⁺). Given that the leach run feed was the same size as for Figure A-1, it can be seen that the residue is much finer, when the different magnifications are taken into account. This is consistent with the gangue being inside the nearly pure pyrite crystals.

The overall SEM elemental scan and its companion XRD work showed that this residue float fraction (density <3.0) was mainly silica plus talc. Weights showed the residue floats to be 2% of the original pyrite. Other work showed the sinks to be mainly chalcopyrite - CuFeS₂, amounting to about 1% of the original pyrite.

The implications of the data are to confirm the chemical analysis of the solid pyrite, which indicated 96.5% FeS₂, 2.5% gangue minerals and 0.8% trace metals.

Table A-1: Comparison of Sink-Float and Visual Analyses

All figures are expressed as w/o of the original pyrite material which remained undissolved

| Leach Residue | Analysis by sink-float | | | Analysis by Microscope | | |
|---------------|------------------------|------------|----------|------------------------|------------|----------|
| | % S | % Sulfides | % Gangue | % S | % sulfides | % Gangue |
| S-4 | 3 | 1 | 2 | 2 | 2 | 2 |
| S-6 | 3 | 22 | 0 | 1 | 22 | 2 |
| S-8 | 3 | 1 | 2 | 3 | 1 | 2 |

Table A-1 shows that the rapid and easy microscopic analysis compares very well to the more rigorous analysis by heavy-liquid following Soxhlet dissolution of S^o. The implication for the extraction calculations is that errors due to visual analysis of residues will be acceptable, generally less than 2%.

The **Frontispiece** shows a portion of the solids from run S-48 at 50 minutes. At this point, iron extraction was 55%, sulfate in solution was 40%. The photograph shows pyrite crystals, pitted from nitric acid attack, bound together with waxy translucent elemental sulfur.

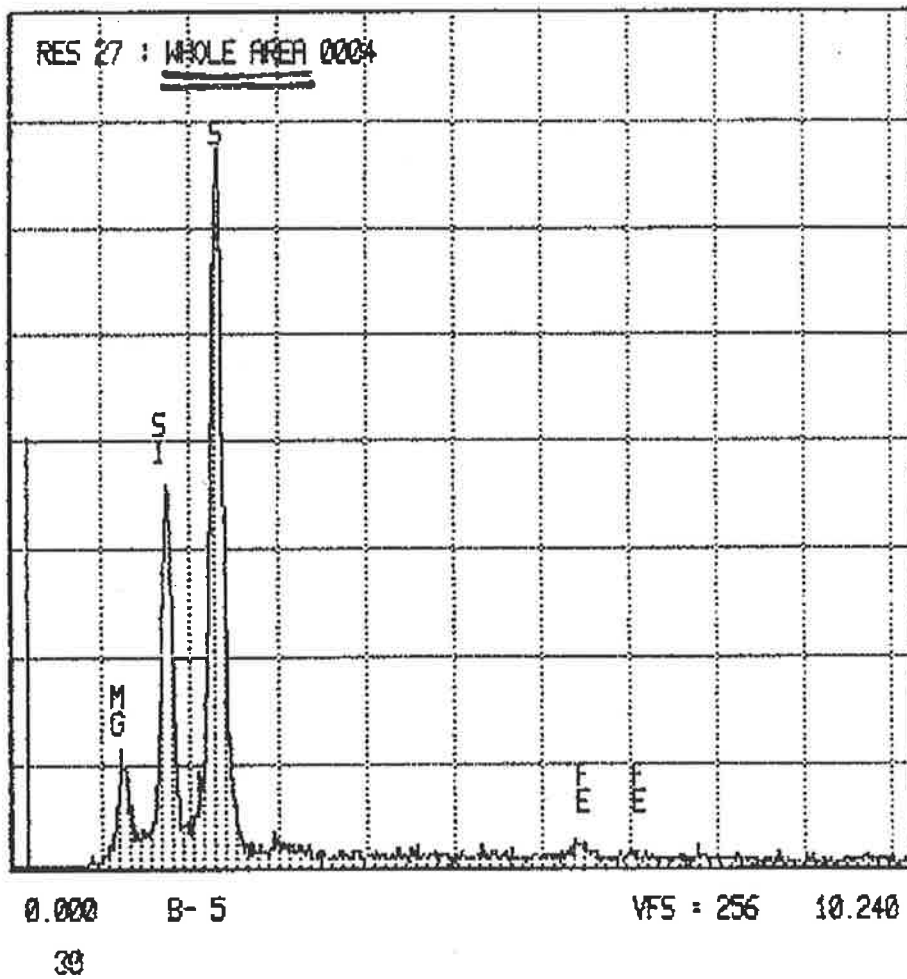
Conditions: Gumeracha pyrite, 125-180 μm, 2.6 M HNO₃, 270 rpm, 80°C, April 23, 1993.

Figure A-3 SEM Microphotograph (250x) of HNO₃ Leach Residue



C.E.M.S.A. Uni of Adelaide Philips 505 WED 03-JUN-92 16:08

Cursor: 0.000keV = 0 ROI (1) 0.000: 0.000



The residue of figure A-3 is from leach test S-7 Gumeracha pyrite, 90/125 mm, 2.6 M HNO₃, 50°C, 128 rpm. These early results confirmed that residues were mostly elemental sulfur and gangue.

Figure A-4 SEM Microphotograph (2250x) Elemental Sulfur Forming on Pyrite Crystal

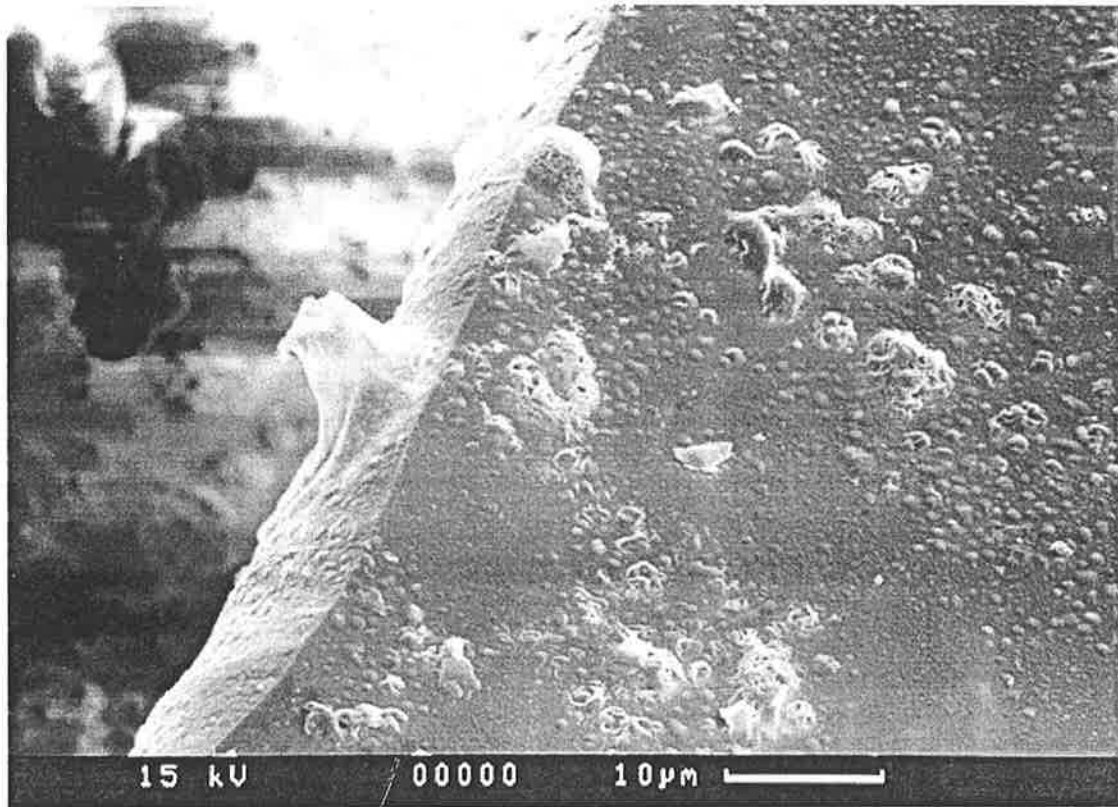
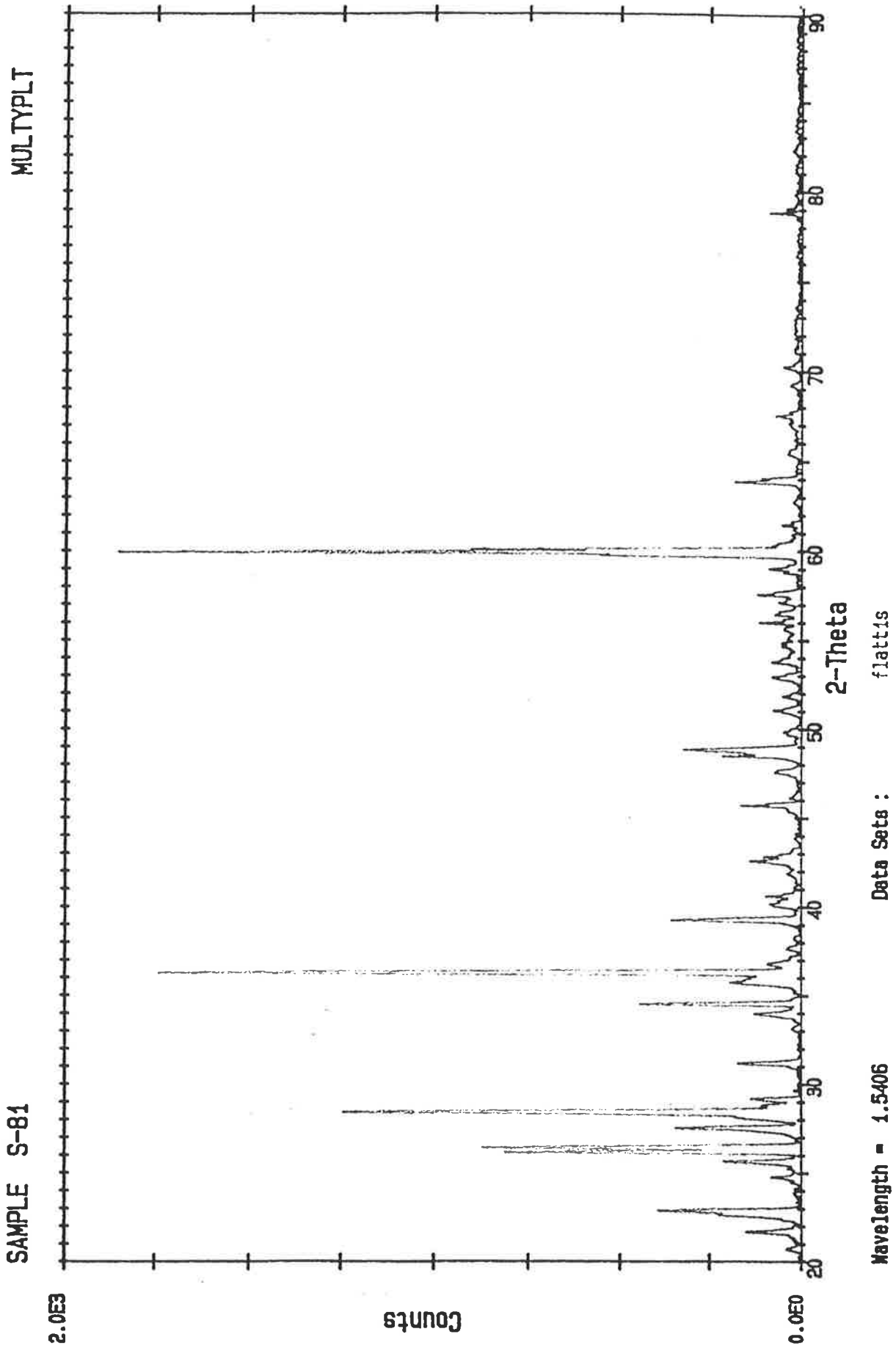


Figure A-4 shows elemental sulfur left behind on the edge of a pyrite crystal. This is the 50 minute sample (61% Fe³⁺ bulk dissolution, 41% SO₄⁼ bulk dissolution) of sample S-48, although there is no guarantee that this crystal is representative. S-48 conditions were: Gumeracha pyrite 125/180 mm, 2.6 M HNO₃, 80°C, 280 rpm

Figure A-5 XRD Scan of HNO₃ Leach Residue
plus Report and Powder Diffraction Table



Input Pattern

| d | I | d | I | d | I | d | I | d |
|-------|----|--------|----|--------|----|--------|----|--------|
| 4.269 | 2 | 3.173 | 8 | 2.4410 | 4 | 1.8750 | 11 | 1.6400 |
| 4.092 | 8 | 3.133 | 67 | 2.3850 | 2 | 1.8630 | 17 | 1.6270 |
| 3.917 | 12 | 3.090 | 5 | 2.2910 | 19 | 1.8290 | 2 | 1.6110 |
| 3.875 | 21 | 3.053 | 7 | 2.2430 | 4 | 1.7870 | 4 | 1.5990 |
| 3.590 | 4 | 2.8670 | 8 | 2.2170 | 5 | 1.7620 | 2 | 1.5630 |
| 3.461 | 11 | 2.6340 | 7 | 2.1200 | 7 | 1.7270 | 4 | 1.5410 |
| 3.400 | 43 | 2.5960 | 22 | 2.1070 | 5 | 1.7020 | 4 | 1.5070 |
| 3.368 | 46 | 2.5160 | 8 | 1.9810 | 9 | 1.6770 | 3 | 1.4790 |
| 3.230 | 18 | 2.4720 | 93 | 1.9060 | 3 | 1.6510 | 2 | 1.4560 |

100

50 lines in pattern.

Identified Phases:

JCPDS= SI ML/X At% Identity . . .
 24-0733D 131 24/9 33 Sulfur / Sulfur, syn = S
 Ierr:50,150 derr:2.0 Bground:1 dmax/min:4.431/1.089

Summary Report:

| d | I | Full | Resid | 24-0733: | 33% |
|--------|----|------|-------|----------|------|
| d | I | I | I | d | I |
| 4.269 | 2 | 2 | | | |
| 4.092 | 8 | None | | 4.060 | 4.0 |
| 3.917 | 12 | 7 | | 3.918 | 5.3 |
| 3.875 | 21 | None | | 3.854 | 33 |
| 3.590 | 4 | None | | 3.570 | 2.3 |
| 3.461 | 11 | None | | 3.447 | 12 |
| 3.400 | 43 | 42 | | 3.384 | 1.3* |
| 3.368 | 46 | 46 | | <3.336 | 7.3> |
| 3.230 | 18 | None | | 3.219 | 14 |
| 3.173 | 8 | 8 | | | |
| 3.133 | 67 | 67 | | <3.113 | 6.6> |
| 3.090 | 5 | None | | 3.084 | 5.0 |
| 3.053 | 7 | 7 | | | |
| 2.8670 | 8 | 8 | | <2.848 | 5.6> |
| 2.6340 | 7 | None | | 2.625 | 3.6 |
| | | | | <2.617 | 3.0> |
| 2.5960 | 22 | 22 | | | |
| 2.5160 | 8 | 8 | | <2.502 | 2.3> |
| | | | | <2.487 | 1.7> |
| 2.4720 | 93 | 93 | | | |
| 2.4410 | 4 | 4 | | <2.426 | 4.0> |
| 2.3850 | 2 | None | | 2.378 | 1.3 |
| | | | | <2.369 | 2.0> |
| 2.2910 | 19 | 17 | | 2.289 | 2.0* |
| 2.2430 | 4 | 4 | | | |

| | | | | d Å | Int. | h k l |
|---|-------------------|------------------------|-------------------|-------|------|-------|
| alpha-S | | | | 7.69 | 6 | 1 1 1 |
| Sulfur | | | | 5.76 | 14 | 1 1 3 |
| | | | | 5.68 | 6 | 0 2 2 |
| Sulfur, syn | | | | 4.60 | 2 | 2 0 2 |
| | | | | 4.19 | 2 | 1 1 5 |
| Rad: CuKα1 | λstd: 1.5405 | Filter: | d-sp: D.S. -114.6 | | | |
| Cutoff: 50.0 | Ins: Densitometer | i/loor: | | 4.06 | 12 | 2 2 6 |
| Ref: de Wolff, P., Technisch Physische Dienst, Delft, the Netherlands, 1000 | | | | 3.91 | 12 | 1 3 1 |
| Grant-in-Aid | | | | 3.85 | 100 | 2 2 2 |
| | | | | 3.57 | 8 | 1 3 3 |
| Sys: orthorhombic | | | | 3.44 | 40 | 0 2 6 |
| S.G.: Fdd (70) | | | | | | |
| a: 10.45 | b: 12.84 | c: 24.46 | A: C: | | | |
| A: | B: | C: | Z: 128 | 3.38 | 4 | 2 2 4 |
| Ref: ibid. | | | | 3.33 | 26 | 3 1 1 |
| | | | | 3.21 | 60 | 0 4 0 |
| Dx: 2.08 | Dy: 2.07 | SS/FON: F0=30(1023,44) | | 3.11 | 25 | 3 1 3 |
| | | | | 3.08 | 18 | 1 3 5 |
| ea: 1.9579 | rsb: 2.0377 | ey: 2.2452 | Sigt: 2θ: 69 deg. | | | |
| Ref: Dana's System of Mineralogy, 7th Ed., I | | | | 3.06 | 2 | 0 0 6 |
| | | | | 2.842 | 18 | 0 4 4 |
| | | | | 2.688 | 2 | 3 3 1 |
| Color: Yellow | | | | 2.673 | 2 | 2 4 2 |
| CAS no.: 7704-34-8. Other data 21-1068. Also called: briarstone. O.O. Cell: | | | | 2.621 | 14 | 1 3 7 |
| a=12.940, b=24.401, c=10.450, a/b=0.5299, c/b=0.4272. F0: of128. Validates | | | | | | |
| by calculated pattern 24-733. To replace 1-478. Met: 32.06. Volume[00]: | | | | 2.614 | 4 | 4 0 0 |
| 3281.98. | | | | 2.569 | 8 | 3 3 3 |
| | | | | 2.501 | 6 | 2 4 4 |
| | | | | 2.424 | 14 | 3 1 7 |
| | | | | 2.404 | 2 | 4 0 4 |

| d Å | Int. | h k l | d Å | Int. | h k l | d Å | Int. | h k l |
|-------|------|--------|-------|------|--------|-------|------|--------|
| 2.375 | 4 | 4 2 2 | 1.838 | 2 | 1 5 9 | 1.531 | 2 | 0 0 16 |
| 2.366 | 4 | 3 3 5 | 1.823 | 4 | 2 4 10 | 1.515 | 2 | 3 5 11 |
| 2.288 | 6 | 0 2 10 | 1.791 | 12 | 2 6 6 | 1.504 | 2 | 1 7 9 |
| 2.215 | 2 | 2 0 10 | 1.754 | 8 | 5 3 5 | 1.490 | 2 | 2 8 4 |
| 2.146 | 4 | 1 1 11 | 1.725 | 8 | 6 0 2 | 1.475 | 2 | 6 2 8 |
| 2.112 | 106 | 3 1 9 | 1.698 | 8 | 1 3 13 | 1.461 | 2 | 7 1 3 |
| 2.098 | 2 | 2 2 10 | 1.665 | 2 | 6 2 2 | 1.439 | 4 | 4 4 12 |
| 2.057 | 2 | 5 1 1 | 1.658 | 2 | 2 0 14 | 1.424 | 4 | 0 8 8 |
| 2.041 | 2 | 2 4 8 | 1.647 | 6 | 3 5 9 | 1.419 | 2 | 7 1 5 |
| 2.003 | 2 | 3 5 3 | 1.622 | 6 | 6 2 4 | 1.391 | 2 | 3 5 13 |
| 1.988 | 4 | 4 0 6 | 1.607 | 6 | 4 0 12 | 1.362 | 2 | 5 7 3 |
| 1.957 | 2 | 2 6 2 | 1.601 | 2 | 6 0 6 | 1.354 | 4 | 7 3 5 |
| 1.926 | 2 | 4 4 4 | 1.585 | 4 | 4 6 4 | | | |
| 1.900 | 86 | 5 1 5 | 1.563 | 2 | 4 4 10 | | | |
| 1.856 | 2 | 3 1 11 | 1.542 | 2 | 3 7 5 | | | |

The residue from leach test S-81 was immersed in liquid nitrogen shortly after filtering (within an hour of test completion). It was analysed by XRD for crystal morphology and shown to be the orthorhombic S_{α} . No change was observed over several months, which was not surprising, once this first sample was recognised as already being the stable form of elemental sulfur.

Overall, the SEM and XRD work of this appendix confirmed the chemical evidence of pyrite purity and the visual and analytical evidence of elemental sulfur formation during nitric acid oxidation of pyrite.